INVESTIGATION OF THE PROJECTED IMPACTS OF CLIMATE CHANGE ON THE HYDROLOGY OF LABRADOR'S CHURCHILL RIVER BASIN USING MULTI-MODEL ENSEMBLES

by

© Jonas Roberts

A Thesis submitted to the

School of Graduate Studies

in partial fulfillment of the requirements for the degree of

Doctorate of Philosophy

Faculty of Engineering and Applied Science

Memorial University of Newfoundland

February 2015

St. John's Newfoundland and Labrador

Abstract

This manuscript thesis presents four stand-alone papers which all contribute to the investigation of projected impacts of climate change on the hydrology of Labrador's Churchill River Basin. The overarching goal of this undertaking was to provide useful information to Nalcor Energy, a hydroelectric developer, regarding the change in the amount and timing of water in the Churchill River between a base period (1971-2000) and a future period (2041-2070).

Three separate multi-model approaches used data from the North American Regional Climate Change Assessment Program to look at the impacts of climate change on the Churchill River: (i) Bias-corrected precipitation and temperature data forced a hydrologic model to investigate the changes in mean daily streamflow for the Pinus River, a sub-basin of the Churchill River; (ii) A new approach (dubbed "fullstream analysis") took advantage of the full range of simulated hydrological variables from each ensemble member and was used to study the expected changes in mean annual runoff of the entire basin, and; (iii) Weighted multi-model ensembles examined the simulated impacts of climate change on mean monthly runoff for the entire basin.

Several results were common across the various approaches. Ensemble mean annual increases in runoff were found to be similar, between 8.9% and 14.6%. Further to this, an increase in cold-season runoff amounts, an earlier onset of the spring melt (though not

necessarily a larger spring melt) and no discernable change in the late summer and early fall runoff were found.

In an effort to further understand sources of error and uncertainty of the climate models used, water balances were investigated and the annual cycle of residuals quantified. Residual magnitudes varied widely between months and models and were dependent on whether one examined atmospheric or terrestrial balances. Water balance residuals remained relatively consistent between time periods implying they are systemic and not climate dependent.

Acknowledgements

First and foremost I thank Rebecca Roberts for her love, patience and support throughout the entire PhD journey. Without you, nothing is possible. Also, thank you for Felix – the world's happiest baby.

I had no intentions of undertaking a PhD until I was approached by Dr. Ken Snelgrove with this interesting project. Ken, you have provided essential support and guidance from the beginning of this undertaking and the outcome would have been of much lower quality without your supervision. Also, thanks to Amy Pryse-Phillips for her collaborative efforts.

I'd like to send a huge thank you to Nalcor Energy for providing the initial research question as well as generous funding. In particular I would like to thank Marion Organ who has been a very supportive point of contact within the organization.

This program would have been much lonelier without the regular 'business meetings' with Tristan Hauser. Thank you for all of your ideas and questions, but primarily for your friendship.

The climate model output was provided free of charge by the North American Regional Climate Change Assessment Program (NARCCAP). I would like to thank the NARCCAP team for their efforts, especially Dr. Seth McGinnis, who responded to all my

queries with patience and thoroughness, as well as Dr. Melissa Bukovsky, who helped shed some light on the shadowy inner workings of the ensemble members.

Finally, thank you to all who provided generous financial support through the program including the Natural Sciences and Engineering Research Council of Canada, Mitacs, the Government of Newfoundland and Labrador, and TD Canada Trust.

Table of Contents

List of Tables

List of Figures

List of Acronyms and Symbols

Acronyms

AHCCD – Adjusted Historical Canadian Climate Data

ccsm - NCAR Community Climate Model version 3

CDF – Cumulative distribution function

cgcm3 - Canadian Global Climate Model version 3

CLARIS - A Europe-South America Network for Climate Change Assessment and Impact Studies in La Plata Basin

CRCM – Canadian Regional Climate Model

CV – Coefficient of variation

DOE – Design of experiments

ECMWF - European Centre for Medium-range Weather Forecasts

ECP2 - Experimental Climate Prediction Center Regional Spectral Model

ENSEMBLES – European integrated climate change research study (2004-2009)

ERA-40 - ECMWF 40 years Re-Analysis

GCM – General circulation model

GEWEX - Global Energy and Water Exchanges Project

gfdl - Geophysical Fluid Dynamics Laboratory Climate Model version 2.1

GrADS - Grid Analysis and Display System

hadcm3 - United Kingdom (UK) Hadley Centre Climate Model version 3

HRM3 - Hadley Regional Model 3

IPCC – Intergovernmental Panel on Climate Change

MM5I - MM5 - PSU/NCAR mesoscale model

NARCCAP – North American Regional Climate Change Assessment Program

NCAR – National Center for Atmospheric Research

NCEP – National Centers for Environmental Prediction

NSERC - Natural Sciences and Engineering Research Council of Canada

PDF – Probability density function

PRUDENCE - Prediction of Regional scenarios and Uncertainties for Defining EuropeaN Climate change risks and Effect

RCM – Regional Climate Model

RCM3 - Regional Climate Model version 3

REA - Reliability Ensemble Averaging

RMSD – Root mean square difference

RMSR – Root mean square residual

SRES - Special Report on Emissions Scenarios (of the IPCC)

UCAR – University Corporation for Atmospheric Research

WCRP – World Climate Research Program

WRFG - Weather Research and Forecasting model

Symbols

a – precipitation bias correction parameter corresponding to the mean of observed data

b – precipitation bias correction parameter corresponding to the coefficient of variation (CV) of observed data

C – condensation

C_p – specific heat

∂t - the period of time over which a variables tendency is determined

$-\nabla_H \vec{Q}$ - Atmospheric moisture convergence

ε_A - Atmospheric moisture balance residual

ε_T - Terrestrial moisture balance residual

E – evaporation or evapotranspiration

e_s – saturation vapour pressure

evps – surface evaporation rate

f – pressure scaling factor

g – gravity

$\vec{g}$ = apparent gravity vector

$\vec{F}_{friction}$ = force due to friction

hfls – surface latent heat flux

L_v – latent heat of vapourization of water

$\vec{\Omega}$ = angular velocity of the earth

p – pressure

P - precipitation

$P - E$ - The balance between precipitation (P) and evapotranspiration (E)

q – specific humidity

Q – heating unit per unit mass

$\bar{Q}$ - vertically integrated horizontal water vapour flux

ρ - density

R_g – gas constant

R_v – gas constant of water vapour

t - time

T – temperature

u – zonal wind component

v – meridional wind component

$\vec{v}$ - wind vector

w – vertical wind component

List of Appendices

1. Introduction

Climate change is already having a noticeable impact on earth's hydrological cycle (Trenberth *et al.* 2003; Dery *et al.* 2009). As the changing climate's influence becomes more apparent, the need to investigate its potential future impacts increases. Small changes in the distribution of precipitation can significantly alter mean annual streamflow (Muzik 2001) and even modest perturbations in natural inflow tend to have amplified impacts on reservoir storage levels (Christensen *et al.* 2004; Minville *et al.* 2008). These impacts and others are of concern to hydroelectric developers and water managers whose strong dependence on climatological factors, such as the balance between precipitation and evaporation, make them vulnerable to climate regime changes.

The overarching goal of this work is to produce a thorough and useful projection of the impact of climate change on the hydrologic system within Labrador's Churchill River Basin, specifically the amount and timing of runoff. The Churchill River Basin covers approximately 92 500 km^2 and extends from Labrador City in the west to Happy Valley-Goose Bay in the east. There is an existing hydroelectric project on the river (the 5,428 MW Churchill Falls Generating Station), one currently under construction (the 824 MW Muskrat Falls Project) and one that is proposed for the future (the 2250 MW Gull Island Project). With over 8500 MW of combined generating capacity and potential, the Churchill River Basin is an important region for Newfoundland and Labrador, and for

Canada in general. The impacts of climate change on the river need to be addressed to facilitate its effective use for the coming decades.

To ensure a thorough examination of the potential impacts of climate change, multiple analysis approaches will be used which, together, incorporate the full range of hydrological data from an ensemble of regional climate models. Hydrological data used in this thesis includes land-atmosphere interactions such as precipitation and evaporation, runoff and terrestrial water storage, as well as atmospheric moisture convergence and precipitable water content. The three multi-model approaches include driving a hydrological model with bias corrected precipitation and temperature data, using all components of the atmospheric and terrestrial water balances to approximate mean annual runoff and employing a weighted ensemble of the climate models' land-surface schemes runoff output.

For the analysis to be useful for water resources managers a quantified representation of uncertainty will also be presented. While there are many sources and forms of uncertainty (discussed in detail in Section 2.6), the uncertainty referred to and represented throughout this work is the spread of climate model output from the multi-model ensembles. If all models projected the same climate change signals then uncertainty is minimal, while if there is a large discrepancy between ensemble members then uncertainty is large.

One of the ways uncertainty is represented in this thesis is through the use of empirical probability distribution functions (PDFs) (or alternatively cumulative distribution

functions (CDFs)), which give the likelihood (based on the output of the climate models used) of a change that falls along a continuous spectrum.

Another representation of uncertainty is through the use of "spaghetti plots." This is simply plotting the results of all individual ensemble members together so one is able to easily see the spread of available simulations.

The final representation of uncertainty employed is the plotting of 80% and 90% uncertainty ranges around a mean ensemble value. If the base period streamflow falls below the 80% uncertainty range for future streamflow, for example, one can say there is 80% likelihood that there will be an increase in streamflow from the base period to the future. Uncertainty ranges are especially useful for hydrograph plots to show the projected changes, and confidence in those changes, of streamflow throughout the year

This manuscript format thesis contains four stand-alone research papers, presented as Chapters 3 through 6, plus a broad literature review found in Chapter 2. At the beginning of each chapter (after each abstract) there is a preface to discuss how the research paper ties in with the previous chapter and how it contributes to the thesis as a whole. Additional material, including supplementary calculation details and results, that may not have been included in the respective research papers for publication or space considerations will also be presented in the prefaces.

1.1. Research Contributions

The primary research contributions of this work are as follows:

1. A procedure for climate researchers with limited resources to investigate the impacts of climate change on runoff in their watersheds of interest, while capturing a range of uncertainty. This includes the development of the "fullstream" analysis approach.
2. An understanding of climate change impacts on the hydrology of the Churchill River Basin including a probabilistic projection and a quantified representation of uncertainty.

Secondary contributions include:

1. The quantification of the NARCCAP models' mean annual cycle of atmospheric and terrestrial water balance components and residuals. Atmospheric water balance residuals were found to be consistently higher than their terrestrial counterparts.
2. Atmospheric and terrestrial water balance residuals were found to be consistent between base and future periods (for each ensemble member), implying that they are systemic in nature and not climate dependent.
3. Recommendations to climate modeling groups and consortiums regarding post-processing and publishing variables.
4. Regional climate models have a substantially larger contribution to uncertainty in

runoff's climate change signal than general circulation models.

5. Choice of runoff approximation (i.e. upstream, midstream or downstream when using fullstream analysis – see Chapter 5) also had a larger contribution to uncertainty in runoff's climate change signal than general circulation models.
6. Relatively little difference in the impacts of climate change on the annual streamflow cycle was found between different weighting schemes, including equally weighted models.

1.2. Co-authorship Statement

The Canadian Water Resources Journal published Chapter 3, entitled "Modeling the Potential Impacts of Climate Change on a Small Watershed in Labrador, Canada" in 2012 (Roberts et al. 2012). Jonas Roberts, the thesis author was the primary and corresponding author, Amy Pryse-Phillips, a masters student, was the second author and Dr. Ken Snelgrove was third author. All authors were part of the same research group, which was led by Dr. Snelgrove. For the work in Chapter 3, the design of the research was developed with input from all members of the group. Mr. Roberts was responsible for the writing of the manuscript, extracting and bias-correcting the climate data as well as preparing it for input into the hydrological model. He was also responsible for all data analysis, discussion and plots within the manuscript. Ms. Pryse-Phillips was responsible for setting up and running the hydrological model WATFLOOD and providing feedback on the writing of the manuscript. Dr. Snelgrove's role was primarily guidance in the

research and writing of the manuscript. He also wrote one portion of the FORTRAN code which facilitated the bias correction process.

For the remainder of the thesis, Mr. Roberts performed the entirety of the research, literature review, data collection and preparation, analysis and writing. Dr. Snelgrove, in his supervisory role, provided guidance for the entire process.

2. Literature Review

2.1.Summary

There is a need for water resource managers and developers to investigate the impacts of climate change on the hydrology in their regions of interest. An ensemble of GCMs dynamically downscaled using a variety of RCMs is an effective way to capture a wide range of uncertainty for simulations of future climate. Comparing historical simulations of models against observations is useful for bias correction, required for hydrological modeling, and determining model skill, which can be applied to determine ensemble member weights. The results of simulating the hydrological impacts of climate change can be effectively presented via a probabilistic approach and the use of probability distribution functions (PDFs).

There are a vast number of studies exploring the potential impact of climate change on the hydrology of various basins, large and small, around the world. Some studies use runoff output directly from the land-surface schemes of climate models, while others bias correct climate model output (directly or via statistical downscaling) before using it to force hydrological models. Another method, which is also widely used for validating the representation of the water cycle in climate models, involves calculating the atmospheric moisture convergence along with the atmospheric and terrestrial water balances. Each of these methods has advantages and disadvantages, which are discussed in detail in the

following literature review. Previous studies only rarely employed more than one of the above methods and have never used all three methods to explore uncertainty.

2.2. Climate Change

Earth's climate is controlled by complex interactions between solar forcing, various properties of the atmosphere, ocean and land-surface along with a multitude of feedback mechanisms. The climate is not constant and irreversible changes can be induced by changing the strength of any of its interacting or driving variables, such as the solar radiation balance.

According to Le Treut *et al.* (2007) there are three fundamental ways to change the solar radiation balance and thus the climate system. The first method is to alter the incoming solar radiation, either by solar output or orbital fluctuations. The second is to change the albedo of the earth so a greater or lesser amount of shortwave radiation is reflected back into space. The last method requires modifying the longwave radiation emitted to space, which relates to atmospheric greenhouse gas concentrations and cloud radiating feedback. The climate system responds to all these changes directly or via feedback mechanisms.

Global temperature change due to increased concentration of greenhouse gases in the atmosphere is dictated by the strength of various feedback mechanisms, the effective heat capacity of the ocean and how heat transport to deep oceans depends on changes at the surface (Allan and Ingram 2002).

2.3. Effects of Climate Change on the Hydrological Cycle

As climate and hydrological cycles have a complex interdependency (Peixoto and Oort 1992), we know that climate change is affecting water resources (Trenberth *et al.* 2003; Maurer 2007).

There are several robust responses of the hydrological cycle to projected climate change. Held and Soden (2006) studied model runs generated for the fourth IPCC assessment (IPCC 2007) and found that there will be a decrease in convective mass fluxes (to maintain the balance between precipitation and the boundary layer mixing ratio) but an increase in horizontal moisture transport, as well as an associated enhancement of the evaporation-precipitation pattern and its variance. These responses stem from the increased amount of water vapour that can be held in a warmer lower troposphere and result in a general intensification of the hydrological cycle. Here, dry areas are expected to get drier and wet areas are expected to get wetter (Bates *et al.* 2008; Trenberth 1998). Unfortunately, it is substantially harder to quantify the range of possible changes in the hydrological cycle than the global mean temperature because of fewer observations and weak physical constraints (Allan and Ingram 2002).

For typical temperatures of the lower troposphere, the Clausius-Clapeyron Equation 2.1 predicts that the saturation vapour pressure (e_s) will increase by 6 to 7% for each degree Celsius temperature (T) increase (L_v and R_v are the latent heat of vapourization and gas constant for water vapour, respectively). However, Allen and Ingram (2002) showed the energy constraints reduce that increase to 3.4% per degree, due to the limiting ability of

the atmosphere to radiate away heat created from condensation. As such, the hydrological cycle is controlled more by the availability of energy rather than the availability of moisture, though extreme event intensity will increase primarily with an increase in moisture. Additionally, regional changes in precipitation are dependent on local changes in atmospheric circulation (Allan and Ingram 2002).

$$\frac{de_s}{dT} = \frac{L_v e_s}{R_v T^2} \qquad (2.1)$$

It has been shown that small changes in the distribution of precipitation can significantly alter mean annual streamflow (Muzik 2001) and even modest perturbations in natural inflow have amplified impacts on reservoir storage levels (Christensen *et al.* 2004; Minville *et al.* 2008). As such, it is important for water managers to investigate the potential impacts that climate change will have on their regions of interest. To do so requires the application of climate models.

2.4. Climate Modelling

Observations, theory and models are all required for climate research (Rummukainen 2010). Numerical models are built on theories based in the physical sciences, while observations are used to calibrate and validate the simulations.

According to physical theory, there are seven equations and corresponding variables that govern the state and evolution of the atmosphere (Peixoto and Oort 1992). Equation 2.2 is based on Newton's second law (conservation of momentum) and can be broken down

into three velocity component parts. Equation 2.3 is the continuity equation or the conservation of mass, while Equation 2.4 is the conservation of water mass. Equation 2.5 is the first law of thermodynamics (conservation of energy) and Equation 2.6 is the equation of state. The variables corresponding to the governing equations include three velocity components u, v, w, (represented by the vector $\vec{v}$) pressure p, temperature T, specific humidity q, and density ρ. After various approximations and simplifications these equations are used as the computational basis for numerical climate models.

$$\frac{D\vec{v}}{Dt} = -\frac{1}{\rho}\vec{\nabla}p - \vec{g} + \vec{F}_{friction} - 2\vec{\Omega}\times\vec{v} \qquad (2.2)$$

$$\frac{\partial\rho}{\partial t} = -\nabla\cdot(\rho\vec{v}) \qquad (2.3)$$

$$\frac{\partial pq}{\partial t} = -\nabla\cdot(p\vec{v}q) + \rho(E - C) \qquad (2.4)$$

$$Q = C_p\frac{dT}{dt} - \frac{1}{\rho}\frac{dp}{dt} \qquad (2.5)$$

$$p = \rho R_g T \qquad (2.6)$$

Where:

$\vec{g}$ = apparent gravity vector

$\vec{F}_{friction}$ = force due to friction

$\vec{\Omega}$ = angular velocity of the earth

E = evaporation

C = condensation

Q = heating rate per unit mass

C_p = specific heat

R_g = gas constant

The most powerful tool used for the simulation of historical and future climate is the General Circulation Model (GCM). However, due to the low spatial resolution of GCMs, they are insufficient for regional climate change analysis (Gagnon *et al.* 2009). GCMs typically have spatial resolution from 200 km to 500 km, and are unable to resolve subgrid scale features such as topography and clouds (Grotch and MacCracken 1991; Fowler *et al.* 2007). This necessitates the need for approximations and physical parameterizations. It is well established that GCM output requires downscaling to effectively examine the impacts of climate change on basin scale hydrology (Dibike and Coulibaly 2005; Sharma *et al.* 2011).

Downscaling Techniques

Downscaling can be grouped into two broad categories: dynamic and statistical. Dynamic downscaling involves the nesting of a high resolution, physically based regional climate model (RCM) within a coarser resolution global model. Statistical downscaling, on the other hand, employs statistical methods to determine the state of various climatic variables, typically at the point scale. Table 2.1 provides an overview of the advantages and disadvantages of statistical and dynamic downscaling (modified from Wilby and Wigly 1997; Fowler *et al.* 2007).

This research will focus on various processes of basin scale hydrology. Since RCMs are based on the physical principles of conservation of energy, mass and momentum (Laprise 2008; Gagnon *et al.* 2009) and are more comprehensive than statistical downscaling methods (Rummukainen 2010), dynamic downscaling will be used. Statistical

downscaling will not be explored further here; For further information on statistical downscaling Fowler *et al.* (2007) and Themeβl *et al.* (2011) provide a broad overview of the most common approaches including regression models, weather typing and weather generators.

Table 2.1 – Advantages and Disadvantages of Statistical and Dynamic Downscaling

	Statistical Downscaling	Dynamic Downscaling
Advantages	- Computationally cheap. - Can provide point-scale climatic variables. - Can be used to derive any climatic variable. - Transferable to other regions. - Based on accepted statistical procedures. - Directly incorporates observations into method.	- Resolves more atmospheric processes at smaller scale than GCMs. - Gives broad selection of variables for entire simulated domain. - Responses are based on physically consistent processes.
Disadvantages	- Need long and reliable observation record for calibration. - Dependent on choice of predictors. - Must assume stationarity between predictor and predictands. - Climate system feedbacks are not included. - Dependent on GCM forcing. - Domain size, region and season affect downscaling skill.	- Computationally expensive. - Limited number of available scenario ensembles. - Strongly dependent on GCM boundary forcing.

The primary disadvantage of dynamic downscaling is the computational effort required (Maurer 2007), so it is generally not feasible to run a large ensemble with multiple RCMs for small studies such as a PhD thesis. However, there are international regional climate modelling efforts covering (or planning to cover) most geographic regions on earth, including North America (NARCCAP), South America (CLARIS), Europe

(ENSEMBLES and PRUDENCE) and east Asia (RGMIP) (Rummukainen 2010). Projects like these improve realism of control simulations and more accurately represent variability and extreme event statistics at a higher spatial and temporal resolution (Fowler *et al.* 2007).

A state-of-the-art RCM's representation of atmospheric climate processes is "as complex as in comprehensive GCMs" (Rummukainen 2010). In fact, they represent local climate variability and extremes better than GCMs. With resolutions of roughly 50 km they are able to realistically simulate regional features such as orographic precipitation (Frei *et al.* 2003), extreme events (Fowler *et al.* 2005; Frei *et al.* 2006) and regional scale anomalies and non-linear effects (Leung *et al.* 2003). They also improve the simulation of meso-scale precipitation processes and therefore produce better higher moment statistics than GCMs (Schmidli *et al.* 2006).

RCMs are able to produce many complex processes involved in the hydrological cycle, including those based on principles of energy and water conservation. As such, they can be useful in quantifying runoff in regions of sparse *in situ* observations (Music *et al.* 2009). However, the complexity of many land-surface and groundwater processes can limit the ability of various RCM land-surface schemes to adequately reproduce observed regimes on a regional scale (Music *et al.* 2009). RCMs are useful tools for quantitative studies of the hydrological cycle on subcontinental scales, however deficiencies in land-surface models and biases in the forcing GCMs can induce errors in RCM simulations (Music and Caya 2007). Other RCM errors are created due to modelling approximations

and the nesting approach (Music *et al.* 2009). A conceptual issue which plagues RCM simulation is that their output is strongly influenced by their GCM forcing data, resulting in "garbage in, garbage out" situations. In other words, if there is a large bias in the GCM forcing then there will be a large bias in the RCM output.

GCM biases cascade through the RCM and subsequently the hydrological performance of an RCM is dependent on the ability of the driving GCM (Music *et al.* 2009). In light of these biases, Sharma *et al.* (2011) found that further downscaling RCM data improved the performance of the hydrological model over raw RCM data (magnitude and timing of changes were more consistent when downscaled data was used). Regardless of the method used, the general patterns of changes in future flow are quite similar using either raw or downscaled data. This improvement might be attributed to the inherent bias correction in statistical downscaling and is not necessarily related to an increase in resolution.

This thesis uses dynamically downscaled climate model simulations (RCMs driven by GCMs) from the freely available North American Regional Climate Change Assessment Program (NARCCAP) for all simulations of future and base period climates.

2.5. Hydrological Impact Modeling

Hydrological impacts are strongly dependent on the GCM. Differences between competing GCMs relate primarily to the spatial variability and magnitude of precipitation rather than the change in temperature (Thorne 2011). Differences in annual runoff from a

RCM when forced with GCMs versus observations have been shown in certain cases to be comparable to a RCMs internal variability (Music *et al.* 2009). Ludwig *et al.* (2009) found that "modified climatic boundary conditions cause dramatic deviances in hydrological model response." Ludwig *et al.* (2009) also showed that the uncertainties introduced by hydrological models can be of similar magnitude to the climate model output scenario used as inputs. They also emphasized that physically based model processes are vital to ensure the predictive power of hydrological models. The magnitude and distribution of climate change combined with specific basin characteristics determine which impacts are most important locally (Menzel 2002; Matondo 2004; Xu *et al.* 2011).

Several studies have shown that in order to achieve realistic results, preprocessing is required to remove biases in climate output fields before they can be used to force a hydrological model (Feddersen and Andersen 2005; Hansen *et al.* 2006; Christensen *et al.* 2008; Piani *et al.* 2010). As mentioned above, this can be accomplished inherently through statistical downscaling or with direct bias correction methods (discussed later). Even the best RCM-GCM contains biases that mask climate change impacts within regional hydrologic models (Maurer 2007). Hydrological climate change impact studies have used RCM output directly (Wood *et al.* 2004; Graham *et al.* 2007a; Graham *et al.* 2007b), bias corrected RCM output (Wood *et al.* 2004; Fowler and Kilsby 2007; Fowler *et al.* 2007) and other statistical approaches (Fowler *et al.* 2007). While hydrological models driven by raw model output tend to perform poorly (Prudhomme *et al.* 2002), bias corrected RCM output tends to reproduce hydrology fairly well (Wood *et al.* 2004), particularly when corrections are applied sub-monthly (Haerter *et al.* 2011).

There are three generations of land-surface models used within atmospheric models that represent three levels of complexity. The first generation land-surface schemes are based on the "bucket" method, originally proposed by Manabe (1969). Here, the land-surface is represented by a bucket with a single adjustable parameter: bucket depth. Once the bucket fills (i.e. land-surface is saturated), excess water spills over and runoff occurs. Second generation schemes increase complexity (and thus realism) by representing multiple soil levels, surface water and energy balance calculations with some vegetation and canopy processes (Music *et al.* 2009). Newer third generation land-surface schemes include vegetation carbon processes in addition to those of second generation schemes. Ludwig *et al.* (2009) found that complex and middle complexity models behave more similarly than their simple bucket model counterpart, however there remain significant differences (e.g. spring flood intensity, spatial water storage patterns). They make the argument that land-surface model complexity should be included in the uncertainty discussion, though they are uncertain as to what level of complexity is required for effective climate change impact studies.

Runoff

Runoff integrates weather events and water availability over time and space (Frigon *et al.* 2010). There is evidence that simulated runoff is less sensitive to changes in a RCM's physical parameterizations than precipitation, evapotranspiration, moisture flux convergence and terrestrial water storage tendency (Music and Caya 2007). That being said, the physical parameterizations in land-surface schemes do have a substantial impact

on runoff, particularly with first and second generation models. When validating a RCM's runoff output Gagnon *et al.* (2009) suggest not to pair a RCM tile with a weather or hydrometric station, as it is more applicable to consider the entire watershed versus each tile separately.

Observed station discharges lag precipitation events due to routing, prolonged snowmelt, seasonal ponding and other factors. This results in basin storage on a monthly, annual and potentially even longer time scale. High runoff variability can be due to the lack of lakes and routing (rivers), as a simulated water drop located on an upstream tile will move faster than a physical upstream water drop (Gagnon *et al.* 2009). It has also been shown that lakes dampen the spring melt signal (Hirschi *et al.* 2006) and the implementation of a lake model would likely have significant effects on the simulated hydrological regime due to improved representation of surface fluxes of heat, water vapour and momentum (Music *et al.* 2009). Therefore, to compare discharge observations with simulated runoff over a short time frame may not be appropriate if storage and basin lag time are not incorporated (Thomas and Henderson-Sellers 1991; Gagnon *et al.* 2009). Roads *et al.* (2003) and Serreze *et al.* (2003) describe streamflow and river discharge as lagged and routed runoff. As runoff is not directly observed one can approximate it as observed streamflow divided by the drainage area. Similarly, multiplying the model runoff by the drainage area is used in Chapters 4, 5 and 6 to approximate total basin streamflow. Naturalized flow, which negates the effects of damming and water management, is often used for model validation (Music *et al.* 2009), as in Chapter 6.

Atmospheric and Terrestrial Water Balances

To determine the amount of water moving into and out of a basin, one can perform atmospheric moisture convergence and water balance calculations. Water balance and moisture convergence equations can be found in Rasmusson (1968) as well as Peixoto and Oort (1992), and are discussed in Chapter 4.

Terrestrial water storage is a key part of the water balance and hydrological cycle as it determines the partitioning of the water and energy fluxes at the land-surface (Mueller *et al.* 2011). Soil moisture, in particular, is important for regions with high precipitation recycling (Schar *et al.* 1999; Hirschi *et al.* 2006). Seneviratne *et al.* (2004) and Hirschi *et al.* (2006) showed that one can effectively estimate basin scale terrestrial water storage using two water balance equations from reanalysis data plus streamflow measurements. Serreze *et al.* (2003) provides a procedure for calculating precipitation recycling that gives a sense of the importance of land-surface processes on the hydrological budget. One can expect smaller and smaller recycling ratios for decreasing region size (value would be 1 for the entire globe) (Brubaker *et al.* 1993).

Typically, estimates of soil moisture on a large scale differ greatly from model to model (Reichle *et al.* 2004; Hirschi *et al.* 2006). Point scale *in situ* soil moisture measurements are not representative for larger areas, resulting in the need for satellite observation or an atmospheric-terrestrial water balance approach to provide more information on the distribution of terrestrial water storage (Mueller *et al.* 2011).

Derived from terrestrial water balance residuals, the commonly touted critical size for water balance computations using atmospheric reanalysis is on the order of 10^5 km^2. That being said, Hirschi *et al.* (2006) performed water balances on three Churchill River-sized basins (84 144, 85 223 and 94 836 km^2 respectively) with acceptable imbalances. Even at scales much greater than 10^5 km^2, Serreze *et al.* (2003) found that P-E was roughly 9-20% lower than the observed discharge for large arctic basins, though given the uncertainties in computed P-E, the authors considered the water budgets to be reasonably closed. All analyses mentioning critical basin size have used roughly 1 degree resolution and larger, and it is uncertain whether the critical domain size will decrease with higher resolution data sets.

The components and residuals of simulated atmospheric and terrestrial water balances are discussed in detail in Chapters 4 and 5.

2.6. Uncertainty and Bias

It is widely known that the primary factors limiting useful application of model output are the uncertainties inherent in climate and impact modelling (Minville *et al.* 2008; Khalili *et al.* 2006; Ludwig *et al.* 2009). This uncertainty in climate projections and subsequent hydrological response to climate changes complicates the understanding of the impacts on water resources (Minville *et al.* 2008; Treut *et al.* 2008; Xu *et al.* 2011).

Sources

Sources of uncertainty in hydrological impact studies (Déqué *et al.* 2007; Maurer 2007; Thorne 2011) include: (i) amplitude of greenhouse gas concentrations, (ii) formulation and accuracy of GCM algorithms, parameterizations and feedback mechanisms, (iii) high resolution RCMs or alternative downscaling technique, (iv) selection and implementation of a land-surface hydrology model, and (v) sampling uncertainty. Wilby and Harris (2006) examined sources of uncertainty individually and described the "uncertainty cascade" which combines and propagates the above mentioned sources of uncertainty. Sources of uncertainty that can't be objectively deduced from numerical simulations include the reliability of SRES greenhouse gas emissions scenarios, RCM-GCM responses to a previously unobserved climate forcing and unexpected phenomena such as volcanic eruptions.

It is also important to note the effect that non-linearity and chaos play in numerical climate model uncertainty. Lorenz (1963) developed a simple non-linear mathematical model for atmospheric convection, which he derived from the governing equations (Equations 2.2 to 2.6), discussed earlier. In this model, a minuscule difference in initial conditions (for certain parameter values) leads to a divergence of results. In other words, the system is chaotic. This sensitivity to initial conditions holds true for more complex climate models and contributes to a model's uncertainty.

The primary constraint on quantifying the impacts of climate change on water resources and the hydrological system are GCM projection uncertainty (Minville *et al.* 2008; Wilby

and Harris 2006; Xu *et al.* 2011). Differences between individual GCMs result in a larger impact on simulating hydrological change than differing emissions scenarios (Graham *et al.* 2007a), even though emissions scenarios play a role (Jasper *et al.* 2004). Thorne (2011) found that even with a prescribed $+2^{o}$ global mean temperature change, individual GCMs gave different outcomes for the Liard River Basin in Northern Canada due to the differences in algorithms, parameterizations and feedback mechanisms. It is recommended that multiple GCMs should be selected for use in impact studies (Ghosh and Mujundar 2009; Kingston *et al.* 2011; Thorne 2011).

While GCM structure and physics generally play a majority role in uncertainty, RCM formulation has been found to have a comparable or sometimes dominant influence for simulated variables, depending on the region of study and season (Rowell 2006; Déqué *et al.* 2007; Roberts *et al.* 2012). Relative contributions to uncertainty vary according to spatial domain, region, season and variable (Déqué *et al.* 2005; Fowler *et al.* 2007).

Another source of uncertainty in climate change projections is the current inability of models to adequately simulate the water cycle, particularly its complex and multi-scale processes (Music and Caya 2007). All parameterizations (including large-scale condensation, convection schemes, soil parameterization, snow-albedo feedback, etc.) contribute to biases in RCMs (Hagemann *et al.* 2004; Fowler *et al.* 2007). This implies that variables other than precipitation, such as soil moisture and evapotranspiration (which are all, of course, interrelated – the degree to which depending on region and season, also contribute to runoff bias (Gagnon *et al.* 2009). This helps justify the need to

evaluate atmospheric moisture convergence and water balances, independent of hydrological models driven by bias corrected data, when investigating the impacts of climate change on the hydrology of a basin. This is undertaken in Chapters 4 and 5.

Prudhomme and Davies (2009a and 2009b) and Thorne (2011) found that hydrological uncertainty can be as large as natural variability in the hydrological regime but that GCM uncertainty on monthly mean flow projections is higher still. Kingston *et al.* (2011) found varying parameters and algorithms in a hydrological model contributes little to the uncertainty of the projection. Complex basins have to consider many aspects of uncertainty in hydrological regime simulations (Thorne 2011) but it is important to note climate models contribute more uncertainty than hydrological models (Hingray 2007a; Fowler *et al.* 2007). As such, it is more important to include multiple GCMs and RCMs than multiple hydrological models in a climate change impact study in order to describe the range of uncertainty.

As RCMs are constrained by their lateral boundary conditions, natural variability generally surpasses internal RCM variability (Christensen *et al.* 2001; Braun *et al.* 2012; Frigon *et al.* 2008; Frigon *et al.* 2010). However, sampling uncertainty, which exists because climate statistics are estimated from a finite sample that doesn't cover the entire range of natural variability, is typically marginal.

Model Validation and Representing Uncertainty

Effectively representing the uncertainties involved in climate change impact projection is essential for helping water managers and hydroelectric developers create and adopt

coherent and informed strategies (Dettinger 2004; Kipari and Gleick 2004; Maurer 2007). Employing an ensemble approach and quantifying uncertainty is important for obtaining the best estimate (Déqué *et al.* 2007). Using different models forced with the same greenhouse gas scenarios is one way to evaluate uncertainty (Crossley *et al.* 2000; Déqué *et al.* 2007). Although various greenhouse forcings are required for a more complete assessment of uncertainty (Frigon *et al.* 2010).

Uncertainty of historical simulations is traditionally evaluated by the root mean square error (RMSE) between simulations and observations (predicted versus actual value) while uncertainty in future simulations is represented by the spread of all available projections (Déqué *et al.* 2007; Shrestha *et al.* 2010). Model skill assessment must be unique for each catchment and application as there is no all encompassing assessment criteria (Fowler *et al.* 2007). Historic RCM evaluation is typically done using "perfect boundary conditions" provided by reanalysis based observations, which is important for validating variability and extremes (Mearns *et al.* 2012). NARCCAP's NCEP driven RCMs are used in the analysis of Chapter 4.

There is no established method to evaluate which models best simulate the future (Déqué *et al.* 2007). However, there are many ways one can represent the uncertainty of future projections. These include response intervals, mapping spatial variability, cumulative distribution functions (CDF), empirical probability distribution functions (PDF) among other methods. Any of these representations can be accomplished using either weighted

or unweighted ensembles. Several of these uncertainty representations are utilized throughout this thesis.

The response interval, in which the minimum and maximum ensemble values provide the boundary of a confidence interval, is a simple and useful approach to quantify uncertainty. The response interval's major drawback is that the results strongly depend on the most and least sensitive models and are subject to any outliers in the sample. Additionally, adding more models simply increases the amplitude of the intervals (Déqué *et al.* 2007). The Gaussian assumption reduces the width of the confidence interval boundaries. The Gaussian character of mean responses is increased by means of the Central Limit Theorem, averaging over several experiments and grid spaces (Déqué *et al.* 2007). The Central Limit Theorem requires that variables are independent, identically distributed and random, which is difficult to confirm with the relatively small sample size used in this thesis. This should be kept in mind when interpreting results from Chapter 6, where the Gaussian assumption is applied when calculating hydrograph confidence intervals.

Thorne (2011) represented uncertainty by mapping "spatial variability of the absolute value between the maximum and minimum projected change between seven GCMs" by season. This approach allows one to determine the regions of higher uncertainty, which is useful for larger basins (such as the Liard River Basin, 275 000 km^2). Thorne found that projected changes in precipitation varied more than temperature spatially and in magnitude.

Ghosh and Mujunder (2009) use weighted ensembles to address inter-GCM uncertainty and account for "partial ignorance uncertainty," which arises when some GCM output is not available. They create bands around CDFs generated by all GCMs. In particular they use an imprecise CDF which is an envelope that includes all GCMs but also the uncertainty from missing GCMs.

Déqué *et al.* (2007) use variance decomposition to take full advantage of design of experiments (DOE) theory for individual statistics – data reconstruction reduces the bias in the overall estimation of uncertainty due to overrepresentation by a certain RCM or GCM. This approach is used in Chapter 5 to isolate and compare the magnitudes of each source of uncertainty.

An ensemble approach using probabilistic methods is very useful for representing projection uncertainty and is discussed in detail in Section 2.7.

Bias Correction Methods

Several studies have shown that in order to achieve realistic streamflow simulations preprocessing is required to remove biases in climate output fields prior to use in hydrological models (Feddersen and Andersen 2005; Hansen *et al.* 2006; Christensen *et al.* 2008; Piani *et al.* 2010).

A simple and widely used statistical downscaling method is the change factor approach (aka. shift, scaling factor, delta-change, perturbation, etc). Here, the difference between the base period and future simulations is imposed on observations (Graham *et al.* 2007a;

Fowler *et al.* 2007) and as such, inherently accounts for systemic bias. Caveats for this method include i) the assumption that GCMs are better at modelling relative change than absolute amounts (i.e. assume a constant bias in time), ii) simple examination of point locations will not take into account changes in variability and spatial patterns, and iii) it produces an unchanging temporal sequence of wet and dry days (Rummukainen 2010; Maurer 2007). An emerging alternative is to rescale time series from RCMs, allowing for changes in variability and extremes, which is important for impact modelling (Graham *et al.* 2007a; Shrestha *et al.* 2010).

Maurer (2007) uses an empirical CDF mapping bias correction from Wilks (2006) to ensure simulated precipitation and temperature CDFs line up with the corresponding observations.

The methods used by Roberts *et al.* (2012), originally from Leander and Buishand (2007) and Shabalova *et al.* (2003), employ a simple non-linear transformation, Equation 2.7, that corrects both the mean and coefficient of variation of precipitation and led to a better representation of uncertainty. They used a straightforward linear approach for correcting bias in the mean and variance of temperature, Equation 2.8. Corrections for both precipitation and temperature were performed on a 5-day mean basis, which is an appropriate correction timescale for hydrological models (Haerter *et al.* 2011; Roberts *et al.* 2012).

$$P^* = aP^b \tag{2.7}$$

$$T^* = \overline{T}_{obs} + (T_{RCM} - \overline{T}_{RCM}) \frac{\sigma(T_{obs})}{\sigma(T_{RCM})} \tag{2.8}$$

Where: P*, T* = corrected precipitation, temperature

P = uncorrected precipitation

a, b = correction parameters corresponding to mean, CV

σ = standard deviation

T_{RCM} = uncorrected model temperature

T_{obs} = observed temperature

$\overline{T}$ = climatological average temperature

Other methods for addressing model bias are statistical downscaling and numerical weather generators. Rahman *et al.* (2012) apply such concepts when assessing the impacts of climate change on a southern Ontario watershed. Others, such as Minville *et al.* (2008), use a combination of the change factor method and a stochastic weather generator. Themeβl *et al.* (2011) provides a thorough comparison of various precipitation bias correction techniques.

Bias correction is imperfect, however it remains a useful and necessary tool for helping to determine climatic change in hydrological regimes between current and future timeframes (Roberts *et al.* 2012).

2.7. Ensemble Projections

An ensemble approach incorporating multiple RCMs nested in various GCMs can be employed to provide a useful measure of uncertainty (Murphy *et al.* 2004; Kotlarski *et al.* 2005). It is well known that no single climate model is best at simulating all climate variables and their various statistics. A single projection represents only one of many possible realizations of the future climate and is not robust (Christensen and Christensen 2007; Maraun *et al.* 2010). A comprehensive assessment of climate change driven hydrological projections requires a wide spectrum of modelling choices (Frigon *et al.* 2010). The design of experiments approach, such as that used by the North American Regional Climate Change Assessment Program (NARCCAP), helps define the range of fundamental uncertainty. The need for robust decision making tools for water management that encompasses future uncertainties (Fowler *et al.* 2007) can be met in part by the probabilistic representation of these ensemble projections (Hunt 2005). That being said, there is no broad consensus on which approach is best for constructing the probability density functions (PDFs) that graphically relate results.

Among the first probabilistic treatment of climate change simulations were Allen *et al.* (2000) and Wigley and Roper (2001). Since then, research on climate change modelling uncertainty has advanced on several fronts (Ghosh and Mujundar 2009). New and Hulme (2000) used Bayesian Monte Carlo simulation to provide a probabilistic quantification of uncertainty and Raisanen and Palmer (2001) used 17 models in their probabilistic approach. Giorgi and Mearns (2002 and 2003) created the Reliability Ensemble

Averaging (REA) weighting approach in their probabilistic analysis where they varied model parameters. A regional application of the probabilistic approach began in 2003 (Stott 2003, Tebaldi *et al.* 2004b). Murphy *et al.* (2004) used 53 ensemble members to create PDFs and explore intra-model variability. Tebaldi *et al.* (2004a and 2005) used a Bayesian approach and REA to create PDFs, though they did not consider temporal variability. Wibly and Harris (2006) used a probabilistic framework to explore the uncertainty cascade and compare relative influences. More recently, regional PDFs have been created to represent climate change impact assessments within hydrological systems (Ekstrom *et al.* 2007; Hingray *et al.* 2007a). Furrer *et al.* (2007) investigated a similar approach at the grid point scale. Ghosh and Mujundar (2007 and 2008) used non-parametric kernal density estimation to create PDFs and explored equally weighted and non-equally weighted GCMs.

Multiple GCMs produce a variety of climate change signals even when forced with identical climate forcing (Meehl *et al.* 2007; Rummukainen 2010). Similarly, RCMs have large differences even when forced with identical boundary conditions (Jacob *et al.* 2007; Eum *et al.* 2012). This discrepancy between model projections is justification for use of an ensemble of RCMs and GCMs to produce realistic climate change assessment. Combining ensemble member simulations generally increases the skill, reliability and consistency of results (Tebaldi and Knutti 2007; Eum *et al.* 2012).

A weighted multi-model ensemble typically improves performance over a single model (Palmer *et al.* 2004; Kendon *et al.* 2008; Eum *et al.* 2012). Quantifying the likelihood of

each model's simulation is required to avoid potentially erroneous analysis as each model has different skill and simulation capability (New and Hulme 2000; Eum *et al.* 2012; Shrestha *et al.* 2010). Eum *et al.* (2012) also found that improvements were due to the reliability and accuracy of the RCMs rather than the ensemble size, though many models are still required due to the uncertainties of future climate.

All weighting schemes are based on a subjective measure of model skill in reproduction of past climate characteristics (van der Linden and Mitchell 2009). Eum *et al.* (2012) has a thorough review of various weighting methods. A straightforward and widely used method is the Reliability Ensemble Averaging (REA) (Giorgi and Mearns 2002). This approach has two weighting criteria: i) accuracy of historical simulation and ii) level of convergence with other models while simulating the future. It is not clear how to most effectively consider model performance when constructing future climate projections (Weigel *et al.* 2010; Frigon *et al.* 2010), though intuitively a model with larger biases in current climate simulation should be given lower confidence in future projections. That being said, a low bias in base period simulations doesn't necessarily mean a model will accurately reproduce the future climate. Also, there is no consistent relationship between skill of present and future simulations (Jun *et al.* 2008; Knutti *et al.* 2010), though the amplitude of climate variable responses from the past are indicative of the likelihood of future amplitudes (Eum *et al.* 2012). Ghosh and Mujundar (2009) feel convergence is an important weighting criteria to prevent an overly strong influence of outliers. While the robustness of responses across models must be considered (Fowler *et al.* 2007), weighting ensemble members based on the convergence of future simulations may result

in discarding important information regarding possible, yet unlikely, situations. An unweighted ensemble is compared to multiple weighted ensembles (most of which use convergence weighting criteria) in Chapter 6.

2.8. Previous Studies

To get an initial idea of the expected change in streamflow, the Intergovernmental Panel on Climate Change's (IPCC) *Technical Paper VI - Climate Change and Water*, describing the effects of climate change on the hydrological cycle (Bates *et al.* 2008), was consulted. The IPCC used a multi-model ensemble, based on the SRES A1B emissions scenario (IPCC 2000), to simulate the projected change in runoff from the base period 1980-1999 to the future 2080-2099. Based on Bates *et al.* (2008), Labrador can expect between a 10 and 20% increase in mean runoff, with at least 80% of the models used in the ensemble agreeing with the direction of change. Unfortunately due to the coarse resolution of the models used in the study, the results represent a very broad spatial scale and it is impossible to evaluate local effects. As such, it is prudent for any hydroelectric developer to investigate local influences and details related to the time evolution of these changes (Roberts *et al.* 2012).

While many studies have been conducted in nearby Quebec and other regions of Canada (Filion 2000; DesJarlais *et al.* 2004; Dibike and Coulibaly 2005; Minville *et al.* 2009; and others), relatively little research has been conducted focusing on the impacts of climate change on Atlantic Canada's energy sector (Vasseur and Catto 2008). Several of the studies examining basins on the Quebec/Labrador peninsula are discussed below.

Gagnon *et al.* (2009) is one of many papers validating various aspects of the Canadian Regional Climate Model (CRCM). They explore the daily maximum and minimum temperature, precipitation and runoff in two small Quebec basins. The CRCM produced reliable results but with significant bias for each variable during at least one season. Total runoff is strongly overestimated (by 30% or more) in both watersheds for most of the annual cycle and is highly variable in the winter and spring, though there is strong simultaneity (r=0.74). The CRCM typically has a cold, wet bias upstream (in the predominant wind regime) of Labrador, though biases have been shown to exhibit different behaviour in two close watersheds. (Plots of regional variation in precipitation bias can be found in Appendix B.)

Frigon *et al.* (2010) explored the sensitivity of annual runoff on lateral boundary condition update frequency along with internal variability and natural climate variability, in various Quebec/Labrador basins, including the upper Churchill Basin. They do not examine the annual cycle, though all simulations show an intensification of the hydrological cycle during climate change. For the Churchill River the change in runoff is 21±6%, with the 6% being the maximum deviation from the median ensemble value. Frigon *et al.* (2010) also showed that the ensemble spread of basin runoff related to natural variability is typically around ±10%.

Music *et al.* (2009) looked at runoff modelling in Quebec/Labrador basins, ranging from 13 000 to 177 000 km^2 in size. Sharma *et al.* (2011) uses CRCM4.2 in a Quebec watershed (9 700 km^2) along with two common downscaling techniques.

Zadeh *et al.* (2012) showed that the mean annual minimum flow in Labrador is strongly related to catchment area (R^2=0.97) and that all examined basins in Labrador can be grouped into one homogeneous hydrological region.

Other Regions

There have also been many studies based in other regions of the world that explore the effects of climate change on hydrology. Methodologies and analysis techniques are as numerous as the publications themselves and a brief sample of this work is discussed below.

Gagnon *et al.* (2009) examined the ability of RCMs (RegCM - Halenka *et al.* (2006), MM5 - Hernandez *et al.* (2006) and CRCM - Caya *et al.* (1995); Caya and Laprise (1999)) to effectively simulate hydrometeorological variables for regions on the order of 10^4-10^6 km^2.

Xu *et al.* (2011) looked at extreme monthly and mean annual discharge. While they discuss Q05 and Q95 flows, their approach is not fully probabilistic. One of their two catchments of interest was a sub-basin of the Yangtze River, where precipitation is roughly 1070 mm/year, similar to that of the Churchill Basin. This paper examined each source of uncertainty individually and plotted each ensemble member's projections against each other.

Shrestha *et al.* (2010) used NARCCAP data to analyse the effects of climate change on mean monthly and seasonal hydrometeorological variables in the Lake Winnipeg

watershed. They only used CRCM-cgcm3 (Music and Caya 2007), HRM3-hadcm3-(Hudson and Jones 2002) and RCM3-gfdl (Pal *et al.* 2007) and attributed all variability in results to the RCMs, while neglecting the impact of the GCMs. They also did not consider different RCM-GCM combinations or use the full range of dates available resulting in an unrepresented sampling error.

Ludwig *et al.* (2009) used three hydrological models of varying complexity for a 709 km^2 basin in Germany. Various flow indicators such as flood frequency, 7-day and 30-day low flows as well as maximum seasonal flow were evaluated in the attempt to determine the level of hydrological model complexity capable of providing the required advice to water managers.

Maurer (2007) used eleven GCMs with two SRES forcing scenarios (A2 and B1) to drive a hydrological model in the Sierra Nevada.

Thorne (2011) found that the magnitude in the river discharge of the Liard River Basin, a sub-basin of the Mackenzie River, showed an overall increase under climate change but was highly uncertain. Thorne (2011) mentioned that reducing uncertainty is difficult due to inherent differences between GCMs as well as "inadequate ground based measurements." The study used HadCM3, CGCM3.1 and CCSM3.0, among other GCMs and found that winter flow and the secondary autumnal streamflow peak is enhanced by warming. Mean annual runoff change ranged from a 3% decrease to a 15% increase and the author attributed this degree of uncertainty to differences between ensemble members in simulated precipitation and temperature. Thorne (2011) did not use a probabilistic

approach or validate the hydrological model once it was calibrated (calibration period was 1973-1990).

Atmospheric Moisture Convergence and Water Balance

Calculating the atmospheric and terrestrial water balances is a useful and common way to validate a model's ability to simulate the hydrological cycle. In order to close the water balance one must calculate the atmospheric moisture convergence, which reflects how much water is advected in or out of a basin via the atmosphere over a period of time. Seneviratne et al. (2004) has a detailed description of the computation of moisture flux convergence. Hewitson and Crane (2006) found these circulation dynamics may be more robust to non-stationarities than parameterized fields, implying a justification for the water balance / atmospheric moisture convergence approach. The studies discussed below illustrate a range of situations in which the moisture convergence and water balance approach is useful. A detailed description of moisture convergence calculations and equations can be found in Section 4.4.

Strong *et al.* (2002) performed an analysis to close the Mackenzie Basin ($1.7x10^6$ km^2) water budget using calculations based on Rasmusson (1968) as part of the Mackenzie Global Energy and Water Cycle Experiment Study. The study's primary objective was to quantify all aspects of the hydrological cycle of the Mackenzie River basin for purposes of investigating the impacts of climate change on the water budget. The task was complicated by the importance of snow cover, soil and water body moisture storage, the size of the basin, corresponding lags in discharge as well as the course resolution of

observational data. Most of the uncertainties involved in closing the atmospheric and surface water balances were due to sparse or erroneous observational data. Strong *et al.* (2002) used the Canadian Meteorological Centre's (CMC) Run-0 operational model runs (Rutherford 1976). (At the time of analysis, North American Regional Reanalysis (NARR) was not yet available.)

Music and Caya (2007) performed a comprehensive validation of water budget components of a basin with respect to the annual mean and annual cycle, again using the standard equations from Rasmusson (1968). In early versions of the CRCM, closure errors in atmospheric water balance calculations were partly attributed to the semi-Lagrangian numerical scheme which induces a slight non-conservation of the prognostic variables (Music and Caya 2007). In more recent versions this error is accounted for by using a small correction to the specific humidity values at each grid point.

Serreze *et al.* (2003) uses NCEP/NCAR global reanalysis (Kalnay *et al.* 1996; Kistler *et al.* 2001) to calculate precipitation minus evapotranspiration (P-E) from the moisture flux convergence for several large arctic basins. All basins exhibit summer maxima in precipitation and minima in P-E. "Unlike P-E computed from analyzed wind and humidity fields forecasted P and E are purely model outputs and suffer from deficiencies in model physics and parameterizations" (Serreze *et al.* 2003). As such, raw NCEP precipitation is not accurate enough for direct hydrologic applications (Serreze and Hurst 2000; Cullather *et al.* 2000). The residual between long-term discharge and P-E means was found to be 9-21% which was satisfactory to the authors as the discharge and P-E

were from independent data sets. Serreze *et al.* (2003) also provides a good synoptic forcing overview.

Hirschi *et al.* (2006) looked at monthly and annual basin means in their water balance analyses of 37 mid-latitude river basins, including several that were of similar size to the Churchill River Basin. They found that ERA-40 reanalysis substantially underestimates the amplitude of the seasonal cycle.

3. Modeling the Potential Impacts of Climate Change on a Small Watershed in Labrador, Canada

3.1. Abstract

Hydroelectric power producers are strongly dependent on the climate to deliver the fuel necessary to generate electricity. This fuel source is watershed runoff, which is manifested as the balance between components of the climate system, primarily precipitation and evapotranspiration. Climate change threatens to alter global hydrological regimes and impacts need to be assessed to determine production vulnerabilities and opportunities. In this paper, dynamically downscaled regional climate models (RCMs) from the North American Regional Climate Change Assessment Program (NARCCAP) have been combined with statistical bias correction techniques to generate 30-year time series of temperature and precipitation for a base period (1980s) and a future period (2050s). These time series are transformed into streamflow using the WATFLOOD hydrological model that has been calibrated for a sub-basin of the Lower Churchill River. Results are consistent with IPCC results and show increasing mean annual streamflow of approximately 9% between the base and future periods with larger increases in winter runoff and little or no change during late summer and fall. Inter-model comparison and probabilistic methods are used to provide further insight into simulation results.

3.2. Preface

This chapter was published in the Canadian Water Resources Journal in 2012 and is referred to as Roberts et al. (2012) throughout the thesis. Some formatting changes were made from the published version to ensure consistency with the remainder of the thesis.

Many hydro-climatology studies use climate model output to drive offline hydrological models to determine the impacts of climate change on the streamflow of a river. Beginning the thesis with this traditional approach provides a baseline analysis for the methods used in later chapters. Setting up and running a hydrological model on a basin the size of the Churchill River Basin is a large undertaking and due to limited time and resources, this chapter focuses on the Pinus River, a 770 km^2 sub-basin of the Churchill River. The Pinus River is one of three tributaries of the Churchill River that has a continuous record of streamflow measurements, which are needed for calibrating the hydrological model, and contains no control structures, making it an appropriate candidate for study. The other two potential gauged and uncontrolled tributaries were the Minipi River (2330 km^2 watershed area upstream of the streamflow gauge) and the East Metchin River (1750 km^2 watershed area upstream of the streamflow gauge). More details on the selection of the Pinus River can be found in Section 3.4.

While not as representative as a hydrological model covering the entire basin, the impacts of climate change found from studying this sub-basin provide insight into the impacts on the Churchill River. Zadeh *et al.* (2012) showed that the mean annual minimum flow in Labrador is strongly related to catchment area (R^2=0.97) and that all examined basins in

Labrador can be grouped into one homogeneous hydrological region. This implies one can infer similar results for other regions in the Churchill Basin from studying the Pinus River. Supporting this inference further, it was found that tributary streamflow volumes of all magnitudes throughout the year are also highly correlated. Between November 1998 and October 2013, the Pinus River streamflow gauge is correlated with the Minipi River and East Metchin River gauges at 0.86 and 0.97 (Pearson correlation coefficient) respectively for mean monthly flows, and slightly less (0.79 and 0.94, respectively) for daily flows.

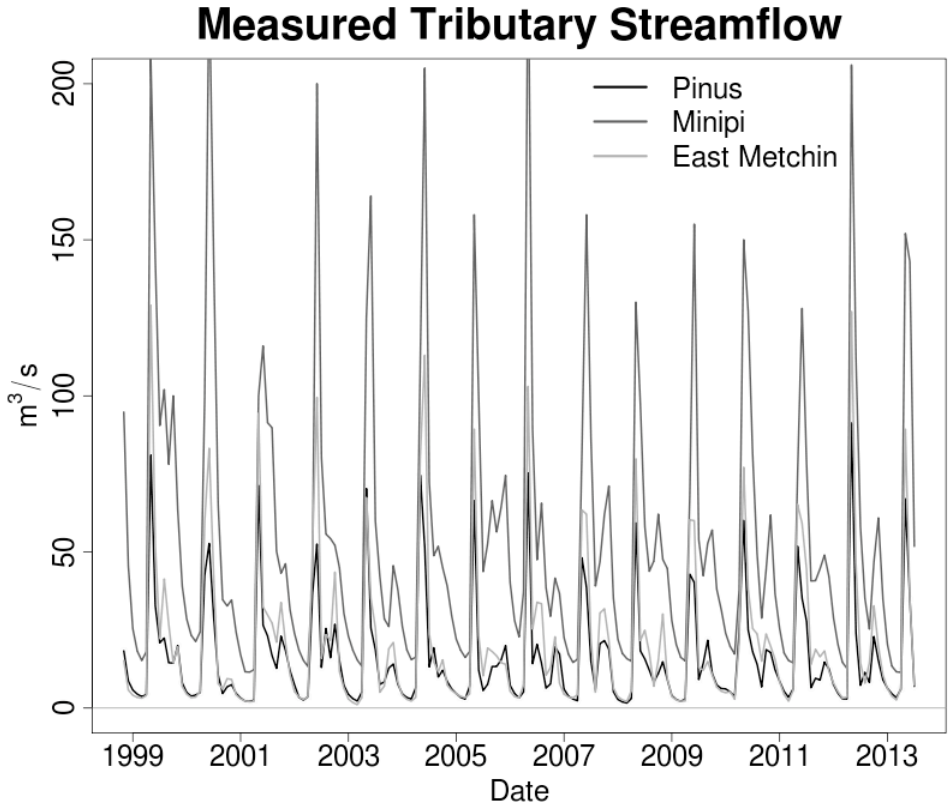

Figure 3.A – Streamflow gauge measurements for uncontrolled tributaries of the Churchill River, from November 1998 to July 2013. (Water Survey of Canada)

The plot of 15 years of mean monthly streamflow measurements for the Pinus, Minipi and East Metchin gauges, in Figure 3.A, shows how the major features of the different hydrographs agree over time. The underlying assumption is that each river will respond to climate change in a similar manner.

Pinus River Peak Flow Magnitude and Timing

Discussion about the magnitude and timing of the spring melt was not included in the paper (p. 44), though are still of interest to water resource managers.

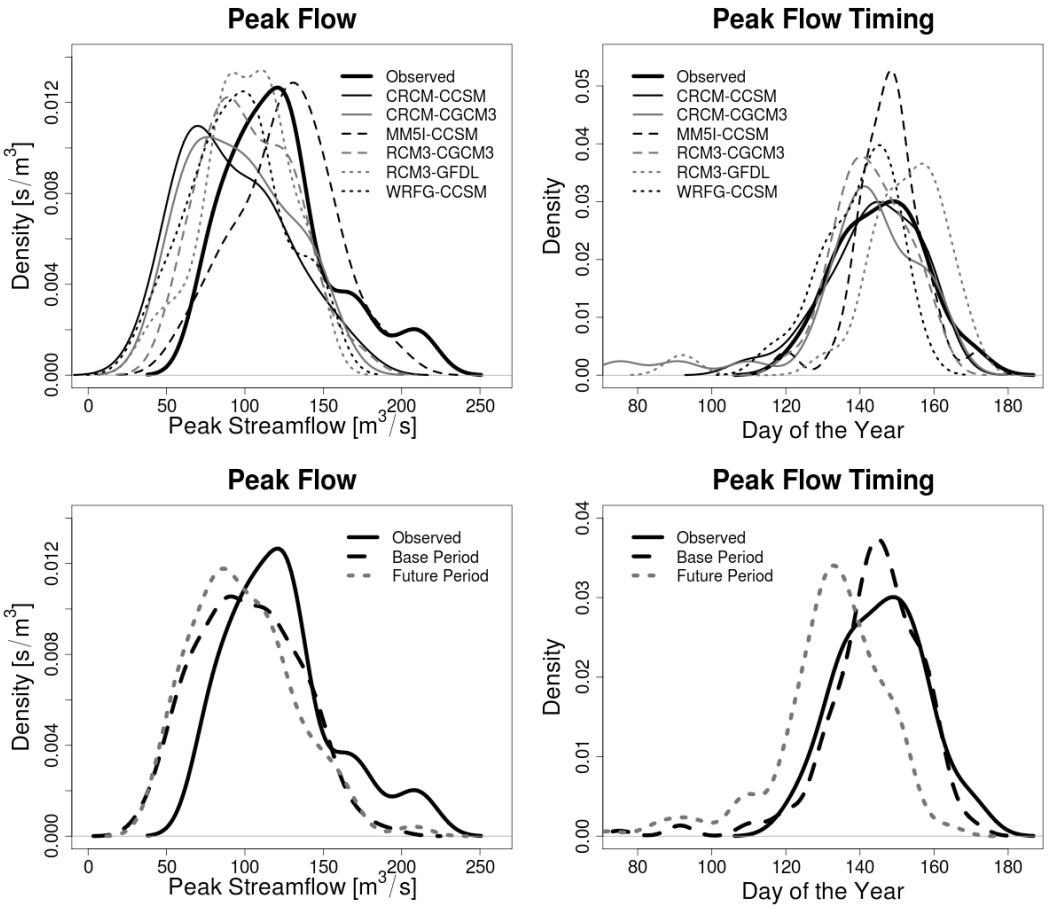

Figure 3.B - Probability distribution functions for peak flow magnitude (left) and timing (right) for ensemble members during the base period (top) and the ensemble means for base and future periods (bottom).

Figure 3.B shows the simulated magnitude and timing of the peak annual flow for each base period ensemble member as they compare to observations. It also includes the mean projected ensemble changes between base and future periods. While there was some variability between ensemble members, the ensemble mean simulation of peak flow timing was a good match to observed values. The peak flow magnitude, however, tended to be underestimated, except for the MM5I-CCSM ensemble member, corresponding to results presented in Figure 3.11.

The projected change in mean peak flow magnitude between the base and future periods is not significantly different (p-value = 0.26, via the Wilcoxon Rank Sum test) while timing of the peak flow occurs significantly earlier in the future (p-value = 1.7×10^{-8}). While more cold-season precipitation may lead one to believe that there would be additional snow-water-equivalent to increase the magnitude of the spring melt, the higher temperatures (discussed in Sections 3.6 and 3.8) lead to additional winter runoff events, mitigating the impact of higher precipitation. The earlier spring melt corresponds with the higher average temperatures.

Bias Correction

The bias correction was undertaken using a combination of FORTRAN code and GrADS scripts. These developed tools are adaptable to any region within the NARCCAP domain and were used by other members of the research group for hydrological studies in Newfoundland's Humber River Basin (Jasim 2014). The primary GrADS scripts for performing the actual bias correction on climate model precipitation and temperature output can be found in Appendix A.

The geographical influence on precipitation bias was also explored. The annual cycles of normalized precipitation biases were calculated for thirteen geographically diverse locations across Canada (e.g. Vancouver, Yellowknife, St. John's, etc) for each ensemble member available at the time of analysis. While the plots may be interesting and may provide motivation for future work, they are outside the scope of this thesis and can be found in Appendix B.

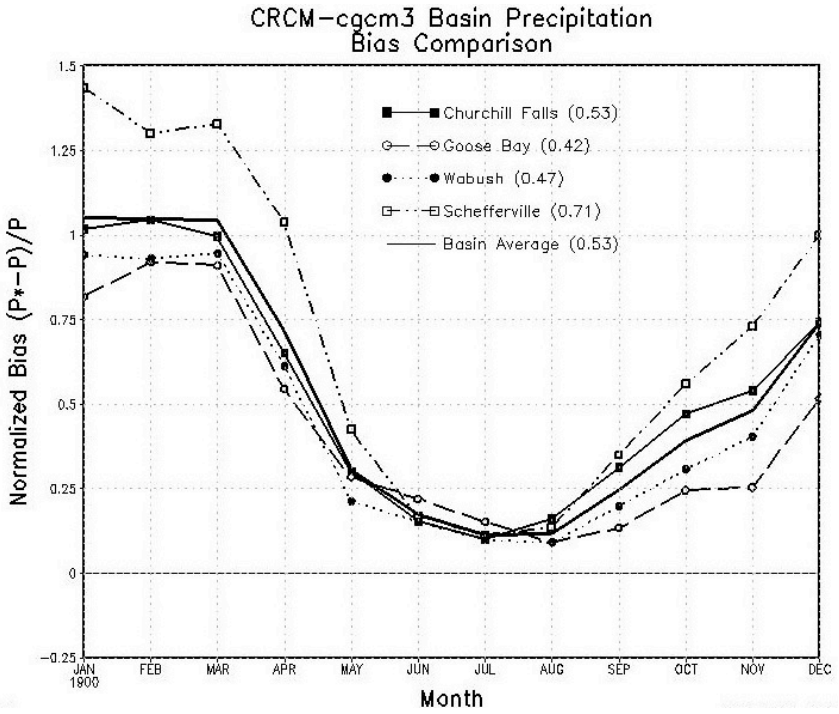

Figure 3.C – Geographical influence on normalized precipitation bias in the Churchill River Basin for CRCM-cgcm3. (Annual averages shown in parentheses.)

Similarly there were four locations in and around the Churchill River Basin where Adjusted Historical Canadian Climate Data precipitation data (Mekis and Hogg 1999), used for observed data, was available (Happy Valley-Goose Bay, Churchill Falls, Labrador City, and Schefferville). Plots of normalized precipitation biases were also

created for these four sites, an example of which can be seen in Figure 3.C. This shows that while the bias is very similar across the basin there are slight differences, which may be attributable to the climate models or the precipitation gauges. Plots for the other ensemble members are available in Appendix B.

3.3. Introduction

As the impacts of climate change become more apparent in day-to-day life, the need to investigate its potential future impacts increases. This is especially true for hydroelectric developers whose strong dependence on climatological factors, such as the balance between precipitation and evaporation, make them especially vulnerable to climate regime changes. It has been shown that small changes in the distribution of precipitation can significantly alter mean annual streamflow (Muzik, 2001) and even modest perturbations in natural inflow have amplified impacts on reservoir storage levels (Christensen *et al.*, 2004; Minville *et al.*, 2008).

In this paper, base period (1971-2000) and future period (2041-2070) hydrological regimes of the Pinus River sub-basin, part of the Lower Churchill watershed, are simulated. The main objective of this work is to develop an initial assessment of how climate change will affect the Lower Churchill River system, proposed site of the Lower Churchill Hydroelectric Project, by modeling future hydrological regime changes in the Pinus River. While many studies have been conducted in nearby Quebec and other regions of Canada (Filion, 2000; DesJarlais *et al.*, 2004; Dibike and Coulibaly, 2005; Minville *et al.*, 2009; and others), relatively little research has been conducted focusing

on the impacts of climate change on Atlantic Canada's energy sector (Vassseur and Catto, 2008).

In addition to this Atlantic Canadian focus, an ensemble approach incorporating multiple regional climate models nested in various general circulation models is employed to provide a useful measure of uncertainty (Murphy *et al.*, 2004; Kotlarski *et al.*, 2005). It is well known that no single climate model is best at simulating all climate variables and their various statistics, as a single projection represents only one of many possible realizations of the future climate and is not robust (Christensen and Christensen, 2007; Maraun *et al.*, 2010).

Climate model output and analysis results are presented as mean annual timeseries and hydrographs as well as probability density functions, similar to Minville *et al.* (2008), where each ensemble member was given equal weight as was each year in all respective projections.

3.4. Background

Lower Churchill Hydroelectric Project

The Churchill River is located in Labrador, Canada. While the existing Churchill Falls generating station has a capacity of nearly 5428 MW, the river's full hydroelectric potential is yet to be developed. There are two potential development sites downstream with a combined capacity of 3074 MW. The Lower Churchill Project encompasses Gull

Island (2250 MW) and Muskrat Falls (824 MW), respectively located 232 km and 291 km downstream of the Churchill Falls station. The Upper Churchill basin has an area of approximately 69 200 km^2, while the Lower Churchill basin adds an additional 23 300 km^2. (Nalcor Energy, 2009)

Pinus River Basin

As a preliminary step to modeling the Lower Churchill watershed, the Pinus River sub-basin, shaded black in Figure 3.1, was selected for study. This basin was chosen partly due to the existence of a streamflow gauge that has been in operation since 1998, the data from which can be used for calibrating the hydrological model. Four other hydrometric stations in the Churchill River Basin had records of sufficient length to be considered for this work. Two of these were in regulated watersheds making model calibration difficult without naturalized flows. The third station was not chosen as it is located at the mouth of a large lake that provides significant attenuation to flows and while these might be negligible over long time frames, details on the elevation-volume relationship and outflow characteristics of the lake are not known. The fourth station was not chosen because it lies in a basin with very flat headlands and the drainage divide is difficult to delineate based on the 1:50 000 scale used. The Pinus River does not have any of the above complications. The watershed area upstream of the streamflow gauge is approximately 770 km^2. The Pinus connects to the Churchill River between Gull Island and Muskrat Falls.

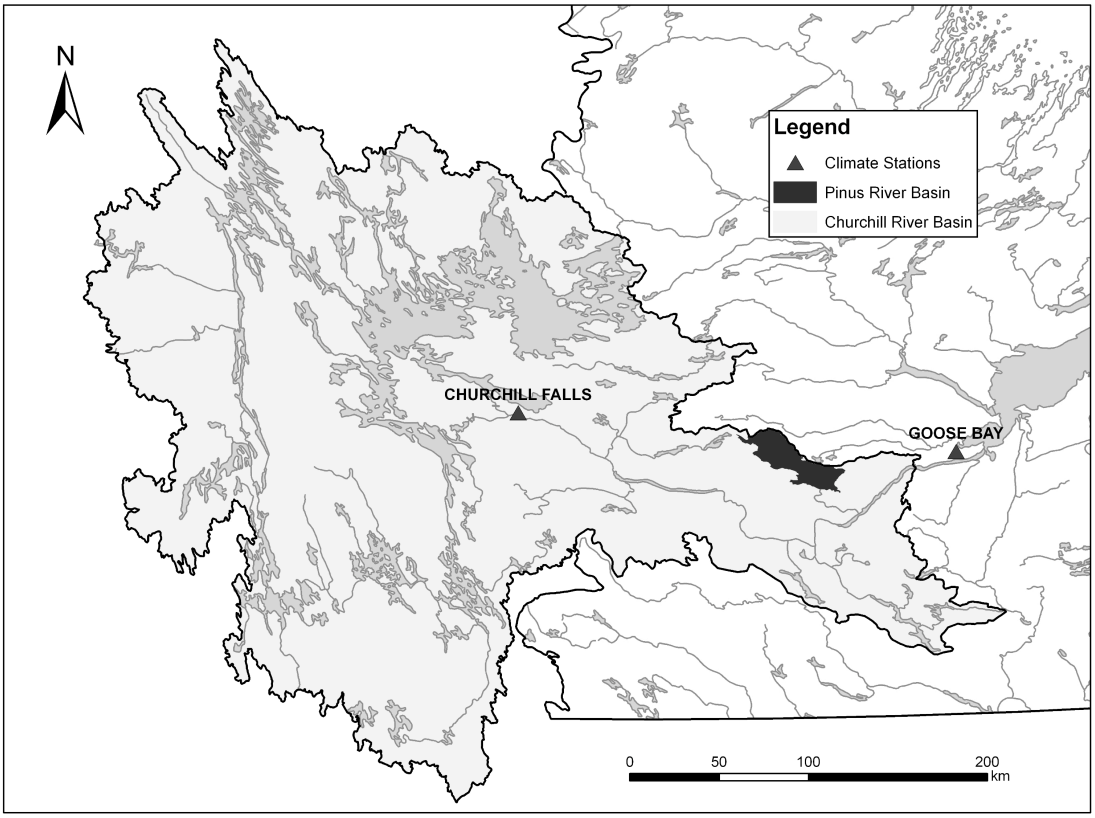

Figure 3.1 - Churchill River Basin and Pinus River Sub-Basin.

Previous Hydrological Forecasting

Short and medium-term forecasts along with long-term projections of reservoir inflow are important for every hydroelectric development. Short-term forecasts consist of hourly predictions required for decisions on operational efficiency, while medium-term forecasts can range from days to weeks and even months ahead (Li *et al.*, 2009). Longer-term projections are important for larger reservoirs with multi-year storage potential. Projections on a multi-decadal scale, including those discussed in this paper, are

fundamental for the planning of future hydroelectric developments such as the Lower Churchill Project.

To get an initial idea of the expected change in streamflow the Intergovernmental Panel on Climate Change's (IPCC) *Technical Paper VI - Climate Change and Water*, which describes the effects of climate change on the hydrological cycle (Bates *et al.*, 2008), was consulted. The IPCC used a multi-model ensemble, based on the SRES A1B emissions scenario (IPCC, 2000), to simulate the projected change in runoff from the base period 1980-1999 to the future 2080-2099.

Based on Bates *et al.* (2008) Labrador can expect between a 10 and 20% increase in mean, with at least 80% of the models used in the ensemble agreeing with the direction of change. Unfortunately due to the coarse resolution of the models used in the study, the results represent a very broad scale and it is impossible to determine local effects. As such, it is prudent for any hydroelectric developer to investigate local influences and details related to the time evolution of these changes.

Data Sources

NARCCAP

The North American Regional Climate Change Assessment Program (NARCCAP) is an international collaboration designed to investigate the uncertainties in future climate projections on the regional level (Mearns *et al.*, 2007; Mearns *et al.*, 2009). NARCCAP data includes a selection of regional climate models (RCMs) of 50 km horizontal

resolution nested within multiple atmosphere-ocean general circulation models (GCMs). Each GCM is driven by the SRES A2 scenario, which falls on the higher CO2 emissions end of the IPCC emissions scenario spectrum (IPCC, 2000).

NARCCAP's ensemble approach allows the representation of uncertainties introduced by GCM choice, which has been found to have the greatest impact on uncertainty in most regions and seasons in several multi-model ensembles (Deque et al., 2007, Minville *et al.*, 2008), RCM choice and their respective structural formulations (Maraun *et al.*, 2010). Unfortunately, other important sources of uncertainty including those related to different potential emissions scenarios, modification of various parameter settings, internal variability induced by choice of initial conditions, and choice of spatial resolution (Kotlarski *et al.*, 2005) are not represented.

The timeframes covered are from 1968 to 2000 for the base period and from 2038 to 2070 for the future period, including three years of model spin up data at the beginning of each run, which is not included in this analysis.

Due to budget constraints not all of NARCCAP's possible RCM-GCM combinations are being run. Each GCM will be coupled with half the RCMs and each RCM will be coupled with half the GCMs, resulting in a representative sample of twelve simulations (both future and current). The results of all 12 simulations were not ready for distribution at the time this work was conducted and as such, this study samples six of the seven available data sets, shown in Tables 3.1 and 3.2. (The only available data set that was not

incorporated in this study was HRM3-hadcm3 due to inconsistencies arising from hadcm3's 360-day year.) The six ensemble members in this study use a variety of grid sizes and map projections, vertical coordinate systems and number of vertical levels, dynamics and physics schemes, land surface schemes and vegetation classes, and timesteps among other varying parameters and characteristics (refer to http://www.narccap.ucar.edu).

Table 3.1 - Details of NARCCAP's RCMs and GCMs.

Regional Climate Models			
NARCCAP Name	**Aliases**	**Modelling Group**	**Full Name**
CRCM	MRCC	Ouranos / UQAM	Canadian Regional Climate Model / le Modèle Régional Canadien du Climat
MM5I	MM5, MM5P	Iowa State University	MM5 – PSU/NCAR mesoscale model
RCM3	RegCM3	UC Santa Cruz	Regional Climate Model version 3
WRFG	WRFG	Pacific Northwest National Laboratory	Weather Research & Forecasting model
Driving General Circulation Models			
Model	**Sponsor**	**Ensemble Member Used**	**Full Name**
CCSM3 (ccsm)	NCAR	b30.030e (ctl), b30.042e (fut)	Community Climate System Model
CGCM3.1 (cgcm3)	CCCMA	CGCM #4	Third Generation Coupled Global Climate Model
GFDL CM2.1 (gfdl)	NOAA-GFDL	20C3M, run2; sresa2, run1	Geophysical Fluid Dynamics Laboratory GCM

Table 3.2 - NARCCAP ensemble members used.

		GCM		
		cgcm3	ccsm	gfdl
RCM	CRCM	X	X	
	MM5I		X	
	RCM3	X		X
	WRFG		X	

The output from these models was bias corrected and used as input for the WATFLOOD hydrological model, from which daily streamflow values were obtained for the base and future periods mentioned above.

Observed Data

To independently validate the RCM-GCM results the base period output was compared to Adjusted Historical Canadian Climate Data (AHCCD) precipitation data (Mekis and Hogg, 1999) and Environment Canada's surface air temperature station data for Goose Bay, Labrador (referred herein as observed data). AHCCD precipitation data was used because of the persistent problem of wind-induced undercatch by precipitation gauges, while the AHCCD temperature data was not used as it was found to be very similar to actual gauge measurements. While some gridded data sets are available for the region of interest (such as CANGRID, which uses AHCCD data but only covers up to 1990; or Agri-Geomatics which covers up to 2003 but does not use corrected data and does not have the required mean daily temperature data), Goose Bay's AHCCD precipitation and measured temperature data were selected for use as it was believed they provided the most accurate and complete weather record for the study region.

Biases were found between base period simulations and the observed data for both precipitation and temperature, with the largest biases occurring for precipitation and in winter. The bias correction process and results are discussed later in detail.

WATFLOOD Hydrological Model

WATFLOOD is a grouped response unit based numerical hydrological model (Kouwen *et al.*, 1993) that is suitable for short-term flood forecasting (Cranmer *et al.*, 2001) and has been shown to effectively translate climate patterns from corrected climate model data into hydrological responses (Sung *et al.*, 2006; Dibike and Coulibaly, 2007). WATFLOOD uses conceptual equations to represent vertical water budget processes and a physically based model for horizontal routing processes (Bingeman *et al.*, 2006).

WATFLOOD can be considered a hydrological model of intermediate complexity. It represents water balances well but does not represent energy-related processes, such as evaporation, with the same degree of sophistication. An advantage of this simplistic representation of energy processes is that only precipitation and temperature data are required as inputs. Thus the evaporation component, which employs Hargreaves equation, ignores the effects of humidity, wind and radiation. Despite these simplifications, a useful result is achieved for the purpose of comparing average flows in different climate periods.

WATFLOOD Calibration

As there are no climate observation stations in the Pinus River basin, precipitation and temperature data from nearby Goose Bay, approximately 90 km east of the basin centroid, was used for WATFLOOD calibration. There was a slight lapse adjustment made to the observed Goose Bay temperature data to compensate for the difference in

elevation between the two locations – the Goose Bay climate station is at an elevation of approximately 50 m whereas the Pinus River basin has an elevation range of between 360 and 480 m, resulting in colder temperatures in the Pinus River basin.

More than ten years, 1998 to 2008, of measured daily streamflow data on the Pinus River were available from the Water Survey of Canada for WATFLOOD model calibration. The intent of the calibration, which was based on the mean annual cycle streamflow values of the observation record (not shown), was not to fit the measured daily flows exactly but to reproduce the "climate signal" (i.e. monthly average flows, timing of spring runoff, baseflow recession periods, etc.). As with any model, the chosen hydrological model cannot give a full picture of reality; however, it is important that the model represents well the main features of the system dynamics relevant to the particular study (Dibike and Coulibaly, 2007). As such, the model was calibrated using monthly summaries of the measured data alone and validated against the ten years of daily hydrometric data, shown in Figure 3.2. Good agreement was found with the daily results. The Nash-Sutcliffe model efficiency coefficient (Nash and Sutcliffe, 1970) for the validation in Figure 3.2 was 0.80 while the r-squared correlation coefficient was 0.81. These were deemed acceptable values for the purpose of climate change impacts assessment on average basin flows.

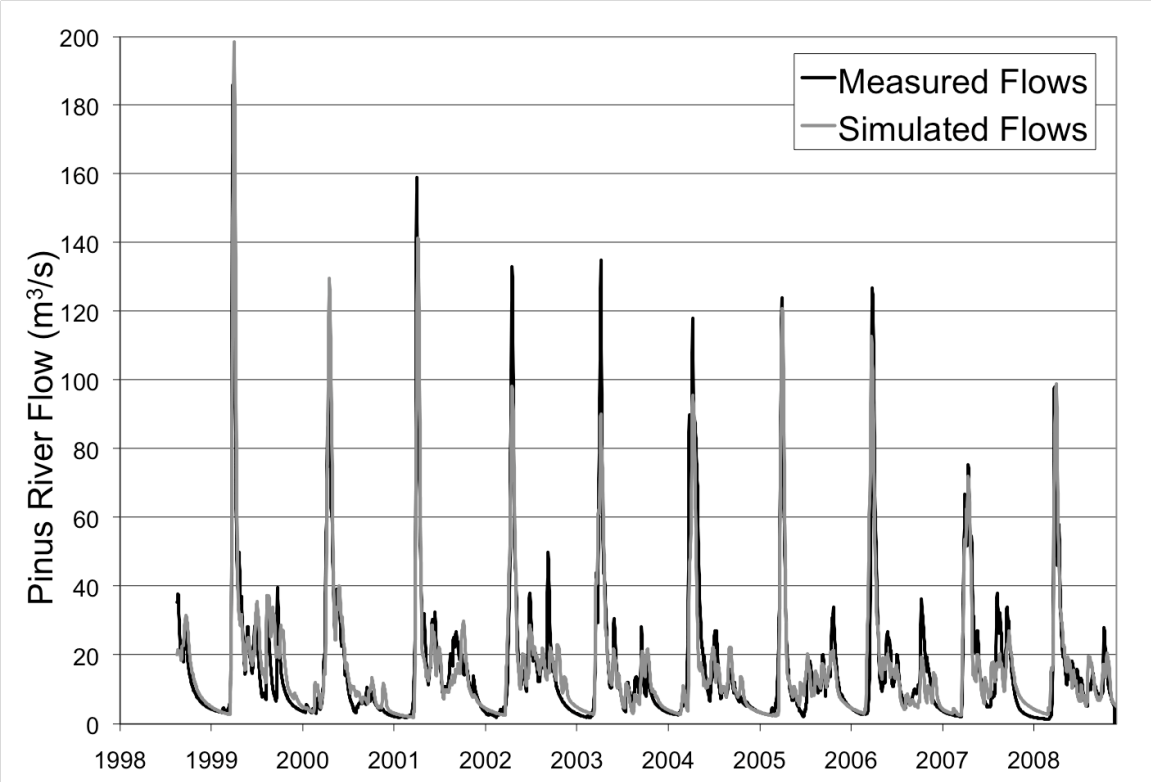

Figure 3.2 - Observed and WATFLOOD simulation daily average flows

Due to the short period of record of the hydrometric gauge and the approximate nature of the calibration, no additional data was used for a separate model validation. If this model continues to be used for impacts research, additional years of streamflow data should be withheld from the monthly calibration process to perform a separate, more independent model validation based on unseen daily measurement. For now, the validation is not fully independent since the model has already 'seen' the monthly summaries of the data through calibration.

3.5. RCM-GCM Bias Corrections

Each of the six ensemble members was found to have varying biases for the location of interest in both temperature and precipitation. In particular, it was found that there was a relatively consistent cold bias throughout the year (likely due in part to the elevation difference between the RCM grid spaces used and the observation station in Goose Bay), while winter precipitation was greatly underestimated.

Several studies have shown that in order to achieve realistic results some form of preprocessing is required to remove biases in climate output fields before they can be used to force a hydrological model (Feddersen and Andersen, 2005; Hansen *et al.*, 2006; Christensen *et al.*, 2008; Piani *et al.*, 2010). As such, model outputs were corrected to statistically match observations from the same period, the benchmark standard of bias correction procedure acceptability (Wood *et al.*, 2004). These corrections, as described in detail below, were then applied to the corresponding future periods.

Precipitation Bias Correction

While linear scaling corrections are commonly used for bias correction, Leander and Buishand (2007) found that a simple nonlinear transformation, first used by Shabalova *et al.* (2003), correcting both mean and coefficient of variation (CV) led to a better reproduction of observed precipitation. They recommended a straightforward linear approach for correcting bias in the mean and variance of temperature. While Leander and Buishand suggested that basin averages be used in the bias corrections there are no

observation stations within the Pinus basin. As a result the authors compared data from the nearby Goose Bay station to the RCM grid points closest to Goose Bay.

Corrected precipitation values were determined using Equation 3.1.

$$P^* = aP^b \qquad (3.1)$$

Where P* is the corrected precipitation, P is the uncorrected model precipitation, while *a* and *b* are the correction parameters corresponding to mean and CV respectively. To reduce sampling variability these factors were determined for 5-day periods (73 periods throughout the year) using data from the 30 preceding and 30 proceeding days (for a total of 65 days of data per year for each 5-day period) and averaged over the entire base period (1971-2000). Parameter *b* was first determined iteratively (using the Newton-Raphson method) by ensuring that the CV of the corrected precipitation matched that of the observed, then parameter *a*, which depends on the value of b, was determined by matching the means of the corrected and observed precipitation. Then it was a simple matter of using Equation 3.1 for each of the 73 5-day periods.

Figure 3.3 shows the impact of the bias correction on the CRCM-cgcm3 ensemble member for the base period simulation along with a comparison of each model's normalized precipitation bias. By inspection it is apparent that the corrected precipitation is a much better fit to observations than the uncorrected data. It is also evident that precipitation biases were consistently greatest in the cold season.

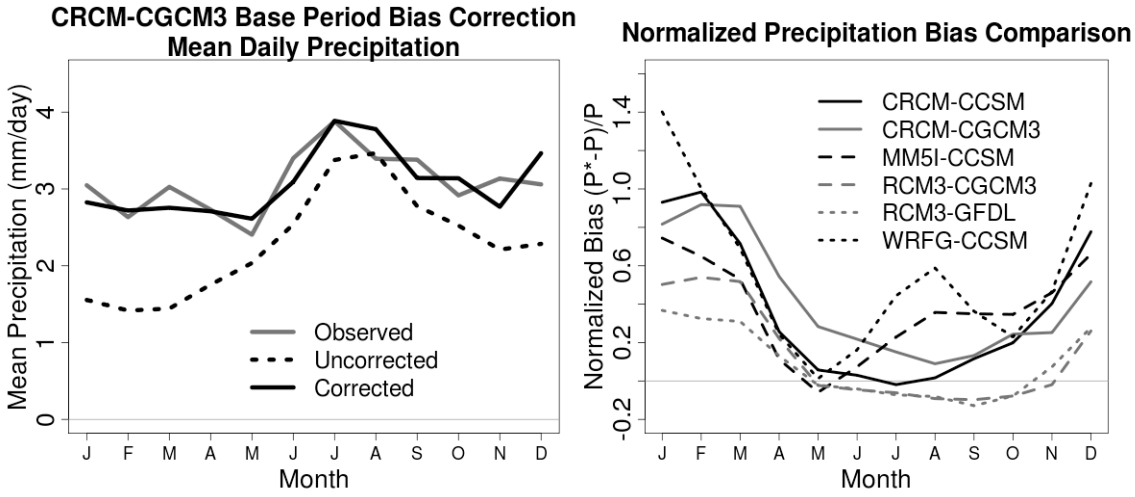

Figure 3.3 - Examples of base period simulated precipitation bias corrections for the CRCM-cgcm3 ensemble member (left) and a comparison of normalized precipitation bias (right).

Temperature Bias Correction

The temperature bias corrections were completed using Equation 3.2, simplified from Leander and Buishand (2007), as previously mentioned there was no need for spatial averaging.

$$T^* = \overline{T}_{obs} + (T_{RCM} - \overline{T}_{RCM}) \frac{\sigma(T_{obs})}{\sigma(T_{RCM})} \qquad (3.2)$$

Where T* is the bias-corrected temperature, T_{RCM} is the uncorrected model temperature, T_{obs} is the observed data, $\overline{T}$ is the climatological average temperature for each 5-day period and σ is the standard deviation. Reducing sampling variability was achieved in a manner identical to the precipitation bias correction.

A typical example of the bias correction for CRCM-cgcm3 is found in Figure 3.4, along with a comparison of the ensemble's normalized temperature biases. Similar to precipitation, it is apparent that the corrected temperature data is a much better fit to observations than the uncorrected data. The normalized temperature biases show that the variability of biases between ensemble members was greatest in the cold season.

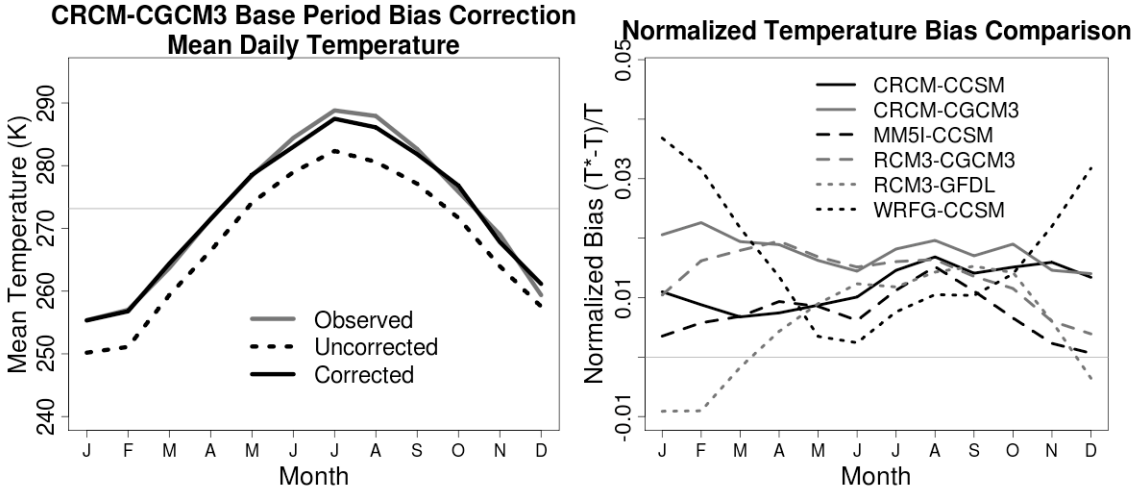

Figure 3.4 - Examples of base period simulated temperature bias corrections for the CRCM-cgcm3 ensemble member (left) and a comparison of normalized temperature bias (right).

Bias Correction Assumptions

When applying a bias correction derived from the comparison between base period model output and observations to some future period, it is assumed that the correction will still be valid for a future, potentially different climate. Unfortunately, this necessary assumption of stationary seasonality cannot be validated or invalidated until the future timeframe is upon us (Trenberth *et al.*, 2003).

The bias correction method discussed above uses a two-month correction window as it moves over the data. While there may be some time bias due to the potential future shifting of seasons, there is a significant overlap that helps to mitigate any negative influence potential non-stationarity may have.

Bias correction is imperfect, however it remains a useful and necessary tool for helping to determine the climatic changes in hydrological regimes between current and future timeframes.

Alternatives

Other methods for addressing model bias are statistical downscaling and numerical weather generators. Rahman *et al.* (2012) apply such concepts when assessing the impacts of climate change on a southern Ontario watershed. Others, such as Sushama *et al.* (2006) do not apply any bias correction methods and simply analyze the differences between the base period and future period model outputs, while Minville *et al.* (2008) use a combination of the change factor method and a stochastic weather generator. See Themeβl *et al.* (2011) for a thorough comparison of various precipitation bias correction and statistical downscaling techniques. Leander and Buishand's bias correction was chosen because of its simplicity and effectiveness in reproducing the observed climate. One should keep in mind the primary caveat of bias correction, which is that the process is not physically based implying the model output cannot be assumed to be physically consistent across all of its variables and caution should be used while interpreting results.

3.6. Bias Corrected Climate Simulation Results

In this section the base and future period results of the bias corrected precipitation and temperature bias are presented alongside observations.

Simulated Precipitation

Corrected mean results of the precipitation simulation (Figure 3.5 and Table 3.3) show that monthly precipitation is consistently higher in the future period simulations than in the base period, except for a small decrease in October. The largest increases occur in winter, with an increase of almost 25% in February, while the smallest occur in spring, with increases typically around 6%. The mean simulated base period precipitation and observed precipitation are both 3.1 mm/day, while the mean daily simulated future precipitation is 3.4 mm/day, over a 9% increase.

Note that individual ensemble members show a high variability of precipitation change, with a difference of over 1 mm/day in some months. This illustrates the importance of using an ensemble approach – some uncertainty was exposed in the simulations, represented by the different climate realizations manifested as a range of possible changes in monthly precipitation rates. It also indicates that the mechanisms involved in simulating rainfall are not robust or consistent across the various RCMs and GCMs. When looking at the variability of mean change projected by any particular GCM or RCM (e.g. ccsm paired with three different RCMs or CRCM paired with two different GCMs), the same overall pattern of inconsistency emerges.

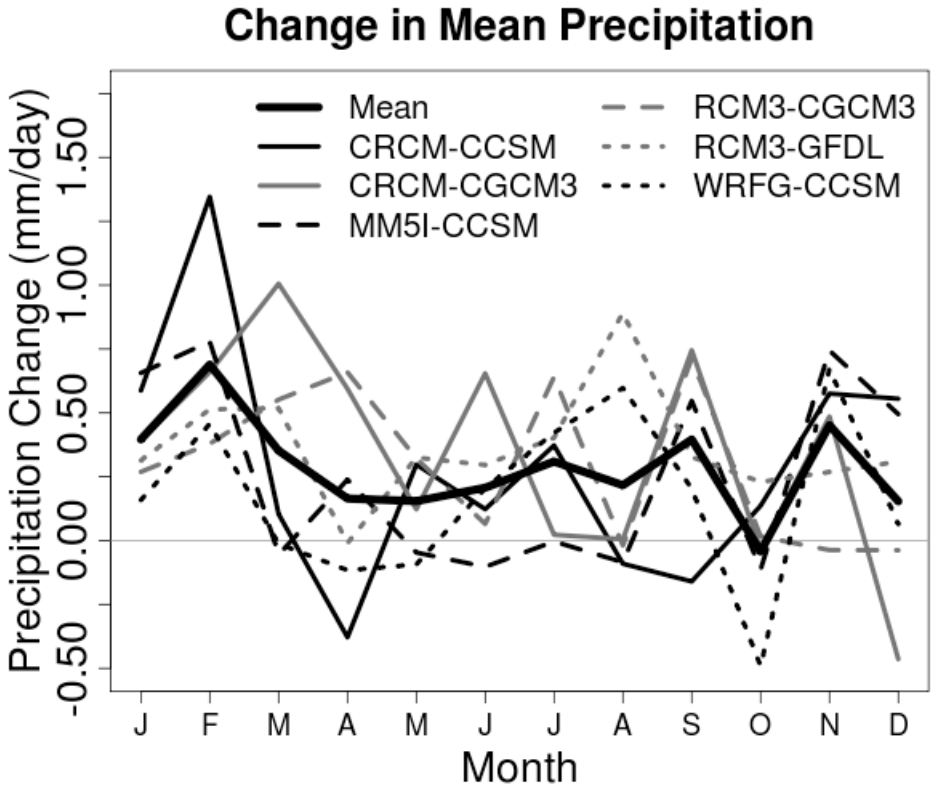

Figure 3.5 - Changes in daily precipitation from simulated base period to future period. Ensemble mean represented by thick black line.

Probability density functions (PDFs) of corrected and uncorrected base and future period simulated precipitation from ensemble mean daily precipitation values are plotted with the observed precipitation in Figure 3.6. It is assumed that each ensemble member projection has an equal probability of occurrence and that each day within respective projections has equal likelihood of being representative. All PDFs were created using a smoothed empirical distribution with Gaussian kernal density estimation. The probability that the precipitation rate, in Figure 3.6, will be below a given value is represented by the area under the curve to the left of said value. As such the total area under a PDF is equal to one, while there is equal likelihood (50%) that the precipitation rate could be above or

below the median value. The units of density on the y-axis are the inverse of the x-axis units (e.g. for precipitation rate, density units are $(mm/day)^{-1}$).

Table 3.3 – Ensemble mean monthly and annual changes in precipitation rates.

Month	Mean Precipitation Rate (mm/day)			Increase in Precipitation (mm/day)	Increase in Precipitation (%)
	Observations	Current Period Simulation	Future Period Simulation		
January	3.0	2.8	3.2	0.4	14.3
February	2.6	2.8	3.5	0.7	24.9
March	3.0	2.8	3.2	0.4	12.5
April	2.7	2.8	2.9	0.2	6.0
May	2.4	2.6	2.8	0.2	5.9
June	3.4	3.2	3.4	0.2	6.4
July	3.9	3.7	4.0	0.3	8.3
August	3.4	3.6	3.8	0.2	6.1
September	3.4	3.3	3.6	0.4	12.2
October	2.9	3.2	3.2	0.0	-1.3
November	3.1	3.0	3.4	0.4	15.3
December	3.1	3.2	3.3	0.2	4.8
Annual	**3.1**	**3.1**	**3.4**	**0.3**	**9.4**

Figure 3.6 shows there can be appreciable variation in total precipitation from day-to-day, month-to-month and year-to-year within any simulated period. This implies that even though the mean precipitation is expected to increase, any given future period year could have less accumulated precipitation than a base period year. This variability is important to keep in mind when using simulation results in impact studies.

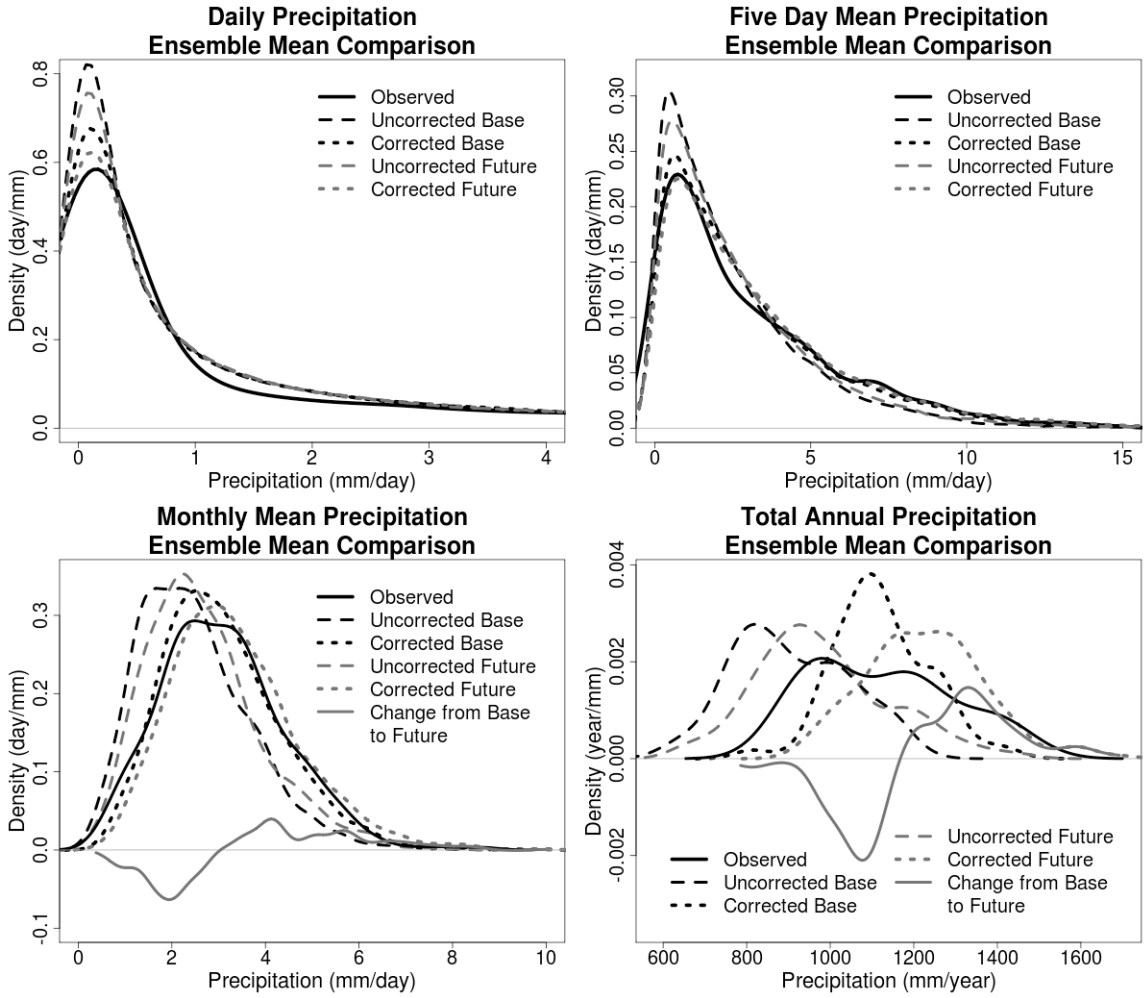

Figure 3.6 - Probability density functions for ensemble daily mean (top left), five-day mean (top right), monthly mean (bottom left) and annual precipitation rates.

The four plots in Figure 3.6 are the distributions for mean daily, five-daily, monthly and annual precipitation. Haerter *et al.* (2011) showed that bias correction improvements are limited to the specific timescale at which the corrections take place and in our work the bias correction focuses on a five-day timescale. Qualitatively the five-day PDF for the corrected base period matches the observations fairly well, as do the daily and monthly timescales. However, while the mean of the corrected base period annual timescale is aligned with observations the year-to-year variance is lower (with a range of roughly 900

to 1450 mm/year compared to the observed range of roughly 800 to 1600 mm/year), indicating that the models did not sufficiently capture interannual variability and the bias correction was unable account for it. Another contributing factor to the discrepancy is that for the annual timescale PDF there were significantly less data points available - only 30 for observations and 172 for the entire ensemble (not all ensemble members had full 30 year runs available, which is why the total is not 180) - for the creation of PDFs, while the daily, five-daily and monthly had 62 780, 12 556 and 2064 points respectively. In other words, the simulated and observed PDFs might have matched better if more data points were available, especially for the observed data set. A similar pattern is found in temperature and streamflow PDFs presented later.

The difference between the base and future period precipitation is shown in the monthly and annual plots. By inspection it is apparent that there will be fewer months and years with less precipitation and more with greater precipitation, contributing to the overall increase in precipitation discussed earlier.

Simulated Temperature

Similar to precipitation, mean monthly temperature is found to increase from base period to future period simulations. As shown in Figure 3.7 and corresponding Table 3.4, the greatest temperature increases occur between November and February, averaging roughly 3.5 K, while the rest of the year experiences a steady mean temperature increase of roughly 2.0 K. Keep in mind that, as with precipitation, projected monthly changes in temperature vary between individual ensemble members (Figure 3.7), with the lowest

variation occurring in late winter. All ensemble members do agree that there will be a temperature increase in each month. The mean annual temperature for the base period simulation is 272.6 K (compared to the observed 272.8K) while the mean annual temperature for the future period is 2.6 K warmer at 275.2 K.

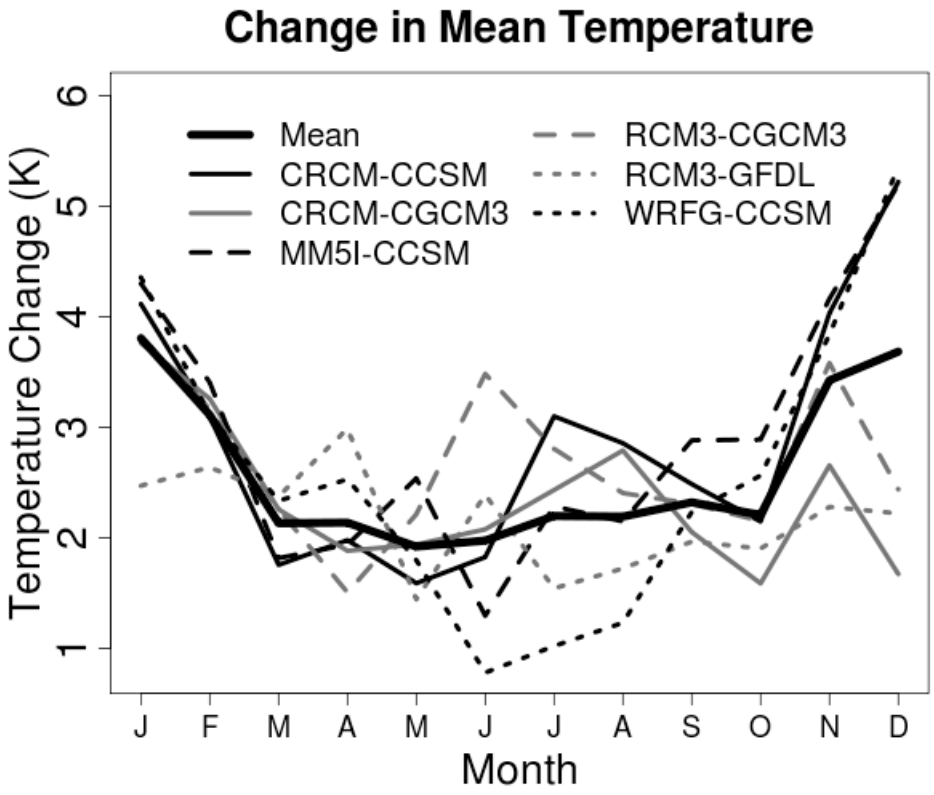

Figure 3.7 - Mean change in temperature from base to future period simulations.

February and March appear to have the strongest consensus across all ensemble members on the change in mean temperature, indicating that the temperature change projections for these two months are relatively robust. There is consistency across ccsm driven ensemble members, except for June, July and August, indicating that throughout most of the annual cycle there is relatively little uncertainty introduced by the RCM. Cgcm3 is less

consistent suggesting a heavier RCM influence on mean temperature change. Both CRCM simulations are in good agreement, except for November and December, implying that in this particular case the GCMs contribute less to uncertainty. RCM3 sees a variety of good and poor agreement throughout the year, which may be an indication of similar amounts of uncertainty introduced by both RCM3 and the driving GCMs.

Table 3.4 – Ensemble mean monthly and annual changes in temperature.

Month	Mean Temperature (K)			Increase in Temperature (K)
	Observations	Current Period Simulation	Future Period Simulation	
January	255.4	255.5	259.3	3.8
February	257.0	257.3	260.4	3.1
March	263.7	264.0	266.1	2.1
April	271.5	271.3	273.4	2.1
May	278.4	278.0	280.0	1.9
June	284.4	283.6	285.6	2.0
July	288.8	288.1	290.3	2.2
August	287.9	287.1	289.3	2.2
September	282.6	282.1	284.4	2.3
October	275.8	276.4	278.6	2.2
November	269.0	268.2	271.6	3.4
December	259.4	260.2	263.9	3.7
Annual	**272.8**	**272.7**	**275.2**	**2.6**

The mean daily, five-daily, monthly and annual temperature PDFs in Figure 3.8 provide further insight into the projected temperature changes. In particular there is relatively little overlap between the corrected base and future simulations on an annual timescale,

indicating that the majority of years in the future are projected to be warmer than most of the warmest base period years. The "Change from Base to Future" line in the annual plot highlights this. Similarly for the monthly timescale, though there is some variability as to the direction of change for non-extreme months, it is apparent that there will be fewer months with very cold temperatures and more months with higher temperatures.

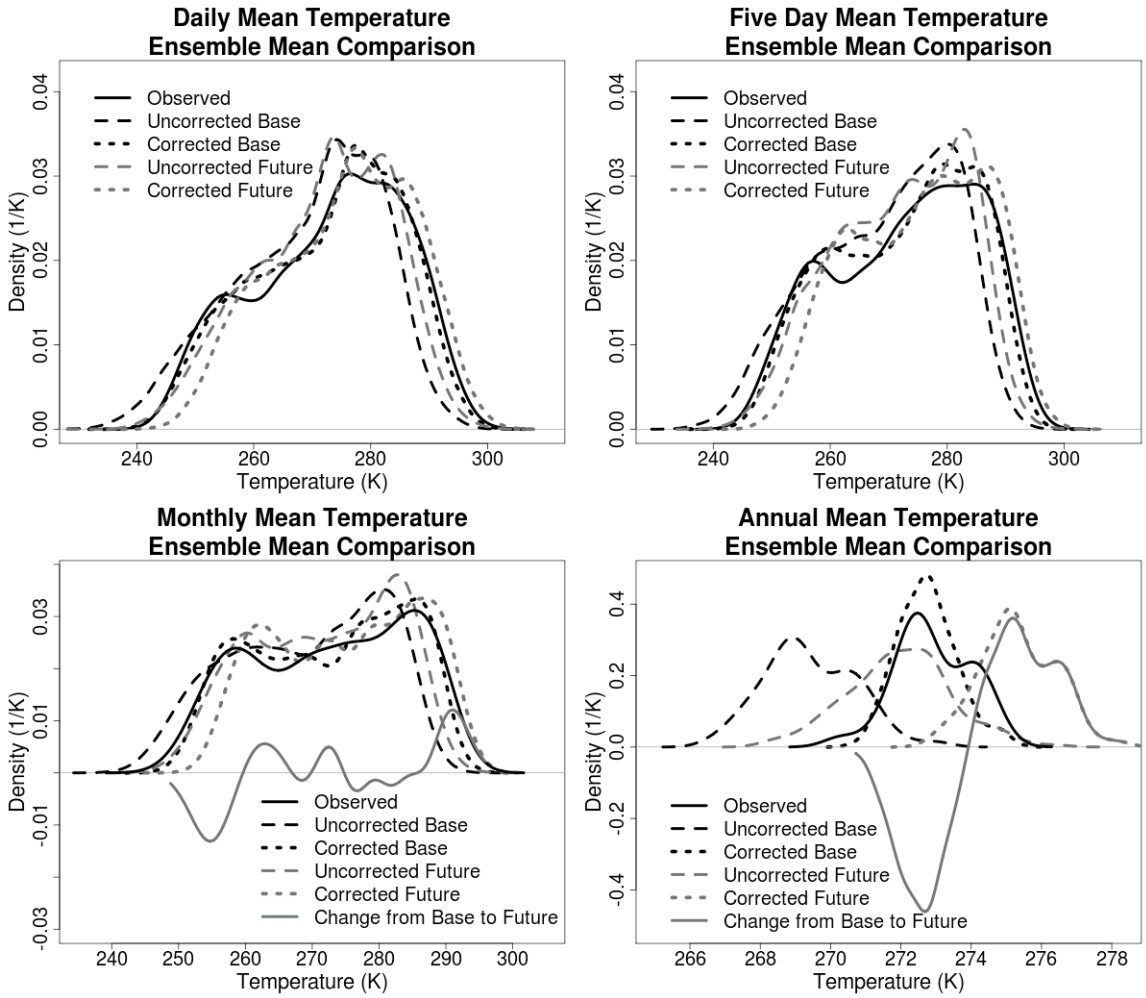

Figure 3.8 - Probability density functions for ensemble daily mean (top left), five-day mean (top right), monthly mean (bottom left) and annual temperature.

As with precipitation, the annual mean simulated temperature has a slightly lower variability than the observed. Differences in the PDF shapes are due to reasons discussed previously.

3.7. Hydrological Simulation Results

By using the corrected results corresponding to the Goose Bay grid coordinates from the base and future period climate simulations, discussed above, as inputs to the WATFLOOD hydrological model, streamflow for the two timeframes was able to be simulated. In this section a comparison of mean hydrographs, annual and seasonal flow as well as a look at peak flow timing and magnitude are presented.

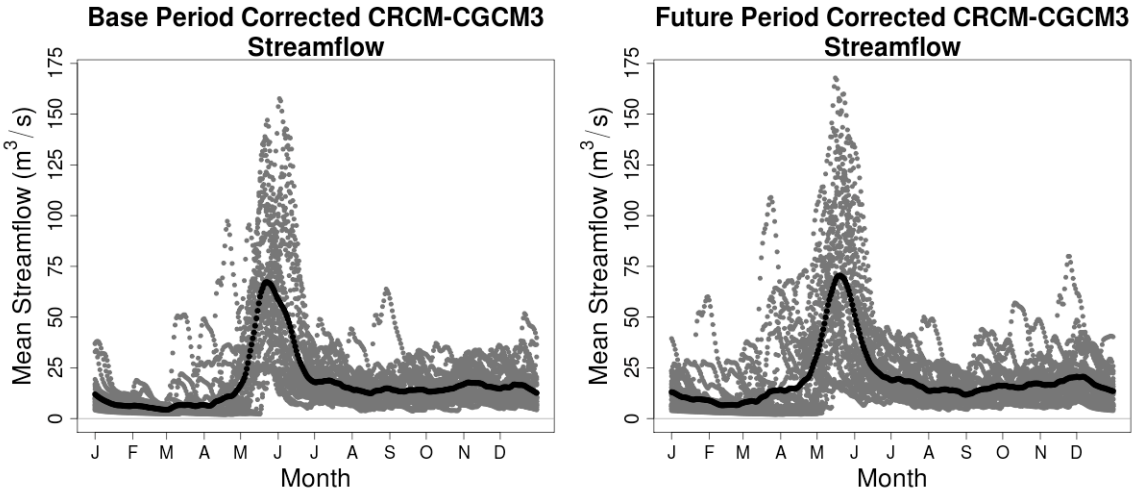

Figure 3.9 - Examples of mean streamflow values for the base (left) and future periods from the CRCM-cgcm3 ensemble member. 30-year mean streamflow represented by black points.

An example (CRCM-cgcm3) of the simulated daily streamflow values (grey) along with the 30-year means (black) for both timeframes is found in Figure 3.9. It is clear from

these plots that while the mean hydrograph is a useful indicator of climatic norms there is notable variance from year to year, especially in the peak spring flows. Differences in base and future period plots are discussed below.

Mean Hydrographs

The differences between the ensemble mean base and future period simulated hydrographs, along with the observation simulation hydrograph are shown in Figure 3.10 and the corresponding Table 3.5. (The "observed" hydrograph in Figure 3.10 and all subsequent hydrographs refer to the WATFLOOD simulation using observed climatological variables as input.) There are four noteworthy changes from the mean base period to the future period simulations:

1 The spring melt, spanning April, May and June, is occurring roughly two weeks earlier though it appears to be slightly smaller in magnitude. April experiences the highest relative increase of any month, over 109%, caused by the earlier onset of the spring melt. The upshot of the earlier melt is that June is simulated to have a 33% decrease in streamflow.

2 November to March streamflow increases substantially.

3 July to October streamflow experiences no substantial change.

4 On a mean annual basis streamflow increases by 8.9%, from 17.6 to 19.2 m^3/s.

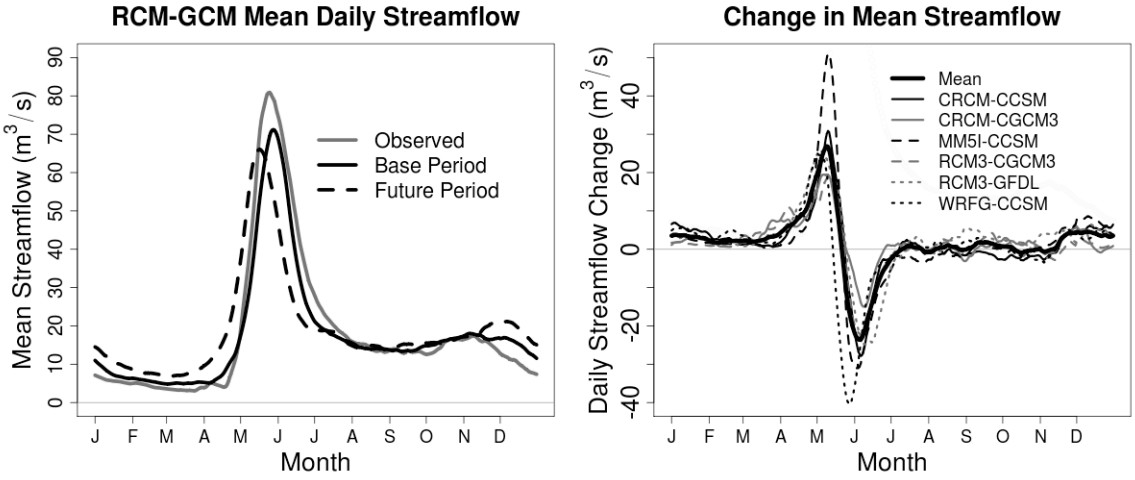

Figure 3.10 - Comparison of 30-year ensemble mean simulated base and future period streamflow (left) and the change in 30-year ensemble mean simulated streamflow, from base to future period (right).

While there is some inter-model variability throughout the year, the variability of change in spring melt signal is most noticeable. MM5I-ccsm and WRFG-ccsm both show large changes in the spring melt, the former shows an increase and the latter a decrease. One can infer from the difference between these simulations that uncertainty in the projection of the spring melt magnitude is largely due to the RCM rather than the GCM, as both models were driven by ccsm.

To determine whether there is a statistically significant difference between the (simulated) base and future periods a Wilcoxon Rank Sum Test was performed using monthly means from all six ensemble members. The statistical significance of the differences between observed and simulated streamflow was not evaluated. This test was chosen due to the skewed distribution of the mean monthly streamflow values. The results, in Table 3.5, show there was a difference statistically significant to 1% for the months of November through June, as indicated by the p-value (p-values less than 0.01

imply a statistical significance level of 1%). The remaining four months proved not to be significantly different between the base and future periods, while mean annual streamflow is shown to be significantly higher.

Table 3.5 – Ensemble mean monthly and annual changes in streamflow.

Month	Mean Streamflow (m^3/s)			Increase in Streamflow (m^3/s)	Increase in Streamflow (%)	p-value (statistical significance)
	Observed WATFLOOD Simulation	Current Period Simulation	Future Period Simulation			
January	5.8	7.8	11.1	3.3	42.2	$2.0x10^{-9}$
February	4.3	5.5	7.6	2.0	36.8	$7.3x10^{-9}$
March	3.4	5.1	7.8	2.7	52.7	$1.7x10^{-7}$
April	6.9	8.7	18.2	9.5	109.3	$1.3x10^{-13}$
May	60.2	49.2	57.5	8.3	16.8	0.00040
June	48.9	40.9	27.3	-13.5	-33.1	$4.1x10^{-9}$
July	20.7	17.8	17.7	-0.1	-0.7	0.61
August	14.4	14.3	14.5	0.2	1.6	0.58
September	13.3	13.8	15.0	1.2	8.4	0.19
October	15.1	16.1	15.9	-0.1	-0.7	0.99
November	15.8	17.2	19.0	1.8	10.5	0.0071
December	10.0	14.8	18.8	4.0	26.8	$8.5x10^{-7}$
Annual	**18.2**	**17.6**	**19.2**	**1.6**	**8.9**	**$4.0x10^{-5}$**

*Small discrepancies may exist due to rounding

It is worthwhile to look at the individual hydrographs produced by the six ensemble members to see if, at least qualitatively, the results discussed above are consistent across all ensemble members. In Figure 3.11 each ensemble member shows that the spring melt begins earlier, winter streamflow increases and late summer and fall streamflow remains relatively unchanged. The magnitude of the spring melt decreases for two thirds of the ensemble members. From this figure one can also compare the mean observed hydrograph to the mean base period hydrographs from ensemble members. Initial inspection reveals that, while the ensemble members do not perfectly reproduce the observed hydrograph they represent the main features of the annual cycle (e.g. winter base flow, spring melt, etc) fairly well, particularly the MM5I-ccsm hydrograph.

Many RCM driven hydrographs illustrate noticeable differences from the observed that are of similar magnitude to the climate change signal. This is consistently the case for December streamflow and is also prevalent in the timing and magnitude of the spring melt. While the results are still useful for investigating the relative changes between base and future period simulations, caution should be used when interpreting absolute changes. Further comparison and discussion is found below.

Distribution of Annual and Seasonal Mean Flows

While the simulated mean changes are informative, one needs to consider the distributions of the results to gain a more useful and robust understanding of the potential impacts of climate change.

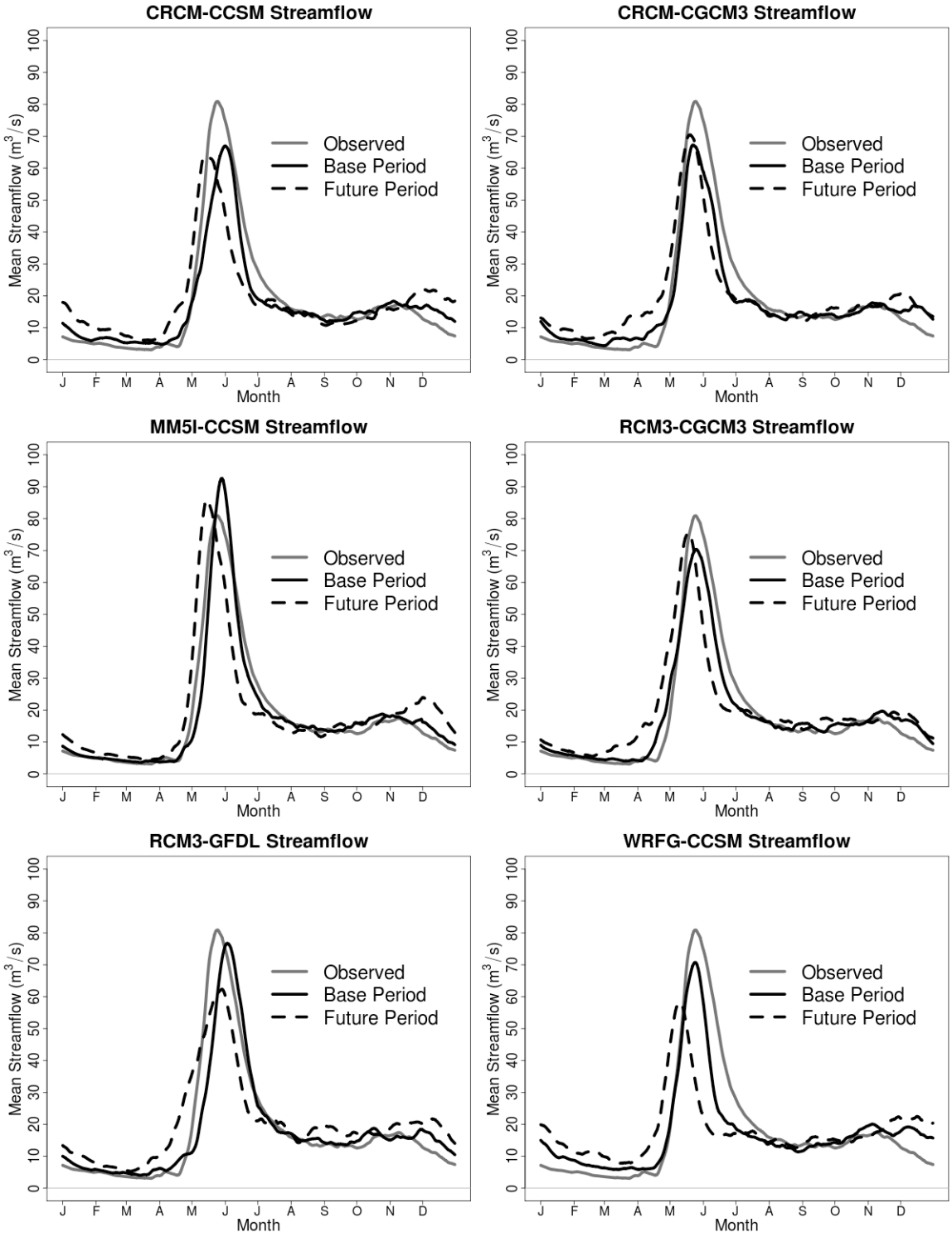

Figure 3.11 - Mean base and future period simulated hydrographs for the six ensemble members.

Figures 3.12 and 3.13 show the PDFs for mean annual and seasonal flow respectively, including a comparison between base period ensemble member results and observed.

Even though there is significant overlap in the mean annual flows there is a clear increase in magnitude from the base to the future period, as quantified in Table 3.5. The ensemble mean is similar to that of the observed hydrograph however the latter has a greater spread of values, most notably on the higher end of flow rates. This is most likely a propagation of the precipitation and temperature bias correction timescale issues discussed previously.

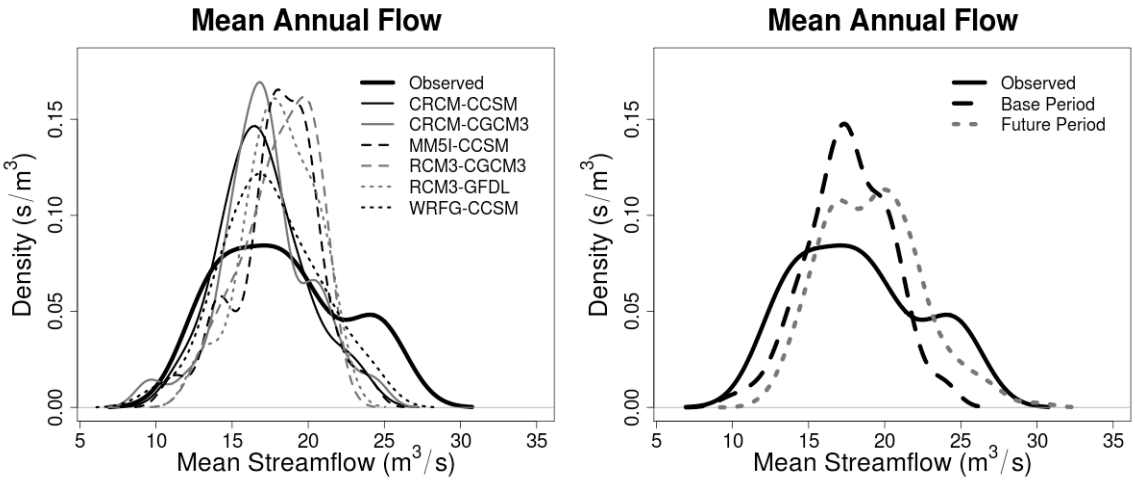

Figure 3.12 - Probability density functions of mean annual flows for ensemble members during the base period (left) and the ensemble means for base and future periods.

By breaking down the flow by season, one is able to gain better insight into what time of the year the significant changes in streamflow are likely to occur. The changes in mean winter (November to March) flow magnitude are statistically significant (p-value = 1.7×10^{-8}) while any changes in spring (April to June) and summer (July to October) are not (p-values of 0.24 and 0.79 respectively). In all three seasons the PDFs become flatter and wider from base to future periods, indicating higher variability in the future.

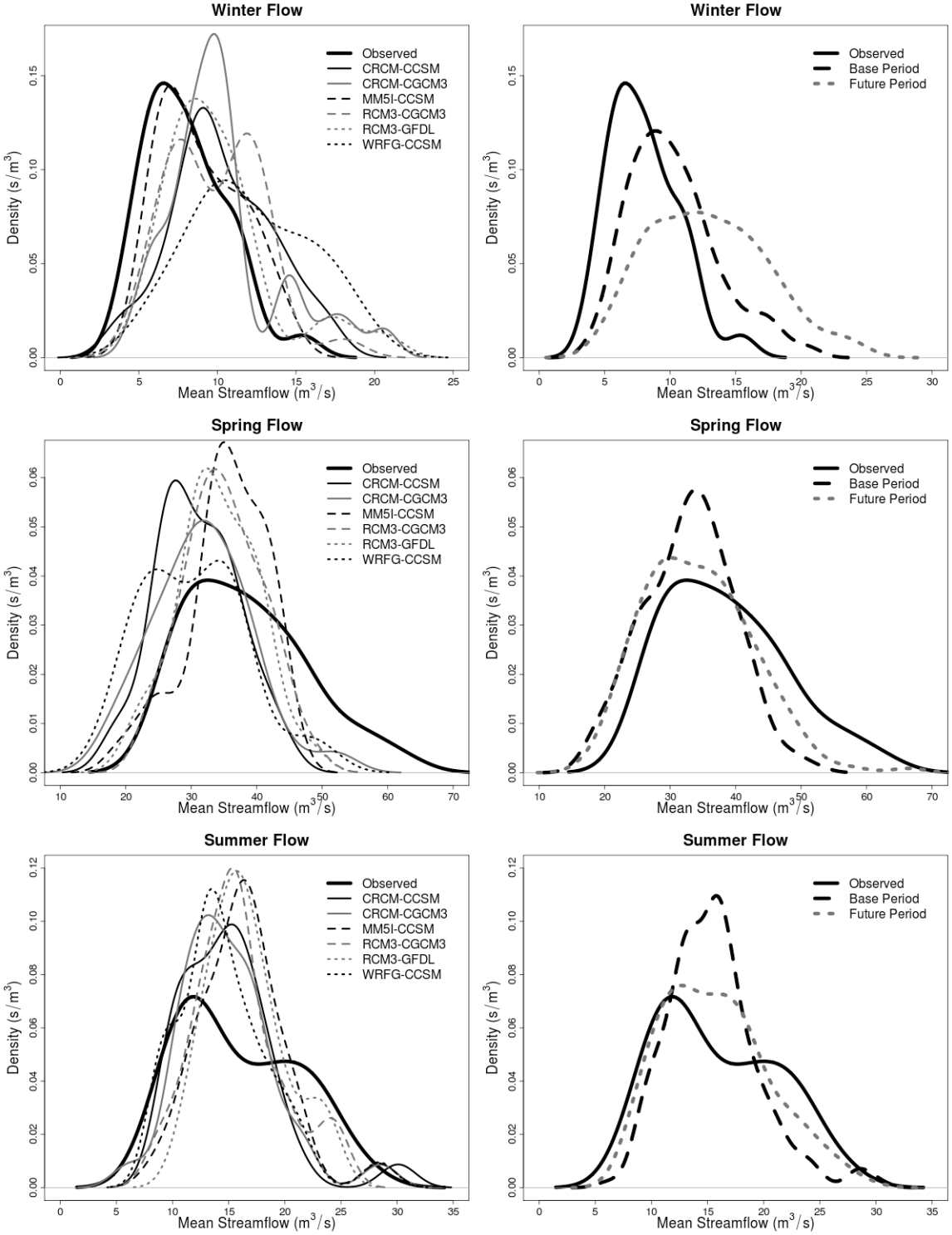

Figure 3.13 - Probability distribution functions for mean winter (November to March), spring (April to June) and summer (July to October) flows, with ensemble member base period results on the left.

There is greatest agreement amongst ensemble member base period simulations in summer, while winter shows the least agreement. During spring and summer, the ensemble member distributions are slightly to the left of the observed indicating a small underestimation of flow, while the opposite is true of winter.

3.8. Discussion of Results

Various amounts of bias in both precipitation and temperature were identified for each of the six ensemble members. The greatest magnitudes and variances of bias between ensemble members occurred in the cold season, while the opposite is true for the warm season. WRFG-ccsm appeared to have the largest overall precipitation bias for the region of interest, while RCM3-gfdl had the lowest. Most of the temperature biases found were relatively consistent throughout the year, with the exception of WRFG-ccsm and RCM3-gfdl whose biases appeared more seasonal. The bias corrections brought the base period simulations for all ensemble members in line with observations. The mean annual bias corrected simulated precipitation was 3.1 mm/day while observations also suggest an average of 3.1 mm/day; the mean annual bias corrected simulated temperature was roughly 272.6 K while observations suggest an average of 272.8 K.

Climate simulations suggest that both mean annual precipitation and temperature will increase from the base period to the future period, with greater increases expected during the cold season. Based on WATFLOOD simulations of the Pinus River Basin, the increase in precipitation over the span of a year will have a greater impact on streamflow

than increased evaporation that accompanies higher temperatures, resulting in an 8.9% mean increase in streamflow. This is an expected result for the latitude of the study region; the intensification of the hydrological cycle is expected to accompany climate change and most of the moisture in the atmosphere deposited as precipitation over Labrador originates from lower latitudes, thousands of kilometers away (Bates *et al.*, 2008; Trenberth, 1998). However, if only July through October are examined, where there is no statistically significant mean increase in streamflow, then the increase in precipitation appears to be balanced by increased evaporation and other processes in the simulation.

The mean annual increase in simulated streamflow corresponds well with previous work by Bates *et al.* (2008) which predicts a 10 to 20% increase in streamflow by the years 2080-2099. The Bates *et al.* simulation follows the SRES A1B scenario that assumes a path for atmospheric carbon dioxide concentrations similar to that of the A2 scenario up to the middle of the 21st century, after which the A1B scenario becomes more conservative (IPCC, 2000).

Breaking down the mean flow by season (as previously defined), the simulations show summer experiences no significant change while winter experiences a statistically significant increase. This increase can be partly explained by the increase in winter precipitation from 2.9 mm/day to 3.3 mm/day. For this additional precipitation to translate into streamflow there needs to be an increase in the amount of time temperature is above freezing. Figure 3.14 shows the empirical cumulative distribution function

(CDF) for mean daily winter temperatures. From the intersection of the CDFs with the vertical lines representing the freezing point, one sees the percentage of days with mean temperatures below freezing decrease from 92.1% to 85.4%, progressing from the base to the future period. In other words, the amount of time spent above freezing in the winter nearly doubles in the future.

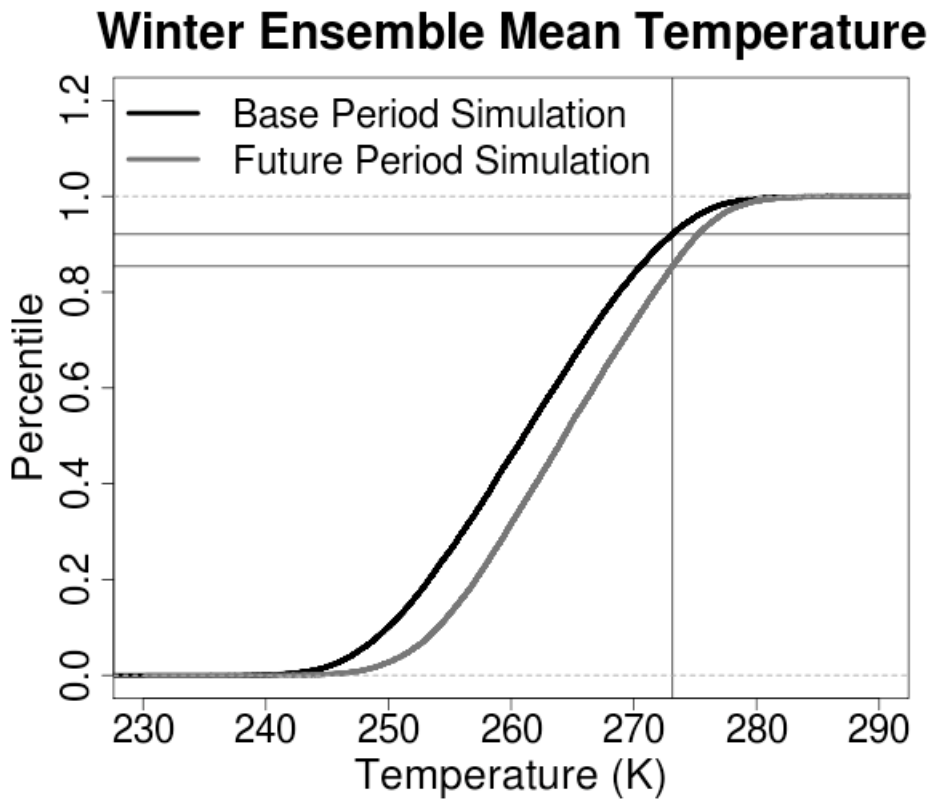

Figure 3.14 - Empirical cumulative distribution function for mean daily winter temperatures. Vertical line indicates freezing point, 273.15 K.

While mean spring flow and the magnitude of the peak spring flow experience no significant change, the timing of the spring melt does occur earlier by roughly two weeks. These results correspond with previous work presented by Bourque and Simonet (2008), which project a higher mean winter flow and an earlier spring melt for a northern Quebec

watershed. Higher winter temperatures contribute to an increase in runoff throughout the winter, leaving less water trapped in the snowpack to feed the spring melt. There is however a mean increase in precipitation throughout the winter that acts to enhance the snowpack volume. These competing factors provide insight into why some ensemble members suggest an increase in the volume of mean and peak melt while others show a decrease, resulting in no statistically significant change.

Sources of Uncertainty

An unavoidable assumption that one must make when using future climate projections from a model validated by comparison to the current climate is that the relationship between model output and reality will remain stationary. While bias corrections ensure statistical consistency between base period model output and observations, the process is not physically based and one has to assume that the validity of statistical corrections will also remain stationary in future climates.

By incorporating six different RCM-GCM combinations in this study a broader understanding of the uncertainty of the simulations, introduced by the RCMs and GCMs, is developed and thus a more useful approximation of mean changes in precipitation, temperature and streamflow is produced. However, this approach does not capture the full range of uncertainty that would be introduced by different emissions scenarios, other climate and hydrological models not included in the study as well as factors and processes that may be poorly represented in the models used.

By examining the range of NARCCAP's projected precipitation and temperature changes (Figures 3.5 and 3.7) one is able to see a measure of uncertainty introduced by the various RCMs and GCMs. There is a wide spread of values projected throughout the year for precipitation indicating that caution should be used if applying only the ensemble mean in an impact study as there is a range of equally likely realizations of potential future precipitation. There was good agreement in late winter for temperature change projections indicating that the ensemble mean is robust for that time of year, while the rest of the year showed a much wider spread.

Upon closer examination of individual RCMs and GCMs it becomes apparent that there was a level of uncertainty introduced by both the regional models and their driving GCMs. For example, in temperature change projections, all three ccsm runs (CRCM, MM5I and WRFG) had strong agreement throughout the year, indicating that relatively little uncertainty was introduced by the RCMs, however the wider variety of ccsm precipitation change projections indicate the RCMs introduced appreciable uncertainty. Agreement between ensemble member projections for both precipitation and temperature vary throughout the annual cycle, signifying that model uncertainty is dependent on the time of year.

There is also uncertainty introduced by using a hydrological model that relies primarily on temperature (Hargreaves equation) to simulate evapotranspiration. While WATFLOOD was adequately calibrated to the energy processes of the current climate, non-stationary future conditions may result in less accurate hydrological simulations. In

order to capture the uncertainty of using an empirical evapotranspiration routine one would have to use also a hydrological model of greater complexity, with a more physically based representation of the land-surface energy balance.

3.9. Conclusions and Recommendations

The results of this study indicate there will be a mean annual increase in streamflow of nearly 9% in the Pinus River sub-basin, from the base period (1971-2000) to the future period (2041-2070). This increase is expected to manifest itself primarily as an increase in cold season (November to April) streamflow, caused by higher precipitation and temperatures over the same period. Conversely, no significant change in streamflow is expected to occur from July through October. Some simulated hydrograph features, namely December flow and the precise timing and magnitude of spring melt, should be interpreted with caution as differences between base period simulations and observations were often of similar magnitude to the climate change signal.

The WATFLOOD hydrological model was driven by bias corrected RCM-GCM combinations from six ensemble members. The ensemble mean of the bias corrected climate output suggested a mean annual increase in precipitation of nearly 0.3 mm/day and a mean annual temperature increase of roughly 2.6 K. Both precipitation and temperature increases were greatest during the cold season.

The range of results in mean projections from different ensemble members demonstrates the uncertainty introduced by various RCMs and GCMs, while the probability density

functions provide a probabilistic measure of climate variability. These measures of uncertainty and climate variability must be kept in mind when conducting impact studies as simply employing the mean results ignores the range of possible outcomes.

The following list is recommended work that will contribute to a more complete understanding of the impacts that climate change may have on the Lower Churchill Hydroelectric Generation Project:

- Include more NARCCAP ensemble members as they become available to more effectively capture the range of uncertainty introduced by RCMs and GCMs. The inclusion of models driven by other emissions scenarios should also be considered, however only the A2 scenario is available through NARCCAP so another data source would be required.

- As an alternative to the bias correction process used in this paper, attempt a statistical downscaling approach that includes stochastic weather generation or some method that is able to accurately reproduce the short and long timescales of the observed data.

- Expand the hydrological modeling to the entire Churchill River watershed. Additional climate and streamflow measuring stations for model calibration would be invaluable in this effort.

- Consideration should be given to the use of a more complex hydrological model,

able to more effectively represent energy balance processes.

- As this study focused primarily on mean streamflow, there should be some effort to examine the effects of climate change on extreme hydrological conditions, such as floods and droughts, in the Churchill River watershed.

- A reservoir or power generation model should be used to determine how the altered flow regimes translate into changes in potential power production.

3.10. Acknowledgements

This paper is part of a broader study at Memorial University in collaboration with Nalcor Energy that examines the effects of climate change on the Lower Churchill Hydroelectric Generation Project. This work would not be possible without the generous financial support of Nalcor. In particular the collaborative efforts of Marion Organ have been tremendously valuable. We would like to recognize Dr. Nicholas Kouwen for his help with setting up and running WATFLOOD. We would also like to thank NSERC for providing financial support.

We wish to thank the North American Regional Climate Change Assessment Program (NARCCAP) for providing access to the data used in this paper. NARCCAP is funded by the National Science Foundation, the U.S. Department of Energy, the National Oceanic and Atmospheric Administration, and the U.S. Environmental Protection Agency Office of Research and Development.

Finally, we'd like to thank the two anonymous reviewers for providing valuable feedback and suggestions.

3.11. References

Bates, B. C., Kundzewicz, Z. W., Wu, S., & Palutikof, J. P. (2008). Climate change and water. Intergovernmental Panel on Climate Change Technical Paper IV. Geneva: IPCC Secretariat, 210 pp.

Bingeman, A. K., Kouwen, N., & Soulis, E. D. (2006). Validation of the hydrological processes in a hydrological model. *Journal of Hydrologic Engineering, 11*(5), 451-463. DOI:10.1061/(ASCE)1084-0699(2006)11:5(451).

Bourque, A. & Simonet, G. (2008). Quebec. In D. S. Lemmen, F. J. Warren, J. Lacroix, & E. Bush (Eds.) *From impacts to adaptation: Canada in a changing climate 2007* (pp. 171-226). Ottawa: Government of Canada.

Christensen, J. H., Boberg, F., Christensen, O.B., & Lucas-Picher, P. (2008). On the need for bias correction of regional climate change projections of temperature and precipitation. *Geophysical Research Letters, 35*(20), L20709. DOI:10.1029/2008GL035694.

Christensen, J. H., & Christensen, O.B. (2007). A summary of the PRUDENCE model projections of changes in European climate by the end of this century. *Climatic Change, 81*(1), 7-30. DOI:10.1007/s10584-006-9210-7.

Christensen, N. S., Wood, A. W., Voisin, N., Lettenmaier, D. P., & Palmer, R. N. (2004). The effects of climate change on the hydrology and water resources of the Colorado River basin. *Climatic Change, 62*, 337-363. DOI:10.1023/B:CLIM.0000013684.13621.1f.

Cranmer, A. J., Kouwen, N., & Mousavi, S.F. (2001). Proving WATFLOOD: modelling the nonlinearities of hydrologic response to storm intensities. *Canadian Journal of Civil Engineering, 28*(5), 837-855. DOI:10.1139/l01-049.

DesJarlais, C., Bourque, A., Decoste, R., Demers, C., Deschamps, P., & Lam, K.-H. (2004). *Adapting to climate change*. Montreal, QC: Ouranos, 83 pp.

Dibike, Y. B., & Coulibaly, P. (2005). Hydrologic impact of climate change in the Saguenay watershed: comparison of downscaling methods and hydrologic models. *Journal of hydrology, 307*(1), 145-163. DOI:10.1016/j.jhydrol.2004.10.012.

Feddersen, H., & Andersen, U. (2005). A method for statistical downscaling of seasonal ensemble predictions. Tellus A, 57(3), 398-408. DOI:10.1111/j.1600-0870.2005.00102.x.

Filion, Y. (2000). Climate change: implications for Canadian water resources and hydropower production. *Canadian Water Resources Journal, 25*(3), 255-269. DOI:10.4296/cwrj2503255.

Haerter, J. O., Hagemann, S., Moseley, C., & Piani, C. (2011). Climate model bias correction and the role of timescales. *Hydrology and Earth System Sciences, 15*(3), 1065-1079. DOI:10.5194/hess-15-1065-2011.

Hansen, J. W., Challinor, A., Ines, A. V. M., Wheeler, T., & Moron, V. (2006). Translating climate forecasts into agricultural terms: advances and challenges. *Climate Research, 33*(1), 27-41. DOI:10.3354/cr033027 .

IPCC. [Nakicenovik, N., & Swart, R. (Eds.)]. (2000). *Emissions Scenarios*. UK: Cambridge University Press, 570 pp.

Jasim, F. (2014). *Development of a base model for flood forecasting studies in the Humber River Basin (NL) and selection of an appropriate model forcing dataset*. St. John's, NL: Memorial University of Newfoundland.

Kotlarski, S., Block, A., Böhm, U., Jacob, D., Keuler, K., Knoche, R., ... & Walter, A. (2005). Regional climate model simulations as input for hydrological applications: evaluation of uncertainties. *Advances in Geosciences, 5*, 119-125.

Kouwen, N., Soulis, E. D., Pietroniro, A., Donald, J., & Harrington, R. A. (1993). Grouped response units for distributed hydrologic modeling. *Journal of Water Resources Planning and Management, 119*(3), 289-305. DOI:10.1061/(ASCE)0733-9496(1993)119:3(289).

Leander, R., & Buishand, T. A. (2007). Resampling of regional climate model output for the simulation of extreme river flows. *Journal of Hydrology, 332*(3), 487-496. DOI:10.1016/j.jhydrol.2006.08.006.

Li, H., Luo, L., Wood, E. F., & Schaake, J. (2009). The role of initial conditions and forcing uncertainties in seasonal hydrologic forecasting. *Journal of Geophysical Research: Atmospheres (1984–2012), 114*(D4), 114. DOI:10.1029/2008JD010969.

Maraun, D., Wetterhall, F., Ireson, A. M., Chandler, R. E., Kendon, E. J., Widmann, M., ... & Thiele-Eich, I. (2010). Precipitation downscaling under climate change: recent developments to bridge the gap between dynamical models and the end user. *Reviews of Geophysics, 48*(3). DOI:10.1029/2009RG000314.

Mearns, L. O., Gutowski, W. J., Jones, R., Leung, L. Y., McGinnis, S., Nunes, A. M. B., & Qian, Y. (2007) updated 2011. The North American Regional Climate Change Assessment Program dataset. *National Center for Atmospheric Research Earth System Grid data portal, Boulder, CO*. http://www.earthsystemgrid.org/browse/viewProject.htm?projectId=ff3949c8-2008-45c8-8e27-5834f54be50f (accessed September 2010).

Mearns, L. O., Gutowski, W., Jones, R., Leung, R., McGinnis, S., Nunes, A., & Qian, Y. (2009). A regional climate change assessment program for North America. *Eos, Transactions American Geophysical Union, 90*(36), 311-311. DOI:10.1029/2009EO360002.

Mekis, E., & Hogg, W. D. (1999). Rehabilitation and analysis of Canadian daily precipitation time series. *Atmosphere-Ocean, 37*(1), 53-85. DOI:10.1080/07055900.1999.9649621.

Minville, M., Brissette, F., Krau, S., & Leconte, R. (2009). Adaptation to climate change in the management of a Canadian water-resources system exploited for hydropower. *Water Resources Management, 23*(14), 2965-2986. DOI:10.1007/s11269-009-9418-1.

Minville, M., Brissette, F., & Leconte, R. (2008). Uncertainty of the impact of climate change on the hydrology of a nordic watershed. *Journal of Hydrology, 358*(1), 70-83. DOI:10.1016/j.jhydrol.2008.05.033.

Murphy, J. M., Sexton, D. M., Barnett, D. N., Jones, G. S., Webb, M. J., Collins, M., & Stainforth, D. A. (2004). Quantification of modelling uncertainties in a large ensemble of climate change simulations. *Nature, 430*(7001), 768-772. DOI:10.1038/nature02771.

Muzik, I. (2001). Sensitivity of hydrologic systems to climate change. *Canadian Water Resources Journal, 26*(2), 233-252. DOI:10.4296/cwrj2602233.

Nalcor Energy. (2009). *Project planning and description. Vol. 1 Part A of Lower Churchill Hydroelectric Generation Project environmental impact statement*. St. John's, NL: Nalcor Energy, 344 pp.

Piani, C., Haerter, J. O., & Coppola, E. (2010). Statistical bias correction for daily precipitation in regional climate models over Europe. *Theoretical and Applied Climatology, 99*(1-2), 187-192. DOI:10.1007/s00704-009-0134-9.

Rahman, M., Bolisetti, T., & Balachandar, R. (2012). Hydrologic modelling to assess the climate change impacts in a Southern Ontario watershed. *Canadian Journal of Civil Engineering, 39*(1), 91-103. DOI:10.1139/l11-112.

Shabalova, M. V., van Deursen, W. P., & Buishand, T. A. (2003). Assessing future discharge of the river Rhine using regional climate model integrations and a hydrological model. *Climate Research, 23*(3), 233-246.

Sung, R. Y. J., Burn, D. H., & Soulis, E. D. (2006). A case study of climate change impacts on navigation on the Mackenzie River. *Canadian Water Resources Journal, 31*(1), 57-68. DOI:10.4296/cwrj3101057.

Sushama, L., Laprise, R., Caya, D., Frigon, A., & Slivitzky, M. (2006). Canadian RCM projected climate‐change signal and its sensitivity to model errors. *International Journal of Climatology, 26*(15), 2141-2159. DOI:10.1002/joc.1362.

Themeßl, M. J., Gobiet, A., & Leuprecht, A. (2011). Empirical‐statistical downscaling and error correction of daily precipitation from regional climate models. *International Journal of Climatology, 31*(10), 1530-1544. DOI:10.1002/joc.2168.

Trenberth, K. E. (1998). Atmospheric moisture residence times and cycling: Implications for rainfall rates and climate change. *Climatic change, 39*(4), 667-694. DOI:10.1023/A:1005319109110.

Trenberth, K. E., Dai, A., Rasmussen, R. M., & Parsons, D. B. (2003). The changing character of precipitation. *Bulletin of the American Meteorological Society, 84*(9), 1205-1217. DOI:10.1175/BAMS-84-9-1205.

Vasseur, L., & Catto, N. (2008). Atlantic Canada. In Lemmen, D. S., Warren, F. J., Lacroix, J., & Bush, E. (Eds.) *From impacts to adaptation: Canada in a changing climate 2007*. Ottawa: Government of Canada, pp 119-170.

Wilby, R. L. (1997). Non‐stationarity in daily precipitation series: Implications for GCM down‐scaling using atmospheric circulation indices. *International Journal of Climatology, 17*(4), 439-454. DOI:10.1002/(SICI)1097-0088(19970330)17:4<439::AID-JOC145>3.0.CO;2-U.

Wood, A. W., Leung, L. R., Sridhar, V., & Lettenmaier, D. P. (2004). Hydrologic implications of dynamical and statistical approaches to downscaling climate model outputs. *Climatic change, 62*(1-3), 189-216. DOI:10.1023/B:CLIM.0000013685.99609.9e.

Zadeh, S. M., Lye, L. M., & Khan, A. A. (2012). Regional Frequency Analysis of Low Flow Using L-moments for Labrador, Canada. *Annual General Conference of the Canadian Society of Civil Engineers, Edmonton, Canada*.

4. Atmospheric and Terrestrial Water Balances of Labrador's Churchill River Basin, as Simulated by the North American Regional Climate Change Assessment Program

4.1. Abstract

In an effort to understand the sources of uncertainty and the physical consistency of climate models from the North American Regional Climate Change Assessment Program (NARCCAP), an ensemble of general circulation models (GCMs) and regional climate models (RCMs) was used to explore climatological water balances for the Churchill River Basin in Labrador, Canada. NCEP driven RCMs were used to support the analysis of the GCM-RCM ensemble and quantify certain structural uncertainties in the RCMs. This study quantifies mean atmospheric and terrestrial water balance residuals, as well as their annual cycles. Mean annual atmospheric water balances had consistently higher residuals than the terrestrial water balances, due in part to the influences of sampling of instantaneous variables and the interpolation of atmospheric data to published pressure levels. Atmospheric and terrestrial water balance residuals for each ensemble member were found to be consistent between base and future periods, implying that they are systemic and not climate dependent. With regard to the annual cycle, there was no pattern

found across time periods or ensemble members as to whether the monthly terrestrial or atmospheric root mean square residual was highest. Due to the interdependence of hydrological cycle components, the complexity of climate models and the variety of methods and processes used by different ensemble members, all causes of the water balance residuals were impossible to isolate. That being said, the residuals created by interpolating a model's native vertical resolution onto NARCCAP's published pressure levels and the subsequent vertical interpolation were quantified and several other sources were explored. In general, residuals were found to be predominantly functions of the RCM choice (as opposed to the GCM choice) and their respective modelling processes, parameterization schemes and post-processing.

4.2. Preface

This chapter has been submitted for publication in Atmosphere-Ocean (as a companion paper for Chapter 5) and is currently under review.

The previous chapter examines a single RCM tile from each of the ensemble members and looks at the relatively small sub-basin of the Churchill River. Part of the motivation for choosing a 770 km^2 sub-basin, as opposed to the entire 92 500 km^2 Churchill River watershed area, was that the collaborator who setup and ran the hydrological model WATFLOOD (Amy Pryse-Phillips) was under the time constraints of a masters degree and the size of the full basin was prohibitive in this respect. This was a good first step in the overall investigation into the impacts of climate change on the Churchill River, however the study needed to be expanded to the entire basin.

This chapter sets the stage for Chapters 5 and 6 by exploring underlying sources of uncertainty and the internal physical consistency within each ensemble member, as it relates to the movement of moisture. No analyses of the climate change signals are undertaken in this chapter but this work is necessary for the analysis in Chapter 5.

Future Period Water Balance

The base period water balance component breakdown is presented as Figure 4.2 and discussed in Section 4.5, however a similar plot for the future period was omitted for the sake of brevity. This plot is shown in Figure 4.A.

Existence of Large Water Balance Residuals

It is generally expected that atmospheric and terrestrial water balance residuals within any given climate model would be limited to rounding error and post-processing issues. The calculations and analysis presented in this chapter found this situation to not always to be the case. It may cross the reader's mind that the analysis may be wrong and there may be some error in the calculations. This supplementary section, in addition to the main work within the chapter, aims to dispel any doubts about the accuracy and validity of the results by providing full details of the calculations as well as summaries of discussions with NARCCAP team members.

Re-Gridding

GrADS analysis software has the ability to automatically re-grid certain map projections for the purposes of display and analysis (including North Polar Stereographic used by

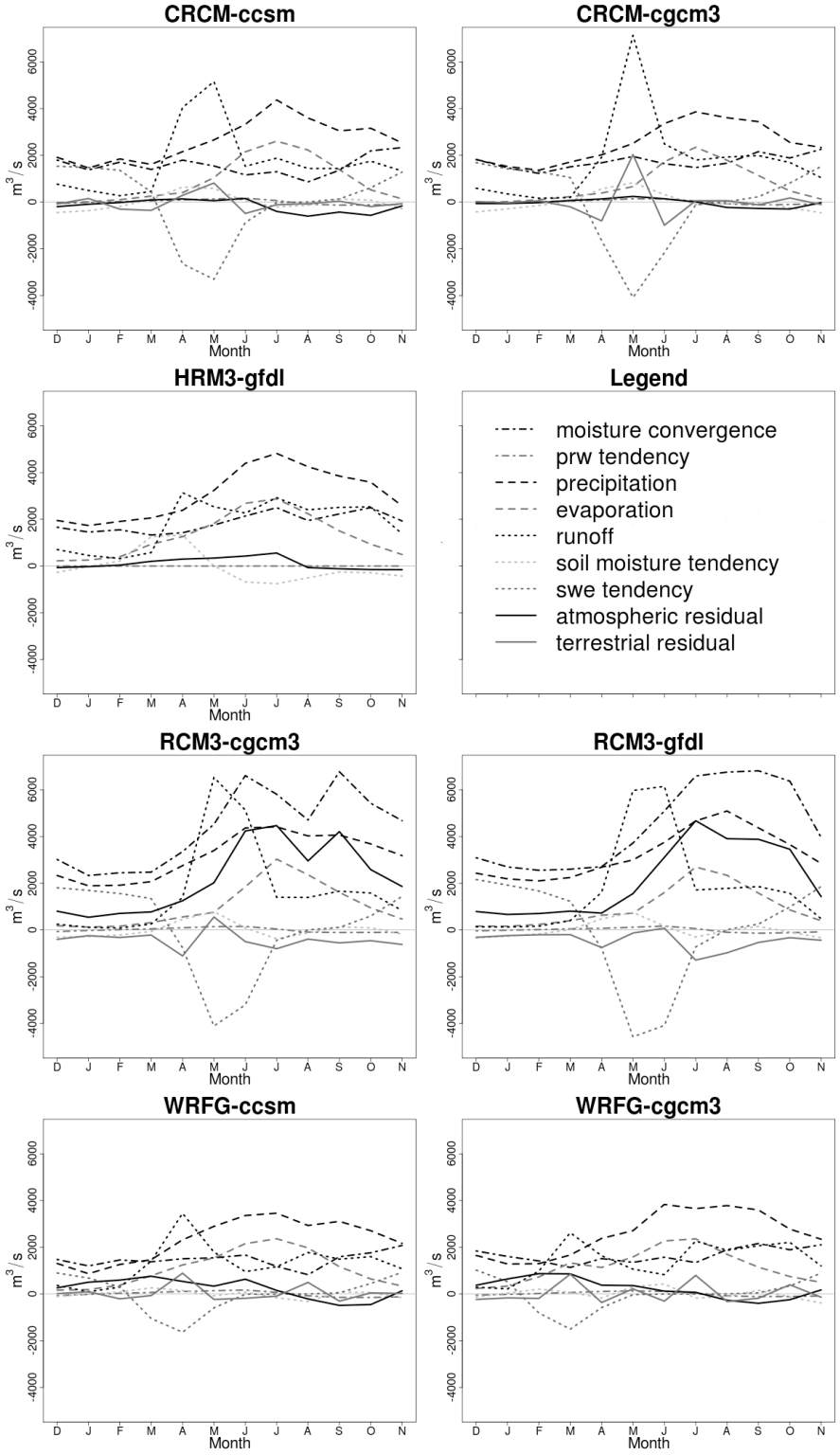

Figure 4.A – Future period water balance component breakdown (as per Figure 4.2)

CRCM and Lambert Conformal used by MM5I and WRFG) however not all of the NARCCAP RCM map projections are supported (including HRM3's Rotated Latitude Longitude projection and RCM3's Transverse Mercator projection). As such, bilinear interpolation (which is used by ECMWF (Bispham 2014)) was used to re-grid all of the RCM 50 km resolution data to a common 0.25 degree grid used for the analysis. As such, the re-gridded grid points each represent an area of approximately 500 km^2 while the original grid points represent 2500 km^2.

In addition to creating a consistent grid between ensemble members, the re-gridding was an important step in the calculation of atmospheric moisture convergence. The common 0.25 degree grid had points following lines of latitude and longitude, which was required to use the GrADS divergence calculation function, *hdivg()* on NARCCAP's published zonal (west to east) and meridional (south to north) wind components. This calculation is discussed later in detail.

The FORTRAN code written to create the information files required for GrADS to perform the bilinear interpolation can be found in Appendix C. This code can re-grid any map projection as long as the latitude and longitude of each grid point is known. To confirm its effectiveness, Figure 4.B compares the GrADS re-gridding of the CRCM topography data to that of the custom re-gridding used for all calculations from this point forward, for Eastern Canada. The results are very similar. Bi-linear interpolation may not perfectly conserve water, though it is unlikely to have any substantial impact on the calculations presented here.

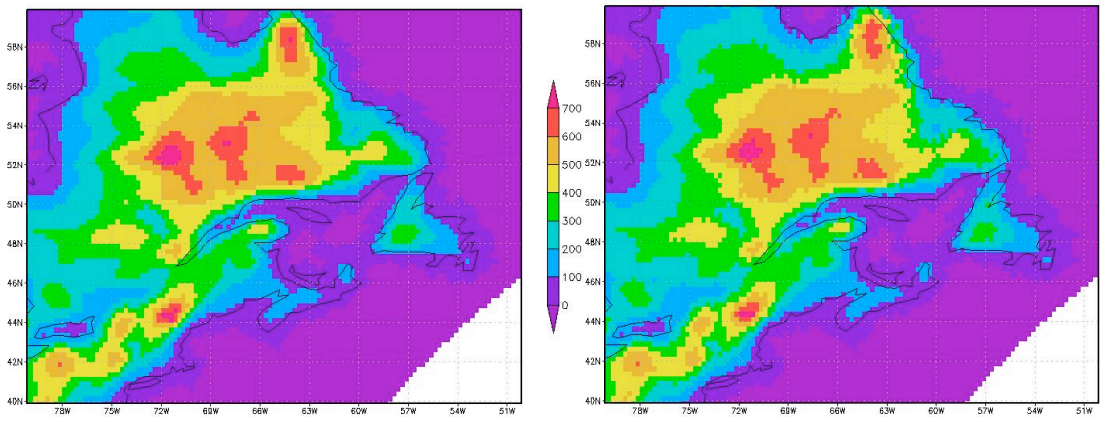

Figure 4.B – GrADS re-gridding of CRCM topography data (left) and custom re-gridding (right). Scale is in metres.

As a check, terrestrial water balance residuals were calculated using ensemble member's original 50 km horizontal grid and found to match those of the regridded values used in this study, to within an order of 1%. An exact match was not expected as data from different grid spaces were incorporated from the boundaries of the basin during the interpolation process. The annual cycles were also very similar.

Basin Masks and Data Extraction

Two data masks were created to represent the Churchill River Basin in the re-gridded map projection. The first mask is the most accurate representation of the basin at a 0.25 degree resolution, and is represented by the grid points inside the thick black line of Figure 4.1. This mask was used when extracting most variables from NARCCAP's published data files, which cover most of North America. The second, extended mask includes the grid points represented by the first mask plus the grid points represented by the thick black line in Figure 4.1. This second mask was required to extract data for the

atmospheric moisture convergence calculations, which require the wind and specific humidity values for surrounding grid points. (More details on this calculation are given below.) Each mask represented the basin with values of "1" and grid points outside the basin with "missing" values, which are ignored during calculations.

Variables that required the first mask were all two-dimensional variables (e.g. precipitation, soil moisture, etc). The wind and specific humidity values were three-dimensional and needed to be extracted for each of NARCCAP's 28 published pressure levels and subsequently stored as one file per variable per ensemble member for analysis purposes. Extraction of each variable was accomplished by applying the mask to the original published data, which was in netCDF format, isolating the smaller domain of data and saving it to new binary files. GrADS has functionality for both netCDF and binary formats. All calculations were then performed on these more manageable basin-specific data files.

Missing Data Calculations

Two required variables, evaporation and precipitable water content, were not published for all ensemble members and were able to be calculated from other published variables. Discussions of these calculations and for which ensemble members they were used are given below.

EVAPORATION

Evaporation is an important variable for this analysis. As such, to ensure consistency the method described here was applied to all ensemble members, regardless of whether or not they had published evaporation rate data. Additionally, the published evaporation rate was defined as the "Surface Evaporation of Condensed Water" and may not include contributions such as evaporation from moist soil and evapotranspiration, while the latent heat flux would. As such, surface evaporation rate, evps, ($kg/m^2/s$) was calculated using published latent heat flux, hfls, (units W/m^2) and the latent heat of vapourization, L_v (units J/kg), via Equation 4.A.

$$evps = \frac{hfls}{L_v} \qquad (4.A)$$

Water's latent heat of vapourization is temperature dependent and so Equation 4.B was used in conjunction with surface temperature, T (^oC) to determine its value. The equation is an empirical cubic polynomial curve fit to the data from Table 2.1 in Rogers & Yau (1984), with fit of R^2=0.999988. This equation is valid for temperatures from -40^{o}C to 40^{o}C and gives units of J/g for L_v.

$$L_v(T) = (-6.14342 * 10^{-5})T^3 + (1.58927 * 10^{-3})T^2 - (2.36418)T + 2.50079 * 10^3 \qquad (4.B)$$

As a check, this method was applied over an ocean tile and calculated results were found to be identical to published evaporation values for RCM3-cgcm3. The same validation was performed over land and there was a small discrepancy due to the more

comprehensive nature of latent heat flux versus the surface evaporation of condensed water. To illustrate, Figure 4.C shows this discrepancy for 3-hourly data of an arbitrarily chosen month. (The data point in Figure 4.C with a difference greater than 35% was quite high as evaporation values were close to zero, making the relative difference appear more substantial.) This difference was negligible compared to other terms in the water balance equations.

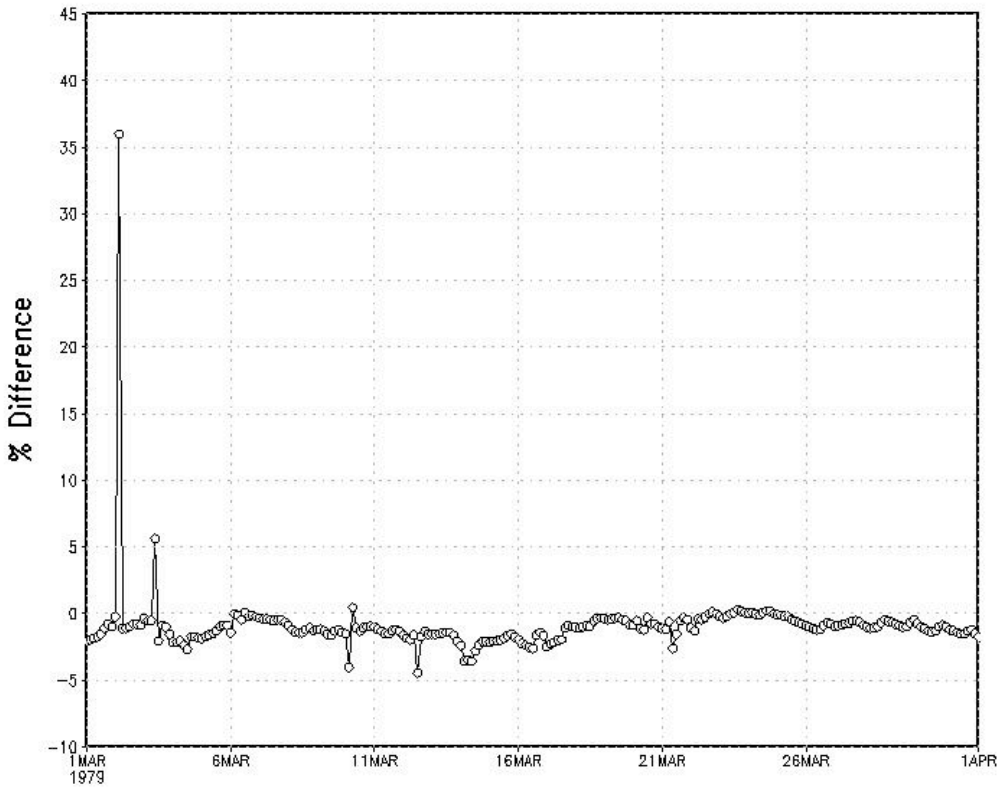

Figure 4.C – Relative difference between evaporation calculated from latent heat flux and temperature and published surface evaporation of condensed water, over land for RCM3-cgcm3.

PRECIPITABLE WATER CONTENT

Precipitable water content (prw), or the total amount of non-condensed water in a column of the atmosphere, was another variable that wasn't available for all ensemble members. This variable was treated as a storage term in the water balance analysis, similar to soil moisture and snow-water-equivalent in the terrestrial environment, and its tendency (how it changes with time) rather than its actual values are of interest. Precipitable water content tendency contributes water volumes several orders of magnitude less than the other terms in the atmospheric water balance equation. As such, the calculation described below was only performed for those ensemble members who did not have published prw values.

Precipitable water content was calculated by vertically integrating the specific humidity from each level of the atmosphere and was used as part of the "Coordinate Systems and Post-Processing" discussion in Section 4.6. The GrADS *vint()* function, which is a sum of mass-weighted layers, was employed for this purpose and is shown in Equation 4.C.

$$v\,\mathrm{int}(p_{sfc},\mathrm{var},p_{top}) = \frac{f}{g}\int_{p_{top}}^{p_{sfc}}(\mathrm{var})\,dp \qquad (4.C)$$

Where: var = the variable of interest (specific humidity when calculating prw)

p_{sfc} = surface pressure (hPa)

p_{top} = pressure of the top atmospheric layer (hPa)

f = pressure scaling factor = 100 Pa/hPa

g = gravity = 9.8 m/s^2

The resulting units of *vint()* are the units of var multiplied by kg/m^2.

The average relative error when looking at calculated precipitable water content values versus those published for CRCM-cgcm3 (base period) was 8.3% (as per Table 4.5), while the relative error for precipitable water content tendency was only 1.7%. To illustrate, an arbitrary month of data from CRCM-cgcm3 comparing the precipitable water tendencies at the 3-hour timescale is shown in Figure 4.D.

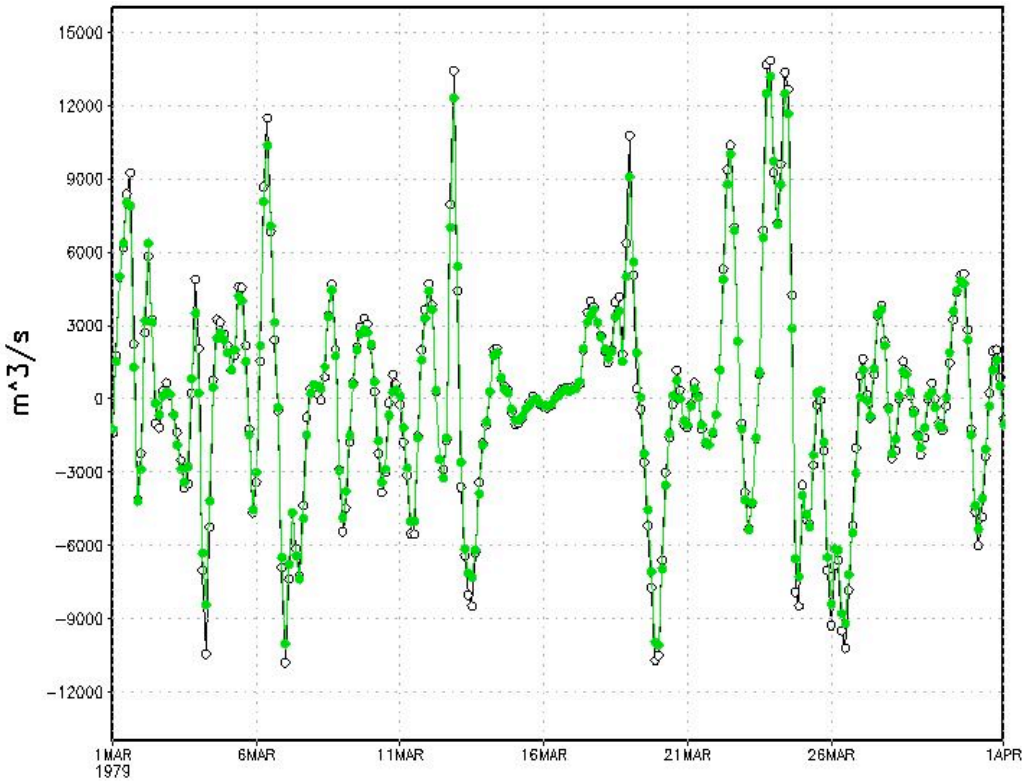

Figure 4.D – 3-hour precipitable water tendencies from published (white circles) and calculated prw (solid grey circles) values.

Atmospheric Moisture Convergence Calculation

While some discussion of the atmospheric moisture convergence calculation is given in Section 4.4, more details are provided here. The variables used in the calculation are zonal and meridional wind components (u and v, respectively, each with units of m/s) and the specific humidity (q, with units of kg of water per kg of air; kg/kg or g/g). All of the atmospheric moisture convergence calculations were performed using 3-hourly data. Once convergence values were found for each 3-hour interval, the monthly totals, presented in this chapter, were calculated. Following the data extraction and application of the basin mask as discussed above, steps of the calculation included:

1. Meridional and zonal water vapour flux, qu and qv (with units of kg/kg * m/s), were determined at each grid point and vertical level by multiplying q with u and v, respectively.

2. The water vapour flux was then integrated from the vertically lowest pressure level (above surface pressure) to 50 hPa (the vertically highest level published by NARCCAP), using *vint()* from Equation 4.C with var represented by qu or qv. The resulting integrated water vapour flux (qu_int and qv_int) had units of kg/m/s.

3. Next, the horizontal divergence (∇_H) of the integrated water vapour flux was taken using GrADS *hdivg()* function. This function operates on qu and qv simultaneously. For a given grid coordinate (x,y), qu_int(x+1,y) is subtracted from qu_int(x-1,y) and divided by the distance separating the coordinates (x+1,y)

and (x-1,y). GrADS determines the distance based on the map information provided in the custom data control files. Similarly the operation is performed on qv_int(x,y+1) and qv_int(x,y-1). The results of each operation are summed together to find the total atmospheric moisture divergence for the grid space (x,y). The results for each grid point within the basin were summed together to find the total basin atmospheric moisture divergence. The negative of this number is the atmospheric moisture convergence (represented by $-\nabla_H \bar{Q}$ in the atmospheric water balance equation). The resulting units are kg/m^2/s, which are then converted to m^3/s by multiplying by the area of the basin (9.25x10^{10} m^2) and by 1 m^3 / 1000 kg water.

Unit Conversion

As streamflow is often reported in cubic metres per second (m^3/s) and hydropower operators find it useful for operational decisions, all of the water balance components were converted to those units for easy comparison. For the Churchill River Basin, the conversion to mm/day, which is a common unit used in hydrology, is 1070.6 m^3/s for 1.00 mm/day.

Many of the NARCCAP variables were published with units of kg/m^2/s (if they were 3-hour averages, such as precipitation) and were converted to m^3/s by applying the multiplication factors mentioned above.

The storage terms precipitable water content and soil moisture were published in kg/m^2 as instantaneous values. They were multiplied by the basin area as above and divided by the time frame (2 months, as represented in seconds – more details in Section 4.6) to obtain the monthly storage term tendency in m^3/s as required for the water balance equations. Similarly, the instantaneous variable snow-water-equivalent was published with units of m of water and was converted to m^3 by multiplying by the basin area and was then divided by the time frame to get m^3/s.

Personal Communication with NARCCAP Personnel

This chapter was sent in full (except for the preface) along with a summary of the results highlighting the large atmospheric water balance residuals in RCM3 and MM5I to Dr. Seth McGinnis, NARCCAP's Data Manager and User Community Manager. The purpose of this was to inform the modeling community about the residuals before the papers were submitted for publication and to see if they were able to provide further insight into their root cause. As a check, Dr. McGinnis conferred with a colleague at University Corporation for Atmospheric Research (UCAR) who concurred that the calculations appeared correct (especially since the balances for other RCMs were well within acceptable limits) and that the residuals were most likely a modeling issue. She characterized the large imbalances as "disappointing, but definitely not shocking." In addition to the reasons discussed in Section 4.6, Dr. McGinnis also mentioned the nesting might make it impossible for any RCM to guarantee a mass balance. For further insight

he suggested contacting his colleague Dr. Melissa Bukovsky, who specializes in model error. (Personal communication with Seth McGinnis, mcginnis@ucar.edu, May 8, 2014.)

Dr. Bukovsky had noticed discrepancies in the RCM3 output in the past and attributed it in part to the fact that the model had no sea ice (in base period, future period or NCEP simulations). This may have had strange effects on moisture transport, especially from the Hudson Bay region. Though it does not explain the apparent loss of water in the atmosphere; From Figure 4.2 one can deduce anomalously high evaporation rates are not a concern for RCM3. She also mentioned some issues with MM5I-ccsm were discovered however she was unable to isolate the problem. (Personal communication with Melissa Bukovsky, bukovsky@ucar.edu, May 19, 2014.)

Water Balance Component Value Check

Each of the water balance components of RCM3-cgcm3 were compared to those of CRCM-cgcm3 (CRCM had minute water balance residuals in comparison with RCM3) to ensure that there were no obvious problems with the magnitudes. All components were found to have comparable values, however those of RCM3 appeared consistently larger. Figure 4.E shows an example plot of this check for atmospheric moisture convergence for the first five years of the base period, which shows that annual cycles and magnitudes are similar and that there were no obvious issues.

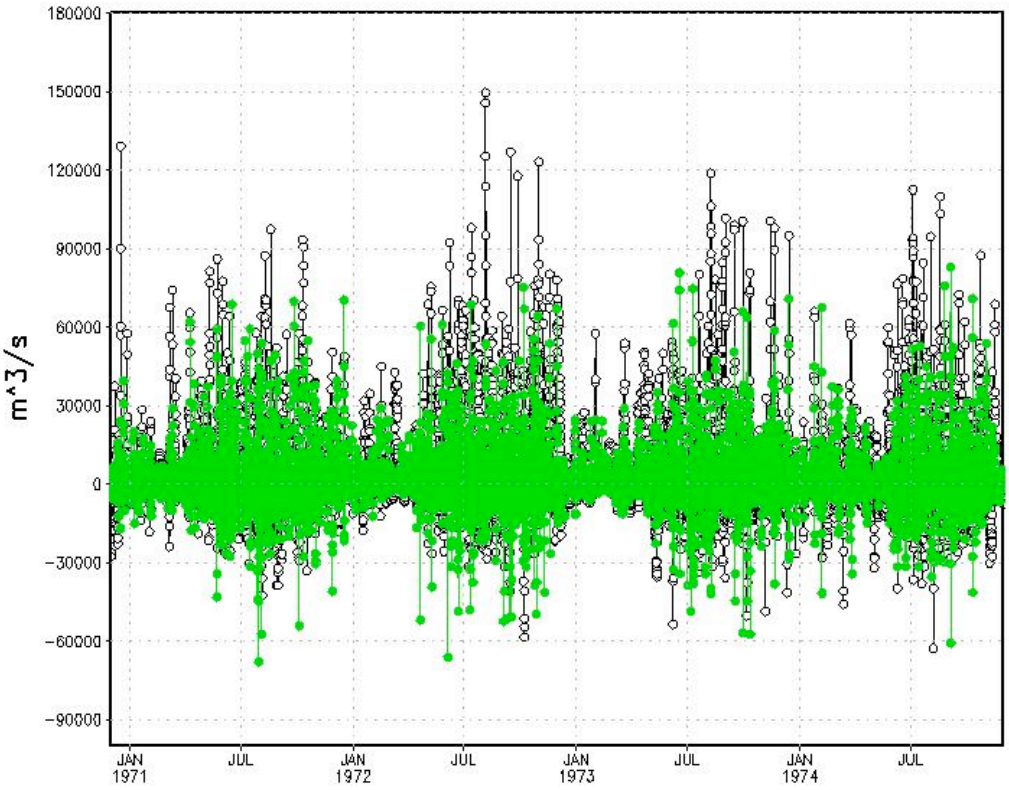

Figure 4.E – Daily basin total atmospheric moisture convergence plots for RCM3-cgcms (white circles) and CRCM-cgcm3 (grey).

4.3. Introduction

There is a growing realization in scientific and engineering communities that a changing global climate requires the use of high-resolution climate models to aid the design and planning of large-scale water resource projects (Dimri 2012). Simple use of historical climate records is inadequate when planning for mean hydrological states and extreme events as both are influenced by climate change (Trenberth et al. 2003). In order to determine the effectiveness of a climate model's ability to simulate the hydrological cycle, and therefore its usefulness to water resource managers, one must examine its atmospheric and terrestrial water balances (Berbery and Rasmusson 1999). It is

recognized that simulation of the water cycle and the wide variety of physical processes involved is a key factor in a model's ability to effectively simulate current and future climates (Chahine 1992, Hack et al. 1998). Hu *et al.* (2005) stated that the "examination of moisture simulation as it relates to climate likely holds the key to our understanding and eventually resolving issues surrounding model uncertainty."

General circulation models (GCMs) and high resolution regional climate models (RCMs) both play an important role in developing an accurate water balance (Berbery and Rasmusson 1999). Moisture is involved in a diverse range of temporal and spatial scales: from minutes to decades and from the micro-physical level up to global circulation. It has been found that water climatologies are different from model to model for a number of reasons (Wang and Paegle 1996), some of which will be explored in this work. Additionally, differences in climate sensitivity (defined as the equilibrium global mean temperature increase caused by doubling atmospheric CO2 concentrations) between climate models can be explained in part by differences in projected moisture levels, where the simulation and parameterization of surface and boundary layer processes are largely responsible (Hu et al. 2005). It is apparent that moisture and its motion is a major climatological factor for any basin (Liu and Stewart, 2003).

Motivation

There are several reasons for undertaking a water balance study. This section discusses a selection of motivations for, and examples of, existing studies.

One motivation is to examine model uncertainty, improve climate model processes and parameterization and validate the physical consistency of climate models. Along this vein, Music and Caya (2007) performed a comprehensive validation of water budget components of a basin with respect to the annual mean and annual cycle. Roads *et al.* (1998) evaluated climate models by examining the vertical distribution of water budget residuals as well as the fit of primary variables to observations. These types of studies typically focus on one or two specific climate models.

Another common objective is to understand the hydrologic processes of a region and how they evolve over time. Strong et al. (2002), part of the Global Energy and Water Exchanges Project (GEWEX), performed water balance study on the Mackenzie River Basin. The primary objective of GEWEX was to quantify all aspects of the hydrological cycle of the Mackenzie River Basin for purposes of investigating the impacts of climate change on the water budget. Jin and Zangvil (2010) calculated moisture convergence, precipitable water, precipitation and evaporation over the Eastern Mediterranean.

A third reason for water balance studies is to obtain approximations for difficult-to-observe variables. Serreze et al. (2003) use NCEP/NCAR global reanalysis to calculate precipitation minus evapotranspiration (P-E) from the moisture flux convergence for several large arctic basins. Seneviratne et al. (2004) and Hirschi et al. (2006) showed that one can effectively estimate basin scale terrestrial water storage using atmospheric and terrestrial water balance equations, plus streamflow measurements.

Accordingly, the purpose of this paper is twofold: (i) To investigate the physical consistency of a selection of RCMs forced by various GCMs over the Churchill River Basin in Labrador, Canada; and (ii) to identify reasons why the atmospheric and terrestrial water budgets do not balance.

Study Region

The Churchill River Basin is located in Labrador, Canada and covers roughly 92 500 km^2. It is the site of the existing Churchill Falls Hydroelectric Facility and the Lower Churchill Hydroelectric Project, the first phase of which is under construction. Figure 4.1 shows the basin outline, topography, and common grid resolution (0.25 degrees) to which all the models in this study were re-gridded.

Early work on water balances was limited to basins larger than $2x10^6$ km^2, due primarily to low radiosonde observation density and sampling frequency (Min and Schubert 1997, Rasmusson 1968). More recently, a commonly touted critical size for water balance computations using atmospheric reanalysis is on the order of 10^5 km^2. That being said, Hirschi et al. (2006) performed water balances on three Churchill River-sized basins (84 144, 85 223 and 94 836 km^2 respectively) with acceptable imbalances. All studies mentioning critical basin size have used observation, analysis and reanalysis data sets with roughly 1 degree resolution and larger. Higher resolution climate models, such as those used in this study (50 km horizontal grid spacing and 3-hour sampling frequency) should be able to provide reliable water balances for domains the size of the Churchill River Basin (Jin & Zangvil 2010). The 0.25 degree grid to which all model output was

regridded does not provide additional information in this respect, though it does allow for better representation of the irregular basin boundaries.

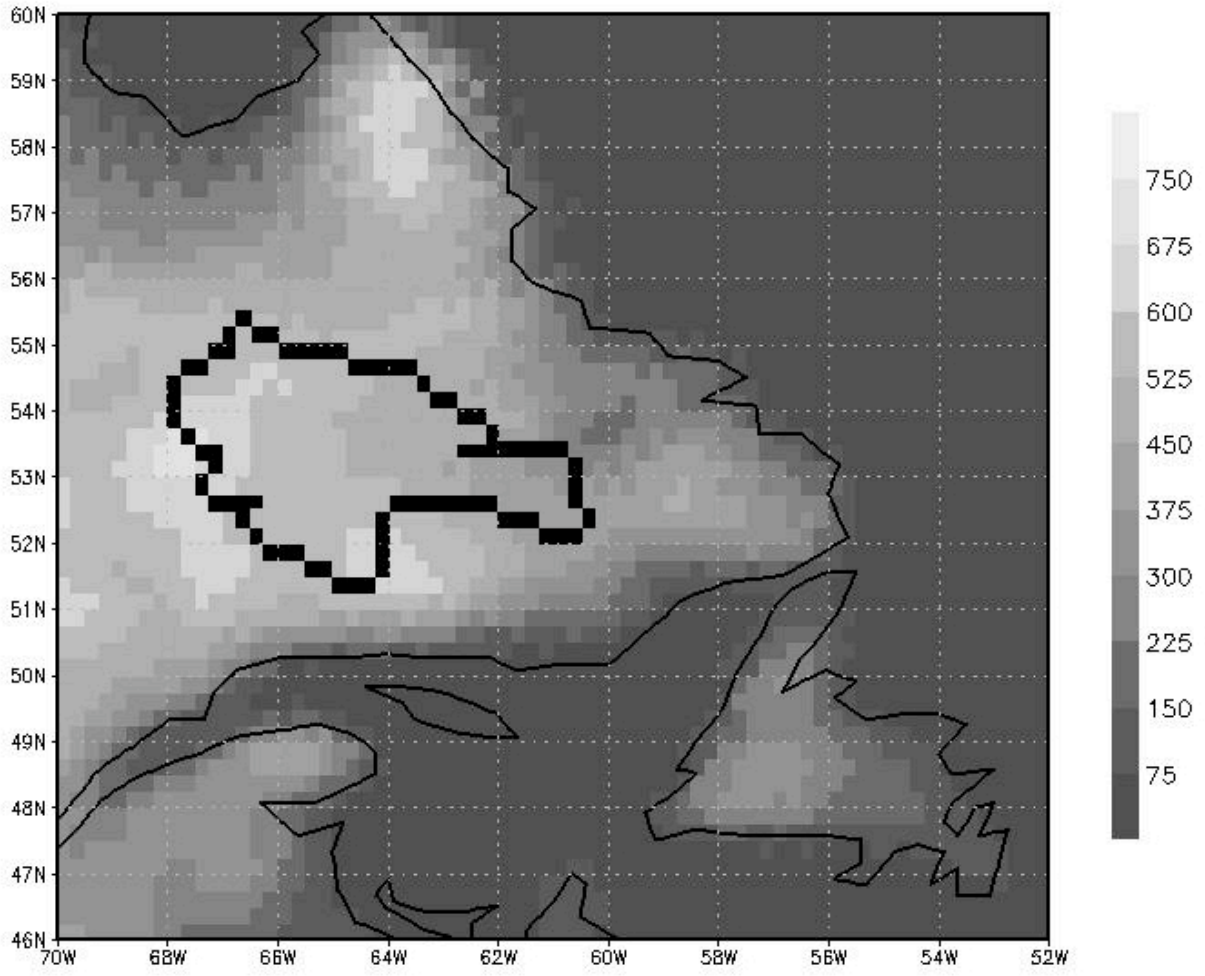

Figure 4.1 - Churchill River Basin (thick black outline) and regional topography (scale in metres). The thin black line represents the coastline.

Literature Review

There is a great deal of interdependence within modelling processes as well as components of the water cycle making the isolation of a single source of imbalance difficult. Every factor and process involved in water cycle simulation is potentially

important and should not be discounted without just cause. The following review highlights potential causes of water balance residuals from the variety of published literature. These potential causes are organized into categories below.

Vertical Coordinate System and Spatial Resolution

The conversion from a model's native vertical coordinate system to published pressure levels has been known to introduce mass imbalances up to a relative magnitude of 100% depending on the region and variable of interest (Serreze et al. 2003, Berbery and Rasmusson 1999, Trenberth 1991). These imbalances are mostly systemic and decrease in magnitude as vertical resolution increases. Similarly, some vertical coordinate systems are more susceptible to the introduction of errors during vertical integration than others (e.g. pressure levels vs. sigma levels (Liu and Stewart, 2003)).

Complex topography leads to difficulties in simulating water vapour transport at lower levels, though a sigma level approach has been shown to better resolve the atmospheric boundary layer and reduce this aspect of bias (Chen et al. 1996, Liu and Stewart 2003). This is not a predominant factor in the current study as the topography of the basin is relatively uncomplicated compared to the mountainous regions of other studies. Errors in surface pressure fields and topography, in addition to the vertical resolution and post-processing, also play a role balancing the water budget (Min and Schubert 1999).

Roads et al. (1998) found that initializing an 18-level climate model with a 28-level analysis simulation produced larger budget imbalances than when vertical levels aligned

(despite the application of a variety of digital filters), showing that discrepancies between GCM and RCM vertical levels are a contributing factor.

Liu and Stewart (2003) postulated that a small domain size and low spatial resolution (e.g. only 15 grid points at 2.5 degree resolution), would not effectively capture local convection events, drastically affecting local water contents.

Temporal Resolution and Sampling Frequency

Inadequate sampling of instantaneous variables (e.g. wind) cannot be compensated for by using long sample periods, and it has been found that moisture convergence is the variable most strongly affected by sampling frequency (Chen et al. 1996). Imbalances as large as the moisture convergence itself over mid-latitude storm tracks were found when using 12-hourly, or even sometimes 6-hourly sampling. This was a result of the low sampling frequency being unable to adequately capture the high variability of the diurnal cycle. Roads et al. (1998) discussed this sampling issue while investigating non-linear fluxes.

As a subset of moisture convergence, the ability to resolve low-level jets also leads to errors, though in North America this issue is concentrated primarily in the great plains regions (Chen et al. 1996). Resolution of the diurnal cycle is important to regions with low-level jets (Berbery and Rasmusson 1999), which are not a major source of influence over the Churchill River Basin. They recommend 8 timesteps per day (3-hour intervals) to effectively capture the diurnal cycle, especially for smaller basins.

Model Processes and Parameterization

Parameterizations of smaller scale turbulent processes, such as condensation, boundary layer moisture flux, boundary layer temperature flux, and net radiation flux (shortwave and longwave) at the surface all contribute to the water budget. Jin & Zangvil (2010) argue that the residuals in atmospheric water balances can be attributed mainly to the theoretical treatment of the water budget equations. They found that assimilating empirical data decreased residuals, though this approach is only viable when using reanalysis models, such as NCEP or ERA-40.

Ruane (2010) found that regions where seasonal precipitation draws primarily from atmospheric moisture convergence are sensitive to dynamical processes (e.g. large-scale waves, circulations or conditions favourable to mesoscale activity) while regions with a high recycling ratio are more sensitive to processes affecting atmospheric stability (e.g. land-surface interaction, boundary layer physics and convective processes).

Global fields of precipitation, temperature and motion strongly depend on land-surface evapotranspiration (Shukla and Mintz 1982), which is generally parameterized as the sum of soil evaporation, vegetation evaporation and vegetation transpiration (Wang and Dickinson 2012). Different land-surface models give a wide range of ratios of transpiration to total evapotranspiration. Parameterized latent heat loss (as evapotranspiration) typically accounts for about 60% of net surface radiation, though it

can vary between models from below 50% to almost 90% (Wang and Dickinson 2012, Trenberth et al. 2009), contributing to inter-model discrepancies.

Terrestrial water storage is a key part of the water balance and hydrological cycle as it determines the partitioning of the water and energy fluxes at the land-surface (Mueller et al. 2011). While the importance of soil moisture's impact on terrestrial water balances is intuitive it is also important for atmospheric water balances in regions with high precipitation recycling. As with the evapotranspiration ratio above, estimates of soil moisture on a regional scale differ greatly from model to model (Hirschi et al. 2006; Reichle et al. 2004; Schär et al. 1999).

Climate Models

The North American Regional Climate Change Assessment Program (NARCCAP) is an international collaboration whose primary purpose is to create high-resolution climate simulation of North America in order to examine uncertainties within the member RCMs and the driving GCMs (Mearns et al. 2009). NARCCAP ensemble members simulate a base period (1971-2000) and a future period (2041-2070) under the IPCC A2 emission scenarios (IPCC 2000) using various map projections at 50 km resolution. To give an idea of the variety of modelling and parameterization strategies employed by different modelling groups, a brief synopses of the RCMs and GCMs used in this study are presented in Tables 4.1 and 4.2 respectively. More information can be found at http://www.narccap.ucar.edu/about/index.html.

Table 4.1 - NARCCAP RCM Characteristics

RCM	Reference	Dynamics Core	Vertical Levels	Vertical Coord-inates	Convective Parameter-ization	Land-Surface Scheme	# Veg. Classes	Spectral Nudging
CRCM	Caya and Laprise (1999)	Nonhydrostatic, compressible	29	Gal-Chen scaled-height	Mass-flux	CLASS	21	Yes
HRM3	Jones et al. (2004)	Hydrostatic, compressible	19	Hybrid terrain following -pressure	Mass-flux (incl. downdraft)	MOSES	53	No
MM5I	Grell et al. (1993)	Nonhydrostatic, compressible	23	Sigma	Kain-Fritsch2 mass flux	NOAH	16	No
RCM3	Giorgi et al. (1993a,b); Pal et al. (2000,2007)	Hydrostatic, compressible	18	Terrain following	Grell (with Frisch-Chapel closure)	BATS	19	No
WRFG	Skamarock et al. (2005)	Nonhydrostatic, compressible	35	Terrain following	Grell	NOAH	24	No

Table 4.2 - NARCCAP GCM Characteristics

GCM	Reference	Horizontal Atmospheric Resolution	Vertical Layers	Top Level	Climate Sensitivity*
ccsm	Collins (2006)	1.4° x 1.4°	26	2.2 hPa	2.7 °C
cgcm3	Flato (2005), Scinocca and McFarlane (2004)	1.9° x 1.9°	31	1 hPa	3.4 °C
gfdl	GFDL (2004)	2.0° x 2.5°	24	3 hPa	3.4 °C
hadcm3	Gordon et al. (2000), Pope et al. (2000)	2.5° x 3.75°	19	5 hPa	3.3 °C

*Climate sensitivity is defined as the projected change in mean global temperatures when a GCM is forced by twice the atmospheric greenhouse gas concentrations as compared to pre-industrial levels.

4.4. Methodology

To determine the movement of moisture into and out of a basin, the atmospheric and terrestrial water balances were calculated for mean monthly climatologies. The equations for each water balance are presented below, 4.1 and 4.2 respectively (see Rasmusson (1968) and Peixoto and Oort (1992) for more details). The units of each component in Equations 4.1 and 4.2 were converted to m^3/s for consistency across each water balance. For the Churchill River Basin 1070.6 m^3/s is approximately 1.00 mm/day.

$$-\frac{\partial W}{\partial t} - \nabla_H \vec{Q} = P - E + \varepsilon_A \qquad (4.1)$$

$$R + \frac{\partial S}{\partial t} = P - E + \varepsilon_T \qquad (4.2)$$

Where: W = precipitable water content of the atmosphere;

$-\nabla_H \vec{Q}$ = atmospheric moisture convergence;

$\vec{Q}$ = vertically integrated horizontal water vapour flux;

$P - E$ = precipitation minus evaporation;

R = land-surface runoff;

S = terrestrial water storage terms, including snow pack and soil moisture;

ε_A = atmospheric water balance residual;

ε_T = terrestrial water balance residual.

The atmospheric moisture convergence, which reflects how much water is advected into or out of a basin via the atmosphere over a period of time, is a large component of atmospheric water balances and Seneviratne et al. (2004) has a detailed description of its computation. The horizontal water vapour flux was calculated for each grid point by multiplying the specific humidity by the meridional and zonal (south to north and west to east respectively) wind components, to get two respective values of flux for each grid point. The vertical integration of the horizontal water vapour flux was then performed in the Grid Analysis and Display System (GrADS), using the *vint()* function, which takes the sum of the mass-weighted layers between the surface (as defined by surface pressure) and the top of the atmosphere (as defined by the uppermost pressure level available, 50 hPa). This provided the total vertical column amount of moisture flux in each of the meridional and zonal directions. The divergence of these vertically integrated values were then calculated for the entire basin, the negative of which was the resulting atmospheric moisture convergence.

Tendencies of the precipitable water content ($\frac{\partial W}{\partial t}$) and terrestrial water storage ($\frac{\partial S}{\partial t}$) terms were calculated on a monthly basis. For example, the precipitable water tendency value for April resulted from the difference between the value of W for May and March, divided by the ∂t of two months.

Evaporation was calculated by dividing surface latent heat flux (W/m^2) by the latent heat of vaporization of water (the temperature dependent values for which were found in

Rogers and Yau (1984)). This was necessary because the NARCCAP variable representing evaporation (evps, "surface evaporation of condensed water") was not published for each model. The calculated evaporation was compared to published evps values (when available) over ocean grid points and was found to be identical, confirming the validity of the evaporation calculation.

4.5. Results

In this section, various components of the atmospheric and terrestrial water balances, including absolute and relative residuals, are discussed. As a point of reference, the Churchill River's observed mean streamflow is roughly 1825 m^3/s (1.70 mm/day) (Water Survey of Canada, 2010) and the mean simulated runoff from all NARCCAP ensemble members used here is 1539 m^3/s (1.44 mm/day) for the base period 1971-2000. Mean ensemble P-E is 1618 m^3/s (1.51 mm/day).

Figure 4.2 shows base period ensemble member simulations and corresponding observations for precipitation and runoff. Monthly precipitation data was extracted from the Global Precipitation Climatology Centre's (GPCC) 0.5 degree resolution data set (Meyer-Christoffer et al., 2011). The gridded GPCC data was checked against four corresponding Environment Canada in-situ meteorological stations in, and around, the Churchill River Basin and any discrepancies in mean monthly values were found to be less than 0.2 mm/day.

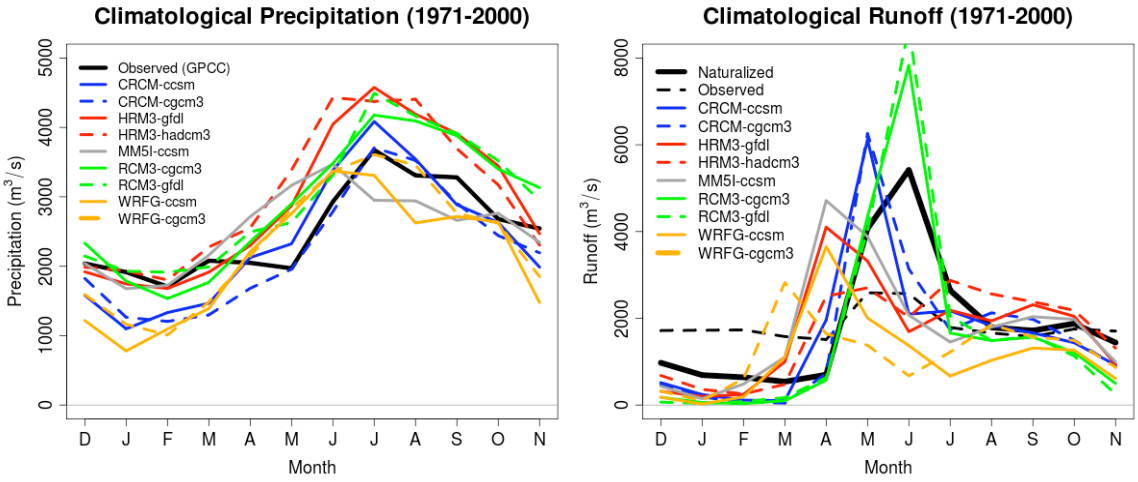

Figure 4.2 - Mean simulated precipitation (left) and runoff (right) compared to observations.

Since roughly three-quarters of the runoff in the Churchill River basin occurs upstream of the Churchill Falls hydroelectric facility a direct comparison between simulated runoff and observed streamflow at the river's outlet would not be useful. Naturalized flow, which negates the effects of damming and water management, is preferred for model validation (Music and Caya, 2007). As such, Figure 4.2 uses naturalized streamflow data, created by Vincent and Latraverse (2000), which accounts for the impact of the reservoirs and control structures of Churchill Falls. They approximated natural inflows into each reservoir (I_N) (i.e. runoff) by applying Equation 4.3.

$$\frac{dS}{dt} = I_N + I_C - O_C \qquad (4.3)$$

Here, dS/dt is the change in reservoir storage, I_C is the controlled inflow into the reservoir (via control structures) and O_C is controlled outflow form the reservoir. Direct precipitation and evaporation over the reservoir are considered to be implicit in the

measured dS/dt. The mean annual observed streamflow is 1825 m^3/s and the mean annual naturalized streamflow is 1875 m^3/s. Observed streamflow is slightly lower due to the additional evaporation from the reservoirs. Both observed and naturalized flow can be seen in Figure 4.2.

The observed precipitation and the naturalized flow both fell within the bounds of the ensemble's simulations, giving one confidence that the simulations provide adequate representations of base period precipitation and runoff. The only exception was simulated November, December and January runoff which was lower than the naturalized flow.

Figure 4.3 plots each ensemble member's base period component breakdown along with the atmospheric and terrestrial residuals. (Note that certain components were not available for all ensemble members.) From Figure 4.3 it is apparent that the precipitable water tendency (the change in precipitable water over time) contributes the least to the water balance from month to month. This is an expected result that has been found by others (Dimri 2012, Berbery and Rasmusson 1999, Chen et al. 1996).

Similar results were found for the future period, however the plot was omitted for space considerations (Figure 4.A).

Over the span of a year, precipitation contributes the most to each water balance, except for RCM3 and MM5I members where atmospheric moisture convergence dominates. Noticeable spikes occur in runoff in spring, which is a direct result of the spring melt's decrease in snow water equivalent stored on the land surface. Soil moisture also increases

as the snowpack melts. HRM3-hadcm3 is the only ensemble member that does not follow this norm – runoff plateaus in April and remains high into the fall. Also, the amplitude of its soil moisture tendency is relatively high compared to other models.

Moisture convergence in consistently positive throughout the year for all ensemble members, indicating that the Churchill River Basin is a moisture sink year round. Both precipitation and evaporation are highest in the summer for all ensemble members.

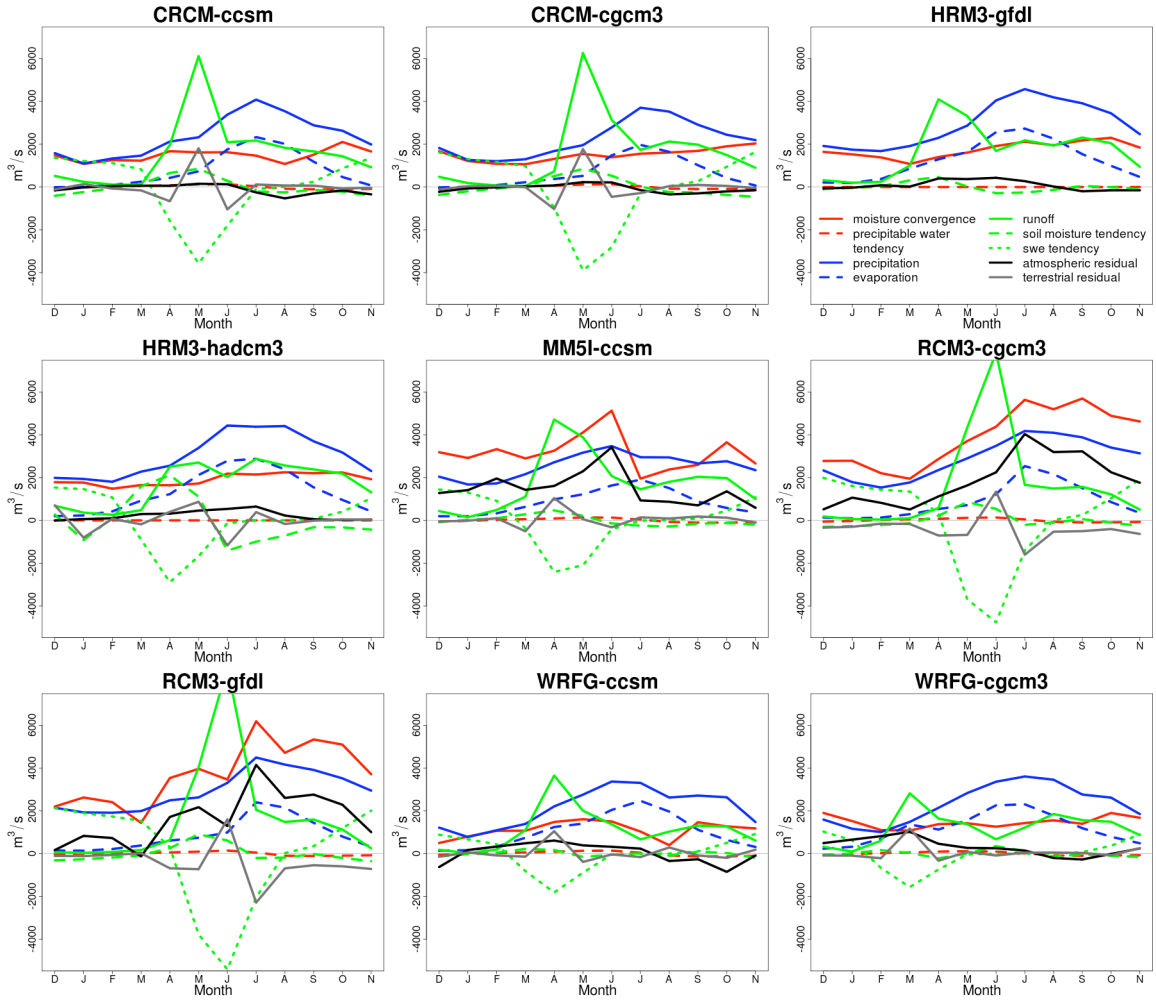

Figure 4.3 - Base period water balance component breakdown.

There are clear differences between ensemble members, the largest of which can be found in atmospheric moisture convergence where RCM3-cgcm3, RCM3-gfdl and MM5I-ccsm are substantially higher than the bulk of the ensemble, especially in the summer and fall months.

While some similarities and differences between moisture balance components for a given time period and ensemble member can be gleamed from the plots, a quantitative summary of the water balance residuals, as found in Tables 4.3a and 4.3b, will give a better idea of water balance closure.

Mean Annual Residuals

The mean terrestrial water balance residual (ε_T) was always much less than the atmospheric (ε_A) for all models and time periods. The future period ε_A was typically larger than the base period with the exceptions of CRCM-cgcm3 and WRFG-cgcm3, while the direction of change in ε_T from base to future varied with each model.

CRCM and HRM3 ensemble members typically had the lowest mean residuals for both base and future periods, while WRFG was only slightly larger. RCM3 models consistently had the highest ε_A and ε_T. The MM5I-ccsm ensemble member had a relatively high atmospheric residual, but a relatively low terrestrial residual (future period data for MM5I-ccsm were not published at the time of analysis).

Table 4.3a – Base period atmospheric and terrestrial water balance residual values (m^3/s) for all available ensemble members

		BASE PERIOD (1971-2000)									
		CRCM ccsm	CRCM cgcm3	HRM3 gfdl	HRM3 hadcm3	MM5I ccsm	RCM3 cgcm3	RCM3 gfdl	WRFG ccsm	WRFG cgcm3	**RMSR**
Atmospheric Residual (m^3/s)	**Dec**	-109	-96	-100	21	1314	648	28	-240	638	**542**
	Jan	1	-12	-30	60	1450	1119	839	194	701	**714**
	Feb	-2	-50	81	97	1910	783	693	274	774	**777**
	Mar	-35	-46	20	294	1313	419	-209	363	943	**583**
	Apr	-103	-58	399	313	1432	976	1595	426	288	**822**
	May	-98	-4	371	455	2025	1402	1987	121	21	**1074**
	Jun	-127	-44	431	534	3157	1980	1006	36	38	**1308**
	Jul	-320	-213	273	643	862	3949	4044	153	100	**1925**
	Aug	-365	-194	23	225	1016	3327	2798	-171	-23	**1498**
	Sep	-85	-107	-198	51	915	3417	2976	-5	-140	**1544**
	Oct	44	-33	-155	18	1571	2431	2470	-593	133	**1286**
	Nov	-164	-1	-147	41	737	1846	1167	104	443	**787**
	MEAN	**-114**	**-71**	**81**	**229**	**1475**	**1858**	**1616**	**55**	**326**	**968**
	RMSR	**164**	**98**	**235**	**311**	**1606**	**2179**	**2025**	**276**	**476**	**1151**
Terrestrial Residual (m^3/s)	**Dec**	-139	-113	N/A	706	-53	-337	-108	-152	-35	**292**
	Jan	134	37	N/A	-805	-14	-301	-112	58	-69	**312**
	Feb	-69	50	N/A	68	99	-156	-59	-83	-207	**112**
	Mar	-159	-6	N/A	-184	-512	-170	20	-139	1135	**455**
	Apr	-664	-1029	N/A	396	1034	-711	-683	1049	-389	**787**
	May	1812	1771	N/A	868	53	-681	-725	-386	50	**1020**
	Jun	-1044	-460	N/A	-1172	-326	1341	1606	-35	-147	**947**
	Jul	118	-282	N/A	383	139	-1606	-2287	-157	-19	**1006**
	Aug	70	43	N/A	-172	85	-531	-685	290	-2	**331**
	Sep	66	99	N/A	-15	179	-506	-540	-82	61	**275**
	Oct	-72	51	N/A	43	125	-407	-591	-194	67	**270**
	Nov	-30	-41	N/A	40	-97	-630	-711	183	309	**361**
	MEAN	**2**	**10**	**N/A**	**13**	**59**	**-391**	**-406**	**29**	**63**	**202**
	RMSR	**640**	**614**	**N/A**	**551**	**358**	**747**	**933**	**352**	**367**	**603**

Tables 4.3b – Future period atmospheric and terrestrial water balance residual values (m^3/s) for all available ensemble members

		FUTURE PERIOD (2041-2070)									
		CRCM ccsm	CRCM cgcm3	HRM3 gfdl	HRM3 hadcm3	MM5I ccsm	RCM3 cgcm3	RCM3 gfdl	WRFG ccsm	WRFG cgcm3	**RMSR**
Atmospheric Residual (m^3/s)	**Dec**	-95	41	-117	N/A	N/A	1038	837	427	769	**607**
	Jan	-61	-17	-26	N/A	N/A	530	684	536	782	**486**
	Feb	-58	-60	38	N/A	N/A	681	672	541	907	**540**
	Mar	-18	-15	201	N/A	N/A	676	706	625	740	**526**
	Apr	-56	-45	296	N/A	N/A	1062	582	327	373	**508**
	May	-204	-38	340	N/A	N/A	1734	1324	53	34	**839**
	Jun	-181	-120	426	N/A	N/A	3934	2773	297	-183	**1833**
	Jul	-527	-84	556	N/A	N/A	4387	4557	17	-118	**2409**
	Aug	-421	-79	-69	N/A	N/A	3134	4105	-58	-176	**1960**
	Sep	-166	-26	-118	N/A	N/A	4429	4159	-199	52	**2299**
	Oct	-322	-92	-153	N/A	N/A	2790	3692	-150	-75	**1756**
	Nov	-2	116	-195	N/A	N/A	2079	1544	381	266	**998**
	MEAN	**-176**	**-35**	**98**	**N/A**	**N/A**	**2206**	**2136**	**233**	**281**	**1171**
	RMSR	**238**	**70**	**263**	**N/A**	**N/A**	**2625**	**2627**	**361**	**489**	**1429**
Terrestrial Residual (m^3/s)	**Dec**	-90	7	N/A	N/A	N/A	-364	-314	20	-31	**200**
	Jan	151	-33	N/A	N/A	N/A	-239	-240	95	-121	**164**
	Feb	-305	50	N/A	N/A	N/A	-320	-204	-206	-111	**222**
	Mar	-356	-205	N/A	N/A	N/A	-217	-198	-67	854	**406**
	Apr	286	-807	N/A	N/A	N/A	-1109	-754	890	-153	**747**
	May	812	2031	N/A	N/A	N/A	557	-129	-233	156	**930**
	Jun	-490	-995	N/A	N/A	N/A	-497	76	-183	-391	**527**
	Jul	-116	53	N/A	N/A	N/A	-802	-1289	-91	650	**677**
	Aug	-70	56	N/A	N/A	N/A	-389	-976	495	-390	**501**
	Sep	35	-120	N/A	N/A	N/A	-552	-532	-307	48	**341**
	Oct	-194	173	N/A	N/A	N/A	-457	-327	47	350	**291**
	Nov	-45	-105	N/A	N/A	N/A	-604	-428	50	-238	**321**
	MEAN	**-32**	**9**	**N/A**	**N/A**	**N/A**	**-416**	**-443**	**43**	**52**	**250**
	RMSR	**328**	**700**	**N/A**	**N/A**	**N/A**	**563**	**578**	**328**	**378**	**500**

For both time periods, CRCM ensemble members had an overall negative mean ε_A, indicating that P-E was typically greater than the contributions of the atmospheric moisture convergence and the precipitable water tendency. All other ensemble members had overall positive mean ε_A, though some months for WRFG models and HRM3-gfdl showed negative residuals. Both RCM3 ensemble members had negative mean terrestrial water balance residuals for both time periods, meaning that P-E was typically greater than the combined contributions of runoff and the terrestrial water storage terms. The other models tended to be on the positive side (though close to zero), with the exception of future period CRCM-ccsm.

Annual Cycle of Residuals

In the discussion of the annual cycle, the root mean square residual (RSMR) gives a better idea than the mean of the magnitudes of ε_A and ε_T across the entire ensemble for each month and for the magnitude of variations from zero for each ensemble member throughout the year.

July had the highest atmospheric RMSR for both time periods, though September's RMSR was relatively close for the future period. Winter and early spring months had the lowest RMSRs. May had the highest terrestrial RMSR for both time periods, but July was a close second for the base period. February had the lowest RMSR for the base period, while January had the lowest for the future. Periods with large ε_A correspond with those

times of year when atmospheric moisture transport, precipitation and evaporation are highest, while large ε_T corresponds with the transition period of the spring melt.

WRFG and MM5I ensemble members had the lowest overall terrestrial RMSR for both time periods and CRCM-ccsm had an equally low RMSR for the future. RCM3-cgcm3 and RCM3-gfdl had the highest overall terrestrial RMSR for the base period while CRCM-cgcm3 had the highest for the future period. RCM3 members had the highest overall atmospheric RMSR for both time periods, while MM5I-ccsm was a distant second for the base period. CRCM-ccsm and CRCM-cgcm3 had the lowest atmospheric RMSR for both time periods.

Whether the terrestrial or atmospheric RMSR was larger depended on the time period in question and on individual ensemble members.

The low mean annual ε_T and high terrestrial RMSR for the CRCM ensemble members means that the month-to-month residuals nearly cancel out over the span of a year but there are substantial residuals when examining individual months, especially during the spring melt. A similar, but less severe, situation occurs in the WRFG and MM5I ensemble members.

Relative Residuals

Table 4.4 presents the mean atmospheric and terrestrial water balance residuals relative to simulated climatological P-E values. The magnitudes of atmospheric residuals range from 2.0 up to 102.8%, while the terrestrial residuals range from 0.1 to 19.5%.

For the most part, there is consistency in the relative size of the residuals between the base and future periods, indicating that the residuals are systemic (the primary exception being WRFG's atmospheric residuals). This is beneficial to climate change analyses as one is still able to gain insight from the differences between base and future periods, even if the residuals are larger than the climate change signal (which is the case for several ensemble members). The climate change signal for P-E ranges from 5.8 to 20.1%, with a mean increase of 8.6%. For a detailed look at the climate change signal of NARCCAP's models over the Churchill River Basin see Chapter 5.

Table 4.4 - Atmospheric and terrestrial residuals relative to climatological P-E for base and future periods, as well as P-E climate change signal $\Delta(P-E)$

		CRCM ccsm	CRCM cgcm3	HRM3 gfdl	HRM3 hadcm3	MM5I ccsm	RCM3 cgcm3	RCM3 gfdl	WRFG ccsm	WRFG cgcm3
1971-2000	$P-E$ (m^3/s)	1592	1583	1663	1687	1684	2028	2091	1084	1147
	ε_A (%)	-7.2	-4.5	4.9	13.6	87.6	91.6	77.3	5.1	28.4
	ε_T (%)	0.1	0.6	N/A	0.8	3.5	-19.3	-19.4	2.7	5.5
2041-2070	$P-E$ (m^3/s)	1739	1761	1761	N/A	N/A	2145	2272	1242	1377
	ε_A (%)	-10.1	-2.0	5.6	N/A	N/A	102.8	94.0	18.8	20.4
	ε_T (%)	-1.8	0.5	N/A	N/A	N/A	-19.4	-19.5	3.5	3.8
$\Delta(P-E)$ (%)		9.2	11.2	5.9	N/A	N/A	5.8	8.7	14.6	20.1

4.6. Discussion

Now that the atmospheric and terrestrial water balance residuals have been identified, this section will shed some light on the sources of imbalance in the current study. As discussed in the literature review of Section 4.3, there are many possibilities including choice of sampling frequency, coordinate system, post-processing, model processes and parameterizations, among others. The impact of each of these will vary and is quantified when possible.

Sampling Frequency

Published precipitation, evaporation and runoff data are averages over a 3-hour timestep (so one can easily find 3-hour totals) while specific humidity, wind components, precipitable water content, snow-water-equivalent and soil moisture are instantaneous values. The 3-hour sampling frequency of this study's RCMs was adequate to capture the diurnal cycle for all averaged and instantaneous variables (Chen et al.l 1996, Roads et al. 1998), however there is some imbalance introduced when sampling instantaneous variables. This is especially true for atmospheric moisture convergence which is the result of multiplying one instantaneous variable (specific humidity) with two others (meridional and zonal wind components). That being said, the sampling frequency was the same for RCM3 as it was for other models and both RCM3 ensemble members experienced relatively similar (and anomalously large) budget residuals for both base and future periods (and NCEP driven runs, see Figure 4.4 and Table 4.5). One would expect the non-linear impact of sampling to be considerably different across ensemble members,

even if they employ the same RCM. As such, it is unlikely that sampling frequency contributed substantially to water balance residuals, especially ε_T. In order to isolate the impact of sampling frequency, cumulative atmospheric moisture convergence values for each time step would be needed in addition to the instantaneous values.

Coordinate Systems and Post-Processing

All ensemble members operate in their own native coordinate systems (see Table 4.1) but the published NARCCAP data have all been interpolated to a common set of pressure levels (by the respective modelling groups) for the sake of data consistency. Published precipitable water values are calculated within each model's native vertical coordinate system. As such, by comparing the manual calculation of precipitable water (from specific humidity at each pressure level) to published values (calculated in a model's native coordinates) one can quantify the residual introduced to a single variable by converting to NARCCAP's pressure levels and undertaking a vertical integration. The range of these results, calculated using Equation 4.4, can be found in Table 4.5.

$$\varepsilon_{relative} = \left(\frac{W_{published} - W_{calculated}}{W_{published}}\right) \times 100\% \qquad (4.4)$$

This effect would be compounded when investigating moisture convergence as one must multiply specific humidity with wind at each level (meaning the values in Table 4.5 are conservative estimates). The mean values are relatively consistent for respective RCM regardless of the forcing GCM or the time period, implying that these residuals are

systemic. By considering the range of relative residuals one gains an appreciation for the potential contribution of conversion to pressure levels and vertical integration. Minimum and maximum values refer to residuals from individual 3-hour timesteps, while the mean spans the 30-year climatology. Some of the more extreme relative residuals were found when a precipitable water value (be it published or calculated) was anomalously small.

Table 4.5 - Range of relative residuals ($\varepsilon_{relative}$) resulting from conversion to pressure levels and the subsequent vertical integration

		CRCM ccsm	CRCM cgcm3	HRM3 gfdl	HRM3 hadcm3	WRFG ccsm	WRFG cgcm3
1971-2000	Min	-6.7 %	-11.3 %	-29.9 %	-27.2 %	N/A*	-15.5 %
	Mean	**8.0 %**	**8.3 %**	**7.3 %**	**5.1 %**	**0.5 %**	**0.9 %**
	Max	28.0 %	28.5 %	23.2 %	30.1 %	82.4 %	14.3 %
2041-2070	Min	-7.4 %	-10.4 %	-37.4 %	N/A	-60.5 %	-12.3 %
	Mean	**8.0 %**	**8.4 %**	**7.2 %**		**1.1 %**	**1.0 %**
	Max	38.2 %	28.6 %	24.2 %		18.1 %	7.3 %

* This value was not available as some precipitable water values were published as zero (an unrealistic value), resulting in an infinite residual.

Unfortunately, published precipitable water data were not available for RCM3 or MM5I so manual vertical integration was used to derive the precipitable water tendency for the water balance of Equation 4.1. Comparing tendencies calculated using published precipitable water data with those derived from manual vertical integration of other ensemble members showed this contributed on the order of 1% to precipitable water tendency values and made no substantial contribution to the overall residuals. Caution should be used when comparing the relative residuals found in the ensemble members of Table 4.5 to RCM3 and MM5I; Their respective atmospheric residuals were significantly

larger than other models and results indicated $\varepsilon_{relative}$ is strongly dependent on RCM choice.

On a climatological basis, mean annual residuals have a smaller magnitude than month-to-month values. During analysis, the time frame over which soil moisture, snow water equivalent and precipitable water tendencies were calculated was found to have an impact on the magnitude of the month-to-month residuals, predominantly because of snow water equivalent tendency during the spring melt. The storage tendency terms were calculated with a ∂t of two months, as represented in seconds (on average, 5 256 000 seconds per two months). If the tendency calculation was performed with a ∂t of one month (i.e. if April's value was the difference between April and March or the difference between May and April) then the magnitude of the storage tendency terms would be different. The impact of this evens out over the span of a year and did not substantially affect mean or RMS residuals.

Residuals at the 3-hour time interval of published data were also calculated and found to be almost identical to the mean annual residuals found above (< 1% difference) despite varying widely from timestep to timestep. The annual cycles of 3-hour residuals followed the same patterns as monthly residuals.

Modelling Processes and Parameterization Schemes

Labrador has a precipitation recycling ratio (i.e. the percentage of precipitation that originates from local evaporation) of roughly 6 to 9%, where a high recycling ratio is

considered to be greater than 20% (Trenberth 1998). Evidence of this can be found in Figure 4.3 where both atmospheric moisture convergence and land-surface evaporation play a significant role. The Churchill River Basin's mid-range recycling ratio implies that atmospheric water balances are influenced relatively equally by parameterizations and dynamical processes. Large-scale moisture advection is the only water balance process that is adequately resolved in most ensemble members. As such, parameterization is required to represent the unresolved processes (e.g. turbulence, convection, evaporation, condensation, radiative fluxes, etc.) with impacts on the water budgets that vary depending on the respective schemes. Some parameterization schemes allow a certain amount of water to be lost within specified accuracy limits (e.g. CRCM's land-surface scheme CLASS has an accuracy limit of $1x10^{-3}$ kg/m^2 (0.001 mm) per time step (Verseghy 2009)). More examples of variation have been found by others in evaporation and soil moisture schemes (see literature review in Section 4.3). The fallibility of parameterizations is further evidenced by unrealistic output values found in NARCCAP data, such as negative runoff and zero precipitable water content.

For a comparison of the isolated effects of the RCMs where the driving model is consistent across all models, Figure 4.4 presents the water balance component breakdown for four of NARCCAP's RCMs driven by NCEP Reanalysis II (Kanamitsu et al. 2002), for the timeframe 1980-2003 (there was insufficient MM5I data and no HRM3 swe data available for analysis). Table 4.6 explicitly lists the corresponding residuals. The differences in residuals between models emphasizes the role that individual RCMs and their respective coordinate systems, parameterizations and modelling processes play in

atmospheric and terrestrial water balances. There are strong similarities between the water balance components and residuals in Figure 4.4 and those in Figure 4.3 for each RCM, confirming the dominant role of the RCM over the forcing model.

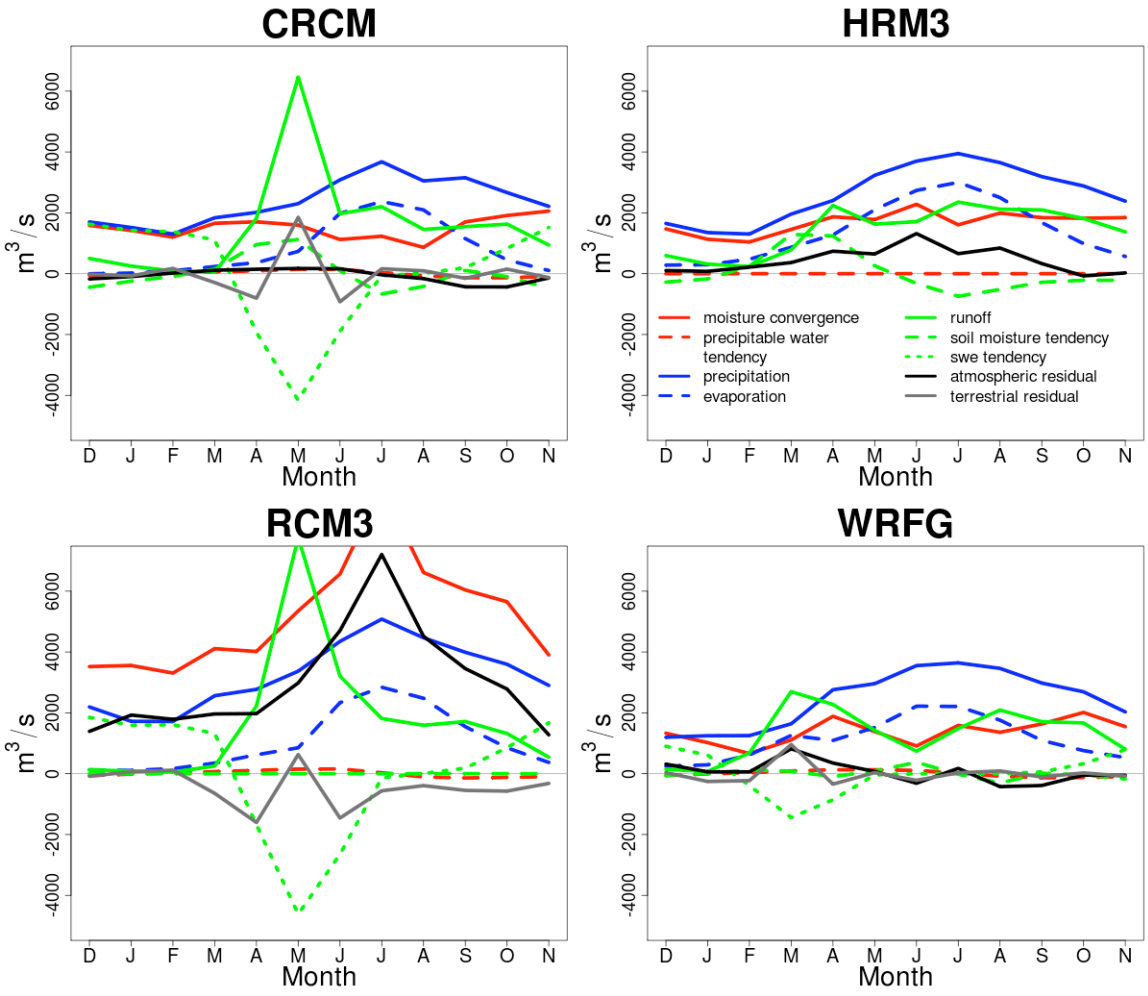

Figure 4.4 - NCEP Reanalysis II driven RCM water balance component breakdown.

Tables 4.6 - Atmospheric and terrestrial water balance residual values (m^3/s) for all available NCEP Reanalysis II driven models.

NCEP (1980-2003)												
Atmospheric Residual		CRCM	HRM3	RCM3	WRFG	RMSR	Terrestrial Residual		CRCM	RCM3	WRFG	RMSR
	Dec	-173	103	1390	314	720		Dec	-20	-85	36	54
	Jan	-96	77	1927	59	966		Jan	-70	63	-256	158
	Feb	20	215	1786	59	900		Feb	172	116	-229	178
	Mar	112	365	1963	818	1080		Mar	-291	-647	958	688
	Apr	147	739	1974	349	1071		Apr	-806	-1604	-344	1055
	May	172	646	2983	72	1529		May	1853	628	35	1130
	Jun	163	1318	4702	-314	2448		Jun	-925	-1458	-218	1005
	Jul	-38	658	7206	174	3619		Jul	162	-563	29	339
	Aug	-162	843	4516	-426	2308		Aug	94	-392	89	238
	Sep	-433	331	3454	-388	1759		Sep	-151	-550	-108	335
	Oct	-436	-74	2782	-46	1409		Oct	150	-573	25	342
	Nov	-142	25	1276	-54	643		Nov	-128	-319	-82	204
	MEAN	-72	437	2997	51	1515		MEAN	3	-449	-6	259
	RMSR	215	588	3430	338	1752		RMSR	655	749	320	604

Geographical Considerations

The influence of regional variation and basin size are also worth exploring. Dimri (2012) found that a similar version of RCM3-ncep had a much smaller water budget residual over the western Himalayas, despite the complex terrain, than was found here over the Churchill River Basin. Their study region was over 3.5 times larger and they investigated a rectangular domain as they weren't interested in a single basin. Music and Caya (2007) studied a similar version of CRCM-ncep over the Mississippi River Basin (3.2×10^6 km^2) and found that their water balance residuals followed a similar annual cycle of those in Figure 4.4 (with largest positive ε_A in late spring and largest negative ε_A in autumn), though they had a consistently smaller magnitude. The largest monthly ε_A was roughly 0.2 mm/day compared to 0.4 mm/day found here. (A previous version of CRCM had

larger mean annual and monthly imbalances. This was mitigated in the current version due to an adjustment applied to specific humidity values at each grid point.)

Another geographical consideration is that the Churchill River Basin is near the eastern lateral boundary of the NARCCAP domain. As the basin lies in a predominantly westerly atmospheric flow it is near the outflow region of each of the RCMs. This relative proximity to the lateral boundary may be introducing residual, particularly in the atmospheric water balance. It has been found that the outflow region in limited area models such as RCMS can exhibit physically inconsistent behaviour due to the requirement for the RCM data to align with that of the forcing GCM (Lucarini et al., 2007; Marbaix et al., 2003). This alignment occurs in the buffer zone where moisture imbalances are common and may result in numerical errors bouncing back into the RCM domain (Liang et al., 2001).

Various

While condensed moisture (e.g. as water or ice in clouds) is not included in the specific humidity or precipitable water variables used in this analysis, the contribution it makes is typically small (on the order of 1%). Atmospheric moisture convergence would also not account for the conversion of water vapour to cloud water or ice within the domain which is subsequently advected outside the domain. It is unlikely this accounts for a substantial portion of the atmospheric residual. Similar to precipitable water, sources of terrestrial

water storage other than soil moisture and snow pack (e.g. canopy interception) are also not accounted for in the water balance.

The only RCM in the current ensemble that used spectral nudging (pushing large-scale variable values for the entire domain closer to those found in the driving GCM) was CRCM and, as shown in Table 4.3, both CRCM ensemble members had relatively low residuals. One should not assume that spectral nudging implies a smaller residual as the onus of water balance closure is then shifted to the driving GCM, which is not guaranteed to be more physically consistent than the RCM. That being said, GCMs do not need to accommodate prescribed lateral boundaries and their respective buffer zones, which was discussed earlier as a potential contributor to RCM water balance residuals. More insight will be gained once simulation results are published for ECP2 (another NARCCAP RCM), which also uses spectral nudging.

In general from Figures 4.3 and 4.4 one can see simulated precipitation and evaporation are relatively consistent across ensemble members and are not substantially affected by the water closure issues, while the atmospheric moisture convergence varies greatly. This implies the potentially large biases in the atmospheric moisture convergence are not strongly communicated to surface hydrology by means of precipitation or evaporation. This physical inconsistency raises concerns about some models' suitability for hydrological analysis.

4.7.Summary and Conclusions

Mean annual atmospheric and terrestrial water balance residuals were quantified as were their mean annual cycles. The atmospheric water balance residuals were consistently higher than the terrestrial residuals, regardless of time period or ensemble member. Some of this difference can be attributed to the residual resulting from the interpolation of atmospheric data to pressure levels and its subsequent integration, found in Table 4.5.

With regard to the annual cycle, the winter and early spring months had the lowest overall RMSRs. The highest atmospheric RMSR was in mid to late summer, while the highest terrestrial RMSR was during the spring melt. There was no pattern across time periods or ensemble members as to whether the terrestrial or atmospheric RMSR was the highest.

Water balance residuals were found to be much more consistent between common RCMs than common GCMs. This implies that residuals are largely a function of RCM and not the driving GCM. Similarly, water balance residuals have been found to be predominantly systemic, implying that anomalies (including inter-annual variation and the climate signal) are better represented than individual field values.

While it wasn't feasible to isolate all root causes of the atmospheric and terrestrial water cycle imbalances this study was able to explore or quantify some causes and eliminate others. At this point, it would be premature to rank the models for physical consistency, as the investigation needs to expand to include additional regions of varying

climatologies and sizes. This can be accomplished by expanding the boundaries of the Churchill River Basin to cover an area greater than 2×10^5 km^2 and comparing the results to those found here and to an equally sized region (elsewhere in North America) modelled by NARCCAP. Additional sources of uncertainty that merit further investigation include the impacts of vertical coordinate system choice (plus vertical coordinate discrepancies between RCM and GCM), parameterization scheme choices, and spectral nudging. Detailed investigation of individual parameterization schemes and dynamic processes is beyond the scope of this paper and would be most effectively investigated by individual modelling teams.

A further check on the suitability of the models' for hydrological studies would come in the form of an energy balance analysis. As water and energy are strongly linked in the climate and in climate models it would be useful to examine whether similar imbalances exist in terrestrial and atmospheric energy balances, providing insight into the root causes of the residuals. If there is a substantial energy imbalance, one can infer the models are flawed and potentially unsuitable for use in climate change impact studies.

One recommendation that should be incorporated into future ensemble studies is to publish accumulated moisture convergence fields calculated using an RCM's native vertical coordinate system. This would provide a consistent variable across all ensemble members without the additional residual introduced by converting to, and performing calculations in, a pressure level coordinate system. (Not to mention drastically reduce the amount of data to download and store!)

While NARCCAP's ensemble is imperfect (as are all simulations), it is still able to provide much useful information, particularly about the impacts of climate change. Water balance errors were found to be largely systemic, meaning that anomalies and changes over time (e.g. under climate change) are more reliable than individual field values (Berbery and Rasmusson 1999, Trenberth 1991). Even if atmospheric and terrestrial water balance residuals exist, models still provide useful information about a basin's moisture flux (Liu and Stewart, 2003). Additionally, long term average moisture convergence and P-E should equal long term average runoff, providing insight for practical applications such as water resource management, as investigated in Chapter 5.

4.8. Acknowledgements

This work would not have been possible without the generous financial support of Nalcor Energy Inc, NSERC, Mitacs and TD Canada Trust.

We wish to thank the North American Regional Climate Change Assessment Program (NARCCAP) for providing access to the data used in this paper. NARCCAP is funded by the National Science Foundation, the U.S. Department of Energy, the National Oceanic and Atmospheric Administration, and the U.S. Environmental Protection Agency Office of Research and Development.

4.9. References

Berbery, E., & Rasmusson, E. (1999). Mississippi moisture budgets on regional scales. *Monthly Weather Review, 127*, 2654-2673. DOI:10.1175/1520-0493(1999)127<2654:MMBORS>.

Bispham, P. (2014). Interpolation: Introduction and Basics. *ECMWF Computer User Training Course 2014*. United Kingdom.

Caya, D., & Laprise, R. (1999). A semi-Lagrangian semi-implicit regional climate model: The Canadian RCM. *Monthly Weather Review, 127*(3), 341-362. DOI:10.1175/1520-0493(1999)127<0341:ASISLR>.

Chahine, M. T. (1992). The hydrological cycle and its influence on climate. *Nature, 359*, 373-380. DOI:10.1038/359373a0.

Chen, S.-C., Norris, C., & Roads, J. (1996). Balancing the atmospheric hydrologic budget. *Journal of Geophysical Research, 101*, 7341-7358. DOI:10.1029/95JD01746.

Collins, W. D., Bitz, C. M., Blackmon, M. L., Bonan, G. B., Bretherton, C. S., Carton, J. A., ... & Smith, R. D. (2006). The community climate system model version 3 (CCSM3). *Journal of Climate*, *19*(11), 2122-2143. DOI:10.1175/JCLI3761.1.

Dimri, A. (2012). Atmospheric water budget over the western Himalayas in a regional climate model. *Journal of Earth System Science, 121*(4), 963-973. DOI:10.1007/s12040-012-0204-8.

Dominguez, F., & Kumar, P. (2005). Dominant modes of moisture flux anomalies over North America. *Journal of Hydrometeorology, 6*(2), 194-209. DOI:10.1175/JHM417.1.

Flato, G. M. (2005). The third generation coupled global climate model (CGCM3). *Environment Canada Canadian Centre for Climate Modelling and Analysis note available at http://www.ec.gc.ca/ccmac-cccma/default.asp?n=1299529F-1.*

GFDL Global Atmospheric Model Development Team. (2004). The new GFDL global atmospheric and land model AM2-LM2: Evaluation with prescribed SST simulations. *Journal of Climate, 17*, 4641-4673. DOI:10.1175/JCLI-3223.1

1629, DOI:10.1029/2003GL017130.

Giorgi, F., Marinucci, M. R., & Bates, G. T. (1993a). Development of a second-generation regional climate model (RegCM2). Part I: Boundary-layer and radiative transfer processes. *Monthly Weather Review, 121*(10), 2794-2813. DOI:10.1175/1520-0493(1993)121<2794:DOASGR>.

Giorgi, F., Marinucci, M. R., Bates, G. T., & De Canio, G. (1993b). Development of a second-generation regional climate model (RegCM2). Part II: Convective processes and

assimilation of lateral boundary conditions. *Monthly Weather Review, 121*(10), 2814-2832. DOI:10.1175/1520-0493(1993)121<2814:DOASGR>.

Gordon, C., Cooper, C., Senior, C. A., Banks, H., Gregory, J. M., Johns, T. C., ... & Wood, R. A. (2000). The simulation of SST, sea ice extents and ocean heat transports in a version of the Hadley Centre coupled model without flux adjustments. *Climate Dynamics, 16*(2-3), 147-168. DOI:10.1007/s003820050010.

Grell, G. A., Dudhia, J., & Stauffer, D. R. (1993). A description of the fifth generation Penn State/NCAR Mesoscale Model (MM5). *NCAR Technical Note NCAR/ TN-398*, 107 pp.

Hack, J. J., Kiehl, J. T., & Hurrell, J. W. (1998). The hydrologic cycle and thermodynamic characteristics of the NCAR CCM3. *Journal of Climate, 11*(6), 1179-1206. DOI:10.1175/1520-0442(1998)011<1179:THATCO>.

Hirschi, M., Seneviratne, S. I., & Schär, C. (2006). Seasonal variations in terrestrial water storage for major midlatitude river basins. *Journal of Hydrometeorology, 7*(1), 39-60. DOI:10.1175/JHM480.1.

Hu, H., Oglesby, R. J., & Marshall, S. (2005). The simulation of moisture processes in climate models and climate sensitivity. *Journal of climate, 18*(13), 2172-2193. DOI:10.1175/JCLI3384.1.

IPCC. [Nakicenovik, N., & Swart, R. (Eds.)]. (2000). *Emissions Scenarios*. UK: Cambridge University Press, 570 pp.

Jin, F., & Zangvil, A. (2010). Relationship between moisture budget components over the eastern Mediterranean. *International Journal of Climatology, 30*(5), 733-742. DOI:10.1002/joc.1911.

Jones, R., Hassell, D., Hudson, D., Wilson, S., Jenkins, G., & Mitchell J. (2004). *Generating high resolution climate change scenarios using PRECIS*. Exeter, UK: Met Office Hadley Centre, 40 pp.

Kanamitsu, M., Ebisuzaki, W., Woollen, J., Yang, S. K., Hnilo, J. J., Fiorino, M., & Potter, G. L. (2002). NCEP-DOE AMIP-II Reanalysis (R-2). *Bulletin of the American Meteorological Society, 83*(11), 1631-1643. DOI:10.1175/BAMS-83-11-1631.

Liang, X.-Z., Kunkel, K. E., & Samel, A. N.(2001). Development of a regional climate model for U. S. Midwest applications. Part 1: Sensitivity to buffer zone treatment. *Journal of Climate, 14*, 4363– 4378. DOI:10.1175/1520-0442(2001)014<4363:DOARCM>2.0.CO;2.

Liu, J., & Stewart, R. (2003). Water vapor fluxes over the Saskatchewan River Basin. *Journal of Hydrometeorology, 4*, 944-959. DOI:10.1175/1525-7541(2003)004<0944:WVFOTS>.

Lucarini, V., Danihlik, R., Kriegerova, I., & Speranza, A. (2007). Does the Danube exist?

Versions of reality given by various regional climate models and climatological data sets. *Journal of Geophysical Research*. *112*, D13103, DOI:10.1029/2006JD008360.

Marbaix, P., Gallee, H., Brasseur, O., & van Ypersele, J. (2003). Lateral boundary conditions in regional climate models: A detailed study of relaxation procedure. *Monthly Weather Review, 131*, 461– 479. DOI:10.1175/1520-0493(2003)131<0461:LBCIRC>2.0.CO;2.

Mearns, L. O., Gutowski, W., Jones, R., Leung, R., McGinnis, S., Nunes, A., & Qian, Y. (2009). A regional climate change assessment program for North America. *Eos, Transactions American Geophysical Union, 90*(36), 311-311. DOI:10.1029/2009EO360002.

Min, W., & Schubert, S. (1997). The climate signal in regional moisture fluxes: A comparison of three global data assimilation products. *Journal of Climate, 10*(10), 2623-2642. DOI:10.1175/1520-0442(1997)010<2623:TCSIRM>.

Pal, J. S., Giorgi, F., Bi, X., Elguindi, N., Solmon, F., Rauscher, S. A., ... & Steiner, A. L. (2007). Regional climate modeling for the developing world: the ICTP RegCM3 and RegCNET. *Bulletin of the American Meteorological Society, 88*(9), 1395-1409. DOI:10.1175/BAMS-88-9-1395.

Pal, J. S., Small, E. E., & Eltahir, E. A. (2000). Simulation of regional‐scale water and energy budgets: Representation of subgrid cloud and precipitation processes within

RegCM. *Journal of Geophysical Research: Atmospheres (1984–2012), 105*(D24), 29579-29594. DOI:10.1029/2000JD900415.

Peixoto, J. P., & Oort, A. H. (1992). *Physics of Climate*. New York, NY: Springer-Verlag, 520 pp.

Pope, V. D., Gallani, M. L., Rowntree, P. R., & Stratton, R. A. (2000). The impact of new physical parametrizations in the Hadley Centre climate model: HadAM3. *Climate Dynamics, 16*(2-3), 123-146. DOI:10.1007/s003820050009.

Rasmusson, E. M. (1968). Atmospheric water vapor transport and the water balance of North America: II. Large-scale water balance investigations. *Monthly Weather Review, 96*(10), 720-734. DOI:10.1175/1520-0493(1968)096<0720:AWVTAT>2.0.CO;2.

Reichle, R. H., Koster, R. D., Dong, J., & Berg, A. A. (2004). Global soil moisture from satellite observations, land surface models, and ground data: Implications for data assimilation. *Journal of Hydrometeorology, 5*(3), 430-442. DOI:10.1175/1525-7541(2004)005<0430:GSMFSO>.

Roads, J. O., Chen, S. C., Kanamitsu, M., & Juang, H. (1998). Vertical structure of humidity and temperature budget residuals over the Mississippi River basin. *Journal of Geophysical Research: Atmospheres (1984–2012), 103*(D4), 3741-3759. DOI:10.1029/97JD02759.

Rogers, R. R., & Yau, M. K. (1984). *A Short Course in Cloud Physics* (Third Edition). United States: Butterworth-Heinemann, 290 pp.

Ruane, A. C. (2010). NARR's atmospheric water cycle components. Part I: 20-year mean and annual interactions. *Journal of Hydrometeorology, 11*(6), 1205-1219. DOI:10.1175/2010JHM1193.1.

Schär, C., Lüthi, D., Beyerle, U., & Heise, E. (1999) The soil–precipitation feedback: A process study with a regional climate model. Journal of Climate, 12, 722–741. DOI:0.1175/1520-0442(1999)012<0722:TSPFAP>.

Schubert, S., Park, C. K., Wu, C. Y., Higgins, W., Kondratyeva, Y., Molod, A., ... & Rood, R. (1995). A multiyear assimilation with the GEOS-1 system: Overview and results. *NASA tech. Memo, 104606*(6), 207.

Scinocca, J. F., & McFarlane, N. A. (2004). The variability of modeled tropical precipitation. *Journal of the atmospheric sciences, 61*(16), 1993-2015. DOI:10.1175/1520-0469(2004)061<1993:TVOMTP>.

Seneviratne, S. I., Viterbo, P., Lüthi, D., & Schär, C. (2004). Inferring changes in terrestrial water storage using ERA-40 reanalysis data: The Mississippi River basin. Journal of climate, 17(11), 2039-2057. DOI:10.1175/1520-0442(2004)017<2039:ICITWS>2.0.CO;2.

Shukla, J., & Mintz, Y. (1982). Influence of land-surface evapotranspiration on the earth's climate. *Science, 215*(4539), 1498-1501. DOI:10.1126/science.215.4539.1498.

Skamarock, W. C., Klemp, J. B., Dudhia, J., Gill, D. O., Barker, D. M., Wang, W., & Powers, J. G. (2005). *A description of the advanced research WRF version 2* (No. NCAR/TN-468+ STR). National Center For Atmospheric Research Boulder Co Mesoscale and Microscale Meteorology Div.

Trenberth, K. E. (1991). Climate diagnostics from global analyses: Conservation of mass in ECMWF analyses. *Journal of climate, 4*(7), 707-722. DOI:10.1175/1520-0442(1991)004<0707:CDFGAC>.

Trenberth, K. E. (1992). *Climate System Modelling*. New York, NY: Cambridge University Press, 788 pp.

Trenberth, K. E. (1998). Atmospheric moisture residence times and cycling: Implications for rainfall rates and climate change. *Climatic change, 39*(4), 667-694. DOI:10.1023/A:1005319109110.

Trenberth, K. E., Dai, A., Rasmussen, R. M., & Parsons, D. B. (2003). The changing character of precipitation. *Bulletin of the American Meteorological Society, 84*(9), 1205-1217. DOI:10.1175/BAMS-84-9-1205.

Trenberth, K. E., Fasullo, J. T., & Kiehl, J. (2009). Earth's global energy budget. *Bulletin of the American Meteorological Society, 90*(3), 311-323. DOI:10.1175/2008BAMS2634.1.

Verseghy, D. L. (2009). CLASS–The Canadian Land Surface Scheme (Version 3.4), Technical Documentation (Version 1.1). *Climate Research Division, Science and Technology Branch, Environment Canada*, 180.

Wang, K., & Dickinson, R. E. (2012). A review of global terrestrial evapotranspiration: Observation, modeling, climatology, and climatic variability. *Reviews of Geophysics, 50*(2). DOI:10.1029/2011RG000373.

Wang, M., & Paegle, J. (1996). Impact of analysis uncertainty upon regional atmospheric moisture flux. *Journal of Geophysical Research: Atmospheres (1984–2012), 101*(D3), 7291-7303. DOI:10.1029/95JD02896.

Water Survey of Canada. (2010). Retrieved from http://www.wsc.ec.gc.ca/applications/H2O/report-eng.cfm?yearb=&yeare=&station=03OE001&report=monthly&year=1971 (Accessed 2013).

5. Uncertainty in Runoff Projections Under Climate Change: Case study of Labrador's Churchill River Basin

5.1. Abstract

An ensemble of seven climate models from the North American Regional Climate Change Assessment Program was used to examine uncertainty in simulated runoff changes from a base period (1971-2000) to a future period (2041-2070), for the Churchill River Basin in Labrador, Canada. Three approximations for mean climatological runoff from each ensemble member were included in the analysis: (i) atmospheric moisture convergence, (ii) the balance between precipitation and evaporation, and (iii) instantaneous runoff output from respective land-surface schemes. Using data imputation (i.e. reconstruction) and variance decomposition it was found that choice of regional climate model (RCM) had the greatest contribution to uncertainty in the climate change signal while the boundary forcing of a general circulation model (GCM) played a smaller, though non-negligible role. It was also found that choice of runoff approximation had a substantial contribution to uncertainty, falling between that of RCM and GCM choice. Mean and median increases in climatological runoff for the basin were found to be 11.2% and 8.9% respectively.

5.2. Preface

This chapter has been submitted for publication in Atmosphere-Ocean (in conjunction with Chapter 4) and is currently under review.

Chapter 3 presented a climate change analysis of a sub-basin of the Churchill River, and this chapter expands the climate change analysis to the entire basin using a different approach. The results presented and discussed in this chapter are supported by the analysis of Chapter 4 as they are based largely on the differences in both the atmospheric and terrestrial water balance components. Much of the information from the preface of the previous chapter (Section 4.2) also applies to this chapter.

Note that if one performs the calculations of mean annual residuals of the previous chapter and this chapter, the results are not identical. There are two reasons for this. First of all, the averages of Chapter 4 were calculated based on mean monthly values (and not all months have the same number of days), whereas here they were calculated using 3-hourly data. Secondly, Chapter 4 incorporates rates of change of the storage terms (∂t), which would were not included in the analysis here.

During the data analysis, the impact of climate change on the atmospheric moisture advection vectors into and out of the Churchill River Basin was also plotted. While these plots are interesting and may provide inspiration for future work, they do not fall within the scope of this chapter or the thesis in general. As such, a sample of these plots for several of the ensemble members can be found in Appendix D.

5.3. Introduction

Climate change is already having a noticeable impact on earth's hydrological cycle (Trenberth et al. 2003; Dery et al. 2009). As the changing climate's influence becomes more apparent, the need to investigate its potential future impacts increases. However, impact assessments are complicated by the uncertainty present in all climate simulations. Uncertainty results from having limited knowledge of how society will develop, how the climate system will react to that development and how to accurately represent the evolution of the climate via computer models. This leads to the inability to predict the impacts of climate change and necessitates the representation of a range of possible outcomes (vis-à-vis uncertainty), for which informed adaptation decisions can be made (Foley 2010).

Primary sources of uncertainty in climate change studies include greenhouse gas emissions scenarios, climate model selection, downscaling method and sampling uncertainty (Déqué et al. 2007; Maurer 2007; Thorne 2011; Shrestha et al. 2011). For hydrological impact studies, the selection and implementation of a land-surface hydrology model and the ability of a climate model to adequately simulate the water cycle, with its complex and multi-scale processes, is also of interest (Music and Caya 2007). Multiple studies (e.g. Mitchell and Hulme 1999; Wilby and Harris 2006) examined several of these sources of uncertainty individually and described the "cascade of uncertainty" and how it propagates through from emissions scenario down to sampling uncertainty.

It is unknown how society will develop in the coming decades and therefore impossible to ascertain total atmospheric greenhouse gas concentrations for the future. There are several greenhouse gas emissions scenarios that provide a range of plausible future pathways for carbon dioxide, methane and other greenhouse gas concentrations (IPCC 2000). In order for a climate study to capture this uncertainty multiple emissions scenarios would need to be employed.

Uncertainty in climate modelling is introduced by an incomplete understanding of the climate system and all of its processes, as well as an inability to fully and accurately represent the processes that are understood. No single model is best at simulating all aspects of the climate system (Christensen and Christensen, 2007; Maraun et al., 2010), meaning a variety of climate models that use different algorithms and parameterization schemes (i.e. a multi-model ensemble) should be used to address this type of uncertainty (Murphy et al. 2004; Kotlarski et al., 2005).

Downscaling of a general circulation model (GCM) can be divided into two approaches: (i) dynamic downscaling where a regional climate model (RCM) of relatively high resolution is driven at its geographic boundaries over a specific region by a global GCM, and; (ii) statistical downscaling where a statistical relationship is established between large scale atmospheric variables and specific local situations (Fowler et al. 2007a). This study focuses on dynamic downscaling, where the choice of RCM introduces an additional level of uncertainty due to differing modelling structures, processes and parameterization schemes. Statistical downscaling methods, which also have been found

to introduce additional uncertainty, though less than that of GCM choice (Chen et al. 2013; Vano et al. 2014), are not discussed further here.

Parameterization schemes are methods of approximating physical processes that occur on too small a scale to be resolved by the climate model. Some examples of processes that require parameterization schemes include large-scale condensation, convection, soil processes, snow-albedo feedback, and evaporation, among others. All parameterizations contribute to bias in RCM output (Hagemann et al. 2004; Fowler et al. 2007), meaning that variables other than precipitation, which is often the primary focus of hydrological studies, also contribute to runoff bias (Gagnon et al. 2009). This creates the need to analyze multiple components of the simulated hydrological system to best capture uncertainty when investigating the impacts of climate change on the hydrology of a basin.

The primary constraint on quantifying the impacts of climate change on water resources and the hydrological system is often touted as GCM projection uncertainty (Minville et al. 2008; Wilby and Harris 2006; Xu et al. 2011; Bennett et al. 2012). Differences between individual GCMs have been found to result in a larger impact on simulated hydrological change than differing emissions scenarios (Graham et al. 2007a), though emissions scenarios still play a role (Jasper et al. 2004). Thorne (2011) found that even with a prescribed +2ºC global mean temperature change, a selection of GCMs gave different outcomes for the Liard River Basin in Northern Canada due to the differences in algorithms, parameterizations and feedback mechanisms. As such, it is recommended that

multiple GCMs should be selected for use in impact studies (Ghosh and Mujundar 2009; Kingston et al. 2011; Thorne 2011).

Regional climate model (RCM) formulation has been found to have a comparable, or sometimes dominant, influence on the uncertainty of simulated variables (Roberts et al. 2012; Rowell 2006; Déqué et al. 2007) and relative contributions to uncertainty vary according to spatial domain, region, season and variable (Déqué al 2005; Fowler et al. 2007). GCMs and RCMs contribute more uncertainty to simulated runoff than hydrological models, though the influence of hydrological model selection becomes stronger during low-flow periods and in arid watersheds (Najafi et al. 2011; Maurer et al. 2010; Velázquez et al. 2013). This increased influence occurs because smaller differences in variable and parameterization values end up having a larger relative impact on the overall water balance equations when the total amount of water is less. As such, it is important to include multiple climate models in a climate change impact study to best capture the range of uncertainty (Hingray 2007a; Fowler et al. 2007). Sampling uncertainty, which exists because climate statistics are estimated from a finite sample that doesn't cover the entire range of natural variability, is typically marginal (Déqué et al. 2007).

There are many components of the hydrological system represented by climate models including the advection of moist air in the atmosphere, precipitation and evaporation as well as runoff. The purpose of this paper is two-fold: (i) To investigate the importance of the role of atmospheric and terrestrial water balance components on uncertainty in the

climate change signal; and (ii) to investigate the projected effects of climate change on the mean runoff of Labrador's Churchill River Basin.

5.4. Background

Churchill River Basin

The Churchill River is located in Newfoundland and Labrador, Canada and has an area of approximately 92 500 km^2. The basin is sparsely populated but contains the sites for existing and future large-scale hydroelectric power production facilities. Figure 5.1 shows the location of the Churchill River Basin outlined in the thick black line. The resolution of Figure 5.1 is the common 0.25 degree grid to which all RCM output was regridded for this study.

The basin is typically snow covered for more than half the year, as snowfall is the most common precipitation type from October to May. Mean annual precipitation ranges from 850 to 950 mm, with a relatively even split between rain and snow. The mean annual temperature ranges from -5 to 0 ^oC, with record winter extremes reaching below -40 ^oC and record summer extremes surpassing 30 ^oC.

Due to the large amount of snow accumulation in the winter, the spring melt is a predominant feature in the annual hydrograph of the Churchill River. However the spring melt signal is subdued by the existence of the Churchill Falls hydroelectric facility and its

associated reservoirs and control structures. Roughly three-quarters of the runoff of the Churchill River originates upstream of Churchill Falls.

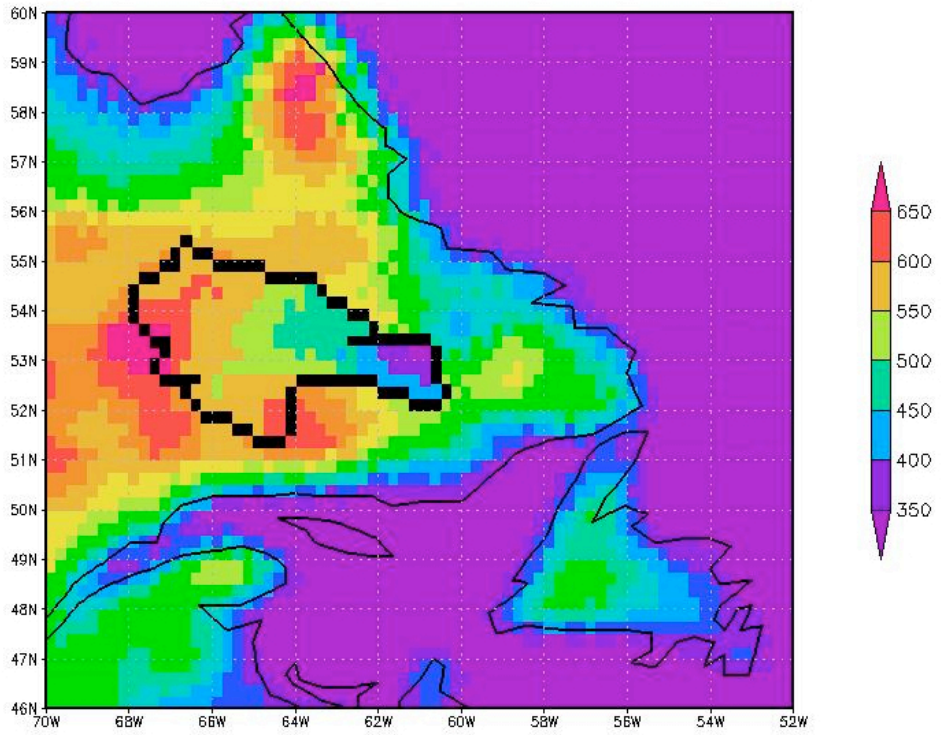

Figure 5.1 - Topography, location and representation of Churchill River Basin (thick black line – coastline is represented by thin black lines). Elevation scale in metres.

It has been shown that even small changes in the distribution of precipitation can significantly alter mean annual runoff (Muzik 2001). Additionally, modest perturbations in natural inflow tend to have amplified impacts on reservoir storage levels (Christensen et al. 2004; Minville et al. 2008). As such, the impact of climate change on the basin's runoff is of great interest.

Climate Models

Frigon et al. (2010) and Eum et al. (2012), among others, recommend using the North American Regional Climate Change Assessment Program (NARCCAP) for climate change and uncertainty analysis. NARCCAP is an international collaboration designed to investigate the uncertainties in future climate projections at a regional level, using a design of experiments (DOE) approach (Mearns et al. 2007; Mearns et al. 2009). It employs a selection of RCMs nested within multiple GCMs. The GCMs provide the initial conditions for the RCMs, as well as boundary conditions including large-scale atmospheric fields, sea surface temperatures and sea ice. This boundary control from the GCMs constrains the RCM simulation to be consistent with the global simulation, while the higher resolution of the RCMs allows for better representation of regional phenomena (Christensen et al. 2007). The land-surface of the GCM does not directly force that of the RCM. Each RCM has its own land-surface scheme that interacts with the lower levels of the RCM atmospheric simulation and evolves without direct input from the GCM land-surface. Each GCM is driven by the SRES A2 scenario, which falls on the higher end of the IPCC emissions scenario spectrum (IPCC 2000). NARCCAP's ensemble approach allows the representation of uncertainties introduced by GCM choice, RCM choice and their respective structural formulations (Maraun et al. 2010). The timeframes covered are from 1968 to 2000 for the base reference period and from 2038 to 2070 for the future period, including three years of model spin up data at the beginning of each run, which are not included in this analysis.

Due to budget constraints not all of NARCCAP's possible RCM-GCM combinations are being run. Each GCM will be coupled with half the RCMs and vice-versa, resulting in a representative sample of twelve simulations. While the various ensemble members each have a 50 km horizontal resolution they employ a variety of map projections, vertical coordinate systems, dynamics and physics schemes, land surface schemes, vegetation classes, and timesteps among other varying parameters and characteristics. Output from the various ensemble members is released incrementally in conjunction with the completion of postprocessing and only those combinations published at the time of analysis are included in this work, as highlighted by Table 5.1. The four RCMs and three GCMs used in this work are briefly discussed below to give an idea of the modelling processes and parameterization schemes represented.

RCM details (more information available at www.narccap.ucar.edu/data/rcm-characteristics.html):

- **CRCM** (Caya and Laprise 1999) uses the CLASS land-surface scheme, has 29 vertical levels in the Gal-Chen scaled height coordinate system, uses nonhydrostatic-compressible dynamics and is the only RCM used here to apply spectral nudging. It employs mass flux cumulus parameterization and removal of supersaturation for explicit moist physics.
- **HRM3** (Jones et al. 2003) uses the MOSES land-surface scheme, has 19 vertical levels in a hybrid terrain following and pressure coordinate system and uses hydrostatic-compressible dynamics. It employs mass flux (including downdraft)

cumulus parameterization and prognostic cloud liquid and ice for explicit moist physics.

- **RCM3** (Giorgi et al. 1993a,b; Paj et al. 2000, 2007) uses the BATS land-surface scheme, has 18 vertical levels in a terrain following coordinate system and uses hydrostatic-compressible dynamics. It employs Grell with Fritsch-Chapell closure cumulus parameterization and SUBEX with prognostic cloud water for explicit moist physics.
- **WRFG** (Skamarock et al. 2005) uses the NOAH land-surface scheme, has 35 vertical levels in a terrain following coordinate system and uses nonhydrostatic-compressible dynamics. It employs Grell cumulus parameterization and prognostic cloud liquid, ice, rain and snow for explicit moist physics.

GCM details (more information available at www.narccap.ucar.edu/about/aogcms.html):

- **ccsm** (Collins 2006) has a horizontal resolution of 1.4x1.4 degrees and an equilibrium climate sensitivity (the mean annual temperature increase resulting from a doubling of pre-industrial CO2 levels (Randel 2007)) of 3.4^{o}C.
- **cgcm3** (Flato 2005, Scinocca and McFarlane 2004) has a horizontal resolution of 1.9x1.9 degrees and an equilibrium climate sensitivity of 2.7^{o}C.
- **gfdl** (GFDL 2004) has a horizontal resolution of 2.0x2.5 degrees and an equilibrium climate sensitivity of 3.4^{o}C.

5.5. Methodology

This study uses a three-pronged approach that incorporates a broad range of simulated hydrological data from an ensemble of RCM-GCMs. This includes the analysis of (i) atmospheric moisture convergence, (ii) the balance between precipitation and evaporation, and (iii) instantaneous runoff, herein referred to as the upstream, midstream and downstream approaches respectively (note: these are analysis approaches and not part of a physical river). The upstream approach examines upper air climatic variables (wind and specific humidity levels) that are primarily driven by model dynamics and minimally influenced by parameterization (Serreze et al. 2003). The midstream approach uses precipitation and evaporation, which occur at the land-surface and are strongly influenced by various parameterization schemes. The downstream approach analyzes the RCM's simulated runoff, which is the end result of the land-surface scheme and a multitude of parameterizations.

Each of the analysis streams can be used as an approximation of mean annual runoff (discussed below) effectively providing three climatological runoff approximations per model. By incorporating hydrological components in these various stages of simulation (i.e. a fullstream approach), one is able to capture a range of intra-modelling uncertainty and provide a more inclusive projection for the amount of runoff in the Churchill River Basin. Note that the uncertainty of the amplitude of future greenhouse gas concentrations is not included in this study as NARCCAP models are driven by a single greenhouse gas scenario.

Water Balance Equations

The fullstream approach used here is based on the atmospheric and terrestrial water balances, Equations 5.1 and 5.2 respectively, which can be found in Rasmusson (1968) and Peixoto and Oort (1992).

$$-\frac{\partial W}{\partial t} - \nabla_H \bar{Q} = P - E \qquad (5.1)$$

$$P - E = R + \frac{\partial S}{\partial t} \qquad (5.2)$$

Here, W is the precipitable water content of the atmosphere, $-\nabla_H \bar{Q}$ is the vertically integrated horizontal atmospheric moisture convergence, P is precipitation, E is evaporation, R is runoff, and S is land-surface water storage (including soil moisture and snowpack).

The terrestrial water storage component in Equation 5.2 tends to zero over long periods of time (as ∂t gets very large), implying that mean climatological runoff can be represented by P – E. Subsequently, mean climatological runoff can also be represented by the atmospheric moisture convergence from Equation 5.1, as the precipitable water tendency is also negligible over long periods. As such, RCMs are able to provide three representations of mean climatological runoff for analysis, corresponding to respective components of the fullstream approach: (i) $-\nabla_H \bar{Q}$, (ii) $P - E$, and (iii) R.

More details on the calculation of the components of Equations 5.1 and 5.2 can be found in Chapter 4.

Variance Decomposition

There are several interpretations of what uncertainty means in climate simulations. For the purposes of this work, uncertainty is treated as the variability in ensemble results of the climate change signal. The approach used in this work follows Déqué et al. (2007), Ferro (2004), and von Storch and Zwiers (1999) and can be used to isolate and compare magnitudes of each source of uncertainty. Variance decomposition is used to take full advantage of DOE for individual statistics while data imputation (the process of replacing missing data with substituted values) reduces the bias in the overall estimation of uncertainty due to overrepresentation by a given GCM or RCM.

The average climate response of the change in the modeled representation of runoff over the entire Churchill River Basin can be denoted by X_{ijk}; where i varies from 1 to 4 according to RCM (R), j varies from 1 to 3 according to GCM (G) and k varies from 1 to 3 according to analysis stream (S). The variance of X can be split into orthogonal positive contributions, as in Equation 5.3, where a dot (•) represents the mean of the index it has replaced.

$$V(X) = R + G + S + RG + RS + GS + RGS \qquad (5.3)$$

Where: $$R = \frac{1}{4}\sum_{i=1}^{4}(X_{i\bullet\bullet} - X_{\bullet\bullet\bullet})^2$$

$$RG = \frac{1}{12}\sum_{i=1}^{4}\sum_{j=1}^{3}(X_{ij\bullet} - X_{i\bullet\bullet} - X_{\bullet j\bullet} + X_{\bullet\bullet\bullet})^2$$

$$RGS = \frac{1}{36}\sum_{i=1}^{4}\sum_{j=1}^{3}\sum_{k=1}^{3}(X_{ijk} - X_{ij\bullet} - X_{i\bullet k} - X_{\bullet jk} + X_{i\bullet\bullet} + X_{\bullet j\bullet} + X_{\bullet\bullet k} - X_{\bullet\bullet\bullet})^2$$

To obtain the total amount of variance contributed by RCMs, for example, one needs to sum up the components of variance in X above which contain R: V(R) = R + RG + RS + RGS. This way one is able to determine the magnitude of varying RCMs, GCMs and analysis streams with respect to climate response uncertainty.

Data Imputation

To analyze the complete matrix of RCM, GCM and analysis stream combinations in an unbiased manner, data imputation is required. This is performed by minimizing the influence of interaction terms from Equation 5.3 (e.g. RG, RGS, etc), as per Déqué et al. (2007).

The first step in the iterative process is to calculate the full average ($X_{\bullet\bullet\bullet}$) and the double averages ($X_{i\bullet\bullet}$, $X_{\bullet j\bullet}$ and $X_{\bullet\bullet k}$) with available data, as they are defined above. This is

relatively straight forward as there are several values for each RCM, GCM and analysis stream meaning a simple average of available values is taken.

Next, one must calculate the simple averages ($X_{ij\bullet}$, $X_{i\bullet k}$ and $X_{\bullet jk}$). Some of these averages cannot be calculated directly due to the missing data (e.g. for $X_{ij\bullet}$, where *i* = CRCM and *j* = gfdl, there is no data available for any of the three analysis streams), so the principle of minimizing interaction terms is used. For example, to minimize the RG interaction term from Equation 5.3 one can set $X_{ij\bullet} = X_{i\bullet\bullet} + X_{\bullet j\bullet} - X_{\bullet\bullet\bullet}$ when $X_{ij\bullet}$ is missing.

One can minimize the RGS interaction term from Equation 5.3 as there are first estimates available for all variables except certain X_{ijk}. Those X_{ijk} that are missing are calculated by setting $X_{ijk} = X_{ij\bullet} + X_{i\bullet k} + X_{\bullet jk} - X_{i\bullet\bullet} - X_{\bullet j\bullet} - X_{\bullet\bullet k} + X_{\bullet\bullet\bullet}$, similar to above.

Now that there are initial estimates for all X_{ijk} one can repeat the above process of calculating full, double and simple averages and minimizing two-term and three-term interaction terms. This iteration continues until the increment of missing X_{ijk} is less than 0.01%.

Results, including imputation results, can be found in Table 5.2 and Figure 5.2.

5.6. Results

Base Period Simulation

Results from the base period simulation of the ensemble members can be found in Table 5.1. The simulated runoff values bookend the Churchill River's observed mean streamflow of roughly 1825 m^3/s (1.7 mm/day) (Water Survey of Canada, 2010) for the time period in question, though no analysis preference is given to ensemble members that most accurately represent reality. Analysis of why each of the three streams have different projections is discussed in Chapter 4.

Table 5.1 - Base period climatological runoff [m^3/s] for each ensemble member and analysis stream

RCM	Stream	GCM		
		ccsm	cgcm3	gfdl
CRCM	up	1482	1510	
	mid	1593	1586	
	down	1610	1606	
HRM3	up			1748
	mid			1665
	down			1697
RCM3	up		3899	3732
	mid		2030	2092
	down		1631	1688
WRFG	up	1114	1474	
	mid	1084	1152	
	down	1119	1218	

Imputation

Ensemble members that have higher than average approximations for simulated runoff in the base period also have higher than average projected runoff changes, likewise for members with lower than average values (Table 5.2). This implies that this "over-estimation" (or "under-estimation") is systemic and also manifests itself in the climate change signal, warranting the study of changes relative to the base period simulation (%). Absolute changes (m^3/s) are also examined to illustrate the climate signal in raw data output and highlight the results from individual RCM-gcm-stream ensemble members.

To determine whether the imputation procedure produced reasonable results a check was completed using the RCM3-cgcm3 ensemble member. Each of the three analysis streams was removed, one at a time, from the data set and then reconstructed using the remaining data (i.e. RCM3-cgcm3-upstream was removed then reconstructed using the imputation method in Section 5.5. Likewise for RCM3-cgcm3-midstream and RCM3-cgcm3-downstream). Root mean square differences (RMSDs) between actual and reconstructed values were calculated and compared to RMSDs from other RCM3 and cgcm3 ensemble members as well as the two remaining streams. As shown in Table 5.3 the RMSD from the actual values is lowest for the reconstructed RCM3-cgcm3 values, indicating that the imputation method is satisfactory.

Table 5.2 - Projected runoff changes, including results of imputation (in grey).

Absolute Change (m^3/s)					Relative Change				
RCM	Stream	GCM			RCM	Stream	GCM		
		ccsm	cgcm3	gfdl			ccsm	cgcm3	gfdl
CRCM	up	83	219	271	CRCM	up	5.6%	14.5%	7.2%
	mid	146	178	147		mid	9.2%	11.2%	8.0%
	down	110	179	113		down	6.8%	11.1%	6.3%
HRM3	up	18	5	121	HRM3	up	12.2%	4.5%	6.9%
	mid	95	152	97		mid	6.0%	7.3%	5.8%
	down	131	196	121		down	7.9%	9.0%	7.2%
RCM3	up	533	456	695	RCM3	up	21.8%	11.7%	18.6%
	mid	121	114	182		mid	6.7%	5.6%	8.7%
	down	99	100	149		down	7.4%	6.1%	8.8%
WRFG	up	357	180	388	WRFG	up	32.1%	12.2%	19.3%
	mid	159	227	178		mid	14.7%	19.7%	15.0%
	down	174	218	165		down	15.5%	17.9%	14.0%

Table 5.3 - Differences between reconstructed RCM3-cgcm3 data and comparable categories

Category		Actual Value	RCM3 -gfdl	CRCM -cgcm3	WRFG -cgcm3	Up stream	Mid stream	Down stream
Absolute Changes (m^3/s)	Upstream	42.95	196.60	279.09	318.55	-	384.16	398.39
	Midstream	17.97	50.41	45.54	95.18	323.94	-	18.56
	Downstream	4.33	53.24	83.46	122.76	360.46	18.56	-
	RMSD	**46.65**	**209.83**	**294.84**	**354.4**	**484.63**	**384.6**	**399.68**
Relative Changes*	Upstream	0.3%	7.2%	3.1%	0.8%	-	5.8%	5.3%
	Midstream	2.8%	0.3%	2.8%	11.3%	3.3%	-	2.3%
	Downstream	1.2%	1.5%	3.8%	10.6%	4.4%	1.7%	-
	RMSD	**3.1%**	**7.4%**	**5.6%**	**15.5%**	**5.5%**	**6.0%**	**5.8%**

*Percentages under Relative Change refer to relative changes in Stream values and not differences between reconstructed values.

PDFs are useful in risk analysis and economic decision making. They recognize that climate projections are not perfect and provide a spectrum of potential outcomes. To fully take advantage of climate projections in PDF form one must compare the costs and risks of an erroneously high runoff projection to those of a low runoff projection. For example, if one were investigating potential climate change impacts for the site of a future dam and hydroelectric development then a runoff projection that is too low may increase the risk of wasting water over a spillway. An erroneously high runoff projection on the other hand may lead to an increase in construction costs (as it would require a higher capacity) without the benefit of increased power generation. The costs and risks of each scenario must be balanced to determine the 'best' projection to use for project design, which is not necessarily the annual mean or median.

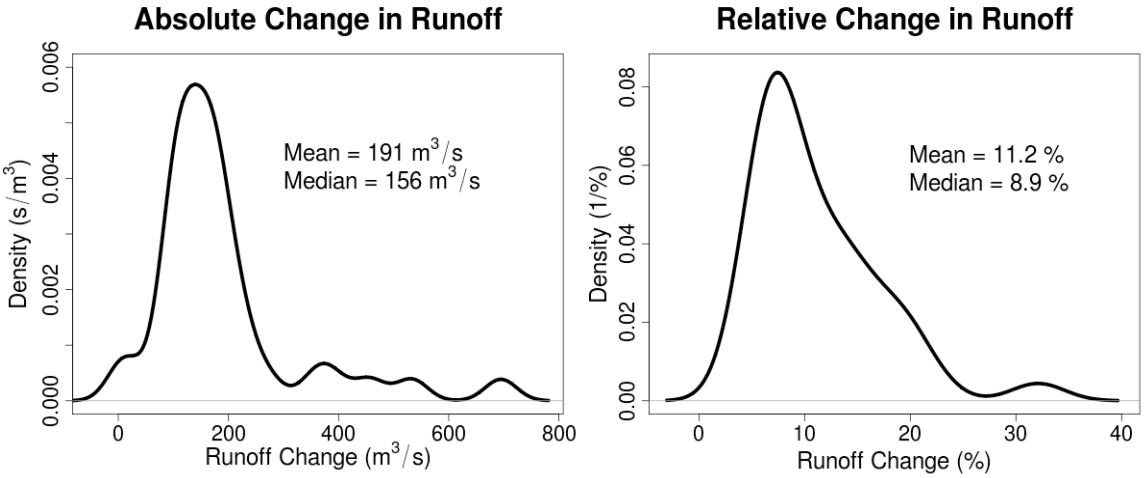

Figure 5.2 - PDFs of absolute (left) and relative changes in runoff (right), including imputed data

The simulations indicate that climatological basin runoff is expected to increase. The ensemble median increase is roughly 155 m^3/s (0.14 mm/day) , or 9%, while the mean

increase is roughly 190 m^3/s (0.18 mm/day), or 11%. There are some outliers on the far right side of the PDF that suggest that runoff increases may be as high as 700 m^3/s (0.65 mm/day), or 35%, but the increase most likely lies between 25 and 250 m^3/s (0.02 and 0.23 mm/day), or 1 and 25%.

Variance Decomposition

Variance decomposition was performed on the full set of data, including imputed values, the results of which are available in Table 5.4. There also exists a subset of the data consisting of two RCMs (CRCM and WRFG), two GCMs (ccsm and cgcm3) and all three streams that contains no holes in the data matrix, negating the need for imputation. Variance decomposition was performed on this subset (also available in Table 5.4) as further confirmation of the validity of the data reconstruction method as well as a quick sensitivity test of the impact of changing the number of RCM-GCM ensemble members.

Table 5.4 - Variance Decomposition Results, in Percentages of Variance Explained

Data	Change	R	G	S	RG	RS	GS	RGS	Total R	Total G	Total S
Full Data Set	**Absolute**	22	2	20	3	44	7	3	71	15	73
	Relative	47	1	11	9	11	9	11	79	31	42
Data Subset	**Absolute**	20	4	5	11	10	10	40	81	65	65
	Relative	28	0	3	8	14	12	36	85	55	64

Total variances do not add up to 100% due to the interaction terms. The term RG, for example, which is the interaction between RCM choice and GCM choice contributes to

both the total variance explained by RCM choice and the total variance explained by GCM choice.

5.7. Discussion

The climate change impacts found here for the Churchill River Basin corroborate those found in other studies. The IPCC used a multi-model ensemble (Bates et al. 2008) based on the SRES A1B emissions scenario (IPCC 2000). The results from this course-resolution study indicate that Labrador can expect between a 10 and 20% increase in mean runoff between 1980-1999 and 2080-2099. Frigon et al. (2010) use a five-member ensemble of various CRCM-cgcm3 configurations to show that the Churchill River, upstream of the existing Churchill Falls hydroelectric facility, can expect a change in runoff to be 21±6% (where 6% was the maximum deviation from the median ensemble value) from the recent past (1961-1990) to the future (2041-2070). Frigon et al. (2010) also showed that the ensemble spread of basin runoff related to natural variability is typically around ±10%. Roberts et al. (2012) used bias corrected precipitation and temperature from an ensemble of six NARCCAP models to drive a hydrological model in a sub-basin of the Churchill River. Their results indicate a roughly 9% increase in mean streamflow.

It is apparent from the variance decomposition of the full set of data that RCM (R) choice plays a major role in contributing to uncertainty whether investigating absolute or relative changes (71% and 79% respectively). Analysis stream choice also has a strong influence

on variability in the climate change signal, with a contribution comparable to RCM choice for absolute changes (73%) and roughly half the RCM contribution for relative changes. GCM choice plays the smallest, though non-negligible, role in contributing to uncertainty.

The results from the data subset corroborate the above results, where RCM choice plays the dominant role in contributing to uncertainty. GCM choice plays a more influential role in the subset analysis while stream choice contributes comparably to uncertainty. This implies that neither the data imputation nor the modification of the ensemble size had a drastic impact on the relative contributions to uncertainty, providing additional confidence in the results.

It is important to note that there are several potentially influential sources of uncertainty that were not included in this study, including greenhouse gas emissions scenario, downscaling method and hydrological model selection. This means it is not a comprehensive overview of climate change projection uncertainty and should be interpreted with caution (Mitchell and Hulme 1999; Chen et al. 2011; Poulin et al. 2011, Bennett et al. 2012).

There are many potential influencers for each contribution to uncertainty. Uncertainty from GCM choice can be attributed to model structure, formulations and climate sensitivity. These factors would influence broad temperature features that, in turn, play a role in evaporation and precipitation. At a basin scale the RCM would play the dominant

role in determining exact values and patterns. In addition to the driving GCM data, differences in RCM vertical coordinate and resolution choice may contribute to variability in upstream runoff projections. Parameterization schemes for precipitation and evaporation contribute to differences in midstream runoff projections, though the parameterization inputs vary between ensemble members and also play a large role. Each RCM has a different land-surface scheme, which contributes to variability in downstream runoff projections. Again, inputs into these schemes vary between members.

While the imputation method used minimizes the contributions of interaction terms, the results of Table 5.4 indicate that interaction is non-negligible when investigating relative contributions to uncertainty. The interaction effect RS contributes an unusually high amount to variance in absolute change of the full data set. This is because the upstream (atmospheric moisture convergence) output of RCM3 was approximately double that of other RCM3 streams and upstream values of other ensemble members. Correspondingly, the absolute difference between base and future period simulations was also noticeably higher. This effect is expectedly less noticeable while analyzing relative changes, implying that the uncertainty contributions for relative (as opposed to absolute) changes provide a more useful interpretation of the results. The three-factor interaction effect of RGS is fairly prominent in the data subset but is less so once the full data set is examined. This effect is likely caused by the imputation method which assumes that higher-order interaction terms are minimal. A larger matrix of data would be beneficial in further understanding the interaction effects.

5.8. Summary and Conclusions

The work presented here provides a useful method of measuring the impacts of climate change on surface runoff in a basin. Results of climatological runoff changes are consistent with a variety of other studies.

The primary contribution of this study highlights the value for investigators to consider multiple aspects of the simulated hydrological cycle in order to capture the broadest range of uncertainty possible, given a set of RCM-GCM output. RCM, GCM and analysis stream all contribute substantially to uncertainty in the climate change signal of the mean basin runoff, with RCM tending to dominate. These results vary from most uncertainty attribution studies because runoff, as opposed to temperature or precipitation, is examined here. While runoff ultimately includes all the factors and inputs that influence mean simulated temperature and precipitation it also incorporates additional parameterizations and inputs such as soil moisture and depth, vegetation classes, evaporation, etc. Many, if not all, of these are strongly dependent on local processes and result in RCM choice being the greatest overall contributor to uncertainty. Choice of analysis stream also plays a substantial role because there are different inputs, processes, parameterizations and assumptions for each, resulting in a variety of approximations for simulated runoff.

Also of note is the difference in relative uncertainty contribution between absolute and relative changes in mean runoff. The primary distinction is the importance of analysis

stream choice, with 73% and 42% of the variance explained for absolute and relative changes respectively. This is caused primarily by the anomalously high atmospheric moisture convergence of RCM3 and its proportional impact on the simulated climate change signal. This implies that with respect to the climate change signal and ensemble member intercomparison it is more insightful to examine relative changes in runoff where RCM, GCM and stream choice explain 79%, 31% and 42% of variance respectively. All of which are substantial and none of which should be ignored.

Future work will include reproducing the analysis on different watersheds to explore regional influence as well as examining the effects of climate change on the annual runoff cycle.

5.9. Acknowledgements

This work would not have been possible without the generous financial support of Nalcor Energy Inc, NSERC, Mitacs and TD Canada Trust.

We wish to thank the North American Regional Climate Change Assessment Program (NARCCAP) for providing access to the data used in this paper. NARCCAP is funded by the National Science Foundation, the U.S. Department of Energy, the National Oceanic and Atmospheric Administration, and the U.S. Environmental Protection Agency Office of Research and Development.

5.10. References

Bates, B. C., Kundzewicz, Z. W., Wu, S., & Palutikof, J. P. (2008). Climate change and water. Intergovernmental Panel on Climate Change Technical Paper IV. Geneva: IPCC Secretariat, 210 pp.

Bennett, K. E., Werner, A. T., & Schnorbus, M. (2012). Uncertainties in Hydrologic and Climate Change Impact Analyses in Headwater Basins of British Columbia. *Journal of Climate, 25*, 5711-5730. DOI:10.1175/JCLI-D-11-00417.1.

Caya, D., & Laprise, R. (1999). A semi-Lagrangian semi-implicit regional climate model: The Canadian RCM. *Monthly Weather Review, 127*(3), 341-362. DOI:10.1175/1520-0493(1999)127<0341:ASISLR>.

Chen, J., Brissette, F. P., Chaumont, D., & Braun, M. (2013). Performance and uncertainty evaluation of empirical downscaling methods in quantifying the climate change impacts on hydrology over two North American river basins. *Journal of Hydrology, 479*, 200-214. DOI:10.1016/j.jhydrol.2012.11.062.

Chen, J., Brissette, F. P., & Leconte, R. (2011). Uncertainty of downscaling method in quantifying the impact of climate change on hydrology. *Journal of Hydrology, 401*, 190-202. DOI:10.1016/j.jhydrol.2011.02.020.

Christensen, J. H., & Christensen, O.B. (2007). A summary of the PRUDENCE model projections of changes in European climate by the end of this century. *Climatic Change, 81*(1), 7-30. DOI:10.1007/s10584-006-9210-7.

Christensen, J. H., Hewitson, B., Busuioc, A., Chen, A. Gao, X. Held, I., … Whetton, P. (2007). Regional Climate Projections. In Solomon, S., Qin, D., Manning, M., Chen, Z., Marquis, M., Averyt, K.B.,… Miller, H. L. (Eds.), *Climate Change 2007: The Physical Science Basis. Contribution of Working Group I to the Fourth Assessment Report of the Intergovernmental Panel on Climate Change* (pp. 847-940). Cambridge, UK and New York, NY: Cambridge University Press.

Christensen, N. S., Wood, A. W., Voisin, N., Lettenmaier, D. P., & Palmer, R. N. (2004). The effects of climate change on the hydrology and water resources of the Colorado River basin. *Climatic Change, 62*, 337-363. DOI:10.1023/B:CLIM.0000013684.13621.1f.

Collins, W. D., Bitz, C. M., Blackmon, M. L., Bonan, G. B., Bretherton, C. S., Carton, J. A., ... & Smith, R. D. (2006). The community climate system model version 3 (CCSM3). *Journal of Climate*, *19*(11), 2122-2143. DOI:10.1175/JCLI3761.1.

Déqué, M., Jones, R. G., Wild, M., Giorgi, F., Christensen, J. H., Hassell, D. C., ... & Van den Hurk, B. (2005). Global high resolution versus Limited Area Model climate change projections over Europe: quantifying confidence level from PRUDENCE results. *Climate Dynamics*, *25*(6), 653-670. DOI:10.1007/s00382-005-0052-1.

Déqué, M., Rowell, D. P., Lüthi, D., Giorgi, F., Christensen, J. H., Rockel, B., ... & van den Hurk, B. J. J. M. (2007). An intercomparison of regional climate simulations for Europe: assessing uncertainties in model projections. *Climatic Change, 81*(1), 53-70. DOI:10.1007/s10584-006-9228-x.

Déry, S. J., Hernández‐Henríquez, M. A., Burford, J. E., & Wood, E. F. (2009). Observational evidence of an intensifying hydrological cycle in northern Canada. *Geophysical Research Letters, 36*(13), L13402, DOI:10.1029/2009GL038852.

Eum, H. I., Gachon, P., Laprise, R., & Ouarda, T. (2012). Evaluation of regional climate model simulations versus gridded observed and regional reanalysis products using a combined weighting scheme. *Climate dynamics, 38*(7-8), 1433-1457. DOI:10.1007/s00382-011-1149-3.

Ferro, C. A. (2004). Attributing variation in a regional climate change modelling experiment. *PRUDENCE working note available at http://prudence.dmi.dk/public/publications/analysis_of_variance.pdf.*

Flato, G. M. (2005). The third generation coupled global climate model (CGCM3). *Environment Canada Canadian Centre for Climate Modelling and Analysis note available at http://www.ec.gc.ca/ccmac-cccma/default.asp?n=1299529F-1.*

Foley, A. M. (2010). Uncertainty in regional climate modelling: A review. *Progress in Physical Geography, 34*: 647-670. DOI:10.1177/0309133310375654 .

Fowler, H. J., Blenkinsop, S., & Tebaldi, C. (2007a). Linking climate change modelling to impacts studies: recent advances in downscaling techniques for hydrological modelling. *International Journal of Climatology, 27*(12), 1547-1578. DOI:10.1002/joc.1556.

Fowler, H. J., Kilsby, C. G., & Stunell, J. (2007b). Modelling the impacts of projected future climate change on water resources in north-west England. *Hydrology and Earth System Sciences, 11*(3), 1115-1126. DOI:10.5194/hess-11-1115-2007.

Frigon, A., Music, B., & Slivitzky, M. (2010). Sensitivity of runoff and projected changes in runoff over Quebec to the update interval of lateral boundary conditions in the Canadian RCM. *Meteorologische Zeitschrift, 19*(3), 225-236. DOI:10.1127/0941-2948/2010/0453.

Frigon, A., Slivitzky, M., Music, B., & Caya, D. (2008). Internal variability of the Canadian RCM's hydrologic variables at the basin scale. *Geophysical Research Abstracts 10*, EGU2008-A-04093.

Gagnon, P., Konan, B., Rousseau, A. N., & Slivitzky, M. (2009). Hydrometeorological validation of a Canadian regional climate model simulation within the Chaudière and Chateauguay watersheds (Quebec, Canada). *Canadian Journal of Civil Engineering, 36*(2), 253-266. DOI:10.1139/L08-125.

GFDL Global Atmospheric Model Development Team. (2004). The new GFDL global atmospheric and land model AM2-LM2: Evaluation with prescribed SST simulations. *Journal of Climate, 17*, 4641-4673. DOI:10.1175/JCLI-3223.1

Ghosh, S., & Mujumdar, P. P. (2009). Climate change impact assessment: Uncertainty modeling with imprecise probability. *Journal of Geophysical Research: Atmospheres (1984–2012), 114*(D18), 113. DOI: 10.1029/2008JD011648.

Giorgi, F., Marinucci, M. R., & Bates, G. T. (1993a). Development of a second-generation regional climate model (RegCM2). Part I: Boundary-layer and radiative transfer processes. *Monthly Weather Review, 121*(10), 2794-2813. DOI:10.1175/1520-0493(1993)121<2794:DOASGR>.

Giorgi, F., Marinucci, M. R., Bates, G. T., & De Canio, G. (1993b). Development of a second-generation regional climate model (RegCM2). Part II: Convective processes and assimilation of lateral boundary conditions. *Monthly Weather Review, 121*(10), 2814-2832. DOI:10.1175/1520-0493(1993)121<2814:DOASGR>.

Graham, L. P., Andréasson, J., & Carlsson, B. (2007). Assessing climate change impacts on hydrology from an ensemble of regional climate models, model scales and linking methods–a case study on the Lule River basin. *Climatic Change, 81*(1), 293-307. DOI:10.1007/s10584-006-9215-2.

Grell, G. A., Dudhia, J., & Stauffer, D. R. (1993). A description of the fifth generation Penn State/NCAR Mesoscale Model (MM5). *NCAR Technical Note NCAR/ TN-398*, 107 pp.

Hagemann, S., Machenhauer, B., Jones, R., Christensen, O. B., Déqué, M., Jacob, D., & Vidale, P. L. (2004). Evaluation of water and energy budgets in regional climate models applied over Europe. *Climate Dynamics, 23*(5), 547-567. DOI:10.1007/s00382-004-0444-7.

Hingray, B., Mezghani, A., & Buishand, T. A. (2007). Development of probability distributions for regional climate change from uncertain global mean warming and an uncertain scaling relationship. Hydrology and Earth System Sciences, 11(3), 1097-1114. DOI:10.5194/hess-11-1097-2007.

IPCC. [Nakicenovik, N., & Swart, R. (Eds.)]. (2000). *Emissions Scenarios*. UK: Cambridge University Press, 570 pp.

Jasper, K., Calanca, P., Gyalistras, D., & Fuhrer, J. (2004). Differential impacts of climate change on the hydrology of two alpine river basins. *Climate Research, 26*(2), 113-129.

Jones, R., Hassell, D., Hudson, D., Wilson, S., Jenkins, G., & Mitchell J. (2004). *Generating high resolution climate change scenarios using PRECIS*. Exeter, UK: Met Office Hadley Centre, 40 pp.

Kingston, D. G., Thompson, J. R., & Kite, G. (2011). Uncertainty in climate change projections of discharge for the Mekong River Basin. *Hydrology and Earth System Sciences, 15*(5), 1459-1471. DOI:10.5194/hess-15-1459-2011.

Kotlarski, S., Block, A., Böhm, U., Jacob, D., Keuler, K., Knoche, R., ... & Walter, A. (2005). Regional climate model simulations as input for hydrological applications: evaluation of uncertainties. *Advances in Geosciences, 5*, 119-125.

Maraun, D., Wetterhall, F., Ireson, A. M., Chandler, R. E., Kendon, E. J., Widmann, M., ... & Thiele-Eich, I. (2010). Precipitation downscaling under climate change: recent developments to bridge the gap between dynamical models and the end user. *Reviews of Geophysics, 48*(3). DOI:10.1029/2009RG000314.

Maurer, E. P. (2007). Uncertainty in hydrologic impacts of climate change in the Sierra Nevada, California, under two emissions scenarios. *Climatic Change, 82*(3-4), 309-325. DOI:10.1007/s10584-006-9180-9.

Maurer, E. P., Brekke, L. D., & Pruitt, T. (2010). Contrasting Lumped and Distributed Hydrology Models for Estimating Climate Change Impacts on California Watersheds. *Journal of the American Water Resources Association, 46*(5), 1024-1035. DOI:10.1111/j.1752-1688.2010.00473.x.

Mearns, L. O., Gutowski, W. J., Jones, R., Leung, L. Y., McGinnis, S., Nunes, A. M. B., & Qian, Y. (2007) updated 2011. The North American Regional Climate Change

Assessment Program dataset. *National Center for Atmospheric Research Earth System Grid data portal, Boulder, CO*. http://www.earthsystemgrid.org/browse/viewProject.htm?projectId=ff3949c8-2008-45c8-8e27-5834f54be50f (accessed September 2010).

Mearns, L. O., Gutowski, W., Jones, R., Leung, R., McGinnis, S., Nunes, A., & Qian, Y. (2009). A regional climate change assessment program for North America. *Eos, Transactions American Geophysical Union, 90*(36), 311-311. DOI:10.1029/2009EO360002.

Minville, M., Brissette, F., & Leconte, R. (2008). Uncertainty of the impact of climate change on the hydrology of a nordic watershed. *Journal of Hydrology, 358*(1), 70-83. DOI:10.1016/j.jhydrol.2008.05.033.

Mitchell, T. D., & Hulme, M. (1999). Predicting regional climate change: living with uncertainty. *Progress in Physical Geography, 23*(1), 57-78. DOI:10.1177/030913339902300103.

Murphy, J. M., Sexton, D. M., Barnett, D. N., Jones, G. S., Webb, M. J., Collins, M., & Stainforth, D. A. (2004). Quantification of modelling uncertainties in a large ensemble of climate change simulations. *Nature, 430*(7001), 768-772. DOI:10.1038/nature02771.

Music, B., & Caya, D. (2007). Evaluation of the hydrological cycle over the Mississippi River basin as simulated by the Canadian Regional Climate Model (CRCM). *Journal of Hydrometeorology, 8*(5), 969-988. DOI:10.1175/JHM627.1

Muzik, I. (2001). Sensitivity of hydrologic systems to climate change. *Canadian Water Resources Journal, 26*(2), 233-252. DOI:10.4296/cwrj2602233.

Najafi, M. R., Moradkhani, H., & Jung, I. W. (2011). Assessing the uncertainties of hydrologic model selection in climate change impact studies. *Hydrological Processes, 25*(18), 2814-2826. DOI:10.1002/hyp.8043.

Pal, J. S., Giorgi, F., Bi, X., Elguindi, N., Solmon, F., Rauscher, S. A., ... & Steiner, A. L. (2007). Regional climate modeling for the developing world: the ICTP RegCM3 and RegCNET. *Bulletin of the American Meteorological Society, 88*(9), 1395-1409. DOI:10.1175/BAMS-88-9-1395.

Pal, J. S., Small, E. E., & Eltahir, E. A. (2000). Simulation of regional‐scale water and energy budgets: Representation of subgrid cloud and precipitation processes within RegCM. *Journal of Geophysical Research: Atmospheres (1984–2012), 105*(D24), 29579-29594. DOI:10.1029/2000JD900415.

Peixoto, J. P., & Oort, A. H. (1992). *Physics of Climate*. New York, NY: Springer-Verlag, 520 pp.

Poulin, A., Brissette, F., Leconte, R., Arsenault, R., & Malo, J. S. (2011). Uncertainty of hydrological modelling in climate change impact studies in a Canadian, snow-dominated river basin. *Journal of hydrology, 409*(3), 626-636. DOI:10.1016/j.jhydrol.2011.08.057.

Randel, D. A., Wood, R. A., Bony, S., Colman, R., Fichefet, T., Fyfe, J., … Taylor, K. E. (2007) Climate models and their evaluation. In Solomon, S., Qin, D., Manning, M., Chen, Z., Marquis, M., Averyt, K.B.,… Miller, H. L. (Eds.), *Climate Change 2007: The Physical Science Basis. Contribution of Working Group I to the Fourth Assessment Report of the Intergovernmental Panel on Climate Change* (pp. 589-622). Cambridge, UK and New York, NY: Cambridge University Press.

Rasmusson, E. M. (1968). Atmospheric water vapor transport and the water balance of North America: II. Large-scale water balance investigations. *Monthly Weather Review, 96*(10), 720-734. DOI:10.1175/1520-0493(1968)096<0720:AWVTAT>2.0.CO;2.

Roberts, J., Pryse-Phillips, A., & Snelgrove, K. (2012). Modeling the Potential Impacts of Climate Change on a Small Watershed in Labrador, Canada. *Canadian Water Resources Journal, 37*(3), 231-251. DOI:10.4296/cwrj2011-923.

Rowell, D. P. (2006). A demonstration of the uncertainty in projections of UK climate change resulting from regional model formulation. *Climatic Change, 79*(3-4), 243-257. DOI:10.1007/s10584-006-9100-z.

Scinocca, J. F., & McFarlane, N. A. (2004). The variability of modeled tropical precipitation. *Journal of the atmospheric sciences, 61*(16), 1993-2015. DOI:10.1175/1520-0469(2004)061<1993:TVOMTP>.

Serreze, M. C., Bromwich, D. H., Clark, M. P., Etringer, A. J., Zhang, T., & Lammers, R. (2002). Large‐scale hydro‐climatology of the terrestrial Arctic drainage system. *Journal of Geophysical Research: Atmospheres (1984–2012), 107*(D2), ALT-1, 28. DOI:10.1029/2001JD000919.

Shrestha, R. R., Berland, A. J., Schnorbus, M. A., & Werner, A. T. (2011). Climate change impacts on hydro-climatic regimes in the peace and Columbia watersheds, British Columbia, Canada. *Pacific climate impacts consortium, University of Victoria*, Victoria.

Skamarock, W. C., Klemp, J. B., Dudhia, J., Gill, D. O., Barker, D. M., Wang, W., & Powers, J. G. (2005). *A description of the advanced research WRF version 2* (No. NCAR/TN-468+ STR). National Center For Atmospheric Research Boulder Co Mesoscale and Microscale Meteorology Div.

Thorne, R. (2011). Uncertainty in the impacts of projected climate change on the hydrology of a subarctic environment: Liard River Basin. *Hydrology and Earth System Sciences, 15*(5), 1483-1492. DOI:10.5194/hess-15-1483-2011.

Trenberth, K. E., Dai, A., Rasmussen, R. M., & Parsons, D. B. (2003). The changing character of precipitation. *Bulletin of the American Meteorological Society, 84*(9), 1205-1217. DOI:10.1175/BAMS-84-9-1205.

Vano, J. A., Udall, B., Cayan, D. R., Overpeck, J. T., Brekke, L. D., Das, T., ... & Lettenmaier, D. P. (2014). Understanding Uncertainties in Future Colorado River streamflow. *Bulletin of the American Meteorological Society, 95*(1), 59-78. DOI:10.1175/BAMS-D-12-00228.1.

Velázquez, J. A., Schmid, J., Ricard, S., Muerth, M. J., Gauvin St-Denis, B., Minville, M., ... & Turcotte, R. (2013). An ensemble approach to assess hydrological models' contribution to uncertainties in the analysis of climate change impact on water resources. *Hydrology and Earth System Sciences, 17*(2), 565-578. DOI:10.5194/hess-17-565-2013.

Von Storch H., & Zwiers, F. W. (1999). *Statistical Analysis in Climate Research*. UK: Cambridge University Press.

Water Survey of Canada. (2010). Retrieved from http://www.wsc.ec.gc.ca/applications/H2O/report-eng.cfm?yearb=&yeare=&station=03OE001&report=monthly&year=1971 (Accessed 2013).

Wilby, R. L., & Harris, I. (2006). A framework for assessing uncertainties in climate change impacts: Low-flow scenarios for the River Thames, UK. *Water Resources Research, 42*(2). doi 10.1029/2005WR004065.

Xu, H., Taylor, R. G., & Xu, Y. (2011). Quantifying uncertainty in the impacts of climate change on river discharge in sub-catchments of the Yangtze and Yellow River Basins, China. *Hydrology and Earth System Science, 15*(1), 333-344.

6. Projected Changes in Runoff for Labrador's Churchill River Basin using Weighted Climate Model Ensembles

6.1. Abstract

Several weighted multi-model ensembles are used to investigate the projected impacts of climate change on streamflow in Labrador's Churchill River Basin. With eight models from the North American Regional Climate Change Assessment Program, six weighting schemes were developed based on five individual weighting criteria. Individual weights were based on differences between historical observations and model simulations covering the same time frame, divergence from the ensemble mean as well as the physical consistency of the model (i.e. the mean annual terrestrial water balance residual). Each month was weighted separately to provide a full annual cycle of the impacts of climate change. Results from the six weighting schemes had similar attributes including an earlier spring melt, an increase in monthly streamflow from October through May and no substantial change in late summer. Differences include varying levels of confidence and different sized ranges of uncertainty. Projected mean annual changes from the weighted ensembles ranged from an increase of 9.8 to 14.6%.

6.2. Preface

This chapter is currently being prepared to submit for publication.

This chapter is intended to round out the research conducted in the thesis. Chapter 3 used output from a bias-corrected multi-model ensemble to drive a hydrological model in a sub basin of the Churchill River to investigate the projected impacts of climate change on the annual hydrological cycle. Chapter 4 took an initial look at the full range of the simulated hydrological components for the entire Churchill River Basin. Mean annual cycles of atmospheric and terrestrial water balances were explored for a range of climate models and reasons for the existence of residuals were discussed. Chapter 5 took advantage of the differences found between mean annual atmospheric moisture convergence, the balance of precipitation and evaporation and the land-surface scheme runoff to find the range of projected mean annual runoff change over the entire basin. Finally, this chapter expands the analysis further by investigating the impacts of climate change on the annual streamflow cycle of the entire Churchill River Basin. A weighted multi-model ensemble of the impacts of climate change on the annual cycle of climate model runoff is presented. By applying six weighting schemes, streamflow projections and ranges of uncertainty are given for each month.

6.3. Introduction

Climate change is projected to impact the earth's hydrological cycle in significant ways (IPCC 2014) and some of these changes are already being observed (Trenberth et al.

2003; Dery et al. 2009). This changing hydrology poses a challenge for those in water resource management as it is no longer sufficient to base decisions exclusively on historical data – climate change projections must also be taken into account. The most powerful tools in projecting climate change are general circulation models (GCMs), which simulate the impact of changing atmospheric greenhouse gas concentrations on the climate, typically at a grid scale of 200 km or larger.

To investigate impacts on a more local level, downscaling, dynamic or statistical, is used. Dynamic downscaling employs a limited area, relatively high-resolution regional climate model (RCM) nested within a lower resolution GCM. Statistical downscaling often employs empirical relationships between larger circulation patterns and a specific location. Dynamic downscaling requires substantial computing power as RCMs are physically based (similar to GCMs), using numerical representations of the Navier-Stokes equations and thermodynamic processes. Parameterizations are used to represent processes that cannot be resolved at the RCM grid scale (e.g. precipitation). Statistical downscaling is computationally much cheaper but is not physically based. Researchers with limited computing power either employ statistical downscaling or access dynamically downscaled data that has been created by others.

In order to investigate the impacts of climate change on the hydrology of a given region, many hydro-climatology studies use climate model output, such as precipitation and temperature, as input for hydrological models to simulate streamflow (Roberts et al. 2012, Fowler et al. 2007, Bennett et al. 2012, and others). That being said, most climate

models include land-surface runoff as one of their outputs, which can be used to approximate streamflow. Roads *et al.* (2003) and Serreze *et al.* (2003) describe streamflow and river discharge as lagged and routed runoff. As runoff is not directly observed, one can approximate it as observed streamflow divided by the drainage area and, conversely, one can also approximate streamflow from simulated runoff.

Uncertainty

It is widely known that one of the primary factors limiting useful application of model output are the uncertainties inherent in climate modelling (Minville *et al.* 2008; Khalili *et al.* 2006; Ludwig *et al.* 2009). This uncertainty in climate projections and simulation of the hydrological response to climate changes complicates the understanding of the impacts on water resources (Minville *et al.* 2008; Treut *et al.* 2008; Xu *et al.* 2011).

While GCM structure and physics has been found to play a majority role in uncertainty, RCM formulation has been found to have a comparable or sometimes dominant influence (Roberts *et al.* 2012; Rowell 2006; Déqué *et al.* 2007). Relative contributions to uncertainty vary according to spatial domain, region, season and variable (Déqué *et al.* 2005; Fowler *et al.* 2007). Effectively representing the uncertainties involved in climate change impact projection is essential for helping water managers and hydroelectric developers create and adopt coherent and informed strategies (Dettinger 2004; Kipari and Gleick 2004; Maurer 2007).

Different GCMs produce a variety of climate change signals even when forced with identical climate forcing (Meehl *et al.* 2007; Rummukainen 2010). Similarly, RCMs have large differences even when forced with identical boundary conditions (Jacob *et al.* 2007; Eum *et al.* 2012). This is justification for use of an ensemble of RCMs and GCMs to produce a best estimate for climate change assessment (Déqué *et al.* 2007). Combining ensemble member simulations generally increases the skill, reliability and consistency of results (Tebaldi and Knutti 2007; Eum *et al.* 2012). These multi-model ensembles can be weighted according to the relative performance of each ensemble member, with regard to certain criteria, or all models can have equal weights (i.e. unweighted).

It has been found that a weighted multi-model ensemble typically improves performance over a single model (Palmer *et al.* 2004; Kendon *et al.* 2008; Eum *et al.* 2012). Quantifying the likelihood of each model's simulation accuracy is suggested by many (New and Hulme 2000; Eum *et al.* 2012; Shrestha *et al.* 2010) to avoid potentially erroneous analysis, as each model has different skill and simulation capability. Eum *et al.* (2012) found that improvements in an ensemble's output were due to the reliability and accuracy of the RCMs rather than the ensemble size, though many models are still required due to the uncertainties of future climate.

It is not clear how to consider model performance when constructing future climate projections (Weigel *et al.* 2010; Frigon *et al.* 2010), though intuitively a model with larger biases in current climate simulation should be given lower confidence in future projections. That being said, a small bias in base period simulations doesn't necessarily

mean a model will accurately reproduce the future climate. Also, there is no consistent relationship between skill of present and future simulations (Jun *et al.* 2008; Knutti *et al.* 2010a,b), though the amplitude of climate variable responses of the past are a robust measure of the likelihood of future amplitudes (Eum *et al.* 2012).

Weighting schemes are based on subjective measures of model skill in reproduction of past climate characteristics (van der Linden and Mitchell 2009, Christensen et al. 2010). A straightforward and widely used method is the Reliability Ensemble Averaging (REA) (Giorgi and Mearns 2002), which uses two weighting criteria: accuracy of historical simulation and level of convergence with other models while simulating the future. In other words, "reliability" in this sense refers to agreement of the ensemble with regard to the reproduction of present day climate and projections of the climate change signal. Ghosh and Mujundar (2009), who use a modified version of REA, feel convergence is an important weighting criteria to prevent an overly strong influence of outliers. Fowler at al (2007) agree that the robustness of responses across models must be considered. Eum *et al.* (2012) has a thorough review of various weighting methods.

Model validation and weighting is a necessarily custom and subjective process that depends on the data available and the specific needs of the end user (van der Linden and Mitchell 2009). By validating and weighting the models, there is an opportunity to explore the impact of weighted versus non-weighted ensembles on the relative changes between base and future simulations. Any agreement between aspects of the weighted

and non-weighted ensemble projections are less sensitive to the subjective weighting criteria and can be taken as an indication of the robustness of those results.

The purpose of this paper is to investigate the projected changes in runoff of Labrador's Churchill River Basin under climate change using weighted multi-model ensembles. REA and modified REA methods are employed and combined with weighting criteria based on a model's physical consistency. Comparisons between the different weighting schemes and an unweighted ensemble are explored to obtain an idea of which projected changes are less sensitive to the applied weights, thus giving one measure of robustness.

6.4. Background

Climate Models

The North American Regional Climate Change Assessment Program (NARCCAP) publishes the output of an ensemble of GCMs and RCMs at a 50 km resolution over North America. The simulations cover a base period of 1971-2000 and a future period 2041-2070. GCMs used in this study include ccsm (Collins et al. 2006), cgcm3 (Flato 2005, Scinocca and McFarlane 2004), gfdl (GFDL 2004) and hadcm3 (Gordon et al. 2000, Pope et al. 2000), while RCMs include CRCM (Caya and Laprise 1999), HRM3 (Jones et al. 2004), RCM3 (Giorgi et al. 1993a,b; Pal et al. 2000, 2007), and WRFG (Skamarock et al. 2005). The models are discussed in detail in Chapters 4 and 5 and on the NARCCAP website (http://www.narccap.ucar.edu/). The eight RCM-GCM combinations used here are found in Table 6.1.

Table 6.1 – RCM-GCM Combinations of Ensemble Members

		GCM			
		ccsm	**cgcm3**	**gfdl**	**hadcm3**
RCM	**CRCM**	X	X		
	HRM3			X	X
	RCM3		X	X	
	WRFG	X	X		

Basin

The Churchill River is located in Labrador, Canada. Near the geographic center of the basin is the Churchill Falls generating station, which has a capacity of nearly 5428 MW. The river's full hydroelectric potential is yet to be developed and there are two potential development sites downstream (on the "Lower Churchill") with a combined capacity of 3074 MW. The Lower Churchill Project encompasses Gull Island (2250 MW) and Muskrat Falls (824 MW), respectively located 232 km and 291 km downstream of the Churchill Falls station. Construction on Muskrat Falls is currently underway. The entire Churchill River Basin covers approximately 92 500 km^2. The basin is represented in Figure 6.1 at the common 0.25 degree grid scale to which all the climate model data was regridded for this work.

Observed and Naturalized Streamflow Data

Since roughly three-quarters of the runoff in the Churchill River Basin occurs upstream of the Churchill Falls hydroelectric facility a direct comparison between simulated runoff and observed streamflow at Muskrat Falls would not be useful. Naturalized flow, which

negates the effects of damming and water management, is preferred for model validation (Music and Caya 2007). As such, this study will use naturalized streamflow data, created by Fortin and Latraverse (2000), which accounts for the impact of the reservoirs and control structures of Churchill Falls. They approximated natural inflows into each reservoir (I_N) (i.e. runoff) by applying Equation 6.1.

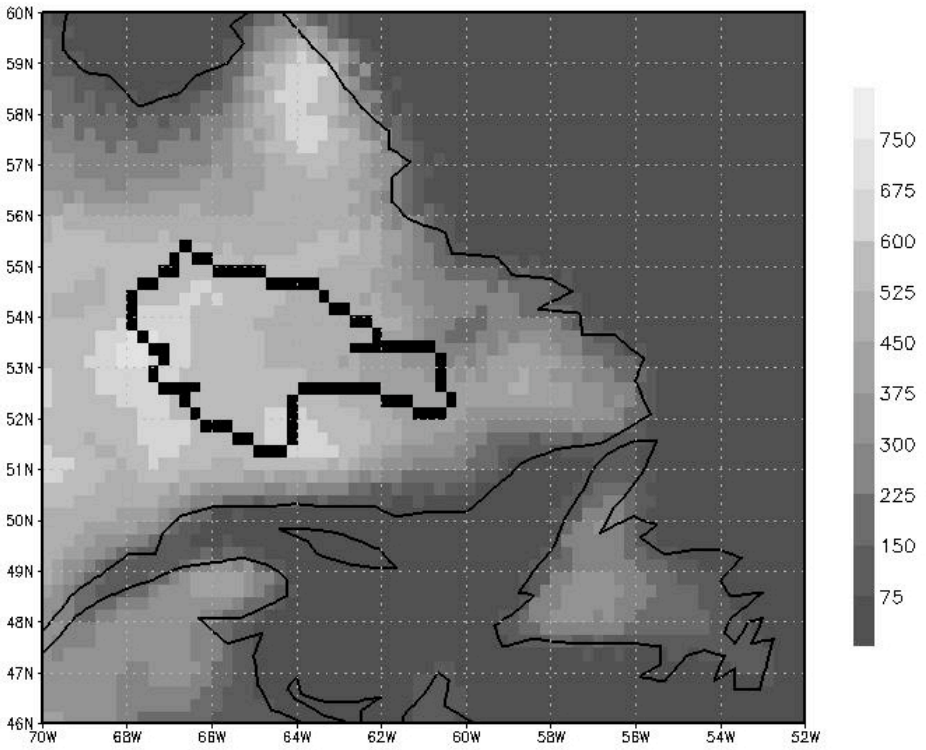

Figure 6.1 – The outline of the Churchill River Basin (thick black line) and the topography (scale in metres)

$$\frac{dS}{dt} = I_N + I_C - O_C \qquad (6.1)$$

Here, dS/dt is the change in reservoir storage, I_C is the controlled inflow into the reservoir (via control structures) and O_C is controlled outflow from the reservoir. Direct

precipitation and evaporation over the reservoir are considered to be implicit in the measured dS/dt. Results of the naturalization procedure for streamflow values from 1972-1999 as applied to Muskrat Falls are presented in Figure 6.2. The mean annual observed streamflow is 1825 m^3/s and the mean annual naturalized streamflow is 1875 m^3/s. Observed streamflow is slightly lower due to the additional evaporation from the reservoirs.

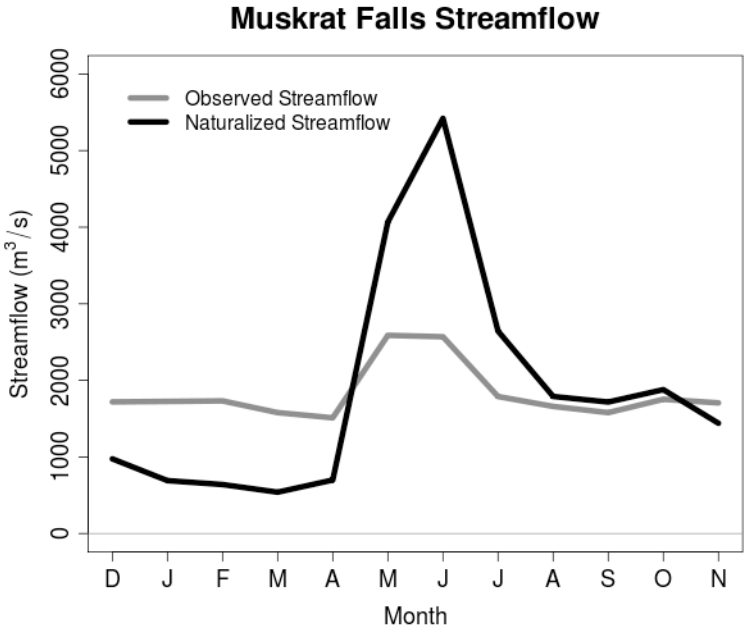

Figure 6.2 – Comparison of observed and naturalized streamflow at Muskrat Falls.

While climate model runoff is not routed like measured and naturalized streamflow, there is still a valid basis to compare streamflow to simulated runoff. (Runoff here refers to the combination of surface and subsurface runoff.) If one made the approximation that the water in rivers and streams within the Churchill River Basin flow at an average of 1 m/s it would take less than 12 days for a drop of water in the headwaters to reach the mouth

of the river at Muskrat Falls (a route of roughly 1000 km), much less than the monthly timescale examined in this study. As such, relatively little error would be introduced by using this approximation.

Throughout this paper "runoff" refers to simulated ensemble member output for either the base or the future period and "streamflow" refers to the naturalized data and the projected changes produced by the weighted ensembles.

6.5. Methodology

Weighting

Five weighting criteria, were used here in various combinations: (i) divergence from the monthly ensemble mean projected change, (ii) reproduction of mean monthly streamflow, (iii) reproduction of the distribution of mean streamflow for each month, (iv) divergence from the monthly ensemble mean streamflow distribution, (v) mean annual physical consistency of models. Once weights were calculated they were subsequently normalized to ensure the sum of all weights equaled one, for easy comparison. Justification for the use of each weighting criteria combination is given in the *Total Weights* subsection, immediately following Equation 6.7.

(i) Divergence from the monthly ensemble mean projected change, WD_i

As per the REA method (Giorgi and Mearns 2002), the weight based on the divergence of an ensemble member's projected change in runoff from the ensemble mean was

calculated according to Equation 6.2. Any values of WD_i that were greater than one, implying that the difference from the ensemble mean was smaller than natural variability, were set to one. $\overline{\Delta R_e}$ is the mean ensemble change in runoff, $\overline{\Delta R_i}$ is the mean change in runoff for ensemble member *i* and σ_{nat} is the standard deviation of naturalized streamflow for the month in question.

$$WD_i = \frac{\sigma_{nat}}{abs(divergence)} = \frac{\sigma_{nat}}{abs(\overline{\Delta R_e} - \overline{\Delta R_i})} \qquad (6.2)$$

(ii) Reproduction of mean monthly streamflow, WB_i

Two methods for determining model weight based on reproduction of observed runoff were used. The first (WB_i) is based on the REA method (Giorgi and Mearns 2002), while the second (WC_i) follows the style of Ghosh and Mujumdar (2009), described further below.

WB_i was calculated according to Equation 6.3. Any WB_i values greater than one, implying that the mean runoff bias for that month was less than the natural variability, were set to one. $\overline{R}_{nat}$ is the mean naturalized streamflow, $\overline{R}_i$ is mean runoff of ensemble member *i* and σ_{nat} is the standard deviation of naturalized streamflow for the month in question.

$$WB_i = \frac{\sigma_{nat}}{abs(bias)} = \frac{\sigma_{nat}}{abs(\overline{R}_{nat} - \overline{R}_i)} \qquad (6.3)$$

(iii) Reproduction of the distribution of mean streamflow, WC_i

WC_i was determined based on a model's ability to accurately simulate various aspects of their corresponding historical observations. For each ensemble member, empirical cumulative distribution functions (CDFs) for both the simulated and naturalized data were compared. Ten equally spaced points on the CDF curves (5^{th}, 15^{th}, 25^{th}, … , 75^{th}, 85^{th}, and 95^{th} percentiles) were used to calculate the root mean square difference ($RMSD_i$) between the simulated and naturalized data. The square root of the inverse was used, as per Equation 6.4, due to the large range of RMSD values (from less than 100 to nearly 5000).

$$WC_i = \frac{1}{\sqrt{RMSD_i}} \qquad (6.4)$$

(iv) Divergence from the monthly ensemble mean streamflow distribution, WF_i

WF_i is similar to WC_i, except $RMSD_i$ is calculated with respect to the ensemble mean CDF as opposed to the naturalized streamflow CDF.

(v) Physical Consistency, WR_i

This weight is based on the residual of the mean annual terrestrial water balance, ε_t found in Equation 6.5 and discussed in depth in Chapters 4. P is precipitation, E is evaporation, R is runoff, and S is land-surface water storage (including soil moisture and snowpack). Annual residual was chosen because some of the variables required for the calculation of

monthly residuals (namely snow water equivalent of the snowpack) were not available for all ensemble members.

$$P - E = R + \frac{\partial S}{\partial t} + \varepsilon_t \qquad (6.5)$$

The terrestrial water storage component in Equation 6.5 tends to zero over long periods of time (as ∂t gets very large), implying that mean climatological runoff should be equal to P – E. This however is not always the case, as discussed in Chapter 4. As with WC_i and WF_i, the inverse of the square root of an ensemble member's relative residual was taken due to the large range of ε_t values (from 0.56% to 32.73%), as shown in Equation 6.6. Any WR_i values greater than one (implying less than 1% residual, which could be attributed to rounding error) were set to one.

$$WR_i = \frac{1}{\sqrt{\varepsilon_t(\%)}} \qquad (6.6)$$

Total Weights

The weights for each ensemble member and for each month were calculated by using various combinations of the above criteria. Since selection of model weights is largely a subjective process, multiple approaches were used as a check for weight selection sensitivity. While many of the weighting criteria are based on the REA approach and may have similarities, common results found across all approaches can increase the confidence in said results.

The six weighting schemes, W_{ni}, are as follows:

(a) $W1_i$ = Unweighted (i.e. equal weights)
(b) $W2_i = WR_i$
(c) $W3_i = WD_i * WB_i$
(d) $W4_i = WF_i * WC_i$
(e) $W5_i = WD_i * WB_i * WR_i$
(f) $W6_i = WF_i * WC_i * WR_i$

(6.7)

$W1_i$ was chosen as a baseline for comparison of the other weighting schemes. $W2_i$ was isolated to investigate the impact of exclusively considering the mean annual physical consistency of ensemble members, which has not been used in model weighting before. $W3_i$ and $W4_i$ were used to compare the impact of two methods of weighting an ensemble members ability to reproduce observations (or naturalized flow in this case). Each of the two approaches has its advantages. The advantage of using $W3_i$ is the simplicity, while the primary advantage of $W4_i$ is the explicit consideration of the interannual variability of monthly flows, including low and high flows represented by the 5^{th} and 95^{th} percentiles respectively. WD_i and WF_i were included because convergence was found to be one of the criteria required to "yield a high reliability for a given model simulation," (Giorgi and Mearns 2002) along with reproduction of observations. $W5_i$ and $W6_i$ were included to explore the interaction between established weighting schemes and the impact of an ensemble member's physical consistency.

The mean change in runoff was calculated according to Equation 6.8 through an iterative process. As the weighting of ensemble members will result in a different ensemble mean,

the divergence weights (WD_i and WF_i) needed to be recalculated. The weights converged quickly, typically within five iterations. (It was found that this iteration process had a relatively minor impact on the end result.) Subsequently, projected future streamflow was calculated as the base period naturalized streamflow plus $\overline{\Delta R}_n$, where n represents the weighting scheme from Equation 6.7.

$$\overline{\Delta R}_n = \frac{\sum_{i=1}^{8} W_{ni} \Delta R_{ni}}{\sum_{i=1}^{8} W_{ni}} \qquad (6.8)$$

Uncertainty Ranges

As per Giorgi and Mearns (2002), uncertainty δ was determined using Equation 6.9. This is based on the equation for root mean square difference, which implies 2δ is centered on the mean projected runoff change $\overline{\Delta R}$ and approximately covers a 68.3% confidence interval. This assumes the projected changes in runoff follow a normal distribution. Further to this, the 95.5% confidence interval is represented by 4δ, while the 80% and 90% confidence intervals can be represented by 2.56δ and 3.29δ respectively. Since the actual distribution of the projected runoff changes are unknown due to the small sample size available, this uncertainty (and the corresponding confidence intervals) should be considered a low estimate. The 80% and 90% confidence intervals were used here for the purposes of illustration.

$$\delta = \sqrt{\frac{\sum_{i=1}^{8} W_i (\Delta R_i - \overline{\Delta R})^2}{\sum_{i=1}^{8} W_i}} \qquad (6.9)$$

6.6. Results

Simulated Monthly Runoff

Figure 6.3 shows the mean hydrographs for each unweighted ensemble member for both base and future periods. Notice the similar patterns produced by ensemble members with common RCMs. This correlation is accounted for by including two ensemble members for each RCM (each forced by a different GCM), ensuring one RCM is not unintentionally more influential in the ensemble projection than any of the others (Weigel et al. 2010). The correlation between GCMs is much smaller and considered unimportant here.

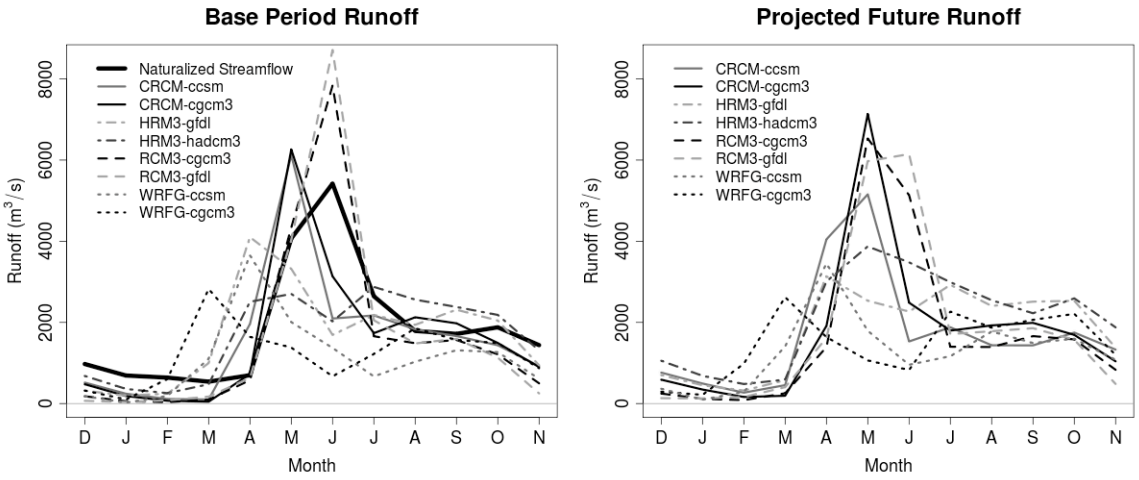

Figure 6.3 – Ensemble member mean hydrographs for base (left) and future periods (right).

Figure 6.4 presents simulated runoff CDFs for every month in the base (black lines) and future period (grey lines) for each ensemble member. Naturalized streamflow is also shown for comparison purposes.

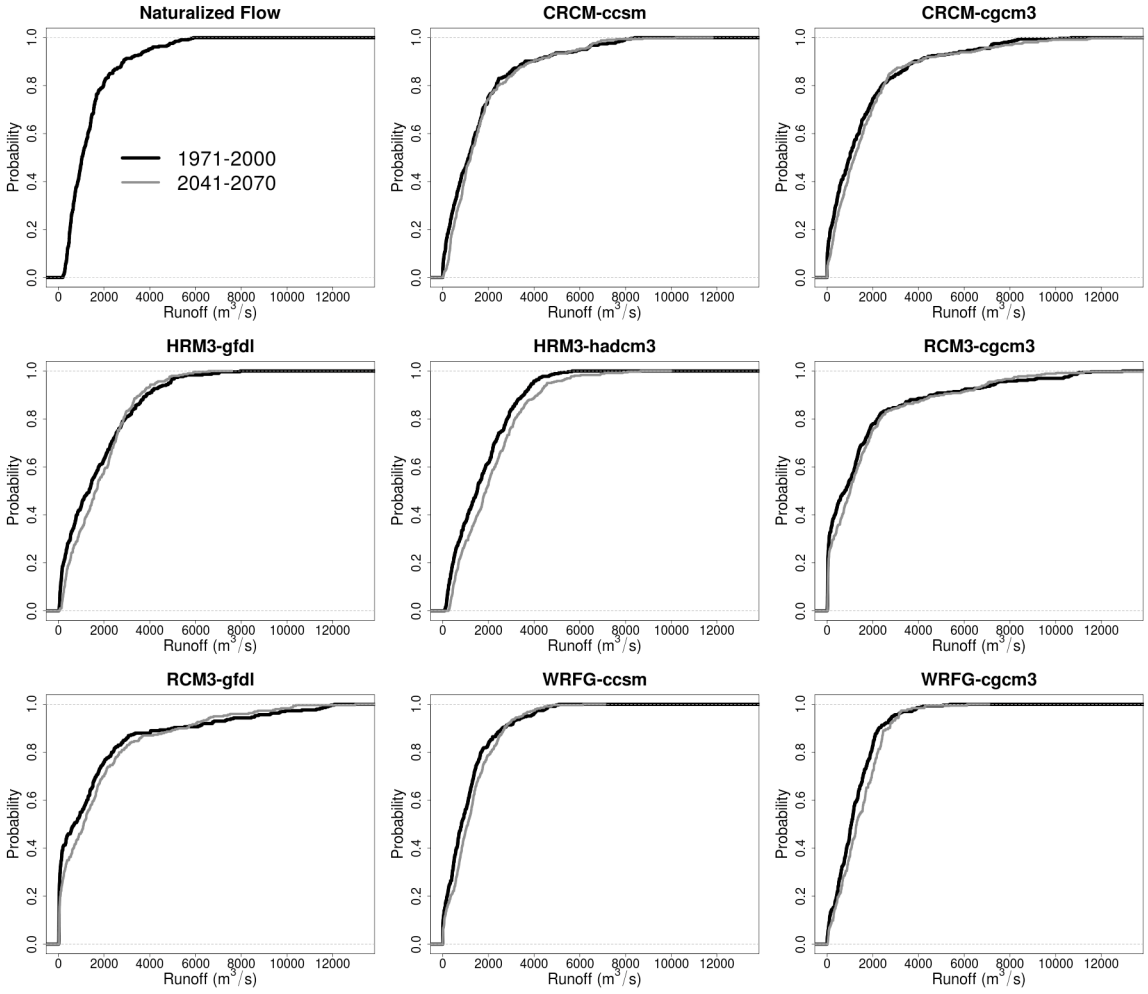

Figure 6.4 – CDFs of naturalized streamflow as well as simulated base period (black lines) and future period (grey lines) for each ensemble member.

Most CDFs have a relatively sharp turn in the distribution between probabilities of 0.8 and 0.9, which illustrates the impact of the spring melt on monthly runoff values. For two months each spring (typically May and June but may vary from year to year and between

ensemble members) the melting snowpack causes a sharp increase in runoff to well over 2000 m^3/s.

There is also a wide range of high runoff values between ensemble members. While many are similar to the naturalized flow which maxes out at around 6000 m^3/s, several ensemble members are up in the 10 000 and even 14 000 m^3/s range. On the low runoff end, most ensemble members have some months with zero runoff (e.g. RCM3-cgcm3) while the naturalized flow doesn't. This may extend from the low winter precipitation biases found in Roberts et al (2012).

Most of the future period CDFs are consistently further to the right than their base period counterparts. This shows monthly runoff generally increases under climate change. Some show an increase in lower end of runoff values (below 0.8 probability) but a decrease or ambiguous change in higher flows (e.g. CRCM-cgcm3, HRM3-gfdl). This implies that while monthly runoff is expected to increase for most of the year, the magnitude of the spring melt may actually decrease or remain constant.

Weights

The normalized weights calculated according Equation 6.7 are plotted by month and ensemble member in Figure 6.5. There is no plot for the unweighted ensemble as all (normalized) values would equal 0.125. Similarly for WR_i, which has only one value per ensemble member for the entire year. These values are found in Table 6.2.

Table 6.2 – Ensemble Member WR_i Values

	CRCM ccsm	CRCM cgcm3	HRM3 gfdl	HRM3 hadcm3	RCM3 cgcm3	RCM3 gfdl	WRFG ccsm	WRFG cgcm3
WR_i	0.047	0.269	0.060	0.269	0.072	0.057	0.133	0.092

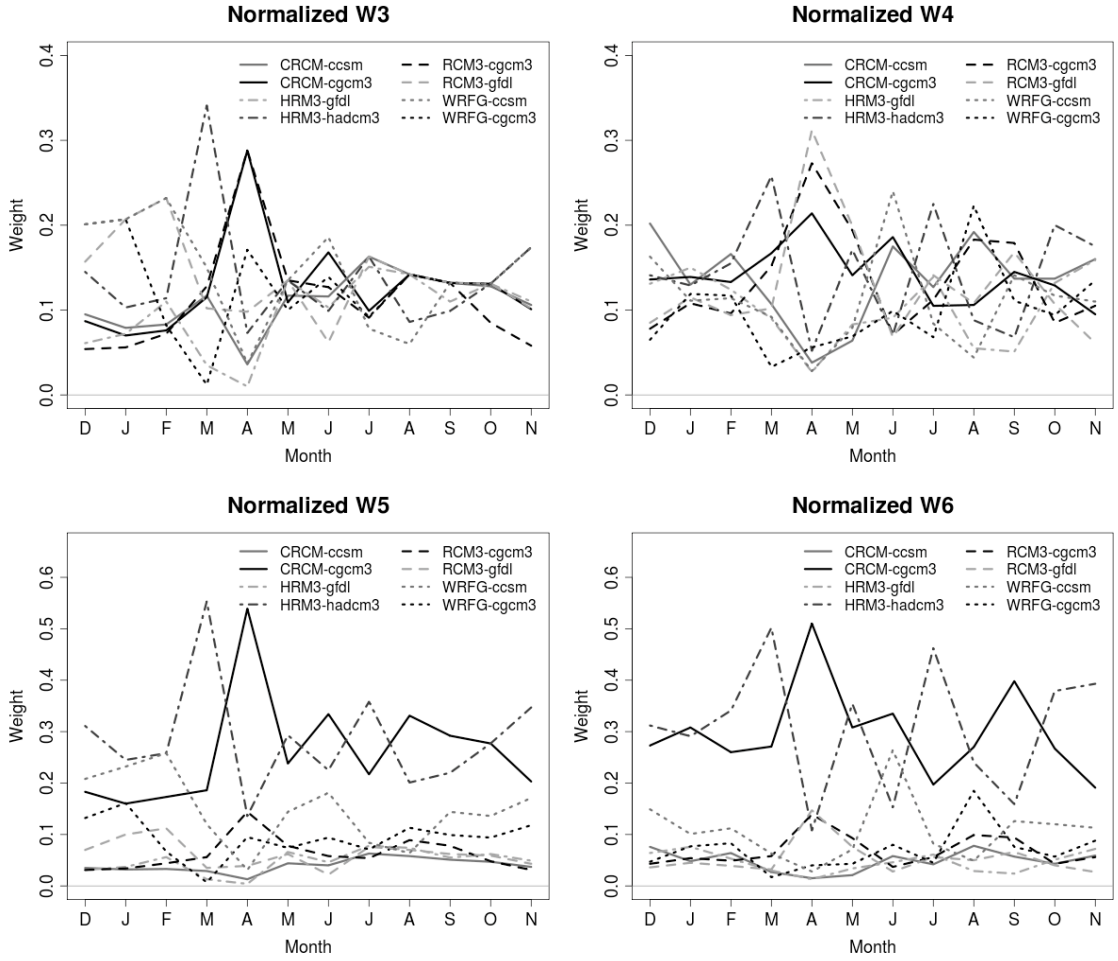

Figure 6.5 – Normalized Weights of W3 (top left), W4 (top right), W5 (bottom left) and W6 (bottom right) weighting schemes

It is clear that including WR_i in the weighting scheme (bottom two plots of Figure 6.5) greatly increases the influence of CRCM-cgcm3 and HRM3-hadcm3, which both had residuals less than 1%. (This low residual may result from tuning between the RCMs and their respective GCMs and not necessarily from each models' physical consistency;

CRCM and cgcm3 are from affiliated Canadian climate modelling centres while HRM3 and HadCM3 are both from the Hadley Centre in the UK.) The difference between the use of simple ensemble means and their CDFs can be seen by comparing the plots on the left to those on the right.

Table 6.3 shows the correlations between the individual weights used in each weighting scheme. WR_i was not included as it has a single value throughout the entire year, making correlation impossible. With one or two exceptions (notably HRM3-hadcm3), the correlations between individual weights within each weighting scheme are relatively low, supporting their selection as weights. The average correlation between individual weights for each weighting scheme is roughly 0.4.

Table 6.3 – Correlations between Weighting Schemes and Individual Weights

Ensemble Member	Individual Weights for Each Scheme			
	W3 (WD,WB)	W4 (WF,WC)	W5 (WD,WB)	W6 (WF,WC)
CRCM-ccsm	0.38	0.06	0.42	0.08
CRCM-cgcm3	N/A	0.23	N/A	0.35
HRM3-gfdl	0.56	0.57	0.55	0.55
HRM3-hadcm3	0.63	0.78	N/A	0.80
RCM3-cgcm3	-0.10	0.34	-0.10	0.28
RCM3-gfdl	0.47	0.25	0.47	0.27
WRFG-ccsm	0.57	0.45	0.48	0.48
WRFG-cgcm3	0.66	0.50	0.67	0.44

Weighted Ensemble Projections

Figure 6.6 shows the mean annual cycle of projected future streamflow, for each weighted ensemble (as defined by Equation 6.7). The upper 80% and 90% uncertainty bounds are represented by the dashed light and dark grey lines respectively, while the lower bounds are represented by dotted lines.

The projected future flow for each of the six plots in Figure 6.6 are quite similar. One common feature is a decrease in June flow and a corresponding increase in April and May flows. This means the spring melt will shift earlier in the year. Additionally, all plots indicate there will be an increase in monthly (cold season) flows, from October through May and no discernable change in late summer.

One of the differences between the six weighting schemes is the size of the confidence intervals, particularly in early spring. Table 6.4 shows by weighting scheme those months where there is greater than 80% confidence projected flows will be different from the base period naturalized flow. The narrowest confidence intervals fall between October and March for all weighting schemes.

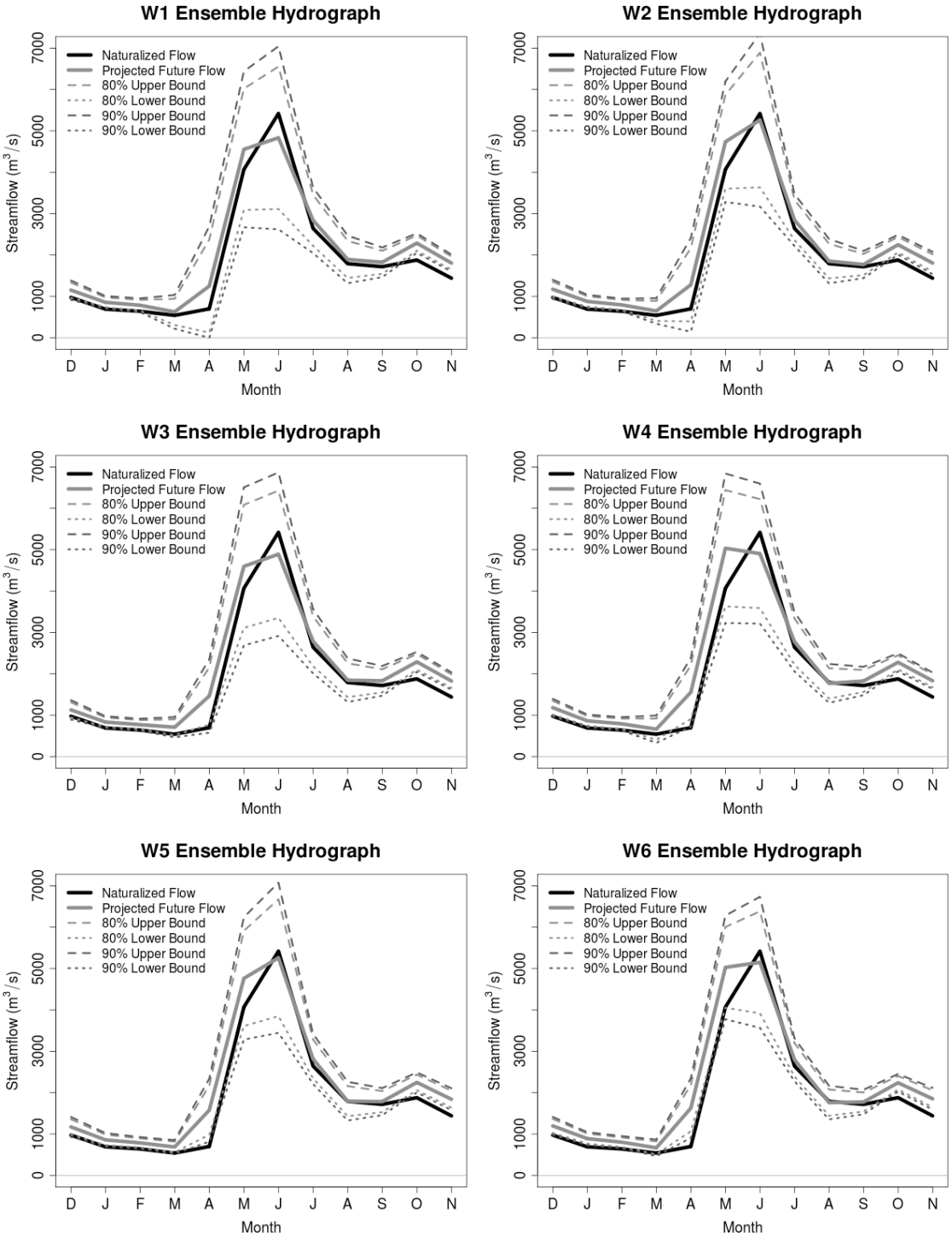

Figure 6.6 - Mean annual cycle of projected future streamflow, with confidence intervals.

Table 6.4 – Months with greater than 80% confidence that future streamflow will be different than base period streamflow. Underline indicates greater than 90% confidence

	Month											
Scheme	**D**	**J**	**F**	**M**	**A**	**M**	**J**	**J**	**A**	**S**	**O**	**N**
W1		X	X								X	X
W2	X	X	X								X	X
W3		X	X		X						X	X
W4	X	X	X		X						X	X
W5	X	X	X	X	X						X	X
W6	X	X	X		X						X	X

Where the mean annual base period naturalized flow is 1875 m^3/s, the mean annual change in streamflow for weighting schemes W1 through W6 are 183, 233, 206, 248, 257, and 273 m^3/s, respectively. This represents a mean annual increase of between 9.8 and 14.6%. Each weighting scheme projects with 90% confidence that an increase in mean annual streamflow will occur.

As a relatively small ensemble size was used to calculate the confidence intervals and not all assumptions can be shown to be valid (e.g. Gaussian distribution of ensemble results), it is prudent to include a spaghetti plot of the projected streamflow changes, as in Figure 6.7. It is important to keep in mind the confidence intervals in Figure 6.6 are synonymous with ensemble uncertainty ranges and should not be interpreted as 'absolute' probability. For instance, if global greenhouse gas emissions do follow the A2 scenario (used to force NARCCAP's GCMs), all projections that fall within the 80% confidence interval do not necessarily have an 80% chance of occurring. The analysis used here is frequentist in

nature and confidence should be interpreted with respect to the uncertainty represented by the eight-member ensemble, not the full spectrum of possible future climates.

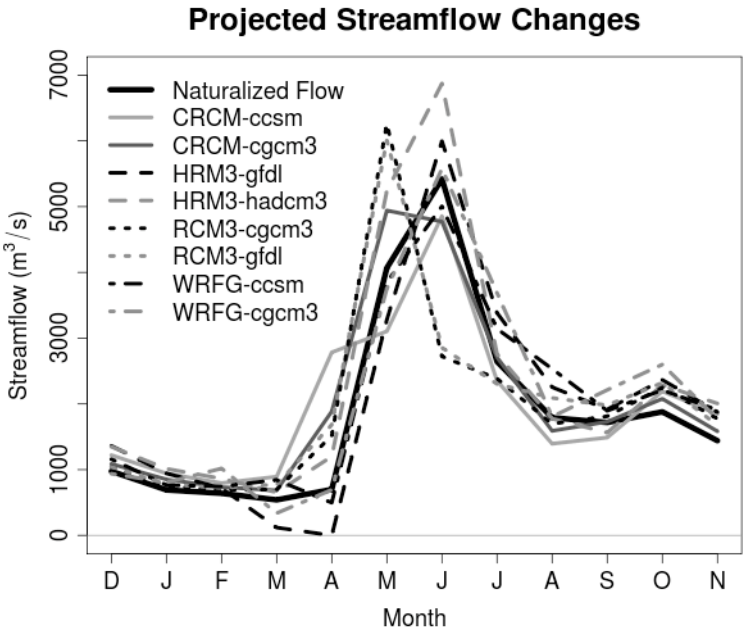

Figure 6.7 – Spaghetti plot of mean annual cycle of projected future streamflow.

Validation

In order to validate the weighting schemes, one ensemble member, CRCM-cgcm3, was selected and removed from the ensemble. CRCM-cgcm3 was chosen as it was one of the highest weighted ensemble members for each of the weighting schemes (Figure 6.5) and its mean hydrograph was relatively similar to that of the naturalized flow (compared with other ensemble members, seen in Figure 6.3). The base period CRCM-cgcm3 simulation was then treated as observed (or naturalized) streamflow and new weights were then calculated for W3 to W6. These new weighted ensemble projections were then compared to the CRCM-cgcm3 future simulation, as in Figure 6.8.

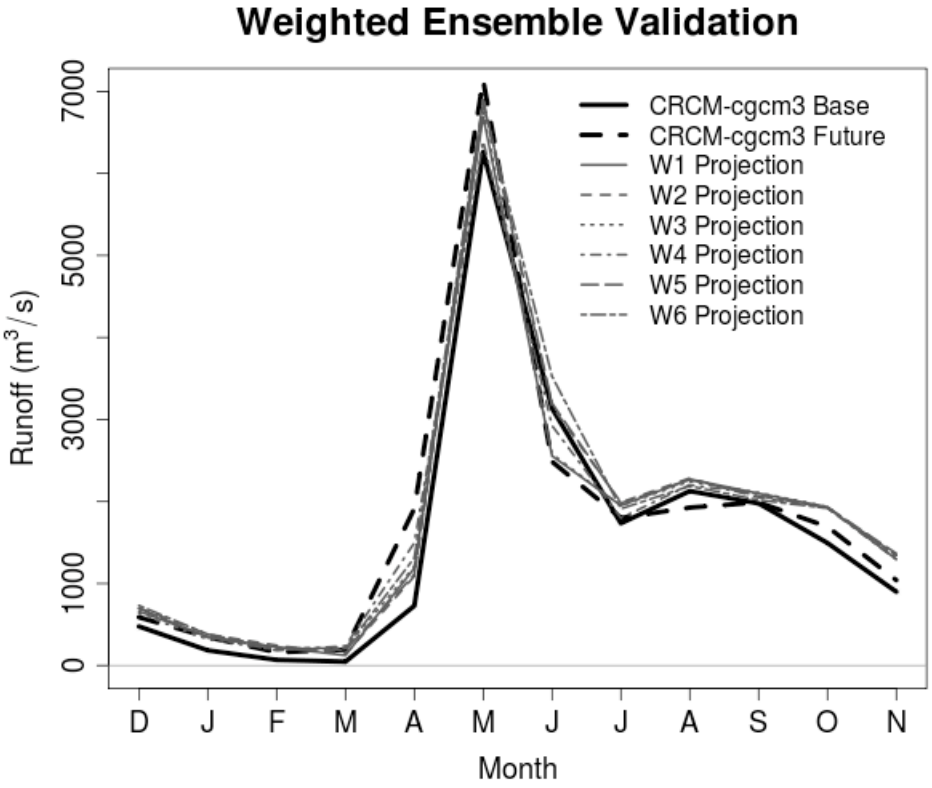

Figure 6.8 – Validation hydrographs for each weighting scheme, as compared to CRCM-cgcm3.

October and November were the only months that fell outside the 80% confidence interval (not shown) for all weighting schemes, primarily because the confidence intervals for those months were relatively narrow. April of W5 also fell outside the range. Table 6.5 shows the RMSD between monthly ensemble projected values and CRCM-cgcm3 future values. W3 had the smallest RMSD while W6 had the largest though there was only about 100 m^3/s difference between them.

Table 6.5 – RMSD between CRCM-cgcm3 future simulation and weighted ensemble projections

Scheme	**W1**	**W2**	**W3**	**W4**	**W5**	**W6**
RMSD (m^3/s)	291	360	279	307	358	384

6.7. Discussion

The projected impact of climate change on the streamflow of the Churchill River Basin found in this study corroborates results of past work. Roberts et al. (2012) used an unweighted, bias-corrected ensemble of NARCCAP precipitation and temperature data to drive a hydrological model for a sub-basin of the Churchill River. They found that the mean annual streamflow was projected to increase by roughly 9%, compared to the 9.8 to 14.6% projected increase found here. Similarly, Chapter 5 found that the mean projected increase in runoff for the entire Churchill River Basin was roughly 11%. Most of the Roberts et al. streamflow increase was projected to occur in the late fall and winter with no significant change occurring during the summer months, which is also what was found here. Both studies indicated an earlier spring melt on average, but not necessarily one with a larger magnitude.

The ranges of uncertainty give one an idea of how confident a projected future streamflow is different from that of the base period. Each weighting scheme produced, with 80% confidence, that future streamflow in October, November, January and February will all be higher than the base period, as per Table 6.4. W5 projects with 80% confidence that streamflow from October to April will be higher in the future. W5 gives the most confidence for increases in streamflow, with five months 90% confident and another two months 80% confident. W6 has similar confidence levels though it has one less month at the 80% level. W1, on the other hand, result in the lowest confidence with

three months at 90% and one month at 80%. W3 and W2 were similar, though each with an additional month at the 80% level.

Another difference between the weighting schemes was the size of the range of uncertainty for March and April, which was noticeably larger for W1 and W2, than W3 through W6. This was because the ensemble members experienced the largest spread of projections for the spring and, for W1 and W2, there was no weight given to models that projected changes close to the ensemble mean, resulting in a larger range of uncertainty.

The inclusion of a model's physical consistency as a weight (W2, W5, W6) caused an increase in June's projected change (rather, less of a decrease). They also had larger mean annual increases in streamflow with an average of 254 m^3/s (13.6%) compared to an average of 212 m^3/s (11.3%) for W1, W3, and W4.

By comparing weighting schemes that used simple means (W3 and W5) with those using CDFs (W4 and W6), it was found that the CDF schemes had a larger increase in streamflow for November through February but the largest differences occurred in April and May (71 and 352 m^3/s respectively higher than simple-mean schemes). The simple-mean schemes had a larger increase in June, and August (by 48 and 56 m^3/s respectively) and there was little difference between the schemes for the remainder of the year. The CDF schemes also produced a larger inter-month variation in the projected changes, with a standard deviation of 372 m^3/s, compared to 296 m^3/s for simple-mean schemes. There was little difference between the two types of schemes with regard to ranges of

uncertainty, except during May and June, where CDF schemes had ranges smaller by 100 and 157 m^3/s respectively.

When looking at the validation, the simple-mean schemes had a smaller RMSD from the validation projection (CRCM-cgcm3) than CDF schemes. This shows that using simple means in the weighting scheme more accurately represents the validation data set, though it doesn't necessarily imply that one would find similar results for the actual future streamflow or even alternative validation data sets. W1 actually had the second smallest RMSDs from the validation data, even though the ensemble projection results were unaffected by any weighting criteria.

6.8. Conclusions

The weighting schemes projected a mean annual increase in streamflow of between 9.8 and 14.6%, when compared to base period naturalized streamflow. For each weighting scheme, at least some future increase in mean annual streamflow was found to occur within the 90% uncertainty range for the ensemble used.

Overall, each of the weighting schemes W1 through W6 produced similar results. Common elements included a decrease in June flow and an increase in April and May flows (as the spring melt moves earlier in the year), an increase in flows from October through May and no substantial change in late summer. The primary differences, other than the magnitude of some changes, was the size of the uncertainty range (i.e. confidence intervals). Though it may be relatively obvious it is worth stating that

weighting schemes that prioritized convergence to the ensemble mean had tighter confidence intervals than those that did not.

There is an inverse relationship between the levels of confidence in projected streamflow changes and the RMSD found during validation. October and November were found by all weighting schemes to have projected increases at the 90% confidence interval, but also performed worst during validation. W4, W5 and W6 all had relatively high levels of confidence in the monthly changes but also had high RMSD during validation. W2, which used only the weight based on physical consistency, performed relatively poorly in the validation and also had relatively low confidence in its projected changes. Low (or high)_confidence in projected changes could mean that the projected future streamflow is similar (different) to that of the base period and should not be used as a measure of ensemble ability. Remember, in this study confidence intervals are synonymous with uncertainty ranges and the ability of each model is indicated by its respective weights.

Results discussed above corroborate the work done by Weigel et al. (2010), who suggest that weighting adds (a relatively small) level of uncertainty to the analysis and that equal weighting (W1) is the "safer and more transparent way to combine models." Weigel et al. also found that weighted ensembles often perform worse than unweighted ensembles partly because there is no consensus on how to objectively derive skill based weights. This is inline with Min and Hense (2006) who show using a Bayesian approach that present day climate (of mean surface temperatures) is better captured by non-trivially weighted ensembles.

Suggestions for future work include the use of a smaller NARCCAP ensemble where the monthly water balance residuals are included. In such a case, there might need to be some kind of compensatory action for unequal representation by correlated RCMs. Also, expansion to include additional weighting criteria based on other observation data sets would likely provide a broader range of projections.

6.9. Acknowledgements

This work would not have been possible without the generous financial support of Nalcor Energy Inc, NSERC, Mitacs and TD Canada Trust.

We wish to thank the North American Regional Climate Change Assessment Program (NARCCAP) for providing access to the data used in this paper. NARCCAP is funded by the National Science Foundation, the U.S. Department of Energy, the National Oceanic and Atmospheric Administration, and the U.S. Environmental Protection Agency Office of Research and Development.

6.10. References

Bennett, K. E., Werner, A. T., & Schnorbus, M. (2012). Uncertainties in Hydrologic and Climate Change Impact Analyses in Headwater Basins of British Columbia. *Journal of Climate, 25*, 5711-5730. DOI:10.1175/JCLI-D-11-00417.1.

Caya, D., & Laprise, R. (1999). A semi-Lagrangian semi-implicit regional climate model: The Canadian RCM. *Monthly Weather Review, 127*(3), 341-362. DOI:10.1175/1520-0493(1999)127<0341:ASISLR>.

Christensen, J. H., Kjellström, E., Giorgi, F., Lenderink, G., & Rummukainen, M. (2010) Weight assignment in regional climate models. *Climate Research, 44*(2-3), 179-194. DOI:10.3354/cr00916.

Collins, W. D., Bitz, C. M., Blackmon, M. L., Bonan, G. B., Bretherton, C. S., Carton, J. A., ... & Smith, R. D. (2006). The community climate system model version 3 (CCSM3). *Journal of Climate*, *19*(11), 2122-2143. DOI:10.1175/JCLI3761.1.

Déqué, M., Jones, R. G., Wild, M., Giorgi, F., Christensen, J. H., Hassell, D. C., ... & Van den Hurk, B. (2005). Global high resolution versus Limited Area Model climate change projections over Europe: quantifying confidence level from PRUDENCE results. *Climate Dynamics*, *25*(6), 653-670. DOI:10.1007/s00382-005-0052-1.

Déqué, M., Rowell, D. P., Lüthi, D., Giorgi, F., Christensen, J. H., Rockel, B., ... & van den Hurk, B. J. J. M. (2007). An intercomparison of regional climate simulations for Europe: assessing uncertainties in model projections. *Climatic Change, 81*(1), 53-70. DOI:10.1007/s10584-006-9228-x.

Déry, S. J., Hernández-Henríquez, M. A., Burford, J. E., & Wood, E. F. (2009). Observational evidence of an intensifying hydrological cycle in northern Canada. *Geophysical Research Letters, 36*(13), L13402, DOI:10.1029/2009GL038852.

Eum, H. I., Gachon, P., Laprise, R., & Ouarda, T. (2012). Evaluation of regional climate model simulations versus gridded observed and regional reanalysis products using a combined weighting scheme. *Climate dynamics, 38*(7-8), 1433-1457. DOI:10.1007/s00382-011-1149-3.

Flato, G. M. (2005). The third generation coupled global climate model (CGCM3). *Environment Canada Canadian Centre for Climate Modelling and Analysis note available at http://www.ec.gc.ca/ccmac-cccma/default.asp?n=1299529F-1.*

Fortin, V., & Latraverse, M. (2000). Une base de données hydrométéorologiques pour le développement d'un indicateur d'hydraulicité. *Logiciels de réseaux Technologies de transport et de distribution (IREQ-2000-268),* Quebec, Canada.

Fowler, H. J., Kilsby, C. G., & Stunell, J. (2007). Modelling the impacts of projected future climate change on water resources in north-west England. *Hydrology and Earth System Sciences, 11*(3), 1115-1126. DOI:10.5194/hess-11-1115-2007.

Frigon, A., Music, B., & Slivitzky, M. (2010). Sensitivity of runoff and projected changes in runoff over Quebec to the update interval of lateral boundary conditions in the

Canadian RCM. *Meteorologische Zeitschrift, 19*(3), 225-236. DOI:10.1127/0941-2948/2010/0453.

GFDL Global Atmospheric Model Development Team. (2004). The new GFDL global atmospheric and land model AM2-LM2: Evaluation with prescribed SST simulations. *Journal of Climate, 17*, 4641-4673. DOI:10.1175/JCLI-3223.1

Ghosh, S., & Mujumdar, P. P. (2009). Climate change impact assessment: Uncertainty modeling with imprecise probability. *Journal of Geophysical Research: Atmospheres (1984–2012), 114*(D18), 113. DOI: 10.1029/2008JD011648.

Giorgi, F., Marinucci, M. R., & Bates, G. T. (1993a). Development of a second-generation regional climate model (RegCM2). Part I: Boundary-layer and radiative transfer processes. *Monthly Weather Review, 121*(10), 2794-2813. DOI:10.1175/1520-0493(1993)121<2794:DOASGR>.

Giorgi, F., Marinucci, M. R., Bates, G. T., & De Canio, G. (1993b). Development of a second-generation regional climate model (RegCM2). Part II: Convective processes and assimilation of lateral boundary conditions. *Monthly Weather Review, 121*(10), 2814-2832. DOI:10.1175/1520-0493(1993)121<2814:DOASGR>.

Giorgi, F., & Mearns, L. O. (2002). Calculation of average, uncertainty range, and reliability of regional climate changes from AOGCM simulations via the "reliability

ensemble averaging"(REA) method. *Journal of Climate, 15*(10), 1141-1158. DOI:10.1175/1520-0442(2002)015<1141:COAURA>2.0.CO;2.

Gordon, C., Cooper, C., Senior, C. A., Banks, H., Gregory, J. M., Johns, T. C., ... & Wood, R. A. (2000). The simulation of SST, sea ice extents and ocean heat transports in a version of the Hadley Centre coupled model without flux adjustments. *Climate Dynamics, 16*(2-3), 147-168. DOI:10.1007/s003820050010.

IPCC. (2014). Chapter 3: Freshwater Resources. In *Climate Change 2014: Impacts, Adaptation, and Vulnerability. Contribution of Working Group II to the Fifth Assessment Report of the Intergovernmental Panel on Climate Change*. New York, NY: Cambridge University Press, 76 pp.

Jones, R., Hassell, D., Hudson, D., Wilson, S., Jenkins, G., & Mitchell J. (2004). *Generating high resolution climate change scenarios using PRECIS*. Exeter, UK: Met Office Hadley Centre, 40 pp.

Khalili, M., Leconte, R., & Brissette, F. (2006, May). On the Use of Multi Site Generated Meteorological Input Data for Realistic Hydrological Modeling in the Context of Climate Change Impact Studies. In *EIC Climate Change Technology, 2006 IEEE* (pp. 1-7). IEEE. DOI:10.1109/EICCCC.2006.277261.

Knutti, R., Furrer, R., Tebaldi, C., Cermak, J., & Meehl, G. A. (2010a). Challenges in combining projections from multiple climate models. *Journal of Climate, 23*(10), 2739-2758. DOI:10.1175/2009JCLI3361.1.

Knutti, R., Abramowitz, G., Collins, M., Eyring, V., Glecker, P. J., Hewitson, B., & Mearns, L. (2010b). Good Practice Guidance Paper on Assessing and Combining Multi Model Climate Projections. In Stocker, T., Dahe, Q., Plattner, G.-K., Tignor, M., & Midgley, P. (Eds.), *Meeting Report of the Intergovernmental Panel on Climate Change Expert Meeting on Assessing and Combining Multi Model Climate Projections*. Bern, Switzerland: IPCC Working Group I Technical Support Unit, University of Bern.

Ludwig, R., May, I., Turcotte, R., Vescovi, L., Braun, M., Cyr, J. F., ... & Mauser, W. (2009). The role of hydrological model complexity and uncertainty in climate change impact assessment. *Advances in Geosciences, 21*(21), 63-71.

Min, S.-K., & Hense, A. (2006). A Bayesian approach to climate model evaluation and multi-model averaging with an application to global mean surface temperatures from IPCC AR4 coupled climate models. *Geophysical Research Letters, 33*(8), L08708, DOI:10.1029/2006GL025779.

Minville, M., Brissette, F., & Leconte, R. (2008). Uncertainty of the impact of climate change on the hydrology of a nordic watershed. *Journal of Hydrology, 358*(1), 70-83. DOI:10.1016/j.jhydrol.2008.05.033.

Music, B., & Caya, D. (2007). Evaluation of the hydrological cycle over the Mississippi River basin as simulated by the Canadian Regional Climate Model (CRCM). *Journal of Hydrometeorology, 8*(5), 969-988. DOI:10.1175/JHM627.1

Pal, J. S., Giorgi, F., Bi, X., Elguindi, N., Solmon, F., Rauscher, S. A., ... & Steiner, A. L. (2007). Regional climate modeling for the developing world: the ICTP RegCM3 and RegCNET. *Bulletin of the American Meteorological Society, 88*(9), 1395-1409. DOI:10.1175/BAMS-88-9-1395.

Pal, J. S., Small, E. E., & Eltahir, E. A. (2000). Simulation of regional‐scale water and energy budgets: Representation of subgrid cloud and precipitation processes within RegCM. *Journal of Geophysical Research: Atmospheres (1984–2012), 105*(D24), 29579-29594. DOI:10.1029/2000JD900415.

Pope, V. D., Gallani, M. L., Rowntree, P. R., & Stratton, R. A. (2000). The impact of new physical parametrizations in the Hadley Centre climate model: HadAM3. *Climate Dynamics, 16*(2-3), 123-146. DOI:10.1007/s003820050009.

Roads, J., Lawford, R., Bainto, E., Berbery, E., Chen, S., Fekete, B., ... & Yarosh, E. (2003). GCIP water and energy budget synthesis (WEBS). *Journal of Geophysical Research: Atmospheres (1984–2012), 108*(D16), 8609. DOI:10.1029/2002JD002583.

Roberts, J., Pryse-Phillips, A., & Snelgrove, K. (2012). Modeling the Potential Impacts of Climate Change on a Small Watershed in Labrador, Canada. *Canadian Water Resources Journal, 37*(3), 231-251. DOI:10.4296/cwrj2011-923.

Rowell, D. P. (2006). A demonstration of the uncertainty in projections of UK climate change resulting from regional model formulation. *Climatic Change, 79*(3-4), 243-257. DOI:10.1007/s10584-006-9100-z.

Scinocca, J. F., & McFarlane, N. A. (2004). The variability of modeled tropical precipitation. *Journal of the atmospheric sciences, 61*(16), 1993-2015. DOI:10.1175/1520-0469(2004)061<1993:TVOMTP>.

Serreze, M. C., Bromwich, D. H., Clark, M. P., Etringer, A. J., Zhang, T., & Lammers, R. (2002). Large‐scale hydro‐climatology of the terrestrial Arctic drainage system. *Journal of Geophysical Research: Atmospheres (1984–2012), 107*(D2), ALT-1, 28. DOI:10.1029/2001JD000919.

Tebaldi, C., & Knutti, R. (2007). The use of the multi-model ensemble in probabilistic climate projections. *Philosophical Transactions of the Royal Society A: Mathematical, Physical and Engineering Sciences, 365*(1857), 2053-2075. DOI:10.1098/rsta.2007.2076.

Trenberth, K. E., Dai, A., Rasmussen, R. M., & Parsons, D. B. (2003). The changing character of precipitation. *Bulletin of the American Meteorological Society, 84*(9), 1205-1217. DOI:10.1175/BAMS-84-9-1205.

Le Treut, H., Gastineau, G., & Li, L. (2008). Uncertainties attached to global or local climate changes. *Comptes Rendus Geoscience, 340*(9), 584-590. DOI:10.1016/j.crte.2008.06.003.

Weigel, A. P., Knutti, R., Liniger, M. A., & Appenzeller, C. (2010). Risks of model weighting in multimodel climate projections. *Journal of Climate, 23*(15), 4175-4191. DOI:10.1175/2010JCLI3594.1.

Xu, H., Taylor, R. G., & Xu, Y. (2011). Quantifying uncertainty in the impacts of climate change on river discharge in sub-catchments of the Yangtze and Yellow River Basins, China. *Hydrology and Earth System Science, 15*(1), 333-344.

7. Summary

This manuscript thesis presented four stand-alone papers (Chapters 3 through 6) which all contributed to the investigation of projected impacts of climate change on the hydrology of Labrador's Churchill River Basin. The initial purpose of this undertaking was to provide useful information to Nalcor Energy regarding the amount and timing of water in the Churchill River in the long-term (i.e. several decades from now), which was required to support design constraints and financing considerations of the Lower Churchill hydroelectric project. A summary specifically for Nalcor Energy can be found in Appendix E.

A broad literature review was conducted in Chapter 2, in addition to those found in Chapters 3 through 6, to provide an overview of the current state of knowledge in the field of climate modelling, uncertainty and impact analysis and to provide context for this work as a whole.

There were three separate multi-model approaches used to look at the impacts of climate change on the Churchill River. Chapter 3 used bias-corrected precipitation and temperature climate model output and hydrologic modeling to investigate the changes in mean daily streamflow for the Pinus River, a sub-basin of the Churchill River. Chapter 5 used a new approach (called fullstream analysis) to study the expected changes in mean annual runoff of the entire basin and took advantage of the full range of simulated hydrological variables from each ensemble member. Chapter 4 was used to support the

analysis conducted in Chapter 5 and provided insight into modelling uncertainty and error. Chapter 6 applied a weighted multi-model ensemble to examine the simulated impacts of climate change on mean monthly runoff for the entire basin.

Climate model output from the North American Regional Climate Change Assessment Program (NARCCAP) was used throughout the thesis. Environment Canada historical meteorological data, Adjusted Historical Canadian Climate Data (AHCCD), data from the Water Survey of Canada and naturalized streamflow data were all used for comparison, bias correction and weighting criteria at various stages of the research.

To a large degree, each of these three approaches corroborated the results of the others. The mean annual increase in runoff/streamflow was found to be 8.9%, 11.2% and between 9.8 and 14.6% for Chapters 3, 5 and 6 respectively. Both Chapters 3 and 6 found there to be an increase in cold-season streamflow volumes, an earlier onset of the spring melt (though not necessarily a larger spring melt) and no discernable change in the late summer and early fall streamflow.

In addition to the information requested by Nalcor, each of the four chapters provides insight into modelling uncertainty and applications for the modeling community at NARCCAP, whose stated primary purpose is "to investigate uncertainties in regional scale projections of future climate and generate climate change scenarios for use in impacts research," (http://www.narccap.ucar.edu/about/index.html). Much of this research was conducted as soon as climate model output became available, which

happened at irregular intervals over the past few years. This is largely why the number of ensemble members used in the analyses increases from Chapter 3 to Chapter 6.

Uncertainty was represented in various ways throughout the thesis. Chapter 3 uses probability distribution functions (PDFs) to present the likelihood of a certain level of precipitation and temperature at various time frames (daily, 5-day, monthly and annual). The differences between base period and future monthly and annual PDFs were also plotted. The mean ensemble hydrograph for base and future periods was shown, as was a spaghetti plot showing how each streamflow changed according to each ensemble member (Figure 3.10), providing a *de facto* response interval. Streamflow changes were also broken down by season. Chapter 5 also used PDFs to communicate mean annual changes in runoff.

Chapter 6 plotted uncertainty ranges around ensemble means of future annual cycles of streamflow. This allows for one to state with 80% and 90% confidence that an increase in streamflow was likely to occur for a given month (though one should keep in mind that 'confidence' is not absolute and refers only to the likelihood with respect to the ensemble and weighting schemes used). Spaghetti plots were also presented showing the variety of base period and future (unweighted) simulations. As model weighting is primarily a subjective process that should include a sensitivity check, the results of a small variety of weighting schemes, including equal weighting, were plotted and discussed.

Overall, this thesis presented the potential impacts of climate change on the mean hydrology of Labrador's Churchill River Basin while representing the uncertainty

embodied in NARCCAP's multi-model ensemble. Given that there were some differences between the output of approaches used and individual ensemble members, in general the mean annual streamflow is expected to increase on the order of 10%. This increase will primarily manifest as additional cold-season (November to March) streamflow. While the work in this thesis attempted to be thorough, there are always avenues to expand and improve the approaches and tools developed as well as additional analysis methods that could be followed. Recommendations for future work are discussed below.

7.1. Recommended Work

There are several sources of uncertainty unrepresented by NARCCAP's ensemble. For instance, only one emissions scenario, A2, was used to force the GCMs. While A2 describes high greenhouse gas emissions relative to many of the other IPCC scenarios it does not capture the range of possible atmospheric concentrations and resulting impacts. NARCCAP also employs only four GCMs, and while they represent a range of climate sensitivities, the most recent IPCC report incorporated several times this number (IPCC 2013). To capture these additional uncertainties data from a source other than NARCCAP would be required.

Several approaches were used in this thesis to investigate the potential impacts of climate change on the Churchill River. That being said, it would still be informative to setup and run a hydrological model, which effectively represents energy balance processes, over the entire basin and force it with bias-corrected climate model output.

The majority of this thesis focused on mean runoff and streamflow, at the annual, monthly or daily scale. There would be some value to water resource managers in investigating the impacts of climate change on extreme hydrological conditions, such as floods and droughts, in the Churchill River watershed. Applying a reservoir or power generation model to determine how the altered streamflow translates into changes in potential power production would prove to be of further value.

This work is focused exclusively within the Churchill River Basin. It would be insightful to examine the water balances of, and apply the fullstream analysis method to watershed areas of similar and larger sizes in different geographic regions across the NARCCAP domain.

Another research opportunity is to use a weighted NARCCAP ensemble where the monthly water balance residuals are included. This would be a smaller ensemble given the current data available but could be expanded to include additional models as more data is published. In such a case, there might need to be some kind of compensatory action for unequal representation by correlated RCMs. Also, expansion to include additional weighting criteria based on other observation data sets would likely provide a broader range of projections.

One recommendation that should be incorporated into future ensemble studies is to publish accumulated moisture convergence fields calculated using an RCM's native vertical coordinate system. This would provide a consistent variable across all ensemble

members without the additional residual introduced by converting to, and performing calculations in, a pressure-level coordinate system.

8. References

Allen M. R., & Ingram, W. J. (2002). Constraints on future changes in climate and the hydrological cycle. *Nature, 419*, 224-232. DOI:10.1038/nature01092.

Allen, M. R., Stott, P. A., Mitchell, J. F. B., Schnur, R., & Delworth, T. L. (2000). Quantifying the uncertainty in forecasts of anthropogenic climate change. *Nature, 407*, 617-620. DOI:10.1038/35036559.

Bates, B. C., Kundzewicz, Z. W., Wu, S., & Palutikof, J. P. (2008). Climate change and water. Intergovernmental Panel on Climate Change Technical Paper IV. Geneva: IPCC Secretariat, 210 pp.

Bennett, K. E., Werner, A. T., & Schnorbus, M. (2012). Uncertainties in Hydrologic and Climate Change Impact Analyses in Headwater Basins of British Columbia. *Journal of Climate, 25*, 5711-5730. DOI:10.1175/JCLI-D-11-00417.1.

Berbery, E., & Rasmusson, E. (1999). Mississippi moisture budgets on regional scales. *Monthly Weather Review, 127*, 2654-2673. DOI:10.1175/1520-0493(1999)127<2654:MMBORS>.

Bingeman, A. K., Kouwen, N., & Soulis, E. D. (2006). Validation of the hydrological processes in a hydrological model. *Journal of Hydrologic Engineering, 11*(5), 451-463. DOI:10.1061/(ASCE)1084-0699(2006)11:5(451).

Bispham, P. (2014). Interpolation: Introduction and Basics. *ECMWF Computer User Training Course 2014*. United Kingdom.

Bourque, A. & Simonet, G. (2008). Quebec. In D. S. Lemmen, F. J. Warren, J. Lacroix, & E. Bush (Eds.) *From impacts to adaptation: Canada in a changing climate 2007* (pp. 171-226). Ottawa: Government of Canada.

Braun, M., Caya, D., Frigon, A., & Slivitzky, M. (2012). Internal Variability of Canadian RCM's Hydrological Variables at the Basin Scale in Quebec and Labrador. *Journal of Hydrometeorology, 13*, 443-462. DOI:10.1175/JHM-D-11-051.1.

Brubaker, K. L., Entekhabi, D., & Eagleson, P. S. (1993). Estimation of continental precipitation recycling. *Journal of Climate, 6*(6), 1077-1089. DOI:10.1175/1520-0442(1993)006<1077:EOCPR>2.0.CO;2.

Caya, D., Laprise, R., Giguere, M., Bergeron, G., Blanchet, J. P., Stocks, B. J., ... & McFarlane, N. A. (1995). Description of the Canadian regional climate model. In *Boreal Forests and Global Change* (pp. 477-482). Netherlands: Springer.

Caya, D., & Laprise, R. (1999). A semi-Lagrangian semi-implicit regional climate model: The Canadian RCM. *Monthly Weather Review, 127*(3), 341-362. DOI:10.1175/1520-0493(1999)127<0341:ASISLR>.

Chahine, M. T. (1992). The hydrological cycle and its influence on climate. *Nature, 359*, 373-380. DOI:10.1038/359373a0.

Chen, J., Brissette, F. P., & Leconte, R. (2011). Uncertainty of downscaling method in quantifying the impact of climate change on hydrology. *Journal of Hydrology, 401*, 190-202. DOI:10.1016/j.jhydrol.2011.02.020.

Chen, J., Brissette, F. P., Chaumont, D., & Braun, M. (2013). Performance and uncertainty evaluation of empirical downscaling methods in quantifying the climate change impacts on hydrology over two North American river basins. *Journal of Hydrology, 479*, 200-214. DOI:10.1016/j.jhydrol.2012.11.062.

Chen, S.-C., Norris, C., & Roads, J. (1996). Balancing the atmospheric hydrologic budget. *Journal of Geophysical Research, 101*, 7341-7358. DOI:10.1029/95JD01746.

Christensen, J. H., & Christensen, O.B. (2007). A summary of the PRUDENCE model projections of changes in European climate by the end of this century. *Climatic Change, 81*(1), 7-30. DOI:10.1007/s10584-006-9210-7.

Christensen, J. H., Hewitson, B., Busuioc, A., Chen, A. Gao, X. Held, I., … Whetton, P. (2007). Regional Climate Projections. In Solomon, S., Qin, D., Manning, M., Chen, Z.,

Marquis, M., Averyt, K.B.,… Miller, H. L. (Eds.), *Climate Change 2007: The Physical Science Basis. Contribution of Working Group I to the Fourth Assessment Report of the Intergovernmental Panel on Climate Change* (pp. 847-940). Cambridge, UK and New York, NY: Cambridge University Press.

Christensen, J. H., Kjellström, E., Giorgi, F., Lenderink, G., & Rummukainen, M. (2010) Weight assignment in regional climate models. *Climate Research, 44*(2-3), 179-194. DOI:10.3354/cr00916.

Christensen, J. H., Boberg, F., Christensen, O.B., & Lucas-Picher, P. (2008). On the need for bias correction of regional climate change projections of temperature and precipitation. *Geophysical Research Letters, 35*(20), L20709. DOI:10.1029/2008GL035694.

Christensen, N. S., Wood, A. W., Voisin, N., Lettenmaier, D. P., & Palmer, R. N. (2004). The effects of climate change on the hydrology and water resources of the Colorado River basin. *Climatic Change, 62*, 337-363. DOI:10.1023/B:CLIM.0000013684.13621.1f.

Christensen, O.B., Gaertner, M. A., Prego, J. A., & Polcher, J. (2001). Internal variability of regional climate models. *Climate Dynamics, 17*(11), 875-887. DOI:10.1007/s003820100154.

Collins, W. D., Bitz, C. M., Blackmon, M. L., Bonan, G. B., Bretherton, C. S., Carton, J. A., ... & Smith, R. D. (2006). The community climate system model version 3 (CCSM3). *Journal of Climate*, *19*(11), 2122-2143. DOI:10.1175/JCLI3761.1.

Cranmer, A. J., Kouwen, N., & Mousavi, S.F. (2001). Proving WATFLOOD: modelling the nonlinearities of hydrologic response to storm intensities. *Canadian Journal of Civil Engineering, 28*(5), 837-855. DOI:10.1139/l01-049.

Crossley, J. F., Polcher, J., Cox, P. M., Gedney, N., & Planton, S. (2000). Uncertainties linked to land-surface processes in climate change simulations. *Climate Dynamics, 16*(12), 949-961. DOI:10.1007/s003820000092.

Cullather, R. I., Bromwich, D. H., & Serreze, M.C. (2000). The atmospheric hydrologic cycle over the Arctic basin from reanalyses. Part I: Comparison with observations and precious studies. *Journal of Climate, 13*(5), 923-937. DOI:10.1175/1520-0442(2000)013<0923:TAHCOT>2.0.CO;2.

Déqué, M., Jones, R. G., Wild, M., Giorgi, F., Christensen, J. H., Hassell, D. C., ... & Van den Hurk, B. (2005). Global high resolution versus Limited Area Model climate change projections over Europe: quantifying confidence level from PRUDENCE results. *Climate Dynamics*, *25*(6), 653-670. DOI:10.1007/s00382-005-0052-1.

Déqué, M., Rowell, D. P., Lüthi, D., Giorgi, F., Christensen, J. H., Rockel, B., ... & van den Hurk, B. J. J. M. (2007). An intercomparison of regional climate simulations for

Europe: assessing uncertainties in model projections. *Climatic Change, 81*(1), 53-70. DOI:10.1007/s10584-006-9228-x.

Déry, S. J., Hernández-Henríquez, M. A., Burford, J. E., & Wood, E. F. (2009). Observational evidence of an intensifying hydrological cycle in northern Canada. *Geophysical Research Letters, 36*(13), L13402, DOI:10.1029/2009GL038852.

DesJarlais, C., Bourque, A., Decoste, R., Demers, C., Deschamps, P., & Lam, K.-H. (2004). *Adapting to climate change*. Montreal, QC: Ouranos, 83 pp.

Dettinger, M. (2004) From climate-change spaghetti to climate-change distribution. Discussion Paper 500-04-028. *Sacramento, California: California Energy Commission*, 20 pp.

Dibike, Y. B., & Coulibaly, P. (2005). Hydrologic impact of climate change in the Saguenay watershed: comparison of downscaling methods and hydrologic models. *Journal of hydrology, 307*(1), 145-163. DOI:10.1016/j.jhydrol.2004.10.012.

Dimri, A. (2012). Atmospheric water budget over the western Himalayas in a regional climate model. *Journal of Earth System Science, 121*(4), 963-973. DOI:10.1007/s12040-012-0204-8.

Dingman, S. L. (2002). *Physical Hydrology* (2nd ed.) New York, NY: Macmillan Publishing Company.

Dominguez, F., & Kumar, P. (2005). Dominant modes of moisture flux anomalies over North America. *Journal of Hydrometeorology, 6*(2), 194-209. DOI:10.1175/JHM417.1.

Ekström, M., Jones, P. D., Fowler, H. J., Lenderink, G., Buishand, T. A., & Conway, D. (2007). Regional climate model data used within the SWURVE project–1: projected changes in seasonal patterns and estimation of PET. *Hydrology and Earth System Sciences, 11*(3), 1069-1083. DOI:10.5194/hess-11-1069-2007.

Eum, H. I., Gachon, P., Laprise, R., & Ouarda, T. (2012). Evaluation of regional climate model simulations versus gridded observed and regional reanalysis products using a combined weighting scheme. *Climate dynamics, 38*(7-8), 1433-1457. DOI:10.1007/s00382-011-1149-3.

Feddersen, H., & Andersen, U. (2005). A method for statistical downscaling of seasonal ensemble predictions. Tellus A, 57(3), 398-408. DOI:10.1111/j.1600-0870.2005.00102.x.

Ferro, C. A. (2004). Attributing variation in a regional climate change modelling experiment. *PRUDENCE working note available at http://prudence.dmi.dk/public/publications/analysis_of_variance.pdf*.

Filion, Y. (2000). Climate change: implications for Canadian water resources and hydropower production. *Canadian Water Resources Journal, 25*(3), 255-269. DOI:10.4296/cwrj2503255.

Flato, G. M. (2005). The third generation coupled global climate model (CGCM3). *Environment Canada Canadian Centre for Climate Modelling and Analysis note available at http://www.ec.gc.ca/ccmac-cccma/default.asp?n=1299529F-1.*

Foley, A. M. (2010). Uncertainty in regional climate modelling: A review. *Progress in Physical Geography, 34*: 647-670. DOI:10.1177/0309133310375654 .

Fortin, V., & Latraverse, M. (2000). Une base de données hydrométéorologiques pour le développement d'un indicateur d'hydraulicité. *Logiciels de réseaux Technologies de transport et de distribution (IREQ-2000-268),* Quebec, Canada.

Fowler, H. J., Blenkinsop, S., & Tebaldi, C. (2007a). Linking climate change modelling to impacts studies: recent advances in downscaling techniques for hydrological modelling. *International Journal of Climatology, 27*(12), 1547-1578. DOI:10.1002/joc.1556.

Fowler, H. J., Ekström, M., Kilsby, C. G., & Jones, P. D. (2005). New estimates of future changes in extreme rainfall across the UK using regional climate model integrations. 1. Assessment of control climate. *Journal of Hydrology, 300*(1), 212-233. DOI:10.1016/j.jhydrol.2004.06.017.

Fowler, H. J., Kilsby, C. G., & Stunell, J. (2007b). Modelling the impacts of projected future climate change on water resources in north-west England. *Hydrology and Earth System Sciences, 11*(3), 1115-1126. DOI:10.5194/hess-11-1115-2007.

Frei, C., Christensen, J. H., Déqué, M., Jacob, D., Jones, R. G., & Vidale, P. L. (2003). Daily precipitation statistics in regional climate models: Evaluation and intercomparison for the European Alps. *Journal of Geophysical Research: Atmospheres (1984–2012), 108*(D3), 4124. DOI:10.1029/2002JD002287.

Frei, C., Schöll, R., Fukutome, S., Schmidli, J., & Vidale, P. L. (2006). Future change of precipitation extremes in Europe: Intercomparison of scenarios from regional climate models. *Journal of Geophysical Research: Atmospheres (1984–2012), 111*(D6), 105. DOI:10.1029/2005JD005965.

Frigon, A., Music, B., & Slivitzky, M. (2010). Sensitivity of runoff and projected changes in runoff over Quebec to the update interval of lateral boundary conditions in the Canadian RCM. *Meteorologische Zeitschrift, 19*(3), 225-236. DOI:10.1127/0941-2948/2010/0453.

Frigon, A., Slivitzky, M., Music, B., & Caya, D. (2008). Internal variability of the Canadian RCM's hydrologic variables at the basin scale. *Geophysical Research Abstracts 10*, EGU2008-A-04093.

Furrer, R., Sain, S. R., Nychka, D., & Meehl, G. A. (2007). Multivariate Bayesian analysis of atmosphere–ocean general circulation models. *Environmental and Ecological Statistics, 14*(3), 249-266. DOI:10.1007/s10651-007-0018-z.

Gagnon, P., Konan, B., Rousseau, A. N., & Slivitzky, M. (2009). Hydrometeorological validation of a Canadian regional climate model simulation within the Chaudière and Chateauguay watersheds (Quebec, Canada). *Canadian Journal of Civil Engineering, 36*(2), 253-266. DOI:10.1139/L08-125.

Garrido, A., & Dinar, A. (2009). *Managing Water Resources in a Time of Global Change: Mountains, Valleys and Flood Plain*. New York, NY: Routledge Press, 272 pp.

GFDL Global Atmospheric Model Development Team. (2004). The new GFDL global atmospheric and land model AM2-LM2: Evaluation with prescribed SST simulations. *Journal of Climate, 17*, 4641-4673. DOI:10.1175/JCLI-3223.1

Ghosh, S., & Mujumdar, P. P. (2007). Nonparametric methods for modeling GCM and scenario uncertainty in drought assessment. *Water Resources Research, 43*(7), W07405, DOI:10.1029/2006WR005351.

Ghosh, S., & Mujumdar, P. P. (2009). Climate change impact assessment: Uncertainty modeling with imprecise probability. *Journal of Geophysical Research: Atmospheres (1984–2012), 114*(D18), 113. DOI: 10.1029/2008JD011648.

Giorgi, F., & Mearns, L. O. (2002). Calculation of average, uncertainty range, and reliability of regional climate changes from AOGCM simulations via the "reliability ensemble averaging"(REA) method. *Journal of Climate, 15*(10), 1141-1158. DOI:10.1175/1520-0442(2002)015<1141:COAURA>2.0.CO;2.

Giorgi, F., & Mearns, L. O. (2003). Probability of regional climate change based on the Reliability Ensemble Averaging (REA) method. *Geophysical Research Letters, 30*(12), 1629, DOI:10.1029/2003GL017130.

Giorgi, F., Marinucci, M. R., & Bates, G. T. (1993a). Development of a second-generation regional climate model (RegCM2). Part I: Boundary-layer and radiative transfer processes. *Monthly Weather Review, 121*(10), 2794-2813. DOI:10.1175/1520-0493(1993)121<2794:DOASGR>.

Giorgi, F., Marinucci, M. R., Bates, G. T., & De Canio, G. (1993b). Development of a second-generation regional climate model (RegCM2). Part II: Convective processes and assimilation of lateral boundary conditions. *Monthly Weather Review, 121*(10), 2814-2832. DOI:10.1175/1520-0493(1993)121<2814:DOASGR>.

Gordon, C., Cooper, C., Senior, C. A., Banks, H., Gregory, J. M., Johns, T. C., ... & Wood, R. A. (2000). The simulation of SST, sea ice extents and ocean heat transports in a version of the Hadley Centre coupled model without flux adjustments. *Climate Dynamics, 16*(2-3), 147-168. DOI:10.1007/s003820050010.

Graham, L. P., Andréasson, J., & Carlsson, B. (2007). Assessing climate change impacts on hydrology from an ensemble of regional climate models, model scales and linking methods–a case study on the Lule River basin. *Climatic Change, 81*(1), 293-307. DOI:10.1007/s10584-006-9215-2.

Graham, L. P., Hagemann, S., Jaun, S., & Beniston, M. (2007). On interpreting hydrological change from regional climate models. *Climatic Change, 81*(1), 97-122. DOI:10.1007/s10584-006-9217-0.

Grell, G. A., Dudhia, J., & Stauffer, D. R. (1993). A description of the fifth generation Penn State/NCAR Mesoscale Model (MM5). *NCAR Technical Note NCAR/ TN-398*, 107 pp.

Grotch, S. L., & MacCracken, M. C. (1991). The use of general circulation models to predict regional climatic change. *Journal of Climate, 4*(3), 286-303. DOI:10.1175/1520-0442(1991)004<0286:TUOGCM>2.0.CO;2.

Hack, J. J., Kiehl, J. T., & Hurrell, J. W. (1998). The hydrologic cycle and thermodynamic characteristics of the NCAR CCM3. *Journal of Climate, 11*(6), 1179-1206. DOI:10.1175/1520-0442(1998)011<1179:THATCO>.

Haerter, J. O., Hagemann, S., Moseley, C., & Piani, C. (2011). Climate model bias correction and the role of timescales. *Hydrology and Earth System Sciences, 15*(3), 1065-1079. DOI:10.5194/hess-15-1065-2011.

Hagemann, S., Machenhauer, B., Jones, R., Christensen, O. B., Déqué, M., Jacob, D., & Vidale, P. L. (2004). Evaluation of water and energy budgets in regional climate models applied over Europe. *Climate Dynamics, 23*(5), 547-567. DOI:10.1007/s00382-004-0444-7.

Halenka, T., Kalvova, J., Chladova, Z., Demeterova, A., Zemankova, K., & Belda, M. (2006). On the capability of RegCM to capture extremes in long term regional climate simulation–comparison with the observations for Czech Republic. *Theoretical and applied climatology, 86*(1-4), 125-145. DOI:10.1007/s00704-005-0205-5.

Hansen, J. W., Challinor, A., Ines, A. V. M., Wheeler, T., & Moron, V. (2006). Translating climate forecasts into agricultural terms: advances and challenges. *Climate Research, 33*(1), 27-41. DOI:10.3354/cr033027 .

Held, I. M., & Soden, B. J. (2006). Robust responses of the hydrological cycle to global warming. *Journal of Climate, 19*(21), 5686-5699. DOI:10.1175/JCLI3990.1.

Hernandez, J. L., Srikishen, J., Erickson, D. J., Oglesby, R., & Irwin, D. (2006). A regional climate study of Central America using the MM5 modeling system: results and comparison to observations. *International journal of climatology, 26*(15), 2161-2179. DOI:10.1002/joc.1361.

Hewitson, B. C., & Crane, R. G. (2006). Consensus between GCM climate change projections with empirical downscaling: precipitation downscaling over South Africa. *International Journal of Climatology, 26*(10), 1315-1337. DOI:10.1002/joc.1314.

Hingray, B., Mezghani, A., & Buishand, T. A. (2007). Development of probability distributions for regional climate change from uncertain global mean warming and an

uncertain scaling relationship. Hydrology and Earth System Sciences, 11(3), 1097-1114. DOI:10.5194/hess-11-1097-2007.

Hirschi, M., Seneviratne, S. I., & Schär, C. (2006). Seasonal variations in terrestrial water storage for major midlatitude river basins. *Journal of Hydrometeorology, 7*(1), 39-60. DOI:10.1175/JHM480.1.

Hu, H., Oglesby, R. J., & Marshall, S. (2005). The simulation of moisture processes in climate models and climate sensitivity. *Journal of climate, 18*(13), 2172-2193. DOI:10.1175/JCLI3384.1.

Hunt, J. C. R. (2005). Inland and coastal flooding: developments in prediction and prevention. *Philosophical Transactions of the Royal Society A: Mathematical, Physical and Engineering Sciences, 363*(1831), 1475-1491. DOI:10.1098/rsta.2005.1580.

IPCC. [Nakicenovik, N., & Swart, R. (Eds.)]. (2000). *Emissions Scenarios*. UK: Cambridge University Press, 570 pp.

IPCC. [Pachauri, R.K., & Reisinger, A. (Eds.)]. (2007). *Contribution of Working Groups I, II, and III to the Fourth Assessment Report of the Intergovernmental Panel on Climate Change.* Geneva, Switzerland: IPCC, 104 pp.

IPCC. [Stocker, T.F., Qin, D., Plattner, G.-K., Tignor, M., Allen, S.K., Boschung, J., … Midgley, P.M. (Eds.)]. (2013). *Climate Change 2013: The Physical Science Basis.*

Contribution of Working Group I to the Fifth Assessment Report of the Intergovernmental Panel on Climate Change. New York, NY: Cambridge University Press, 1535 pp.

IPCC. (2014). Chapter 3: Freshwater Resources. In *Climate Change 2014: Impacts, Adaptation, and Vulnerability. Contribution of Working Group II to the Fifth Assessment Report of the Intergovernmental Panel on Climate Change*. New York, NY: Cambridge University Press, 76 pp.

Jacob, D., Bärring, L., Christensen, O. B., Christensen, J. H., de Castro, M., Deque, M., ... & van den Hurk, B. (2007). An inter-comparison of regional climate models for Europe: model performance in present-day climate. *Climatic Change, 81*(1), 31-52. DOI:10.1007/s10584-006-9213-4.

Jasim, F. (2014). *Development of a base model for flood forecasting studies in the Humber River Basin (NL) and selection of an appropriate model forcing dataset*. St. John's, NL: Memorial University of Newfoundland.

Jasper, K., Calanca, P., Gyalistras, D., & Fuhrer, J. (2004). Differential impacts of climate change on the hydrology of two alpine river basins. *Climate Research, 26*(2), 113-129.

Jin, F., & Zangvil, A. (2010). Relationship between moisture budget components over the eastern Mediterranean. *International Journal of Climatology, 30*(5), 733-742. DOI:10.1002/joc.1911.

Jones, R., Hassell, D., Hudson, D., Wilson, S., Jenkins, G., & Mitchell J. (2004). *Generating high resolution climate change scenarios using PRECIS*. Exeter, UK: Met Office Hadley Centre, 40 pp.

Jun, M., Knutti, R., & Nychka, D. W. (2008). Spatial analysis to quantify numerical model bias and dependence: how many climate models are there?. *Journal of the American Statistical Association, 103*(483), 934-947. DOI:10.1198/016214507000001265.

Kalnay, E., Kanamitsu, M., Kistler, R., Collins, W., Deaven, D., Gandin, L., ... & Joseph, D. (1996). The NCEP/NCAR 40-year reanalysis project. *Bulletin of the American meteorological Society, 77*(3), 437-471. DOI:10.1175/1520-0477(1996)077<0437:TNYRP>2.0.CO;2.

Kanamitsu, M., Ebisuzaki, W., Woollen, J., Yang, S. K., Hnilo, J. J., Fiorino, M., & Potter, G. L. (2002). NCEP-DOE AMIP-II Reanalysis (R-2). *Bulletin of the American Meteorological Society, 83*(11), 1631-1643. DOI:10.1175/BAMS-83-11-1631.

Kendon, E. J., Rowell, D. P., Jones, R. G., & Buonomo, E. (2008). Robustness of future changes in local precipitation extremes. *Journal of Climate, 21*(17), 4280-4297. DOI:10.1175/2008JCLI2082.1.

Khalili, M., Leconte, R., & Brissette, F. (2006, May). On the Use of Multi Site Generated Meteorological Input Data for Realistic Hydrological Modeling in the Context of Climate

Change Impact Studies. In *EIC Climate Change Technology, 2006 IEEE* (pp. 1-7). IEEE. DOI:10.1109/EICCCC.2006.277261.

Kingston, D. G., Thompson, J. R., & Kite, G. (2011). Uncertainty in climate change projections of discharge for the Mekong River Basin. *Hydrology and Earth System Sciences, 15*(5), 1459-1471. DOI:10.5194/hess-15-1459-2011.

Kiparski, M., & Gleick, P. H. (2004). Climate change and California water resources. *The World's water*, *2005*, 157-188.

Kistler, R., Collins, W., Saha, S., White, G., Woollen, J., Kalnay, E., ... & Fiorino, M. (2001). The NCEP-NCAR 50-year reanalysis: Monthly means CD-ROM and documentation. *Bulletin of the American Meteorological society, 82*(2), 247-267. DOI:10.1175/1520-0477(2001)082<0247:TNNYRM>2.3.CO;2

Knutti, R., Furrer, R., Tebaldi, C., Cermak, J., & Meehl, G. A. (2010a). Challenges in combining projections from multiple climate models. *Journal of Climate, 23*(10), 2739-2758. DOI:10.1175/2009JCLI3361.1.

Knutti, R., Abramowitz, G., Collins, M., Eyring, V., Glecker, P. J., Hewitson, B., & Mearns, L. (2010b). Good Practice Guidance Paper on Assessing and Combining Multi Model Climate Projections. In Stocker, T., Dahe, Q., Plattner, G.-K., Tignor, M., & Midgley, P. (Eds.), *Meeting Report of the Intergovernmental Panel on Climate Change*

Expert Meeting on Assessing and Combining Multi Model Climate Projections. Bern, Switzerland: IPCC Working Group I Technical Support Unit, University of Bern.

Kotlarski, S., Block, A., Böhm, U., Jacob, D., Keuler, K., Knoche, R., ... & Walter, A. (2005). Regional climate model simulations as input for hydrological applications: evaluation of uncertainties. *Advances in Geosciences, 5*, 119-125.

Kouwen, N., Soulis, E. D., Pietroniro, A., Donald, J., & Harrington, R. A. (1993). Grouped response units for distributed hydrologic modeling. *Journal of Water Resources Planning and Management, 119*(3), 289-305. DOI:10.1061/(ASCE)0733-9496(1993)119:3(289).

Lammers, R. B., Shiklomanov, A. I., Vörösmarty, C. J., Fekete, B. M., & Peterson, B. J. (2001). Assessment of contemporary Arctic river runoff based on observational discharge records. *Journal of Geophysical Research: Atmospheres (1984–2012), 106*(D4), 3321-3334. DOI:10.1029/2000JD900444.

Laprise, R. (2008). Regional climate modelling. *Journal of Computational Physics, 227*(7), 3641-3666. DOI:10.1016/j.jcp.2006.10.024.

Leander, R., & Buishand, T. A. (2007). Resampling of regional climate model output for the simulation of extreme river flows. *Journal of Hydrology, 332*(3), 487-496. DOI:10.1016/j.jhydrol.2006.08.006.

Leung, L. R., Mearns, L. O., Giorgi, F., & Wilby, R. L. (2003). Regional climate research: needs and opportunities. *Bulletin of the American Meteorological Society, 84*(1), 89-95. DOI:10.1175/BAMS-84-1-89.

Li, H., Luo, L., Wood, E. F., & Schaake, J. (2009). The role of initial conditions and forcing uncertainties in seasonal hydrologic forecasting. *Journal of Geophysical Research: Atmospheres (1984–2012), 114*(D4), 114. DOI:10.1029/2008JD010969.

Liang, X.-Z., Kunkel, K. E., & Samel, A. N.(2001). Development of a regional climate model for U. S. Midwest applications. Part 1: Sensitivity to buffer zone treatment. *Journal of Climate, 14*, 4363– 4378. DOI:10.1175/1520-0442(2001)014<4363:DOARCM>2.0.CO;2.

Liu, J., & Stewart, R. (2003). Water vapor fluxes over the Saskatchewan River Basin. *Journal of Hydrometeorology, 4*, 944-959. DOI:10.1175/1525-7541(2003)004<0944:WVFOTS>.

Lopez, A., Tebaldi, C., New, M., Stainforth, D., Allen, M., & Kettleborough, J. (2006). Two approaches to quantifying uncertainty in global temperature changes. *Journal of Climate, 19*(19), 4785-4796. DOI:10.1175/JCLI3895.1.

Lorenz, E. N. (1963). Deterministic nonperiodic flow. *Journal of the atmospheric sciences, 20*(2), 130-141. DOI:10.1175/1520-0469(1963)020<0130:DNF>2.0.CO;2.

Lucarini, V., Danihlik, R., Kriegerova, I., & Speranza, A. (2007). Does the Danube exist?

Versions of reality given by various regional climate models and climatological data sets. *Journal of Geophysical Research*. *112*, D13103, DOI:10.1029/2006JD008360.

Ludwig, R., May, I., Turcotte, R., Vescovi, L., Braun, M., Cyr, J. F., ... & Mauser, W. (2009). The role of hydrological model complexity and uncertainty in climate change impact assessment. *Advances in Geosciences, 21*(21), 63-71.

Manabe, S. (1969). Climate and Ocean Circulation, I, The Atmospheric Circulation and the hydrology of the Earth's Surface. *Monthly Weather Review, 97*(11), 739-774. DOI:10.1175/1520-0493(1969)097<0739:CATOC>2.3.CO;2.

Maraun, D., Wetterhall, F., Ireson, A. M., Chandler, R. E., Kendon, E. J., Widmann, M., ... & Thiele‐Eich, I. (2010). Precipitation downscaling under climate change: recent developments to bridge the gap between dynamical models and the end user. *Reviews of Geophysics, 48*(3). DOI:10.1029/2009RG000314.

Marbaix, P., Gallee, H., Brasseur, O., & van Ypersele, J. (2003). Lateral boundary conditions in regional climate models: A detailed study of relaxation procedure. *Monthly Weather Review, 131*, 461– 479. DOI:10.1175/1520-0493(2003)131<0461:LBCIRC>2.0.CO;2.

Matondo, J. I., Peter, G., & Msibi, K. M. (2004). Evaluation of the impact of climate change on hydrology and water resources in Swaziland: Part II. *Physics and Chemistry of the Earth, Parts A/B/C, 29*(15), 1193-1202. DOI:0.1016/j.pce.2004.09.035.

Maurer, E. P. (2007). Uncertainty in hydrologic impacts of climate change in the Sierra Nevada, California, under two emissions scenarios. *Climatic Change, 82*(3-4), 309-325. DOI:10.1007/s10584-006-9180-9.

Maurer, E. P., Brekke, L. D., & Pruitt, T. (2010). Contrasting Lumped and Distributed Hydrology Models for Estimating Climate Change Impacts on California Watersheds. *Journal of the American Water Resources Association, 46*(5), 1024-1035. DOI:10.1111/j.1752-1688.2010.00473.x.

Maurer, E. P., & Duffy, P. B. (2005). Uncertainty in projections of streamflow changes due to climate change in California. *Geophysical Research Letters, 32*(3). DOI:10.1029/2004GL021462.

Mearns, L. O., Gutowski, W. J., Jones, R., Leung, L. Y., McGinnis, S., Nunes, A. M. B., & Qian, Y. (2007) updated 2011. The North American Regional Climate Change Assessment Program dataset. *National Center for Atmospheric Research Earth System Grid data portal, Boulder, CO*. http://www.earthsystemgrid.org/browse/viewProject.htm?projectId=ff3949c8-2008-45c8-8e27-5834f54be50f (accessed September 2010).

Mearns, L. O., Gutowski, W., Jones, R., Leung, R., McGinnis, S., Nunes, A., & Qian, Y. (2009). A regional climate change assessment program for North America. *Eos, Transactions American Geophysical Union, 90*(36), 311-311. DOI:10.1029/2009EO360002.

Mearns, L. O., Arritt, R., Biner, S., Bukovsky, M. S., McGinnis, S., Sain, S., ... & Snyder, M. (2012). The North American regional climate change assessment program: overview of phase I results. *Bulletin of the American Meteorological Society, 93*(9), 1337-1362. DOI:10.1175/BAMS-D-11-00223.1.

Mekis, E., & Hogg, W. D. (1999). Rehabilitation and analysis of Canadian daily precipitation time series. *Atmosphere-Ocean, 37*(1), 53-85. DOI:10.1080/07055900.1999.9649621.

Menzel, L., & Bürger, G. (2002). Climate change scenarios and runoff response in the Mulde catchment (Southern Elbe, Germany). *Journal of hydrology, 267*(1), 53-64. DOI:10.1016/S0022-1694(02)00139-7.

Mesinger, F., DiMego, G., Kalnay, E., Mitchell, K., Shafran, P. C., Ebisuzaki, W., ... & Shi, W. (2006). North American regional reanalysis. *Bulletin of the American Meteorological Society, 87*(3), 343-360. DOI:10.1175/BAMS-87-3-343.

Mheel, G. A., Collins, W. D., Friedlingstein, P., Gaye, A. T., Gregory, J. M., Kitoh, A.,… Zhao, Z.-C. (2007). Global climate projections. In Solomon, S., Qin, D., Manning, M., Chen, Z., Marquis, M., Averyt, K. B., … Miller, H. L. (Eds.) *Climate Change 2007: The Physical Science Basis. Contribution of Working Group I to the Fourth Assessment Report of the Intergovernmental Panel on Climate Change*. New York, NY: Cambridge University Press.

Min, S.-K., & Hense, A. (2006). A Bayesian approach to climate model evaluation and multi-model averaging with an application to global mean surface temperatures from IPCC AR4 coupled climate models. *Geophysical Research Letters, 33*(8), L08708, DOI:10.1029/2006GL025779.

Min, W., & Schubert, S. (1997). The climate signal in regional moisture fluxes: A comparison of three global data assimilation products. *Journal of Climate, 10*(10), 2623-2642. DOI:10.1175/1520-0442(1997)010<2623:TCSIRM>.

Minville, M., Brissette, F., Krau, S., & Leconte, R. (2009). Adaptation to climate change in the management of a Canadian water-resources system exploited for hydropower. *Water Resources Management, 23*(14), 2965-2986. DOI:10.1007/s11269-009-9418-1.

Minville, M., Brissette, F., & Leconte, R. (2008). Uncertainty of the impact of climate change on the hydrology of a nordic watershed. *Journal of Hydrology, 358*(1), 70-83. DOI:10.1016/j.jhydrol.2008.05.033.

Mitchell, T. D., & Hulme, M. (1999). Predicting regional climate change: living with uncertainty. *Progress in Physical Geography, 23*(1), 57-78. DOI:10.1177/030913339902300103.

Murphy, J. M., Sexton, D. M., Barnett, D. N., Jones, G. S., Webb, M. J., Collins, M., & Stainforth, D. A. (2004). Quantification of modelling uncertainties in a large ensemble of climate change simulations. *Nature, 430*(7001), 768-772. DOI:10.1038/nature02771.

Murphy, J. M., Sexton, D. M. H., Jenkins, G. J., Booth, B. B. B., Brown, C. C., Clark, R. T., ... & Wood, R. A. (2009). *UK climate projections science report: climate change projections*. Exeter, UK: Met Office Hadley Centre, 192 pp.

Music, B., & Caya, D. (2007). Evaluation of the hydrological cycle over the Mississippi River basin as simulated by the Canadian Regional Climate Model (CRCM). *Journal of Hydrometeorology, 8*(5), 969-988. DOI:10.1175/JHM627.1

Music, B., & Caya, D. (2009). Investigation of the sensitivity of water cycle components simulated by the Canadian Regional Climate Model to the land surface parameterization, the lateral boundary data, and the internal variability. *Journal of Hydrometeorology, 10*(1), 3-21. DOI:10.1175/2008JHM979.1.

Music, B., Frigon, A., Slivitzky, M., Musy, A., Caya, D., & Roy, R. (2009). Runoff modelling within the Canadian Regional Climate Model (CRCM): analysis over the Quebec/Labrador watersheds. *IAHS publication, 333*, 183.

Muzik, I. (2001). Sensitivity of hydrologic systems to climate change. *Canadian Water Resources Journal, 26*(2), 233-252. DOI:10.4296/cwrj2602233.

Najafi, M. R., Moradkhani, H., & Jung, I. W. (2011). Assessing the uncertainties of hydrologic model selection in climate change impact studies. *Hydrological Processes, 25*(18), 2814-2826. DOI:10.1002/hyp.8043.

Nalcor Energy. (2009). *Project planning and description. Vol. 1 Part A of Lower Churchill Hydroelectric Generation Project environmental impact statement*. St. John's, NL: Nalcor Energy, 344 pp.

New, M., & Hulme, M. (2000). Representing uncertainty in climate change scenarios: a Monte-Carlo approach. *Integrated Assessment, 1*(3), 203-213. DOI:10.1023/A:1019144202120.

Pal, J. S., Giorgi, F., Bi, X., Elguindi, N., Solmon, F., Rauscher, S. A., ... & Steiner, A. L. (2007). Regional climate modeling for the developing world: the ICTP RegCM3 and RegCNET. *Bulletin of the American Meteorological Society, 88*(9), 1395-1409. DOI:10.1175/BAMS-88-9-1395.

Pal, J. S., Small, E. E., & Eltahir, E. A. (2000). Simulation of regional‐scale water and energy budgets: Representation of subgrid cloud and precipitation processes within RegCM. *Journal of Geophysical Research: Atmospheres (1984–2012), 105*(D24), 29579-29594. DOI:10.1029/2000JD900415.

Palmer, T., Andersen, U., Cantelaube, P., Davey, M., Deque, M., Doblas-Reyes, F. J., ... & Thomsen, M. C. (2004). Development of a European multi-model ensemble system for seasonal to inter-annual prediction (DEMETER). *Bulletin of the American Meteorological Society, 85*(6), 853-872. DOI:10.1175/BAMS-85-6-853.

Peixoto, J. P., & Oort, A. H. (1992). *Physics of Climate*. New York, NY: Springer-Verlag, 520 pp.

Piani, C., Haerter, J. O., & Coppola, E. (2010). Statistical bias correction for daily precipitation in regional climate models over Europe. *Theoretical and Applied Climatology, 99*(1-2), 187-192. DOI:10.1007/s00704-009-0134-9.

Pope, V. D., Gallani, M. L., Rowntree, P. R., & Stratton, R. A. (2000). The impact of new physical parametrizations in the Hadley Centre climate model: HadAM3. *Climate Dynamics, 16*(2-3), 123-146. DOI:10.1007/s003820050009.

Poulin, A., Brissette, F., Leconte, R., Arsenault, R., & Malo, J. S. (2011). Uncertainty of hydrological modelling in climate change impact studies in a Canadian, snow-dominated river basin. *Journal of hydrology, 409*(3), 626-636. DOI:10.1016/j.jhydrol.2011.08.057.

Prudhomme, C., & Davies, H. (2009a). Assessing uncertainties in climate change impact analyses on the river flow regimes in the UK. Part 1: baseline climate. *Climatic Change, 93*(1-2), 177-195. DOI:10.1007/s10584-008-9464-3.

Prudhomme, C., & Davies, H. (2009b). Assessing uncertainties in climate change impact analyses on the river flow regimes in the UK. Part 2: future climate. *Climatic Change, 93*(1-2), 197-222.

Prudhomme, C., Reynard, N., & Crooks, S. (2002). Downscaling of global climate models for flood frequency analysis: where are we now?. *Hydrological processes, 16*(6), 1137-1150. DOI:10.1002/hyp.1054.

Rahman, M., Bolisetti, T., & Balachandar, R. (2012). Hydrologic modelling to assess the climate change impacts in a Southern Ontario watershed. *Canadian Journal of Civil Engineering, 39*(1), 91-103. DOI:10.1139/l11-112.

Räisänen, J., & Palmer, T. N. (2001). A probability and decision-model analysis of a multimodel ensemble of climate change simulations. *Journal of Climate, 14*(15), 3212-3226. DOI:10.1175/1520-0442(2001)014<3212:APADMA>2.0.CO;2.

Randel, D. A., Wood, R. A., Bony, S., Colman, R., Fichefet, T., Fyfe, J., … Taylor, K. E. (2007) Climate models and their evaluation. In Solomon, S., Qin, D., Manning, M., Chen, Z., Marquis, M., Averyt, K.B.,… Miller, H. L. (Eds.), *Climate Change 2007: The Physical Science Basis. Contribution of Working Group I to the Fourth Assessment Report of the Intergovernmental Panel on Climate Change* (pp. 589-622). Cambridge, UK and New York, NY: Cambridge University Press.

Rasmusson, E. M. (1968). Atmospheric water vapor transport and the water balance of North America: II. Large-scale water balance investigations. *Monthly Weather Review, 96*(10), 720-734. DOI:10.1175/1520-0493(1968)096<0720:AWVTAT>2.0.CO;2.

Reichle, R. H., Koster, R. D., Dong, J., & Berg, A. A. (2004). Global soil moisture from satellite observations, land surface models, and ground data: Implications for data assimilation. *Journal of Hydrometeorology, 5*(3), 430-442. DOI:10.1175/1525-7541(2004)005<0430:GSMFSO>.

Roads, J. O., Chen, S. C., Kanamitsu, M., & Juang, H. (1998). Vertical structure of humidity and temperature budget residuals over the Mississippi River basin. *Journal of Geophysical Research: Atmospheres (1984–2012), 103*(D4), 3741-3759. DOI:10.1029/97JD02759.

Roads, J., Lawford, R., Bainto, E., Berbery, E., Chen, S., Fekete, B., ... & Yarosh, E. (2003). GCIP water and energy budget synthesis (WEBS). *Journal of Geophysical Research: Atmospheres (1984–2012), 108*(D16), 8609. DOI:10.1029/2002JD002583.

Roberts, J., Pryse-Phillips, A., & Snelgrove, K. (2012). Modeling the Potential Impacts of Climate Change on a Small Watershed in Labrador, Canada. *Canadian Water Resources Journal, 37*(3), 231-251. DOI:10.4296/cwrj2011-923.

Rogers, R. R., & Yau, M. K. (1984). *A Short Course in Cloud Physics* (Third Edition). United States: Butterworth-Heinemann, 290 pp.

Rowell, D. P. (2006). A demonstration of the uncertainty in projections of UK climate change resulting from regional model formulation. *Climatic Change, 79*(3-4), 243-257. DOI:10.1007/s10584-006-9100-z.

Ruane, A. C. (2010). NARR's atmospheric water cycle components. Part I: 20-year mean and annual interactions. *Journal of Hydrometeorology, 11*(6), 1205-1219. DOI:10.1175/2010JHM1193.1.

Schär, C., Lüthi, D., Beyerle, U., & Heise, E. (1999) The soil–precipitation feedback: A process study with a regional climate model. Journal of Climate, 12, 722–741. DOI:0.1175/1520-0442(1999)012<0722:TSPFAP>.

Schmidli, J., Frei, C., & Vidale, P. L. (2006). Downscaling from GCM precipitation: a benchmark for dynamical and statistical downscaling methods. *International Journal of Climatology, 26*(5), 679-689. DOI:10.1002/joc.1287.

Schubert, S., Park, C. K., Wu, C. Y., Higgins, W., Kondratyeva, Y., Molod, A., ... & Rood, R. (1995). A multiyear assimilation with the GEOS-1 system: Overview and results. *NASA tech. Memo, 104606*(6), 207.

Scinocca, J. F., & McFarlane, N. A. (2004). The variability of modeled tropical precipitation. *Journal of the atmospheric sciences, 61*(16), 1993-2015. DOI:10.1175/1520-0469(2004)061<1993:TVOMTP>.

Seneviratne, S. I., Viterbo, P., Lüthi, D., & Schär, C. (2004). Inferring changes in terrestrial water storage using ERA-40 reanalysis data: The Mississippi River basin. Journal of climate, 17(11), 2039-2057. DOI:10.1175/1520-0442(2004)017<2039:ICITWS>2.0.CO;2.

Serreze, M. C., Bromwich, D. H., Clark, M. P., Etringer, A. J., Zhang, T., & Lammers, R. (2002). Large‐scale hydro‐climatology of the terrestrial Arctic drainage system. *Journal of Geophysical Research: Atmospheres (1984–2012), 107*(D2), ALT-1, 28. DOI:10.1029/2001JD000919.

Serreze, M. C., & Hurst, C. M. (2000). Representation of mean Arctic precipitation from NCEP-NCAR and ERA reanalyses. *Journal of Climate, 13*(1), 182-201. DOI:10.1175/1520-0442(2000)013<0182:ROMAPF>2.0.CO;2.

Shabalova, M. V., van Deursen, W. P., & Buishand, T. A. (2003). Assessing future discharge of the river Rhine using regional climate model integrations and a hydrological model. *Climate Research, 23*(3), 233-246.

Sharma, M., Coulibaly, P., & Dibike, Y. (2010). Assessing the need for downscaling RCM data for hydrologic impact study. *Journal of Hydrologic Engineering, 16*(6), 534-539. DOI:10.1061/(ASCE)HE.1943-5584.0000349.

Shrestha, R. R., Berland, A. J., Schnorbus, M. A., & Werner, A. T. (2011). Climate change impacts on hydro-climatic regimes in the peace and Columbia watersheds, British Columbia, Canada. *Pacific climate impacts consortium, University of Victoria*, Victoria.

Shrestha, R., Dibike, Y., & Prowse, T. (2010). Modelling Climate Impacts on Hydrologic Processes in the Lake Winnipeg Watershed. *2010 International Congress on*

Environmental Modelling and Software Modelling for Environment's Sake, Fifth Biennial Meeting, Ottawa, Canada.

Shukla, J., & Mintz, Y. (1982). Influence of land-surface evapotranspiration on the earth's climate. *Science, 215*(4539), 1498-1501. DOI:10.1126/science.215.4539.1498.

Skamarock, W. C., Klemp, J. B., Dudhia, J., Gill, D. O., Barker, D. M., Wang, W., & Powers, J. G. (2005). *A description of the advanced research WRF version 2* (No. NCAR/TN-468+ STR). National Center For Atmospheric Research Boulder Co Mesoscale and Microscale Meteorology Div.

Stott, P. A. (2003). Attribution of regional‐scale temperature changes to anthropogenic and natural causes. *Geophysical Research Letters, 30*(14), 1728. DOI:10.1029/2003GL017324.

Strong, G. S., Proctor, B., Wang, M., Soulis, E. D., Smith, C. D., Seglenieks, F., & Snelgrove, K. (2002). Closing the Mackenzie Basin water budget, water years 1994/95 to 1996/97. Atmosphere-Ocean, 40(2), 113-124. DOI:10.3137/ao.400203.

Sung, R. Y. J., Burn, D. H., & Soulis, E. D. (2006). A case study of climate change impacts on navigation on the Mackenzie River. *Canadian Water Resources Journal, 31*(1), 57-68. DOI:10.4296/cwrj3101057.

Sushama, L., Laprise, R., Caya, D., Frigon, A., & Slivitzky, M. (2006). Canadian RCM projected climate-change signal and its sensitivity to model errors. *International Journal of Climatology, 26*(15), 2141-2159. DOI:10.1002/joc.1362.

Tebaldi, C., & Knutti, R. (2007). The use of the multi-model ensemble in probabilistic climate projections. *Philosophical Transactions of the Royal Society A: Mathematical, Physical and Engineering Sciences, 365*(1857), 2053-2075. DOI:10.1098/rsta.2007.2076.

Tebaldi, C., Mearns, L. O., Nychka, D., & Smith, R. L. (2004a). Regional probabilities of precipitation change: A Bayesian analysis of multimodel simulations. *Geophysical Research Letters, 31*(24). DOI:10.1029/2004GL021276.

Tebaldi, C., Smith, R. L., Nychka, D., & Mearns, L. O. (2005). Quantifying uncertainty in projections of regional climate change: A Bayesian approach to the analysis of multimodel ensembles. *Journal of Climate, 18*(10), 1524-1540. DOI:10.1175/JCLI3363.1.

Tebaldi, C., Nychka, D., & Mearns, L. O. (2004b). From global mean responses to regional signals of climate change: simple pattern scaling, its limitations (or lack of) and the uncertainty in its results. In *Proceedings of the 17th Conference on Probability and Statistics in the Atmospheric Sciences*.

Themeßl, M. J., Gobiet, A., & Leuprecht, A. (2011). Empirical‐statistical downscaling and error correction of daily precipitation from regional climate models. *International Journal of Climatology, 31*(10), 1530-1544. DOI:10.1002/joc.2168.

Thomas, G., & Henderson-Sellers, A. (1991). An evaluation of proposed representations of subgrid hydrologic processes in climate models. *Journal of climate, 4*(9), 898-910. DOI:10.1175/1520-0442(1991)004<0898:AEOPRO>2.0.CO;2.

Thorne, R. (2011). Uncertainty in the impacts of projected climate change on the hydrology of a subarctic environment: Liard River Basin. *Hydrology and Earth System Sciences, 15*(5), 1483-1492. DOI:10.5194/hess-15-1483-2011.

Todd, M. C., Taylor, R. G., Osborn, T. J., Kingston, D. G., Arnell, N. W., & Gosling, S. N. (2011). Uncertainty in climate change impacts on basin-scale freshwater resources–preface to the special issue: the QUEST-GSI methodology and synthesis of results. *Hydrology and Earth System Sciences, 15*, 1035-1046.

Trenberth, K. E. (1991). Climate diagnostics from global analyses: Conservation of mass in ECMWF analyses. *Journal of climate, 4*(7), 707-722. DOI:10.1175/1520-0442(1991)004<0707:CDFGAC>.

Trenberth, K. E. (1992). *Climate System Modelling*. New York, NY: Cambridge University Press, 788 pp.

Trenberth, K. E. (1998). Atmospheric moisture residence times and cycling: Implications for rainfall rates and climate change. *Climatic change, 39*(4), 667-694. DOI:10.1023/A:1005319109110.

Trenberth, K. E., Dai, A., Rasmussen, R. M., & Parsons, D. B. (2003). The changing character of precipitation. *Bulletin of the American Meteorological Society, 84*(9), 1205-1217. DOI:10.1175/BAMS-84-9-1205.

Trenberth, K. E., Fasullo, J. T., & Kiehl, J. (2009). Earth's global energy budget. *Bulletin of the American Meteorological Society, 90*(3), 311-323. DOI:10.1175/2008BAMS2634.1.

Le Treut, H., Gastineau, G., & Li, L. (2008). Uncertainties attached to global or local climate changes. *Comptes Rendus Geoscience, 340*(9), 584-590. DOI:10.1016/j.crte.2008.06.003.

Van der Linden, P., & Mitchell, J. (2009). ENSEMBLES: climate change and its impacts: summary of research and results from the ENSEMBLES project. Exeter, UK: *Met Office Hadley Centre*.

Vano, J. A., Udall, B., Cayan, D. R., Overpeck, J. T., Brekke, L. D., Das, T., ... & Lettenmaier, D. P. (2014). Understanding Uncertainties in Future Colorado River streamflow. *Bulletin of the American Meteorological Society, 95*(1), 59-78. DOI:10.1175/BAMS-D-12-00228.1.

Vasseur, L., & Catto, N. (2008). Atlantic Canada. In Lemmen, D. S., Warren, F. J., Lacroix, J., & Bush, E. (Eds.) *From impacts to adaptation: Canada in a changing climate 2007*. Ottawa: Government of Canada, pp 119-170.

Velázquez, J. A., Schmid, J., Ricard, S., Muerth, M. J., Gauvin St-Denis, B., Minville, M., ... & Turcotte, R. (2013). An ensemble approach to assess hydrological models' contribution to uncertainties in the analysis of climate change impact on water resources. *Hydrology and Earth System Sciences, 17*(2), 565-578. DOI:10.5194/hess-17-565-2013.

Verseghy, D. L. (2009). CLASS–The Canadian Land Surface Scheme (Version 3.4), Technical Documentation (Version 1.1). *Climate Research Division, Science and Technology Branch, Environment Canada*, 180.

Von Storch H., & Zwiers, F. W. (1999). *Statistical Analysis in Climate Research*. UK: Cambridge University Press.

Wang, K., & Dickinson, R. E. (2012). A review of global terrestrial evapotranspiration: Observation, modeling, climatology, and climatic variability. *Reviews of Geophysics, 50*(2). DOI:10.1029/2011RG000373.

Wang, M., & Paegle, J. (1996). Impact of analysis uncertainty upon regional atmospheric moisture flux. *Journal of Geophysical Research: Atmospheres (1984–2012), 101*(D3), 7291-7303. DOI:10.1029/95JD02896.

Water Survey of Canada. (2010). Retrieved from http://www.wsc.ec.gc.ca/applications/H2O/report-eng.cfm?yearb=&yeare=&station=03OE001&report=monthly&year=1971 (Accessed 2013).

WCRP. (1994). Arctic Climate System Study (ACSYS): Initial implementation plan. Geneva, Switzerland: *World Climate Research Programme WCRP-85, WMO/TD-627*, 66 pp.

Weigel, A. P., Knutti, R., Liniger, M. A., & Appenzeller, C. (2010). Risks of model weighting in multimodel climate projections. *Journal of Climate, 23*(15), 4175-4191. DOI:10.1175/2010JCLI3594.1.

Wilby, R. L. (1997). Non‐stationarity in daily precipitation series: Implications for GCM down‐scaling using atmospheric circulation indices. *International Journal of Climatology, 17*(4), 439-454. DOI:10.1002/(SICI)1097-0088(19970330)17:4<439::AID-JOC145>3.0.CO;2-U.

Wilby, R. L., & Wigley, T. M. L. (1997). Downscaling general circulation model output: a review of methods and limitations. *Progress in Physical Geography, 21*(4), 530-548. DOI:10.1177/030913339702100403.

Wigley, T. M., & Raper, S. C. (2001). Interpretation of high projections for global-mean warming. *Science, 293*(5529), 451-454. DOI:10.1126/science.1061604

Wilby, R. L., & Harris, I. (2006). A framework for assessing uncertainties in climate change impacts: Low-flow scenarios for the River Thames, UK. *Water Resources Research, 42*(2). doi 10.1029/2005WR004065.

Wilby, R. L., Hay, L. E., Gutowski, W. J., Arritt, R. W., Takle, E. S., Pan, Z., ... & Clark, M. P. (2000). Hydrological responses to dynamically and statistically downscaled climate model output. *Geophysical Research Letters, 27*(8), 1199-1202. DOI:10.1029/1999GL006078.

Wilks, D.S. (2006). *Statistical methods in the atmospheric sciences* (2nd ed.). San Diego, California: Academic Press, p 627.

Wood, A. W., Leung, L. R., Sridhar, V., & Lettenmaier, D. P. (2004). Hydrologic implications of dynamical and statistical approaches to downscaling climate model outputs. *Climatic change, 62*(1-3), 189-216. DOI:10.1023/B:CLIM.0000013685.99609.9e.

Wurbs, R. A. (2006). Methods for developing naturalized monthly flows at gaged and ungaged sites. *Journal of Hydrologic Engineering, 11*(1), 55-64. DOI:10.1061/(ASCE)1084-0699(2006)11:1(55).

Xu, H., Taylor, R. G., & Xu, Y. (2011). Quantifying uncertainty in the impacts of climate change on river discharge in sub-catchments of the Yangtze and Yellow River Basins, China. *Hydrology and Earth System Science, 15*(1), 333-344.

Zadeh, S. M., Lye, L. M., & Khan, A. A. (2012). Regional Frequency Analysis of Low Flow Using L-moments for Labrador, Canada. *Annual General Conference of the Canadian Society of Civil Engineers, Edmonton, Canada*.

9. Appendices

9.1. Appendix A – GrADS Scripts for Precipitation and Temperature Bias Correction

Precipitation Bias Correction Script

```
# Determine a/b values and applies bias correction for precipitation
# Calculates b such that CV(obs)-CV(now) is minimized, then calculates a

"reinit"
"open pr_OBS_time.ctl"
"open pr_NOW_CRCM_cgcm3.ctl"
"open zmask.ctl"
"open pr_FUT_CRCM_cgcm3.ctl"
"set undef 1.0e+20"
"set t 1 12014"
"set z 1 73"
"define OBSpr=abs(pr.1*mask.3)"
"define NOWpr=abs(pr.2*mask.3)"

# Calculate OBScv
"set gxout stat"
k=1
while (k <=73)
  "set z " k
  cvcalc(OBSpr)
  OBScv.k=_cv
  Oave.k=_ave
  k = k + 1
endwhile

# Secant method, want f(bi)=OBScv-NEWcv(bi)=0 --> b=b1-f(b1)*(b1-b0)/(f(b1)-f(b0))
# Calculate NEWcv
k=1
while (k <= 73)
  "set z " k
  b1=0.5
  b.k=2.5
  dif=b1 - b.k

# Calculate initial, then new, f(b1)
```

```
  "NEWprb1=pow(NOWpr,"b1")"
  cvcalc(NEWprb1)
  NEWcv.k=_cv
  fb1 = OBScv.k-NEWcv.k
  while (dif>0.0001|dif<-0.0001)
    b0=b1
    b1=b.k
    fb0=fb1
    "NEWprb1=pow(NOWpr,"b1")"
    cvcalc(NEWprb1)
    NEWcv.k=_cv
    fb1 = OBScv.k-NEWcv.k
    b.k=b1-fb1*(b1-b0)/(fb1-fb0)
    dif=b.k-b1
  endwhile
  "NEWprb2=pow(NOWpr,"b.k")"
  cvcalc(NEWprb2)
  Nave.k=_ave
  a.k=Oave.k/Nave.k
  k = k + 1
endwhile
"undefine OBSpr"
"undefine NOWpr"

# Writes a and b values to binary file ---------------------------------
"set gxout fwrite"
"set fwrite -le -st -cl pr_ab_CRCM_cgcm3.bin"
k=1
while (k <= 73)
  "d " a.k
  "d " b.k
  k=k+1
endwhile
"disable fwrite"

# Apply a.k and b.k as the bias correction factors ----------------------
"set gxout fwrite"
"set fwrite -le -st -cl pr_NEW_CRCM_cgcm3.bin"
"set time 01dec1970"
"set z 1"
"q dims"
dimsout=result
timeline=sublin(dimsout,5)
count=subwrd(timeline,9)
```

```
# Write out missing to keep files equal length
missing=1
while(missing<count)
  "set t "missing
  "d 1.0e+20"
  missing=missing+1
endwhile
k=1
while(count < 12014)
  "set t "count" "count+4
  "d "a.k"*pow(abs(pr.2),"b.k")"
  count = count + 4 + 1
  k=k+1
  if(k=74);k=1;endif
endwhile
"disable fwrite"
"set gxout fwrite"
"set fwrite -le -st -cl pr_FBC_CRCM_cgcm3.bin"
"set time 01dec1970"
"set z 1"
"q dims"
dimsout=result
timeline=sublin(dimsout,5)
count=subwrd(timeline,9)

# Write out missing to keep files equal length
missing=1
while(missing<count)
  "set t "missing
  "d 1.0e+20"
  missing=missing+1
endwhile
k=1
while(count < 12014)
  "set t "count" "count+4
  "d "a.k"*pow(abs(pr.4),"b.k")"
  count = count + 4 + 1
  k=k+1
  if(k=74);k=1;endif
endwhile
"disable fwrite"
```

```
# Calculates the average, stdev and cv ------------------------------
function cvcalc(varname)
  "set gxout stat"
  "d " varname
  statout=result
  aveline=sublin(statout,11)
  stdline=sublin(statout,13)
  _ave=subwrd(aveline,2)
  _std=subwrd(stdline,2)
  _cv=_std/_ave
return rc
```

Temperature Bias Correction Script

```
# Apply the bias correction to NOW(gcm) and FUT

"reinit"
"open ta_OBS_time.ctl"
"open ta_NOW_CRCM_cgcm3.ctl"
"open zmask.ctl"
"open ta_FUT_CRCM_cgcm3.ctl"
"set undef 1.0e+20"
"set t 1 12014"
"set z 1 73"

"define OBSta=ta.1*mask.3"
"define NOWta=ta.2*mask.3"
k=1
while(k<=73)
  "set z "k
  statcalc(OBSta)
  aveOBS.k=_ave
  stdOBS.k=_std
  statcalc(NOWta)
  aveNOW.k=_ave
  stdNOW.k=_std
  k=k+1
endwhile
"undefine OBSta"
"undefine NOWta"

# Applying bias correction and writing out corrected data ------------
"set gxout fwrite"
```

```
"set fwrite -le -st -cl ta_NEW_CRCM_cgcm3.bin"

# Write out missing to keep files equal length
"set time 01dec1970"
"set z 1"
"q dims"
dimsout=result
timeline=sublin(dimsout,5)
count=subwrd(timeline,9)
missing=1
while(missing<count)
  "set t "missing
  "d 1.0e+20"
  missing=missing+1
endwhile
k=1
while(count < 12014)
  "set t "count" "count+4
  "d "aveOBS.k"+("stdOBS.k"/"stdNOW.k")*(ta.2-"aveOBS.k")+("aveOBS.k"-
"aveNOW.k")"
  count = count + 4 + 1
  k=k+1
  if(k=74);k=1;endif
endwhile
"disable fwrite"
"set gxout fwrite"
"set fwrite -le -st -cl ta_FBC_CRCM_cgcm3.bin"

# Write out missing to keep files equal length
"set time 01dec1970"
"set z 1"
"q dims"
dimsout=result
timeline=sublin(dimsout,5)
count=subwrd(timeline,9)
missing=1
while(missing<count)
  "set t "missing
  "d 1.0e+20"
  missing=missing+1
endwhile
k=1
while(count < 12014)
  "set t "count" "count+4
```

```
  "d "aveOBS.k"+("stdOBS.k"/"stdNOW.k")*(ta.4-"aveOBS.k")+("aveOBS.k"-
"aveNOW.k")"
  count = count + 4 + 1
  k=k+1
  if(k=74);k=1;endif
endwhile
"disable fwrite"

# Calculates the average, stdev
function statcalc(varname)
  "set gxout stat"
  "d " varname
  statout=result
  aveline=sublin(statout,11)
  stdline=sublin(statout,13)
  _ave=subwrd(aveline,2)
  _std=subwrd(stdline,2)
return rc
```

9.2. Appendix B – Geographical Influence on Precipitation Bias Plots

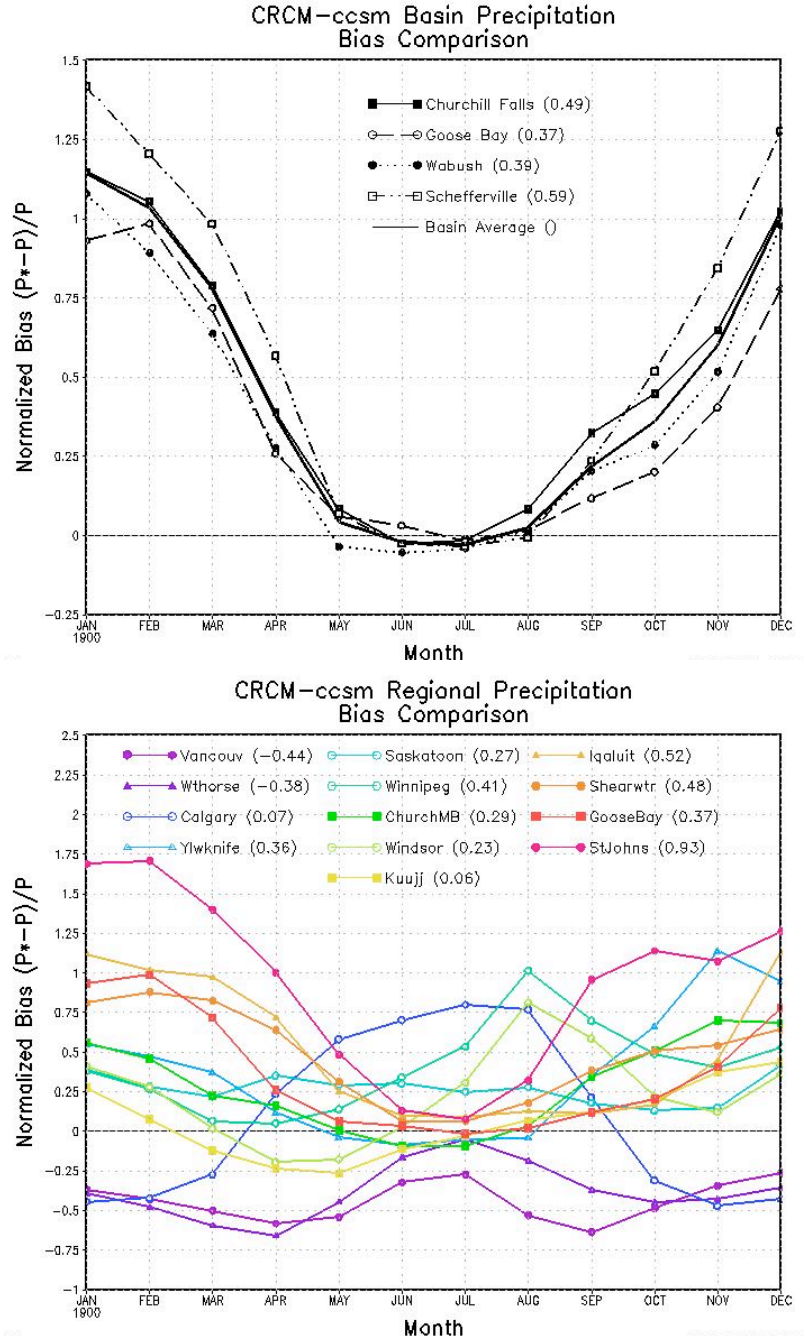

Figure B.1 – Precipitation bias of CRCM-ccsm for various regions in the Churchill River Basin (above) and across Canada (below). (Annual means in parentheses.)

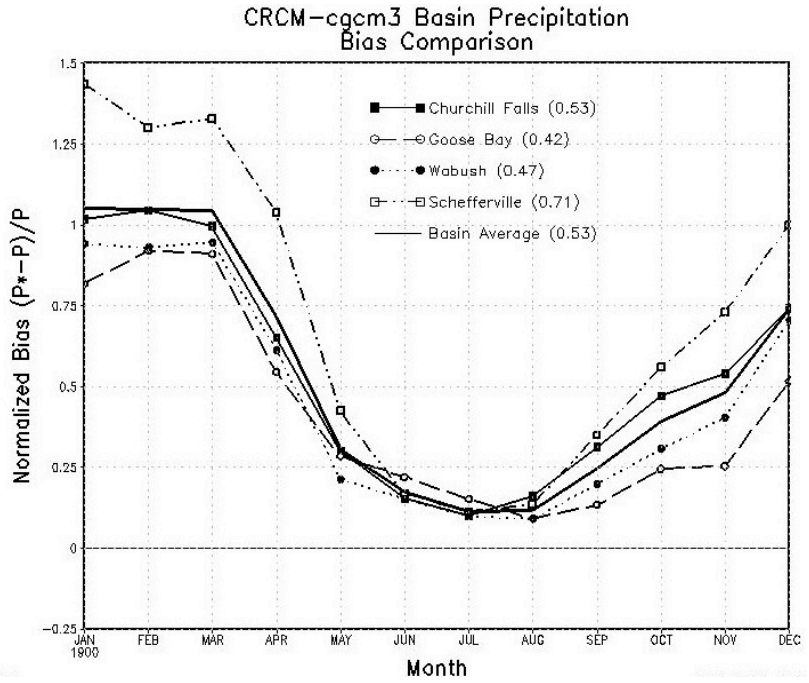

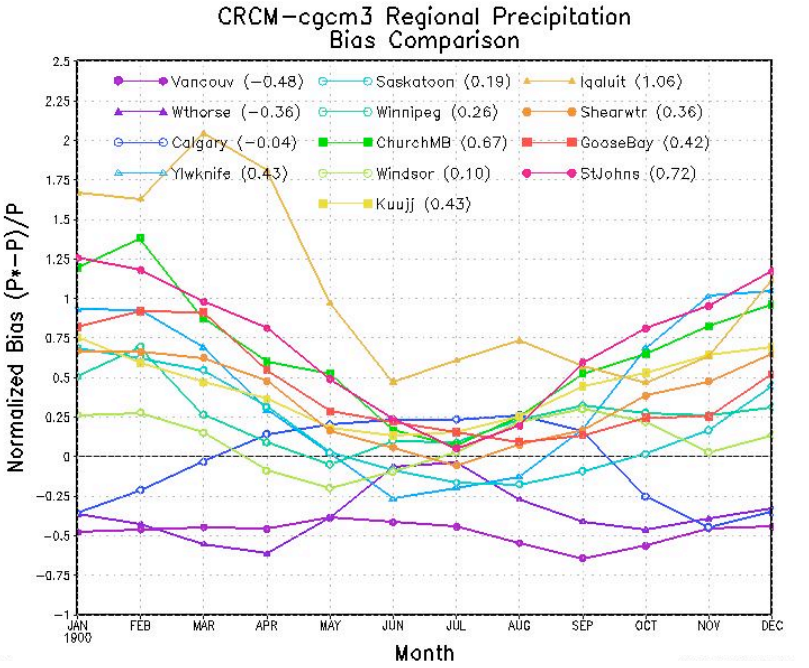

Figure B.2 – As per Figure B.1 for CRCM-cgcm3.

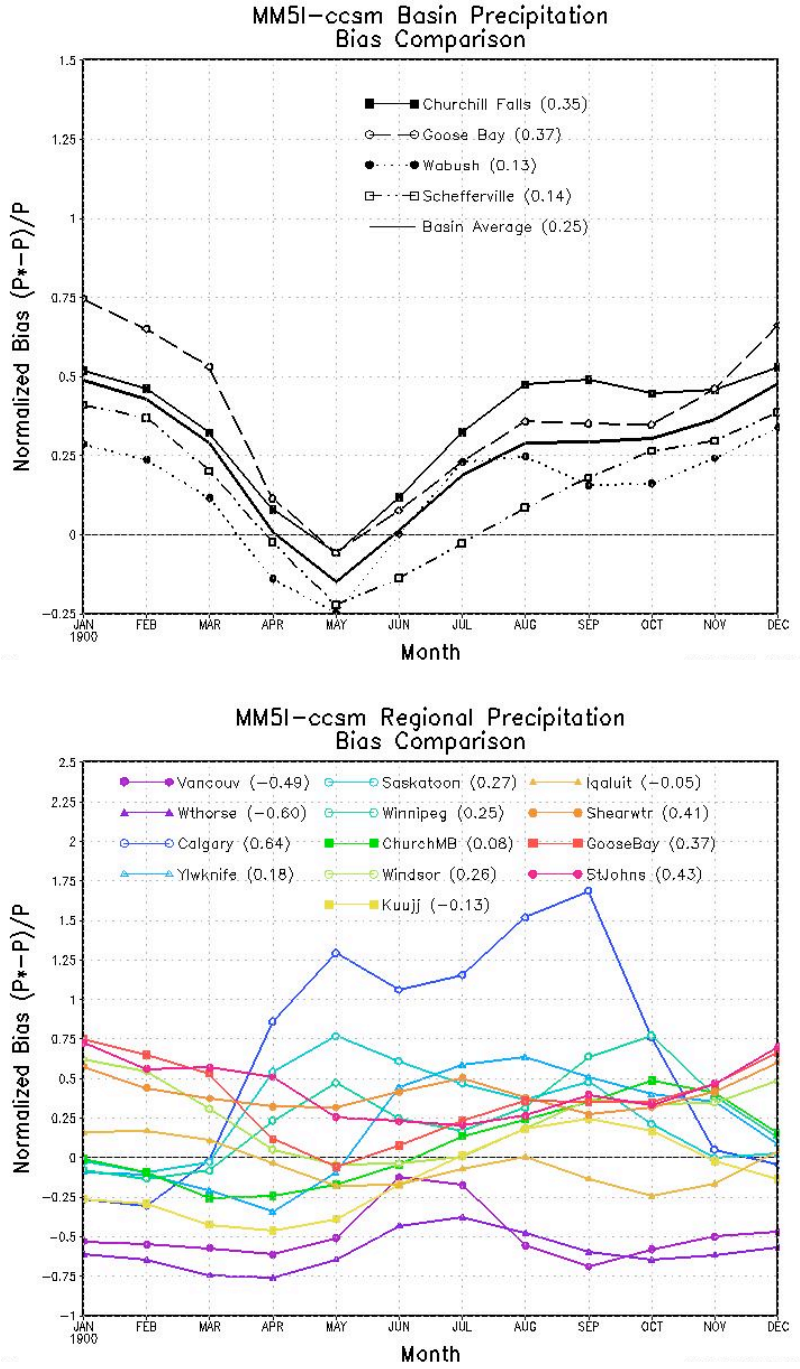

Figure B.3 – As per Figure B.1 for MM5I-ccsm.

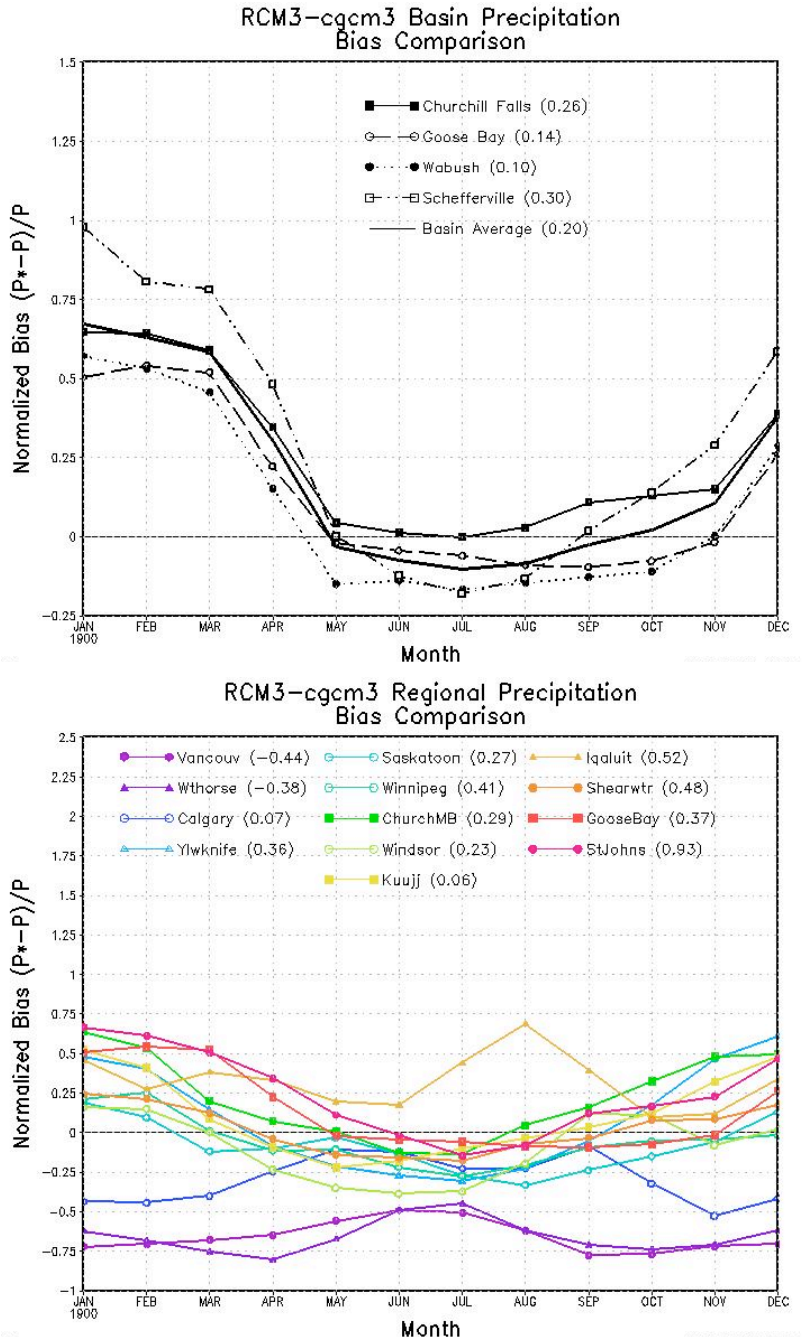

Figure B.4 – As per Figure B.1 for RCM3-cgcm3.

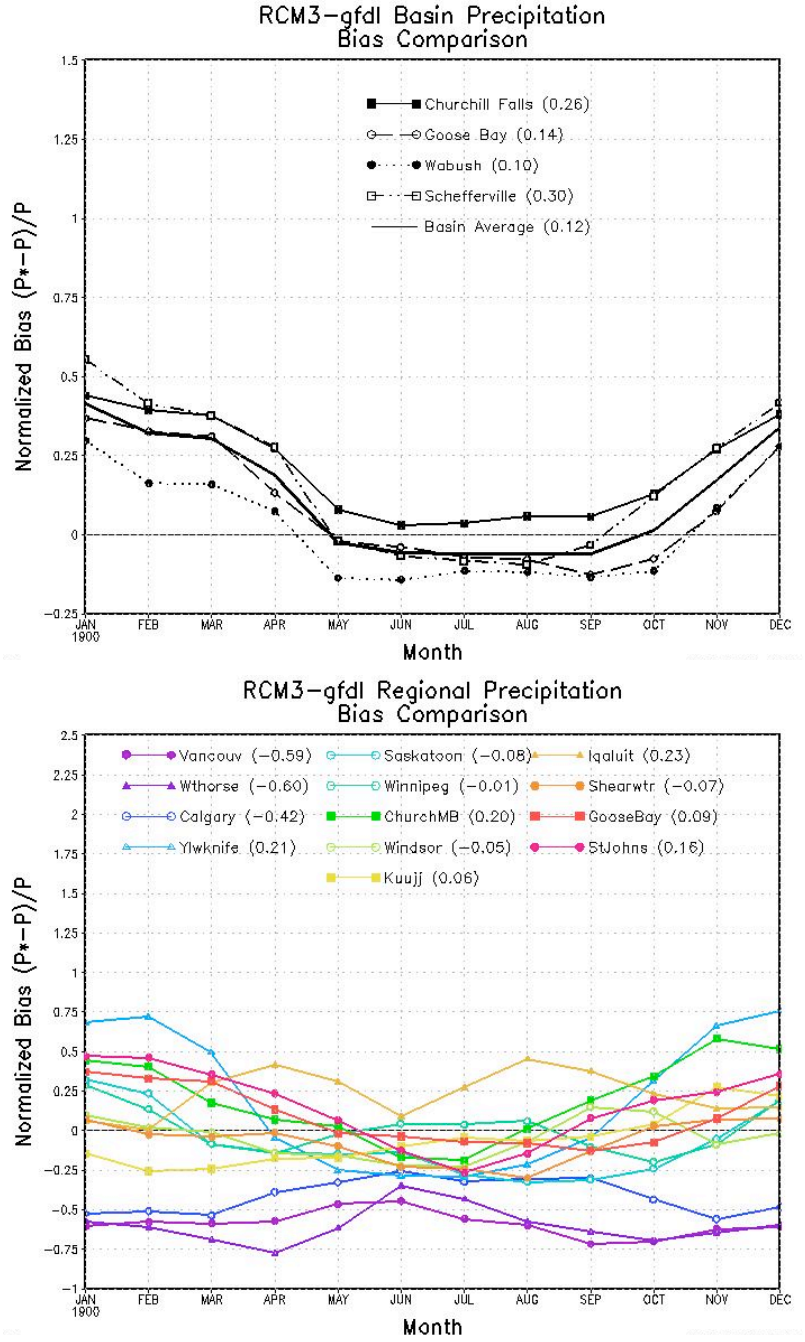

Figure B.5 – As per Figure B.1 for RCM3-gfdl.

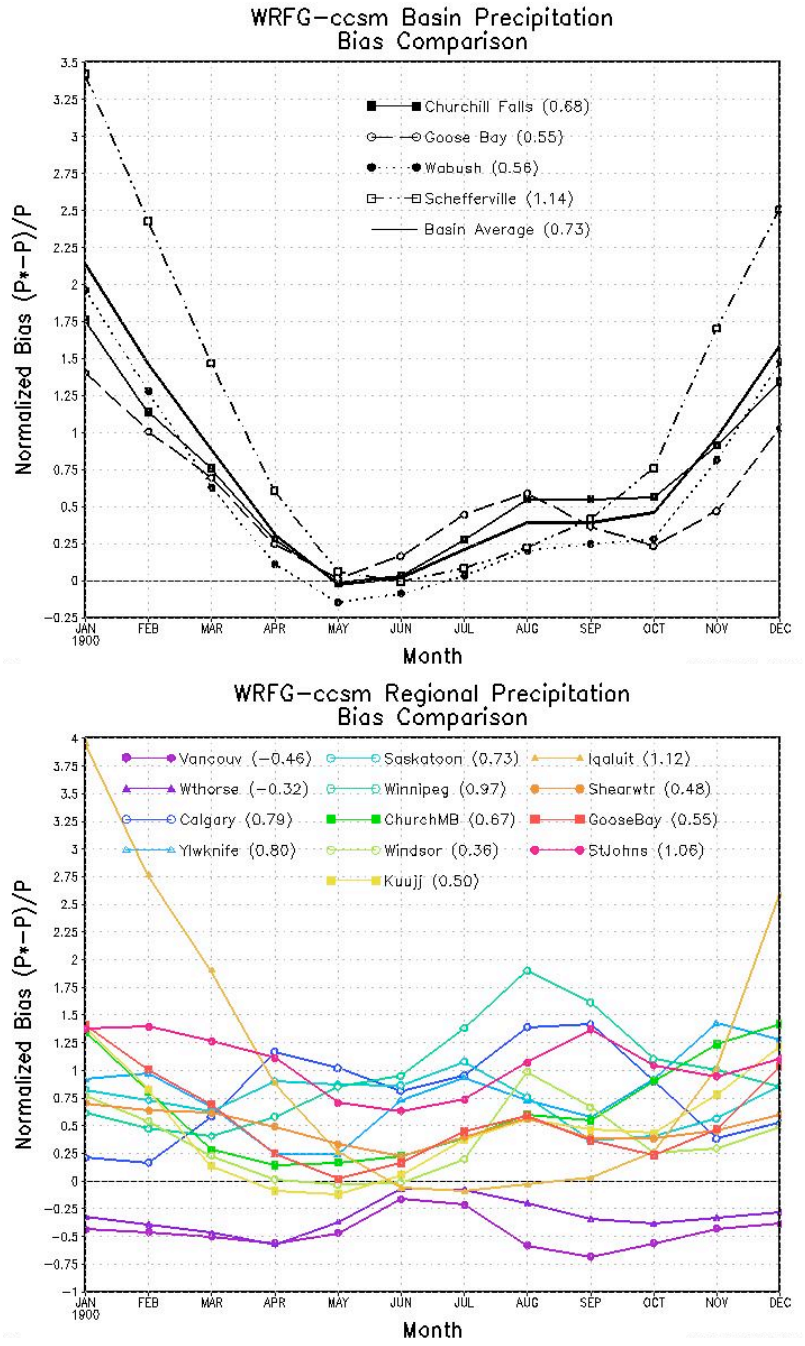

Figure B.6 – As per Figure B.1 for WRFG-ccsm.

9.3. Appendix C – FORTRAN Code for GrADS Bilinear Interpolation

```
! Filename: bilin_create.f90
! Purpose: Identifies where desired GrADS gridpoints are wrt RCM projection and calculates xp, yp where appropriate
!          Creates RCM_BILIN.bin file required by GrADS for re-gridding to common 0.25 degree lat-lon grid

PROGRAM BILIN
IMPLICIT NONE

CHARACTER(LEN=17) :: latfile, lonfile
CHARACTER(LEN=19) :: bilinfile

REAL     :: lat, lat_top, lat_bot, lat_right, lat_left, lat_up, lat_down   ! finding relative location of grads gdpt
REAL     :: lon, lon_top, lon_bot, lon_right, lon_left, lon_1st, lon_2nd   ! finding relative location of grads gdpt
REAL     :: R_lonmin,R_lonmax,R_latmin,R_latmax,R_latm,R_lonl,R_lonr       ! lat-lon boundaries of RCM grid
REAL     :: lata,latb,latc,lona,lonb,lonc,pal,pbl,pcl,abl,bcl,c1,c2,c3,c4  ! used to calc xp,yp

REAL, DIMENSION(720) :: G_lon         !known lon coords for GrADS rectilinear grid
REAL, DIMENSION(360) :: G_lat         !known lat coords for GrADS rectilinear grid

! **** CUSTOMIZE # for each RCM ****************

REAL, DIMENSION(134,104) :: RCM_lon    !*** CUSTOMIZE *** known lon coords for RCM gridpoints
REAL, DIMENSION(134,104) :: RCM_lat    !*** CUSTOMIZE *** known lat coords for RCM gridpoints

! *********************************************

REAL, DIMENSION(720,360) :: Ri         !wanted corresponding RCM i values for each GrADS gridpoint
REAL, DIMENSION(720,360) :: Rj         !wanted corresponding RCM j values for each GrADS gridpoint
REAL, DIMENSION(720,360) :: Rwind      !-999 for no wind rotation

INTEGER  :: mcount, ncount, m, n            ! grads rectilinear grid
INTEGER  :: xcount, ycount, x_grid, y_grid   ! RCM map projection grid
INTEGER  :: xa,xb,xc,ya,yb,yc               ! used to calc xp,yp
INTEGER  :: iunit,junit,ierror              ! read/write, etc

!size of GrADS display grid
m=720    !# of lon gdpoints
n=360    !# of lat gdpoints

! **** CUSTOMIZE # for each RCM ****************

latfile = 'RCM3_lat.txt'
lonfile = 'RCM3_lon.txt'
bilinfile = 'RCM3_BILIN.bin'
R_lonmin = 202.0  ! CRCM:200.0, ECP2:200.0, HRM3:189.0(-171), MM5I:203.0, RCM3:202.0, WRFG:197.0
R_lonmax = 325.0  ! CRCM:326.0, ECP2:328.0, HRM3:337.0(-23),  MM5I:323.0, RCM3:325.0, WRFG:329.0
R_latmin = 19.0   ! CRCM:21.0,  ECP2:18.0,  HRM3:12.0,        MM5I:20.0,  RCM3:19.0,  WRFG:17.0
R_latmax = 77.0   ! CRCM:74.0,  ECP2:73.0,  HRM3:76.0,        MM5I:70.0,  RCM3:71.0,  WRFG:72.0
x_grid = 134      ! CRCM:140,   ECP2:147,   HRM3:155,         MM5I:123,   RCM3:134,   WRFG:134
y_grid = 104      ! CRCM:115,   ECP2:116,   HRM3:130(129-u/va)MM5I:99,    RCM3:104,   WRFG:109

! *********************************************

WRITE (*,*) 'Started'

!populating known lat/lon coords for GrADS rectilinear grid
mcount=0
DO WHILE (mcount <= (m-1))
  G_lon(mcount+1) = 180.125 + mcount*0.25
  mcount=mcount+1
END DO
```

```
ncount=0
DO WHILE (ncount <= (n-1))
  G_lat(ncount+1) = 0.125 + ncount*0.25
  ncount=ncount+1
END DO

!Want corresponding RCM i,j values for each GrADS gridpoint
!Sets all inital value to -999 --> overwrite only if a data point is within projection range

DO mcount=1,m
  DO ncount=1,n
    Ri(mcount,ncount)=-999.0
    Rj(mcount,ncount)=-999.0
    Rwind(mcount,ncount)=-999.0
  END DO
END DO
WRITE (*,*) 'Rectilinear grid arrays populated with initial value of -999.0'

!reads in known lat/lon coords for RCM gridpoints

iunit=10
OPEN (UNIT=iunit, FILE=TRIM(lonfile), STATUS='OLD', ACTION='READ', FORM='FORMATTED', IOSTAT=ierror)
  !do all x for one y coord then y=y+1 and repeat
  DO ycount=1,y_grid     !DO WHILE (ycount <= y_grid)
    DO xcount=1,x_grid   !DO WHILE (xcount <= x_grid)
      READ(iunit,'(F10.6)') RCM_lon(xcount,ycount)
    END DO
  END DO
CLOSE(iunit)

iunit=11
OPEN (UNIT=iunit, FILE=TRIM(latfile), STATUS='OLD', ACTION='READ', FORM='FORMATTED', IOSTAT=ierror)
  DO ycount=1,y_grid     !DO WHILE (ycount <= y_grid)
    DO xcount=1,x_grid   !DO WHILE (xcount <= x_grid)
      READ(iunit,'(F10.6)') RCM_lat(xcount,ycount)
    END DO
  END DO
CLOSE(iunit)

WRITE (*,*) 'RCM lat/lon read'
WRITE (*,*) 'Performing grid interpolation calculations ....'

!identify where grads gdpt is wrt RCM projection and calculate xp, yp where appropriate
DO ncount=1,n     !DO WHILE (ncount<=n)
  DO mcount=1,m  !DO WHILE (mcount<=m)

    lon = G_lon(mcount)
    lat = G_lat(ncount)

    ! Quick rough check for outside of domain
    IF( ( lon >= R_lonmin .AND. lon <= R_lonmax ) .AND. ( lat >= R_latmin .AND. lat <= R_latmax ) ) THEN
    ! continute to refine location of gdpt

      DO xcount=1,(x_grid-1)
        DO ycount=1,(y_grid-1)

          IF (RCM_lat(xcount,ycount+1) == RCM_lat(xcount+1,ycount+1)) THEN
            lat_top=RCM_lat(xcount,ycount+1)
          ELSE
            lat_top=max(RCM_lat(xcount,ycount+1),RCM_lat(xcount+1,ycount+1))
          END IF
          IF (RCM_lat(xcount,ycount) == RCM_lat(xcount+1,ycount)) THEN
            lat_bot=RCM_lat(xcount,ycount)
          ELSE
            lat_bot=min(RCM_lat(xcount,ycount),RCM_lat(xcount+1,ycount))
          END IF
```

```
IF (RCM_lon(xcount+1,ycount) == RCM_lon(xcount+1,ycount+1)) THEN
  lon_right=RCM_lon(xcount+1,ycount)
ELSE
  lon_right=max(RCM_lon(xcount+1,ycount),RCM_lon(xcount+1,ycount+1))
END IF
IF (RCM_lon(xcount,ycount) == RCM_lon(xcount,ycount+1)) THEN
  lon_left=RCM_lon(xcount,ycount)
ELSE
  lon_left=min(RCM_lon(xcount,ycount),RCM_lon(xcount,ycount+1))
END IF


!quick check to see if GrADS gridpoint is close
IF ((lat_bot<=lat .AND. lat<=lat_top) .AND. (lon_left<=lon .AND. lon<=lon_right)) THEN
  !CLOSE --> continue refining domain

  ! determining if the GrADS grid point is within four RCM grid points (ie. within trapezoid)

  !find corresponding coords to above
  IF (lat_top == RCM_lat(xcount,ycount+1)) THEN
    lon_top = RCM_lon(xcount,ycount+1)
  ELSE !if (lat_top == RCM_lat(xcount+1,ycount+1)) THEN
    lon_top = RCM_lon(xcount+1,ycount+1)
  END IF

  !IF (lat_bot == RCM_lat(xcount,ycount) .AND. lon_top /= RCM_lon(xcount,ycount+1)) THEN
  !   lon_bot = RCM_lon(xcount,ycount)
  !ELSE !IF (lat_bot == RCM_lat(xcount+1,ycount)) THEN
  !   lon_bot = RCM_lon(xcount+1,ycount)
  !END IF

  !Test statement
  IF (lon_top == RCM_lon(xcount,ycount+1)) THEN
    lon_bot = RCM_lon(xcount+1,ycount)
  ELSE !IF (lon_top == RCM_lon(xcount+1,ycount+1)) THEN
    lon_bot = RCM_lon(xcount,ycount)
  END IF

  IF (lon_right == RCM_lon(xcount+1,ycount) ) THEN
    lat_right = RCM_lat(xcount+1,ycount)
  ELSE !if (lon_right == RCM_lon(xcount+1,ycount+1)) THEN
    lat_right = RCM_lat(xcount+1,ycount+1)
  END IF

  !IF (lon_left == RCM_lon(xcount,ycount) .AND. lat_right /= RCM_lat(xcount+1,ycount)) THEN
  !   lat_left = RCM_lat(xcount,ycount)
  !ELSE !IF (lon_left == RCM_lon(xcount,ycount+1)) THEN
  !   lat_left = RCM_lat(xcount,ycount+1)
  !END IF

  !Test statement
  IF (lat_right == RCM_lat(xcount+1,ycount)) THEN
    lat_left = RCM_lat(xcount,ycount+1)
  ELSE !IF (lat_right == RCM_lat(xcount+1,ycount+1) THEN
    lat_left = RCM_lat(xcount,ycount)
  END IF

  ! Check to see which region / quadrant of the trapezoid the point falls near / within

  !Finding latitudes of intersection between point's longitude and side of trapezoid
  !TOP HALF (lat_up)
  IF (lon < lon_top) THEN  !TOP LEFT SIDE OF TRAP
    lat_up = lat_left + (lat_top - lat_left)*( (lon - lon_left) / (lon_top - lon_left) )
  ELSE IF (lon == lon_top) THEN
    lat_up = lat_top
  ELSE !IF (lon >= lon_top) THEN  !TOP RIGHT SIDE OF TRAP
```

```
  lat_up = lat_right + (lat_top - lat_right)*( (lon - lon_right) / (lon_top - lon_right) )
END IF

!BOTTOM HALF (lat_down)
IF (lon < lon_bot) THEN  !BOTTOM LEFT SIDE OF TRAP
  lat_down = lat_bot + (lat_left - lat_bot)*( (lon - lon_bot) / (lon_left - lon_bot) )
ELSE IF (lon == lon_bot) THEN
  lat_down = lat_bot
ELSE !IF (lon >= lon_bot) THEN  !BOTTOM RIGHT SIDE OF TRAP
  lat_down = lat_bot + (lat_right - lat_bot)*( (lon - lon_bot) / (lon_right - lon_bot) )
END IF

!Finding lonitutes of intersection between point's latitude and side of trapezoid
!LEFT HALF (lon_1st)
IF (lat < lat_left) THEN ! BOTTOM LEFT SIDE OF TRAP
  lon_1st = lon_left + (lon_bot - lon_left)*( (lat_left - lat) / (lat_left - lat_bot) )
ELSE IF (lat == lat_left) THEN
  lon_1st = lon_left
ELSE !IF (lat >= lat_left) THEN ! TOP LEFT SIDE OF TRAP
  lon_1st = lon_left + (lon_top - lon_left)*( (lat - lat_left) / (lat_top - lat_left) )
END IF

!RIGHT HALF (lon_2nd)
IF (lat < lat_right) THEN ! BOTTOM RIGHT SIDE OF TRAP
  lon_2nd = lon_bot + (lon_right - lon_bot)*( (lat - lat_bot) / (lat_right - lat_bot) )
ELSE IF (lat == lat_right) THEN
  lon_2nd = lon_right
ELSE !IF (lat >= lat_right) THEN ! TOP RIGHT SIDE OF TRAP
  lon_2nd = lon_top + (lon_right - lon_top)*( (lat_top - lat) / (lat_top - lat_right) ) ! was (lon_top-lon_right)
END IF

IF ((lat_down<=lat .AND. lat<=lat_up) .AND. (lon_1st<=lon .AND. lon<=lon_2nd)) THEN ! FALLS WITHIN TRAP
!want corresponding RCM i,j values for each GrADS gridpoint

  !RCM gdpt coords
  !xa=xcount
  !xb=(xcount+1)
  !xc=(xcount+1)
  !ya=(ycount+1)
  !yb=(ycount+1)
  !yc=ycount

  !lat/lon of RCM gdpts
  lata=RCM_lat(xcount,(ycount+1))
  latb=RCM_lat((xcount+1),(ycount+1))
  latc=RCM_lat((xcount+1),ycount)
  lona=RCM_lon(xcount,(ycount+1))
  lonb=RCM_lon((xcount+1),(ycount+1))
  lonc=RCM_lon((xcount+1),ycount)

  ! line length
  pal=SQRT( (lat-lata)*(lat-lata) + (lon-lona)*(lon-lona) )
  pbl=SQRT( (lat-latb)*(lat-latb) + (lon-lonb)*(lon-lonb) )
  pcl=SQRT( (lat-latc)*(lat-latc) + (lon-lonc)*(lon-lonc) )
  abl=SQRT( (latb-lata)*(latb-lata) + (lonb-lona)*(lonb-lona) )
  bcl=SQRT( (latc-latb)*(latc-latb) + (lonc-lonb)*(lonc-lonb) )

  ! See notebook for calculation proof
  c1=(pal/abl)*(pal/abl) - xcount*xcount - (ycount+1)*(ycount+1)
  c2=(pbl/abl)*(pbl/abl) - (xcount+1)*(xcount+1) - (ycount+1)*(ycount+1)
  c3=(pcl/bcl)*(pcl/bcl) - (xcount+1)*(xcount+1) - ycount*ycount
  c4=(pbl/bcl)*(pbl/bcl) - (xcount+1)*(xcount+1) - (ycount+1)*(ycount+1)

  Ri(mcount,ncount)=(c1-c2)/2
  Rj(mcount,ncount)=(c3-c4)/2
```

```
            END IF ! Not within trapezoid
          END IF ! Not close to trapezoid --> continue search
        END DO
      END DO
    END IF ! Not within max RCM boundary --> Move on to next grads gdpt
  END DO
END DO

WRITE (*,*) 'i,j values found and stored'

iunit=20
OPEN (UNIT=iunit, FILE=TRIM(bilinfile), STATUS='REPLACE', ACTION='WRITE', FORM='BINARY',
        ACCESS='STREAM', IOSTAT=ierror)
!writing three matrices (i.e. BILIN file) - varies x then y

DO ncount=1,n
  DO mcount=1,m
    WRITE (iunit) Ri(mcount,ncount)
  END DO
END DO

DO ncount=1,n
  DO mcount=1,m
    WRITE (iunit) Rj(mcount,ncount)
  END DO
END DO

DO ncount=1,n
  DO mcount=1,m
    WRITE (iunit) Rwind(mcount,ncount)
  END DO
END DO

CLOSE(iunit)

WRITE (*,*) 'BILIN file written'
WRITE (*,*) ' '
WRITE (*,*) '!!!!! FINISHED !!!!!'
WRITE (*,*) 'BILIN file should be 3 110 400 bytes'

END PROGRAM BILIN
```

9.4. Appendix D – Atmospheric Moisture Advection Vectors

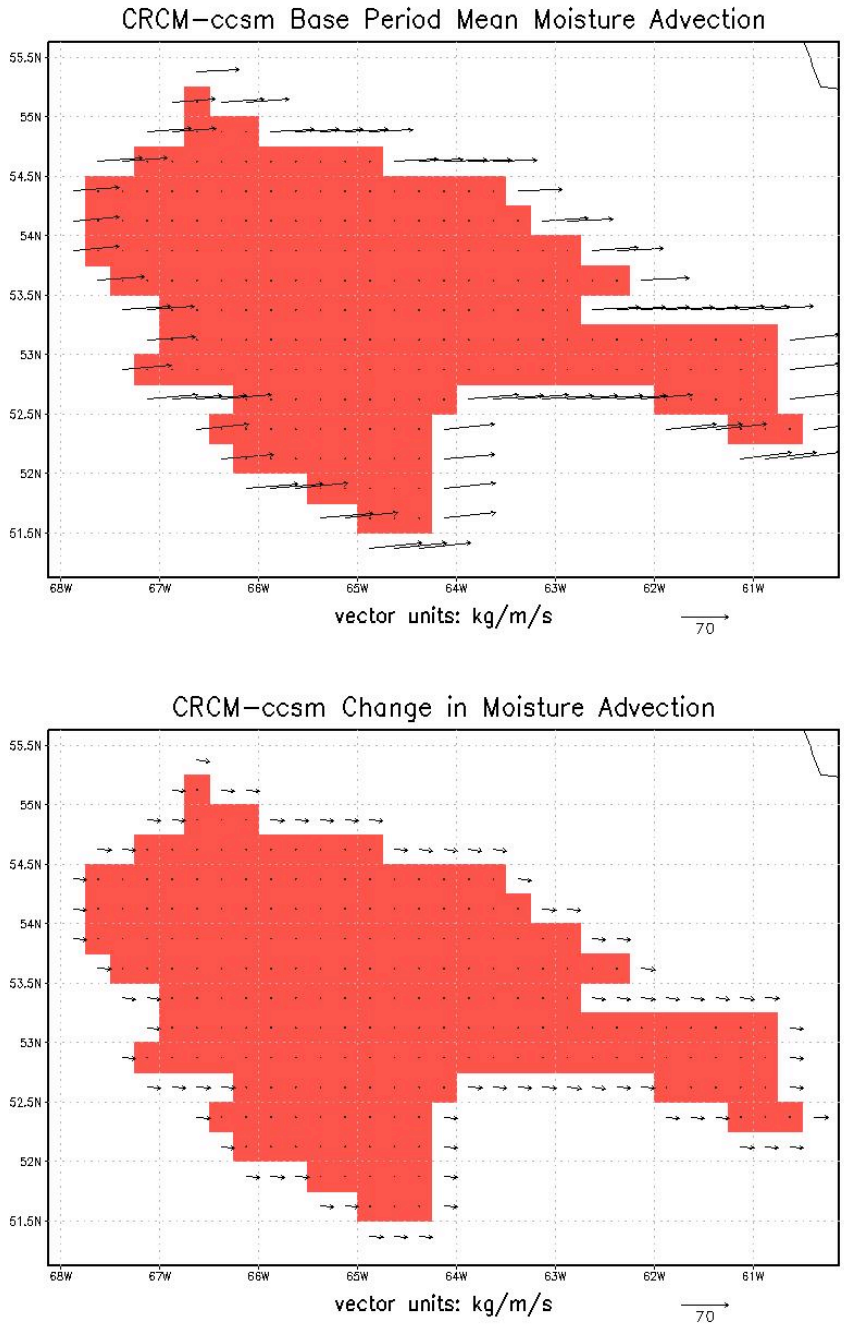

Figure D.1 – CRCM-ccsm mean base period moisture advection vectors (top) and the influence of projected climate change (bottom).

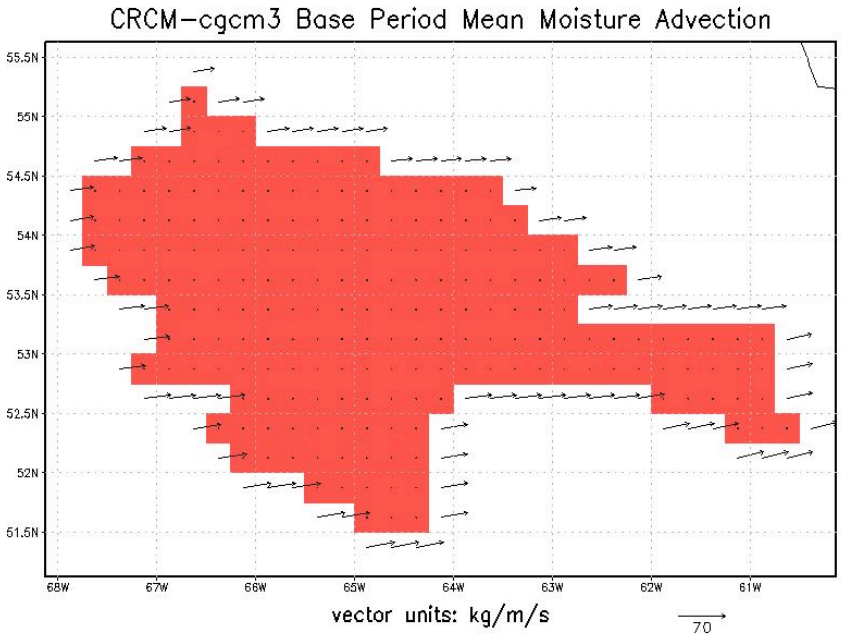

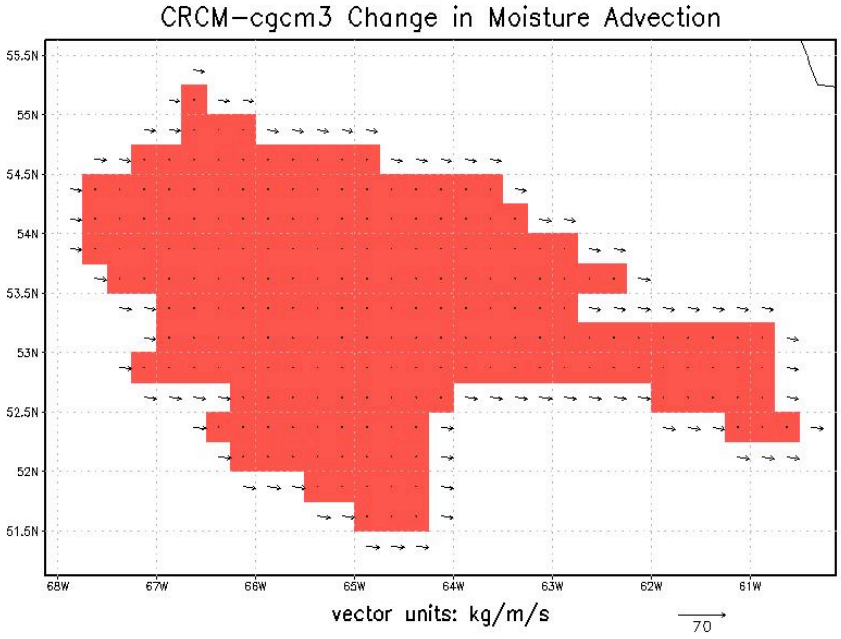

Figure D.2 – As per Figure D.1 for CRCM-cgcm3.

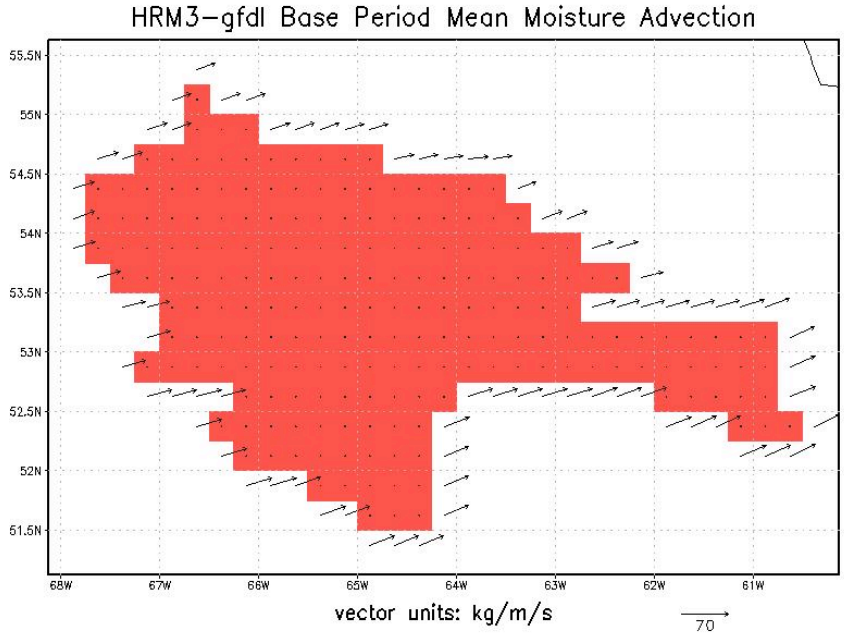

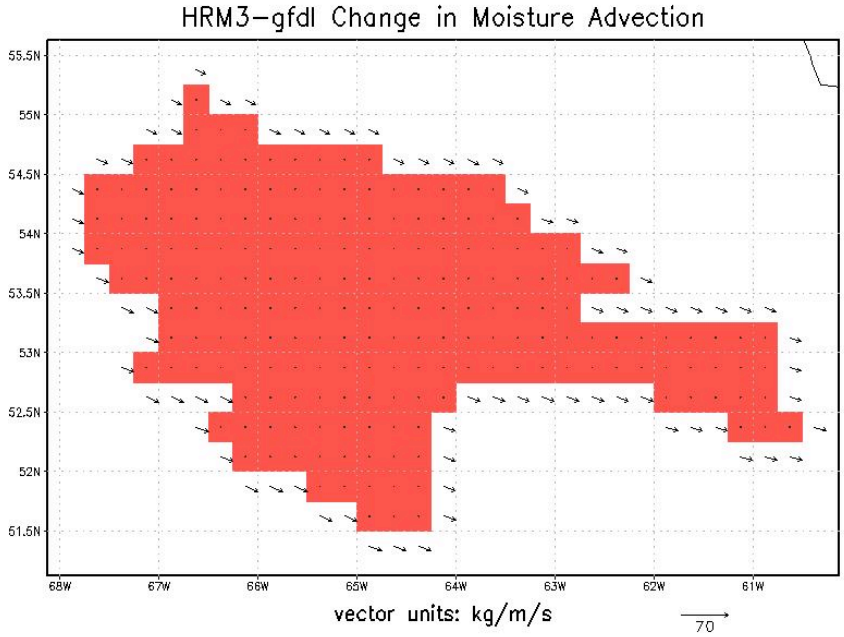

Figure D.3 – As per Figure D.1 for HRM3-gfdl.

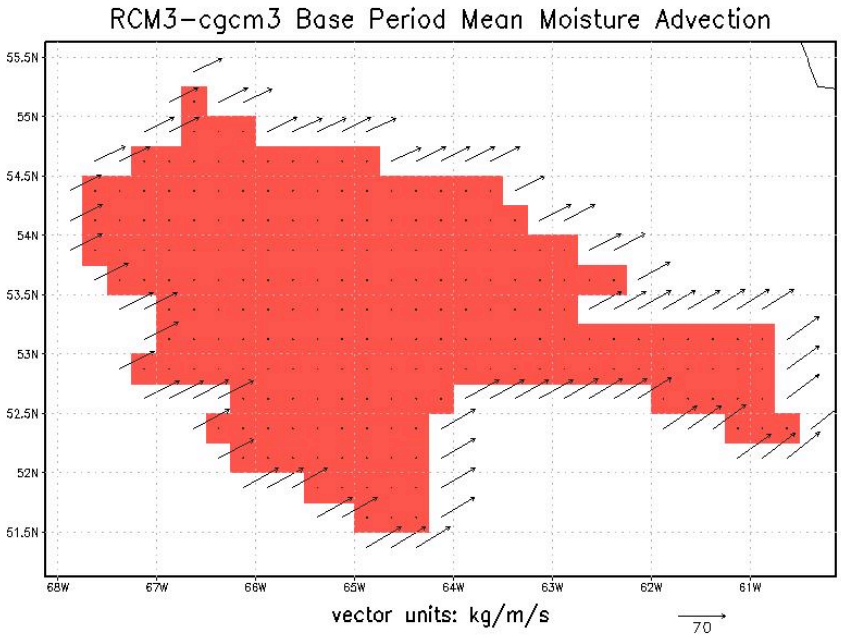

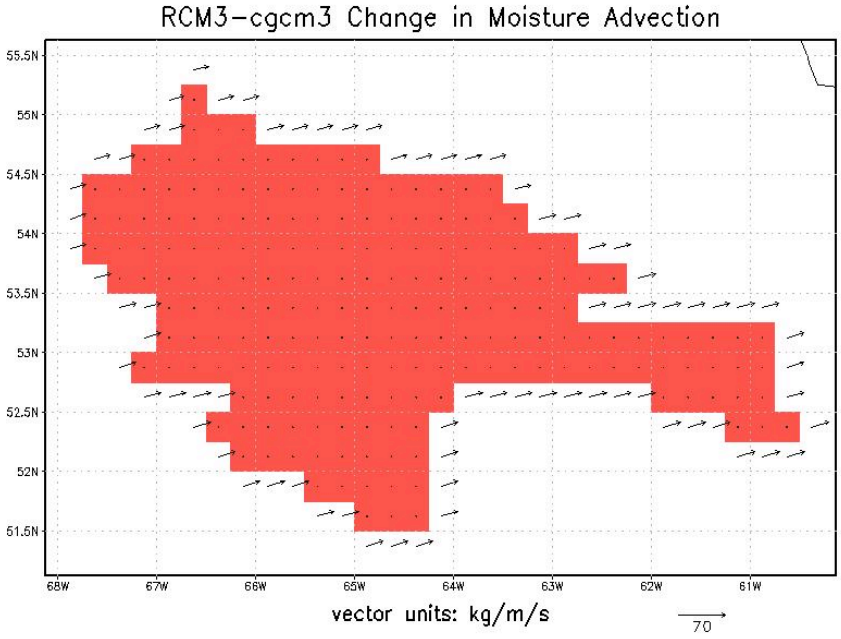

Figure D.4 – As per Figure D.1 for RCM3-cgcm3.

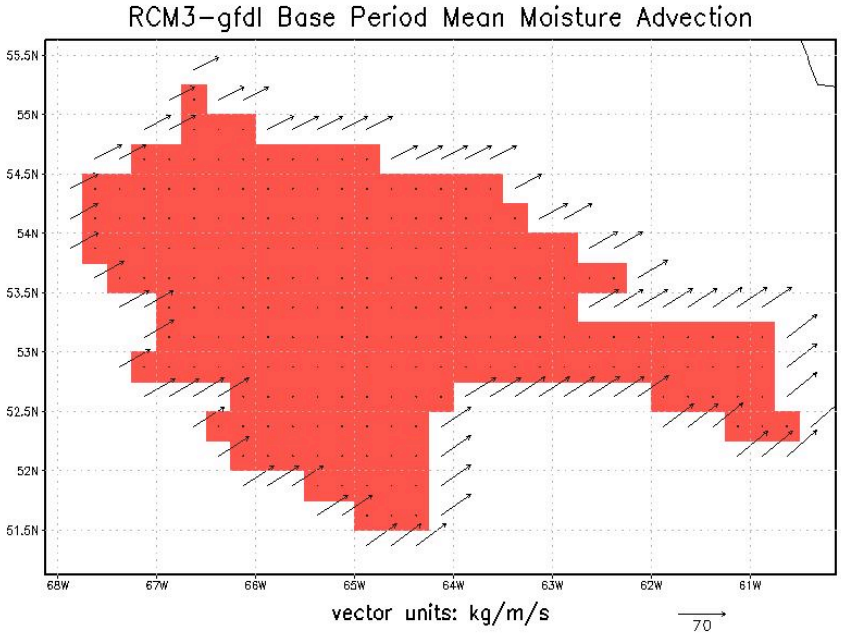

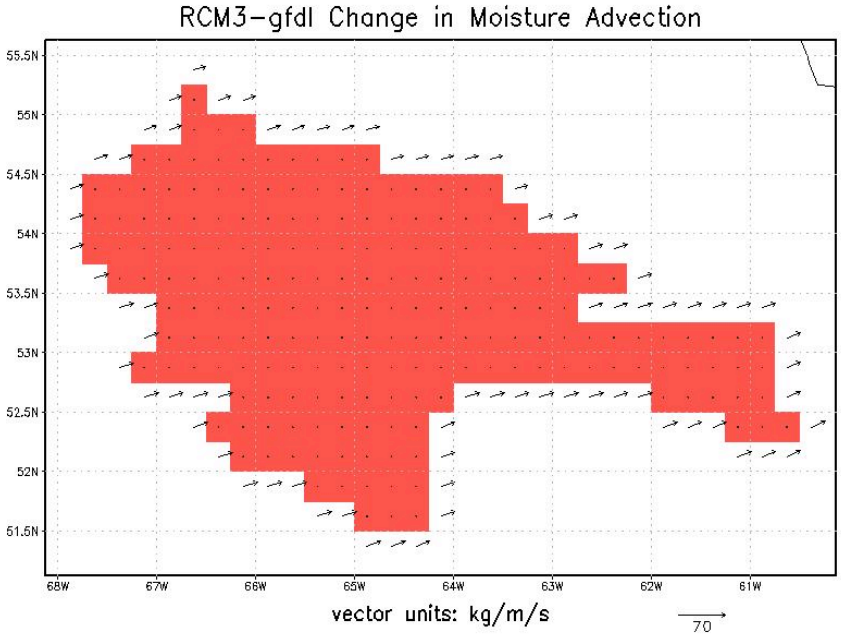

Figure D.5 – As per Figure D.1 for RCM3-gfdl.

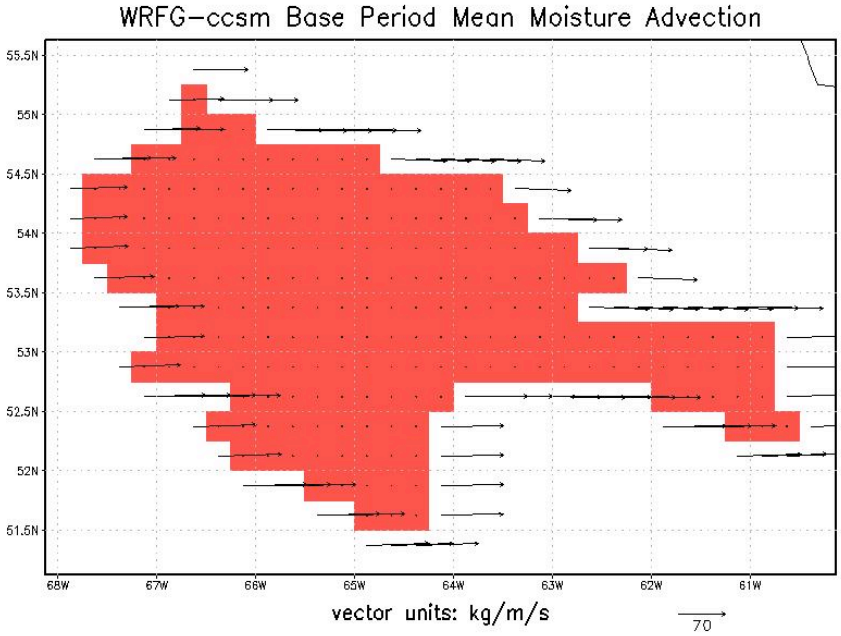

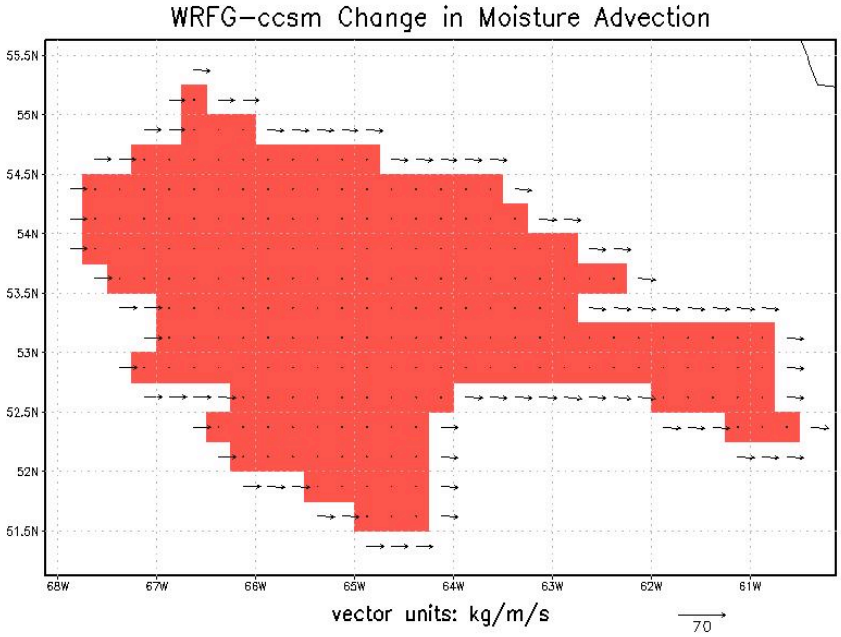

Figure D.6 – As per Figure D.1 for WRFG-ccsm.

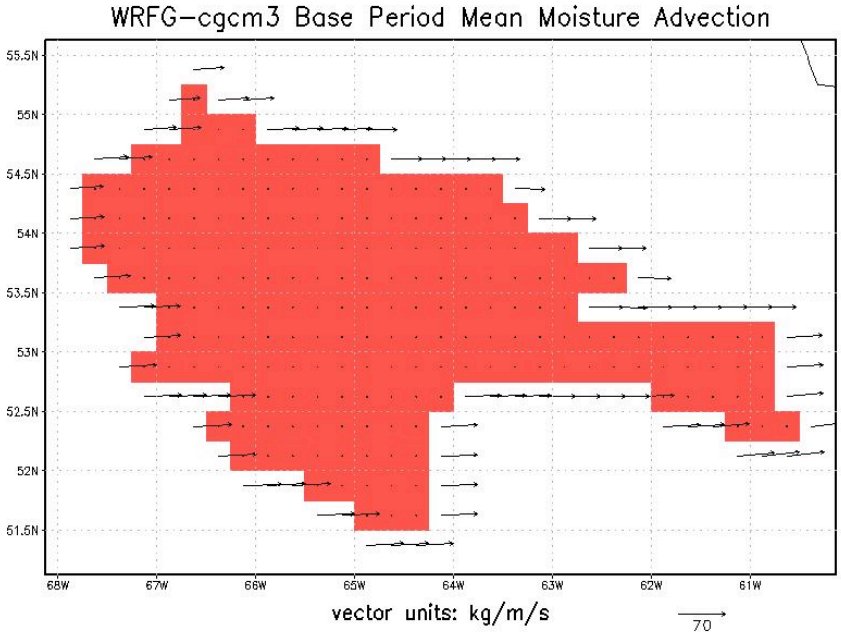

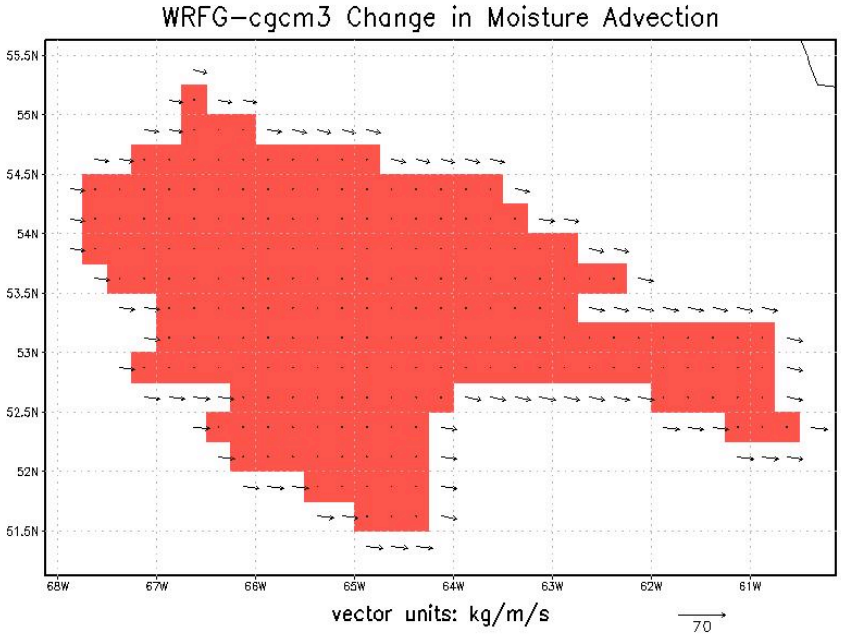

Figure D.7 – As per Figure D1 for WRFG-cgcm3.

9.5. Appendix E – Nalcor Energy Summary

This brief includes a results summary for Jonas Roberts' PhD thesis, the primary objective of which was to investigate the potential impacts of climate change on Labrador's Churchill River. The results presented here are only a fraction of the research discussed in the thesis and if the reader requires additional details it is recommended they consult the full work.

Overview

Three separate multi-model approaches, each using climate model output from the North American Regional Climate Change Assessment Program (NARCCAP), investigated the impacts of climate change on the Churchill River. The first approach used bias-corrected climate model precipitation and temperature data in conjunction with hydrologic modeling to investigate the changes in mean daily streamflow for the Pinus River, a sub-basin of the Churchill River. The second used a new approach (called fullstream analysis) to study the expected changes in mean annual runoff of the entire basin and took advantage of the full range of simulated hydrological variables from each ensemble member. The third approach applied weighted multi-model ensembles to examine the simulated impacts of climate change on mean monthly runoff for the entire basin.

To a large degree, each of these three approaches corroborated the results of the others. The mean annual increase in runoff/streamflow was found to be 8.9%, 11.2% and between 9.8 and 14.6% for the three approaches respectively. There was also found to be an increase in cold-season streamflow volumes, an earlier onset of the spring melt (though not necessarily a larger spring melt) and no discernable change in the late summer and early fall streamflow.

Uncertainty was represented in various ways throughout the thesis. For the Pinus River study, probability distribution functions (PDFs) were used to present the differences between base period and future streamflow. The mean ensemble hydrograph for base and future periods was shown, as were "spaghetti" plots showing how each streamflow changed according to each ensemble member. Streamflow changes were also broken down by season. The fullstream analysis also used PDFs to communicate mean annual changes in runoff.

The results of the weighted ensembles were plotted with uncertainty ranges around ensemble means of future annual cycles of streamflow. This allows for one to state with 80% and 90% confidence that an increase in streamflow was likely to occur for a given month. Spaghetti plots were also presented showing the variety of base period and future (unweighted) simulations. As model weighting is a necessarily subjective process that should include a sensitivity check, the results of a small variety of weighting schemes, including equal weighting, were plotted and discussed.

Pinus River Hydrological Modelling

The differences between the ensemble mean base and future period simulated hydrographs for the Pinus River, along with the observation simulation hydrograph are shown in Figure 1. (The "observed" hydrograph in Figure 1 refers to the WATFLOOD simulation using observed climatological variables as input.) There are four noteworthy changes from the mean base period to the future period simulations:

1 The spring melt, spanning April, May and June, is occurring roughly two to three weeks earlier though it appears to be slightly smaller in magnitude. April experiences the highest increase of any month, over 109%, caused by the earlier onset of the spring melt. The upshot of the earlier melt is that June is simulated to have a 33% decrease in streamflow.

2 November to March streamflow increases substantially.

3 July to October streamflow experiences no substantial change.

4 On a mean annual basis Pinus River streamflow increases by 8.9%, from 17.6 to 19.2 m^3/s.

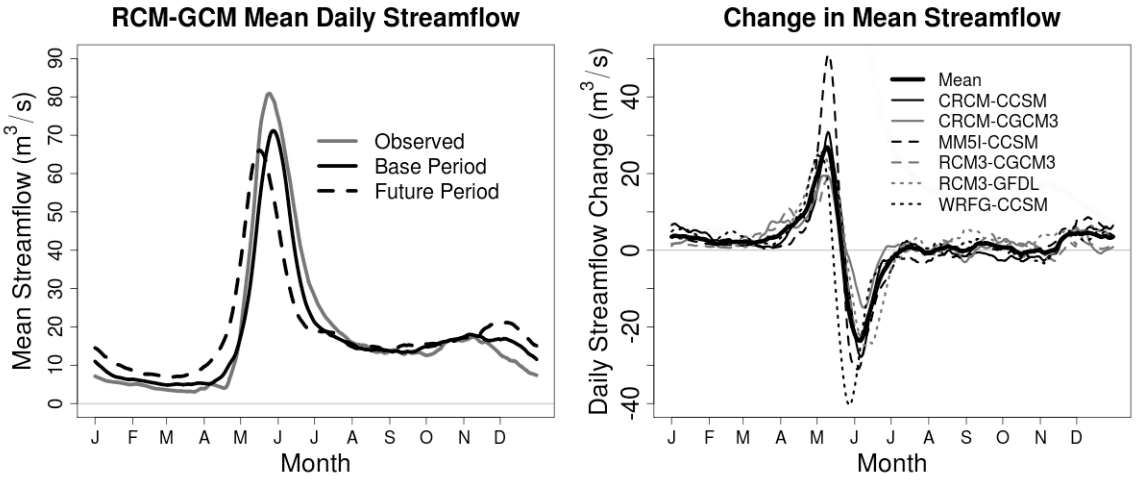

Figure 1 - Comparison of 30-year ensemble mean simulated base and future period streamflow (left) and the change in 30-year ensemble mean simulated streamflow, from base to future period (right).

Even though there is significant overlap in the mean annual flows, shown in Figure 2, there is a clear increase in magnitude from the base to the future period. The ensemble mean is similar to that of the observed hydrograph however the latter has a greater spread of values, most notably on the higher end of flow rates.

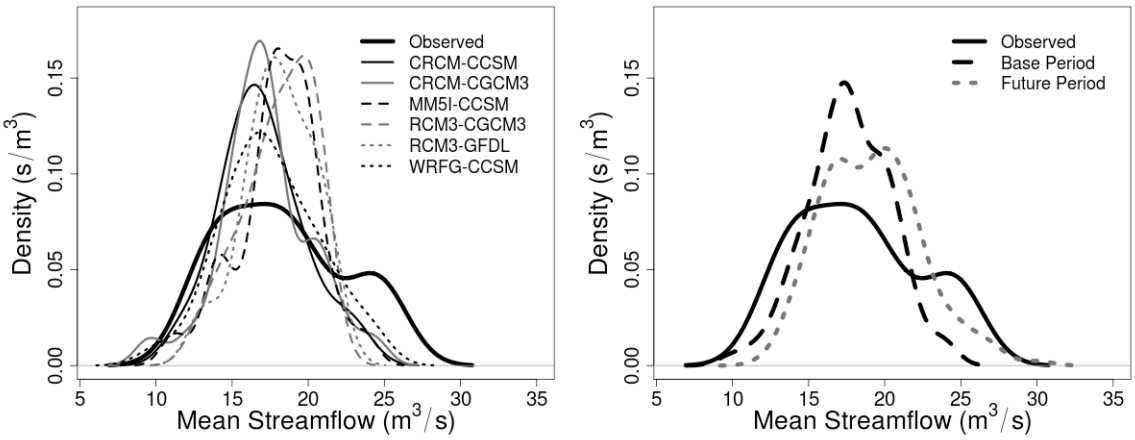

Figure 2. Probability density functions of mean annual flows for ensemble members during the base period (left) and the ensemble means for base and future periods (right).

By breaking down the flow by season in Figure 3, one is able to gain better insight into what time of the year the significant changes in streamflow are likely to occur. The changes in mean winter (defined here as November to March) flow magnitude are statistically significant while changes in spring (April to June) and summer (July to October) are not. In all three seasons the PDFs become flatter and wider from base to future periods, indicating higher variability in the future.

There is greatest agreement amongst ensemble member base period simulations in summer, while winter shows the least agreement. During spring and summer, the ensemble member distributions are slightly to the left of the observed indicating a small underestimation of flow, while the opposite is true of winter.

Fullstream Analysis: Projected Changes in Mean Annual Streamflow of Churchill River Basin

The approach used here is based on the atmospheric and terrestrial water balances in Equations 1 and 2, respectively.

$$-\frac{\partial W}{\partial t} - \nabla_H \bar{Q} = P - E \qquad [1]$$

$$P - E = R + \frac{\partial S}{\partial t} \qquad [2]$$

Here, W is the precipitable water content of the atmosphere, $-\nabla_H \bar{Q}$ is the vertically integrated horizontal atmospheric moisture convergence, P is precipitation, E is evaporation, R is runoff, and S is land-surface water storage (including soil moisture and snowpack).

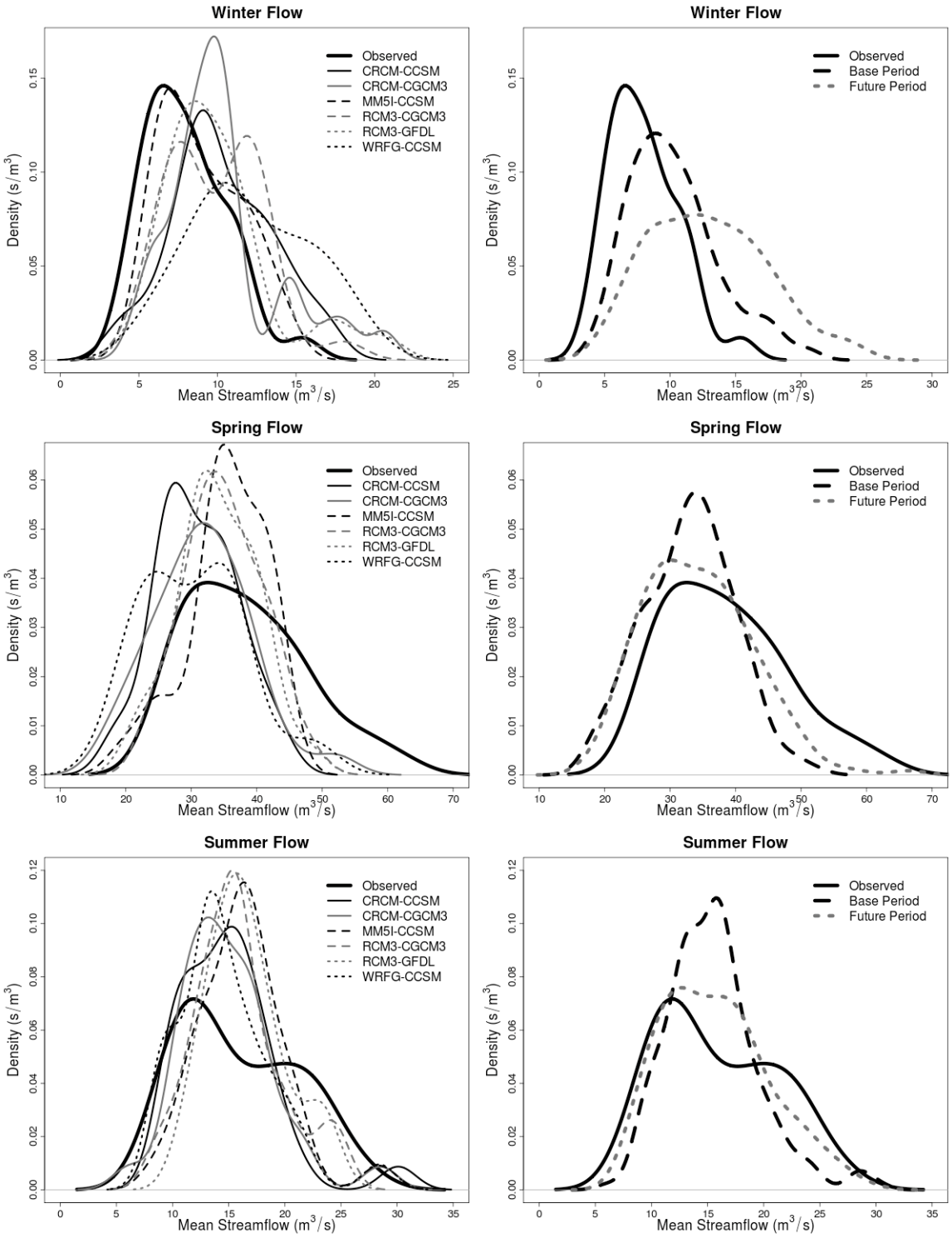

Figure 3. Probability distribution functions for mean winter (November to March), spring (April to June) and summer (July to October) flows, with ensemble member base period results on the left.

The terrestrial water storage component in Equation 2 tends to zero over long periods of time (as ∂t gets very large), implying that mean climatological runoff can be represented by P – E. Subsequently, mean climatological runoff can also be represented by the atmospheric moisture convergence from Equation 1, as the precipitable water tendency is also negligible over long periods. As such, RCMs are able to provide three representations of mean climatological runoff for analysis, corresponding to respective components of the "fullstream" approach: (i) $-\nabla_H \bar{Q}$, (ii) $P - E$, and (iii) R. (Note fullstream does not refer to any physical portion of a river but to the corresponding, and figurative, upstream, midstream and downstream approximations of runoff represented by $-\nabla_H \bar{Q}$, $P - E$ and R respectively.)

The mean annual streamflow measured at Muskrat Falls by the Water Survey of Canada is roughly 1825 m^3/s. Ensemble members that have higher than average approximations for simulated runoff in the base period also have higher than average projected runoff changes, likewise for members with lower than average values. This implies that this "over-estimation" (or "under-estimation") is systemic and also manifests itself in the climate change signal, warranting the study of changes relative to the base period simulation (%), as in Table 1. Absolute changes (m^3/s) are also examined to illustrate the climate signal in raw data output and highlight the results from individual RCM-gcm-stream ensemble members.

Table 1 - Projected runoff changes, including results of data reconstruction (in grey).

Absolute Change (m^3/s)					**Relative Change**				
RCM	**Stream**	**GCM**			**RCM**	**Stream**	**GCM**		
		ccsm	**cgcm3**	**gfdl**			**ccsm**	**cgcm3**	**gfdl**
CRCM	**up**	83	219	271	**CRCM**	**up**	5.6%	14.5%	7.2%
	mid	146	178	147		**mid**	9.2%	11.2%	8.0%
	down	110	179	113		**down**	6.8%	11.1%	6.3%
HRM3	**up**	18	5	121	**HRM3**	**up**	12.2%	4.5%	6.9%
	mid	95	152	97		**mid**	6.0%	7.3%	5.8%
	down	131	196	121		**down**	7.9%	9.0%	7.2%
RCM3	**up**	533	456	695	**RCM3**	**up**	21.8%	11.7%	18.6%
	mid	121	114	182		**mid**	6.7%	5.6%	8.7%
	down	99	100	149		**down**	7.4%	6.1%	8.8%
WRFG	**up**	357	180	388	**WRFG**	**up**	32.1%	12.2%	19.3%
	mid	159	227	178		**mid**	14.7%	19.7%	15.0%
	down	174	218	165		**down**	15.5%	17.9%	14.0%

PDFs, shown in Figure 4, are useful in risk analysis and economic decision-making. They recognize that climate projections are not perfect and provide a spectrum of potential

outcomes. To fully take advantage of climate projections in PDF form one must compare the costs and risks of an erroneously high runoff projection to those of a low runoff projection. For example, if one were investigating potential climate change impacts for the site of a future dam and hydroelectric development then a runoff projection that is too low may increase the risk of wasting water over a spillway. An erroneously high runoff projection on the other hand may lead to an increase in construction costs (as it would require a higher capacity) without the benefit of increased power generation. The costs and risks of each scenario must be balanced to determine the 'best' projection to use for project design, which is not necessarily the annual mean or median.

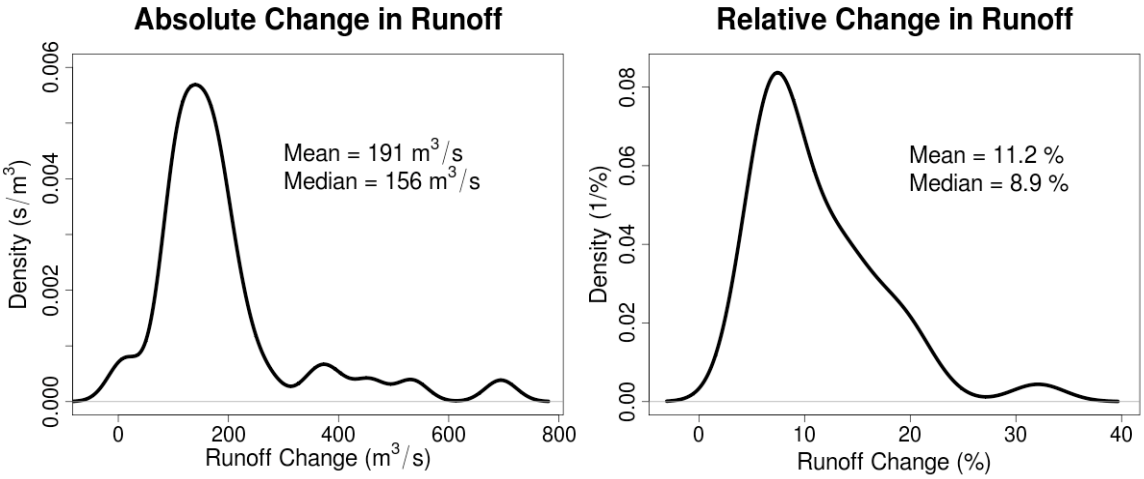

Figure 4 - PDFs of absolute (left) and relative changes in runoff (right), including imputed data

The simulations above indicate that climatological basin runoff is expected to increase. The ensemble median increase is roughly 155 m^3/s (0.14 mm/day), or 9%, while the mean increase is roughly 190 m^3/s (0.18 mm/day), or 11%. There are some outliers on the far right side of the PDF that suggest that runoff increases may be as high as 700 m^3/s (0.65 mm/day), or 35%, but the increase most likely lies between 25 and 250 m^3/s (0.02 and 0.23 mm/day), or 1 and 25%.

Weighted Ensembles: Change in the Annual Streamflow Cycle of the Churchill River Basin

Figure 5 shows the mean hydrographs of climate model runoff for each unweighted ensemble member for both base and future periods.

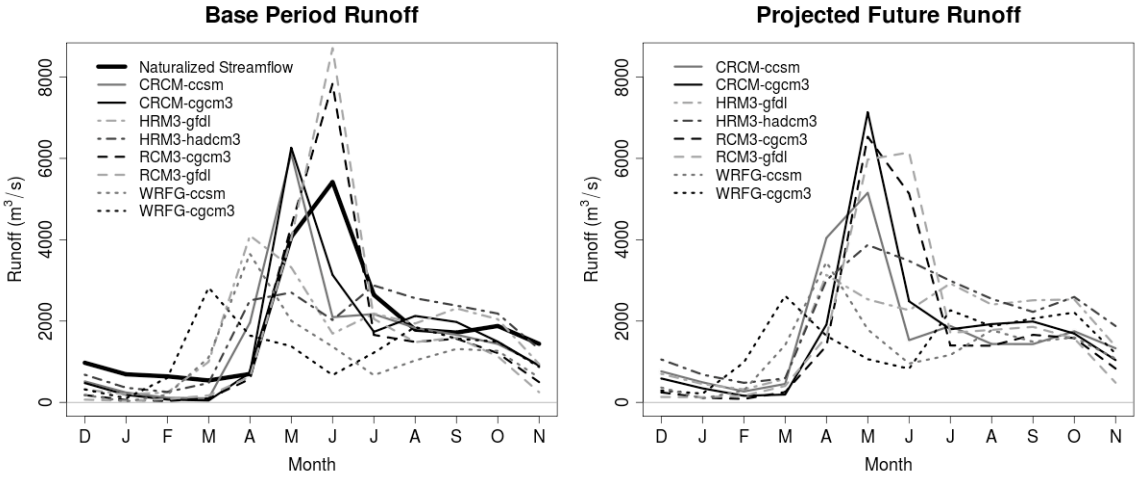

Figure 5 – Ensemble member mean hydrographs for base (left) and future periods (right).

Figure 6 presents simulated runoff CDFs for every month in the base (black lines) and future period (grey lines) for each ensemble member (note the scale differences between plots for the x-axes). Naturalized streamflow (observations accounting for the reservoirs and control structure of Churchill Falls) is also shown for comparison purposes.

Most CDFs have a relatively sharp turn in the distribution between probabilities of 0.8 and 0.9, which illustrates the impact of the spring melt on monthly runoff values. For two months each spring (typically May and June but may vary from year to year and between ensemble members) the melting snowpack causes a sharp increase in runoff to well over 2000 m^3/s.

There is also a wide range of high runoff values between ensemble members. While many are similar to the naturalized flow which maxes out at around 6000 m^3/s, several ensemble members are up in the 10 000 and even 14 000 m^3/s range. On the low runoff end, most ensemble members have some months with zero runoff (e.g. RCM3-cgcm3) while the naturalized flow doesn't.

Most of the future period CDFs are consistently further to the right than their base period counterparts. This shows monthly runoff generally increases under climate change. Some show an increase in lower end of runoff values (below 0.8 probability) but a decrease or ambiguous change in higher flows (e.g. CRCM-cgcm3, HRM3-gfdl). This implies that while monthly runoff is expected to increase for most of the year, the magnitude of the spring melt may actually decrease or remain constant.

Figure 7 shows the mean annual cycle of projected future streamflow, for each of the six weighted ensembles. W1 represents the unweighted (or equally weighted) ensemble., while five weighting criteria, were used in various combinations to create the weighting schemes W2 through W6: (i) divergence from the monthly ensemble mean, (ii) reproduction of mean monthly streamflow, (iii) reproduction of the distribution of mean streamflow for each month, (iv) divergence from the monthly ensemble mean streamflow

distribution, (v) mean annual physical consistency of models. The upper 80% and 90% uncertainty bounds are represented by the dashed light and dark grey lines respectively, while the lower bounds are represented by dotted lines.

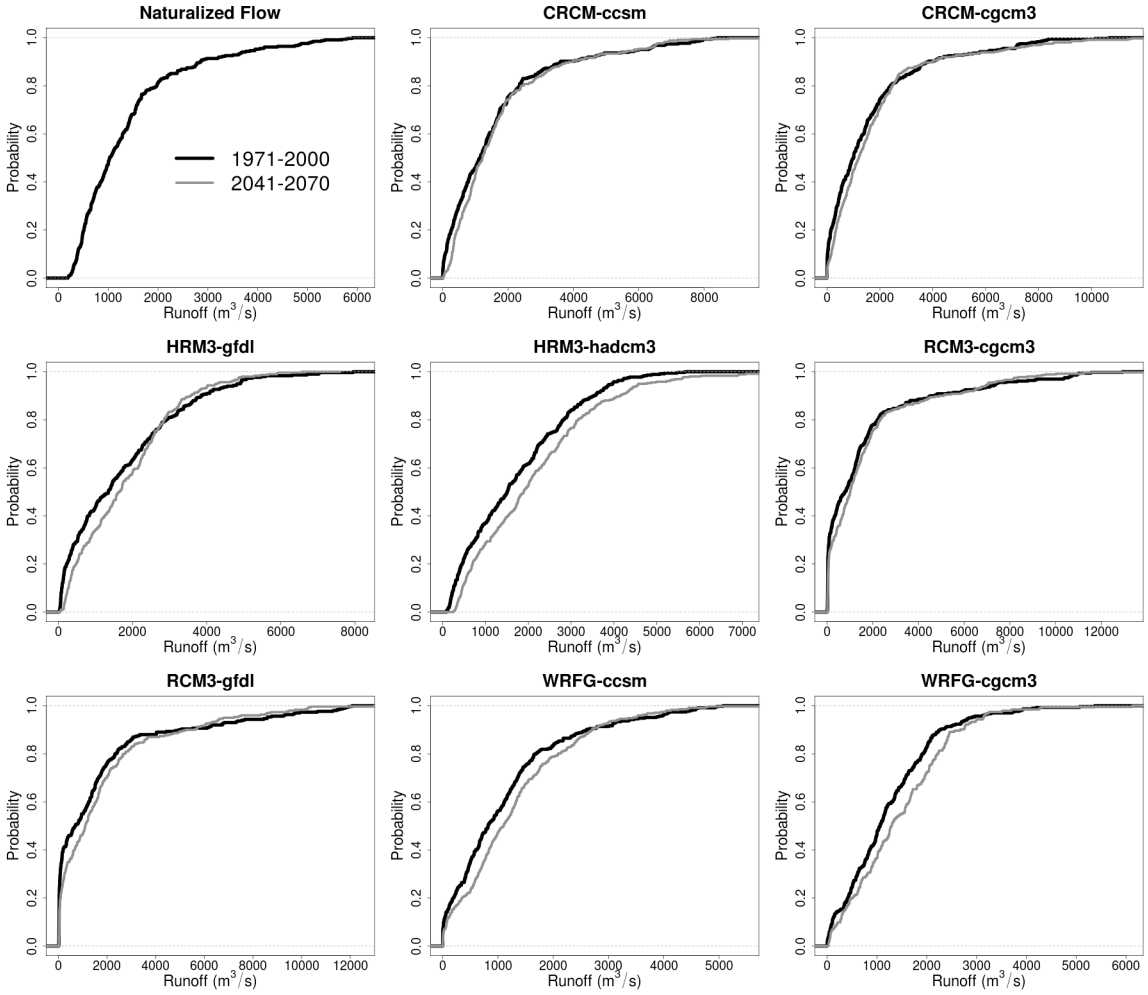

Figure 6 – CDFs of naturalized streamflow as well as simulated base period (black lines) and future period (grey lines) for each ensemble member.

The projected future flows for each of the six weighted ensembles in Figure 7 are quite similar. One common feature is a decrease in June flow and a corresponding increase in April and May flows. This means the spring melt will shift earlier in the year. Additionally, all plots indicate there will be an increase in monthly (cold season) flows, from October through May and no discernable change in late summer.

One of the differences between the six weighting schemes is the size of the confidence intervals, particularly in early spring. Table 2 shows by weighting scheme those months where there is greater than 80% confidence projected flows will be different from the

base period naturalized flow. The narrowest confidence intervals fall between October and March for all weighting schemes.

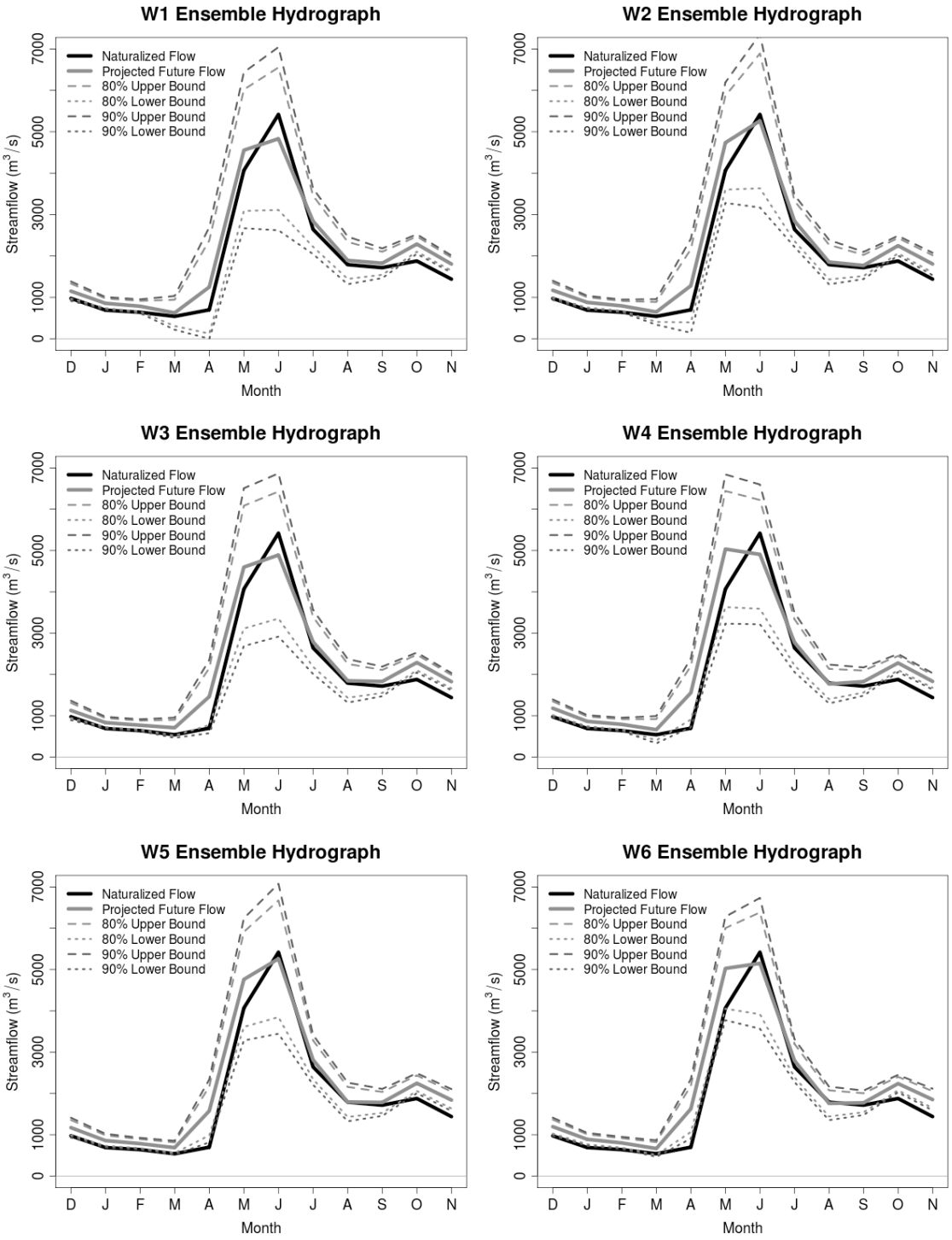

Figure 7 - Mean annual cycle of projected future streamflow, with confidence intervals.

Table 2 – Months with greater than 80% confidence that future streamflow will be different than base period streamflow. Underline indicates greater than 90% confidence

Scheme	D	J	F	M	A	M	J	J	A	S	O	N
W1		X	X								X	X
W2	X	X	X								X	X
W3		X	X		X						X	X
W4	X	X	X		X						X	X
W5	X	X	X	X	X						X	X
W6	X	X	X		X						X	X

Where the mean annual base period naturalized flow is 1875 m^3/s, the mean annual change in streamflow for weighting schemes W1 through W6 are 183, 233, 206, 248, 257, and 273 m^3/s, respectively. This represents a mean annual increase of between 9.8 and 14.6%. Each weighting scheme projects with 90% confidence that an increase in mean annual streamflow will occur.

Conclusion

Overall, the thesis presented the potential impacts of climate change on the mean hydrology of Labrador's Churchill River Basin while representing the uncertainty embodied in NARCCAP's multi-model ensemble. Given that there were some differences between the output of approaches used and individual ensemble members, in general the mean annual streamflow is expected to increase on the order of 10%. This increase will primarily manifest as additional cold-season (November to March) streamflow.